

# Smart Polymeric Materials by Ring-Opening Metathesis Polymerization

by

Mehdi Neqal

A thesis

presented to the University of Waterloo

in fulfilment of the

thesis requirement for the degree of

Doctor of Philosophy

in

Chemistry

Waterloo, Ontario, Canada, 2017

© Mehdi Neqal 2017

## **Examining committee membership**

The following served on the Examining Committee for this thesis. The decision of the Examining Committee is by majority vote.

External Examiners

JEROME CLAVERIE

Professor

JEAN-LUC SIX

Professor

Supervisors

VALERIE HEROGUEZ

DR (CNRS)

MARIO GAUTHIER

Professor

Internal Member

JEAN DUHAMEL

Professor

Internal-external Members

SEBASTIEN LECOMMANDOUX

Professor

VERONIQUE MONTEMBault

Professor

Other Members

VERONIQUE COMA

Associate Professor

FRANK GU

Associate Professor

AURELIEN VOISIN

Engineer (PhD)

## **Author's Declaration**

I hereby declare that I am the sole author of this thesis. This is a true copy of the thesis, including any required final revisions, as accepted by my examiners.

I understand that my thesis may be made electronically available to the public.



## **Abstract**

Microbial contamination in aircraft fuel tanks is a major concern because it can potentially put at risk the safety of the passengers. In these environments, microorganisms develop using the fuel as their carbon source and fuel additives as nutrients, and they can proliferate due to the presence of water from various sources, typically forming a layer below the fuel phase in storage tanks. Fuel degradation and the formation of sludge can cause premature deterioration of engine parts, but most importantly, the microorganisms induce chemical corrosion of the tank walls due to their ability to produce organic acids. Biocide compounds are typically used to inhibit these microorganisms, either with organic molecules dissolved directly in the fuel or the water phase, or most commonly with a chromium-based coating on the walls to hinder chemical corrosion. While organic biocides need to be replenished regularly, chromium is a particularly dangerous compound that is targeted by the REACH legislation (Registration, Evaluation and Authorization of Chemicals) due to its carcinogenic nature.

The main objective of this Thesis was to develop a new system to substitute for the biocides used presently. This system must be less toxic to humans, and remain active for a duration approaching the lifetime of the tank. The approach selected for this project was the development of a smart system of multifunctional polymeric particles that can deliver a biocide following an acidic trigger due to the presence of microorganisms. This system would be integrated in a coating formulation to apply on tank walls, to promote bioactivity and thus inhibit microbial-induced corrosion inside fuel tanks.

The Ring-Opening Metathesis Polymerization (ROMP) of cyclic olefins was discovered in the early 1960s and has become a popular way to produce polymeric materials. The reaction also became applicable in dispersed media, opening the way for the preparation of polymeric particles by ROMP. In particular, dispersion polymerization is seen as an interesting path due to its homogeneous initiation mechanism and low stabilizer concentration requirements.

In this study, particles were synthesized by dispersion ROM copolymerization of norbornene with an  $\alpha$ -norbornene linear macromonomer acting as a reactive stabilizer. Polyglycidol was selected for the backbone of the macromonomer for its water-solubility, its biocompatibility and because it can potentially be highly functionalized. Several macromonomers were synthesized by anionic ring-opening polymerization of protected glycidol initiated by norbornene-methanol. The degree of polymerization was controlled by the monomer/initiator ratio. After hydrolysis to recover the polyglycidol backbone, the hydroxyl functionalities were activated and further derivatized with dodecylamine, a primary amine selected for its antifungal properties and its ability to form a pH-sensitive imine bond with the activated macromonomer. Dispersion ROMP of non-functionalized and dodecylamine-functionalized macromonomers yielded novel polynorbornene-g-polyglycidol-based latexes. The colloidal properties of the non-functionalized core-shell particles were studied with variations in the length of the macromonomer, while highly functionalized particles were obtained using the dodecylamine-functionalized macromonomer.

The antifungal activity of the functionalized macromonomer and the particles was then investigated for the inhibition of *Hormoconis resinae*, a fungal strain typically found in fuel tanks. The use of homogeneous macromonomer solutions heterogeneous particle dispersions and particle films in the microbiological tests required the determination of the most suitable methods and conditions to observe the best antifungal response. Integration of the particles in a commercial coating sprayed on aluminum plates was also attempted to mimic the utilization of the system on tank walls. The ability of the coating to sustain extremely corrosive environment, with and without the particles needed to be verified for the system to be viable.

## Résumé en Français

La contamination microbienne des réservoirs de carburant est un problème majeur dans l'industrie de l'aéronautique qui peut potentiellement affecter la sécurité des voyageurs. En effet, les réservoirs sont un milieu particulièrement propice au développement de microorganismes où le carburant et ses additifs représentent une source abondante de composés carbonés et de nutriments pour ces dernières. La présence d'eau assure aussi le développement de populations et est introduite dans les réservoirs à partir de différentes sources. L'eau forme une phase séparée du carburant au fond des réservoirs, ce qui offre dans un premier temps la possibilité aux microorganismes de se développer à l'interface des deux phases où les substances nécessaires à leur développement sont facilement accessibles. Passé un certain stade de développement, les populations peuvent former des biofilms et se déplacer avec le carburant, ce qui entraîne de multiples conséquences. Les microorganismes se nourrissant du carburant peuvent ainsi le dégrader, ce qui peut mener à l'augmentation de sa viscosité et donc à l'usure prématurée de certaines pièces de l'appareil. De plus, le métabolisme des microorganismes entraîne la production d'acides organiques susceptibles de corroder les parois métalliques des réservoirs. En plus d'une vidange quotidienne de l'eau présente dans les réservoirs, des substances biocides sont habituellement utilisées pour éliminer les populations microbiennes. Ces substances peuvent être des composés organiques dissous dans le carburant devant être régulièrement réapprovisionnés, ou bien de manière plus courante du chrome (VI) sous forme de revêtement à la surface des parois afin de créer une couche passive et d'empêcher la corrosion chimique. Cependant, le chrome appartient à la catégorie des substances cancérigènes, mutagènes et reprotoxiques (CMR) et se trouve maintenant soumis à restriction par la réglementation européenne REACH (Registration, Evaluation and Authorization of Chemicals).

Ce travail de thèse consiste à développer un nouveau système utilisant des substances moins toxiques, non visées par la réglementation REACh, et qui ne nécessitent pas d'entretien régulier sur toute la durée de vie du réservoir. Le choix s'est ainsi porté sur la préparation de particules polymères intelligentes libérant une molécule biocide en environnement acide, témoignant de la présence de microorganismes. Ce système pourrait être incorporé dans un revêtement à appliquer sur les parois d'un réservoir aéronautique afin de lui conférer des propriétés bioactives, et ainsi entraver la corrosion chimique liée à la présence microbienne.

Depuis sa découverte au début des années 1960, la polymérisation par ouverture de cycle par métathèse (ROMP) d'oléfines cycliques est devenue une option très intéressante pour la confection de matériaux polymères. L'utilisation de cette technique a pu être transposée en milieu dispersé pour la préparation de particules polymères. La polymérisation en dispersion, par son amorçage en milieu homogène et ses besoins limités en stabilisant, représente une alternative intéressante.

Pour ce projet, des particules polymères sont synthétisées par copolymérisation en ROMP de norbornène avec un macromonomère  $\alpha$ -norbornène linéaire servant de stabilisant réactif à incorporer dans les particules. La chaîne principale du macromonomère est composée de polyglycidol, un polymère choisi pour sa solubilité dans l'eau, sa biocompatibilité et sa structure multifonctionnalisable. Des macromonomères de degrés de polymérisation différents ont été synthétisés par polymérisation anionique par ouverture de cycle amorcée par le norbornène-méthanol. Une structure linéaire est obtenue par protection du glycidol avant la polymérisation. Après hydrolyse de ces fonctions, les groupements hydroxyl de la chaîne de polyglycidol peuvent être activés pour conjuguer le biocide. Une fonction imine, pH sensible, est choisie pour attacher la dodecylamine, une amine primaire connue pour sa bioactivité, et obtenir un macromonomère multifonctionnel. La ROMP en dispersion utilisant la fonction norbornène terminale des macromonomères, fonctionnalisés ou non, permet la préparation de

latex inédits à base de polynorbornène-*g*-polyglycidol. Une étude sur les particules non fonctionnalisées a permis de confirmer la formation de structures cœur-écorce et de quantifier l'influence du degré de polymérisation du macromonomère ou de la nature de la phase dispersante sur les propriétés colloïdales des objets. L'utilisation du macromonomère fonctionnalisé a quant à lui permis la préparation de particules hautement fonctionnelles pour application en tant qu'agents de décontamination des réservoirs de carburant.

Les propriétés bioactives du macromonomère et des particules fonctionnalisées ont été ensuite vérifiées en testant leur inhibition de la souche fongique *Hormoconis resiniae*, un contaminant typique des réservoirs. Des méthodologies de microbiologie ont été mises au point pour tester différents systèmes de solutions homogènes de macromonomère, de dispersions hétérogènes et de films de particules afin d'en observer les réponses bioactives les meilleures. Afin de simuler l'application finale des particules dans les réservoirs, leur incorporation a été effectuée par pulvérisation sur une surface d'aluminium couverte d'un revêtement commercial. La capacité des particules à ne pas altérer la résistance du revêtement de base à des conditions de corrosion extrêmes a permis de vérifier leur applicabilité dans ce domaine.

## Acknowledgements

*After four special years in PhD, I want to acknowledge the many wonderful people from all around the world I had the chance to meet and the people who were here for me long before too. I am thankful for the opportunity to pursue this project in the frame of the IDS-FunMat program between two Universities: the University of Bordeaux, France where I worked at the « Laboratoire de Chimie des Polymères Organiques » (LCPO) and the University of Waterloo, Canada in the department of Chemistry. I would first like to thank the IDS-FunMat consortium for supporting this project, and the Region of Aquitaine, Pr. Mario Gauthier and the University of Waterloo for the funding of these four years.*

*I wish to express my gratitude to the jury members Pr. Jérôme Claverie, Pr. Jean-Luc Six, Pr. Véronique Montembault, Pr. Jean Duhamel, Dr. Frank Gu, Dr. Aurélien Voisin and Pr. Sébastien Lecommandoux for accepting to review this thesis, for the rich discussion we had during the defence and the many suggestions I benefited from to improve this manuscript.*

Je tiens à remercier les directeurs successifs du LCPO, Pr. Henri Cramail et Pr. Sébastien Lecommandoux, de m'avoir accueilli dans leur laboratoire et m'avoir permis d'évoluer dans un cadre idéal pour mon apprentissage.

Je tiens à exprimer ma plus profonde gratitude à mes deux directeurs de thèse, Dr. Valérie Héroguez et Pr. Mario Gauthier. Mario, je vous remercie de m'avoir accueilli dans votre équipe à Waterloo, et pour m'avoir accordé votre confiance. J'admire votre savoir encyclopédique sur le domaine des polymères et de la chimie en général. Valérie, merci pour votre implication totale de tous les jours, même lorsque j'étais de l'autre côté de l'Atlantique, d'avoir toujours été présente avec un nombre incalculable d'idées, et d'avoir su me garder motivé malgré quelques périodes de traversées du désert. J'ai énormément appris sur moi-même et sur mon futur métier à vos côtés.

Je tiens aussi à remercier Dr. Véronique Coma, grâce à qui l'étude en microbiologie a pu voir le jour. Merci de m'avoir guidé et rassuré sur ce sujet qui me faisait très peur au départ, et pour ta bonne humeur communicative !

Je suis très reconnaissant que ce projet aux applications très ciblées m'ait donné l'opportunité de collaborer avec le milieu industriel. Je voudrais donc remercier Dr. Konstantin Sipos, Dr. Thomas Stimpfling, et Dr. Aurélien Voisin de l'entreprise Rescoll pour les échanges réguliers que nous avons pu entretenir et leur aide précieuse dans l'incorporation de notre système dans des revêtements commerciaux et les tests de corrosion accélérée.

Ce travail n'aurait pas pu être complété sans l'apport scientifique de nombreuses personnes qui m'ont formé aux appareils de mesure, m'ont aidé à préparer mes échantillons, et à analyser mes résultats: Etienne Gontier, Sabrina Lacomme et Melina Petrel du BIC, Christelle Absalon et Patricia Castel du CESAMO, Wiljan Smaal et Sokha Khiev d'ELORPrinTec, Emmanuel Ibarboure, Najim Ounajma, Gilles Pecastaings, Amélie Vax, *Jan Venne* et Anne-Laure Wirotius.

Un grand merci aux personnes qui permettent au LCPO de tourner sans accrocs au quotidien, et qui ont toujours été disponibles pour répondre à la moindre de mes interrogations: Gérard Dimier, Bernadette Guillabert, Corinne Gonçalves, Cédric Le Coz, Claude Le Pierres, Loïc Petrault, Dominique Richard, Catherine Roulinat et Eric Virol.

*Many thanks to Maya Bernier, Sarah Mark (thank you for the tea time conversations whenever I popped in!), Howard Siu and Cathy Van Esch who helped me and the whole department on an everyday basis in Waterloo.*

Je voudrais aussi remercier les différents acteurs du programme IDS-FunMat qui veillent au bon déroulement de notre thèse et aident les nombreux doctorants à résoudre leurs problèmes dans leurs pays d'accueil: Stéphane Carlotti, Marie-Christine Durrieu, Marianne Delmas, Laurent Servant, Audrey Sidobre, Thierry Tassaing et Bernhard Zeimetz.

*I want to express my heartfelt gratitude to all the past and current members of Pr. Mario Gauthier's team. I keep many happy and fun memories of our times together: My C2-166 bros Aklilu and Mosa, Ala, Alvaro, An, Basma, Deepak, Hemali, Joanne, Liying, Natun, Olivier, Paul, Priscilla, Ryan, Tori and Xiaozhou. I also want to thank Pr. Jean Duhamel and all the members from his team with whom we worked in close relationship.*

*I wish to thank Momo and Wayne for the many late night discussions when I stayed on campus long after sundown!*

*Want to thank the unforgettable « IDSers » for all the great times we had in Bordeaux, in Waterloo, and at the training schools!! Abderrezak, Alberto, Anil, Ara, Begüm, Camille, Can, Carole, Dan, David, Erin, Gustavo, Gregor, Edis (wise mate), Hareesh, Jiang, João, Kenny, Laura, Marie, Margot, Marwa, Mathilde(s), Mylène (Heureusement qu'on avait le Grad House, Waterloo l'hiver c'était quand même long!!), Nhi, Paul, Ruihao (Ray), Santosh, Sergey, Sheavon, Shun, Tuyen, Uyxing, Vusala and Zhen.*

J'ai ma petite famille au LCPO : Valérie prend soin de nous et on prend soin de chacun !  
Merci à tous les membres de la Team Héroguez : le trio (ou quatuor, quoique l'occasion se présentait rarement !) du N1-19, Loïc (I break myself!!! Merci pour tout, j'ai beaucoup appris grâce à toi), Arthur (Tu sais ce que c'est ? C'EEEST...!!!) et Margot (Princesse), mais aussi les anciens qui m'ont aussi beaucoup apporté: Floraine, Edgar (WHAAAAAAT????!!!), Hélène et Robert.

Merci à mes anciens du N2-29: Cony (Ma voisine du fond ☺, on aura beaucoup causé !), Khalid, Shusheng et Zoey.

En quatre ans au LCPO, j'ai pu côtoyer plusieurs générations de doctorants/postdocs avec qui j'ai partagé mon quotidien. J'ai adoré causer, traîner, sortir et jouer de la musique avec vous  
Anna, Antoine, Ariane, Beste, Blandine, Boris, Camille, Cédric, Cindy, Christopher, Dam, Dounia, Elise, Erwan, Esra, Estelle, Fiona, Gauvin, Guillaume C., Guillaume G., Hélène,



Jérémy, Julie, Julien B., Julien R., Kevin, Laura, Léa, Louis, Marie, Martin (Câââliiiiiin), Michelle, Mikael, Nicoletta, Nooshin, Pauline, Pierre-Luc, Quentin P., Quentin S., Sofiem, Thomas (mon premier chef !), Ye et bien d'autres... Merci à tous, ces quatre années valaient le coup car vous étiez là !

Un petit mot pour les copains de CBP qui malgré la distance, continuent de prolonger le délire : Alex, Alexis, Arthur, Benji, Clément, Geoffrey, Jo, Johann, Laurie, Mathilde, Maxime (Le Binôôôôme, (HP ≠ Hachis Parmentier)), Nico, Romain, Stefan, Thomas, mes Bretons: Adri, et Damien (Alphonse Daminator) et Les Casseurs Flotteurs: Ronan C., Ronan L., Thibaud (Lélé Le Mix), et Victor (Vicky V, le leader charismatique).

Je voudrais remercier ma famille pour leur soutien et pour m'avoir supporté toutes ces années. Je ne pouvais pas terminer sans te remercier Anne, qui n'a jamais douté de moi et qui continue tous les jours à m'étonner et à m'inspirer !

Mehdi

# Table of Contents

Examining committee membership.....	ii
Author's Declaration .....	iv
Abstract .....	v
Résumé en Français.....	vii
Acknowledgements .....	x
Table of Contents .....	xiv
List of Figures .....	xviii
List of Tables.....	xxiii
List of Schemes .....	xxiv
List of Abbreviations.....	xxv
List of Symbols .....	xxvii

## **Chapter 1: General Introduction ..... 1**

1.1. Opening Remarks .....	2
1.2. Research Objectives and Thesis Outline .....	3

## **Chapter 2: Bibliography – Synthesis of Functional Particles by ROMP ... 6**

2.1. General Concepts of Ring-Opening Metathesis Polymerization (ROMP) .....	7
2.1.1. Discovery of Olefin Metathesis Polymerization.....	9
2.1.2. Mechanism.....	11
2.1.3. Development of ROMP Catalysts .....	12
2.1.3.1. Ill-Defined Metathesis Catalysts.....	12
2.1.3.2. Well-Defined Catalysts.....	13
2.1.3.3. Ruthenium-Based Catalysts .....	13
2.1.3.4. Metal-Free ROMP .....	18
2.2. Particles by Self-Assembly of ROMP Copolymers .....	19
2.2.1. Core-Crosslinked Particles .....	20
2.2.2. Shell-Crosslinked Particles.....	22
2.2.3. Particles Stabilized by Interchain Interactions .....	24
2.3. Particles by Dispersed Medium ROMP Using Non-Reactive Surfactants.....	26
2.3.1. Emulsion ROMP.....	26
2.3.1.1. ROMP in Aqueous Emulsions .....	29
2.3.1.2. ROMP in Non-Aqueous Emulsions.....	30
2.3.2. Miniemulsion ROMP.....	30
2.3.3. Microemulsion ROMP.....	32
2.3.4. Suspension ROMP.....	35
2.3.5. Dispersion ROMP.....	36
2.4. Synthesis of Particles by ROMP Using Macromonomers .....	39
2.4.1. Miniemulsion ROMP.....	39
2.4.2. Suspension ROMP .....	40
2.4.3. Dispersion ROMP.....	41
2.5. pH-Sensitive Functionalized Polymeric Particles .....	43
2.5.1. pH-Sensitive Bonds for the Formation of Drug-Polymer and Drug- Particle Conjugates.....	44
2.5.1.1. Conjugation with Acetal Bonds .....	44
2.5.1.2. Conjugation with Ester Bonds .....	46

2.5.1.3.	Conjugation with Hydrazone Bonds.....	47
2.5.1.4.	Conjugation with Imine Bonds.....	49
2.5.1.5.	Conjugation with pH-Sensitive Triazole Bonds.....	51
2.5.2.	pH-Sensitive Particles Prepared with ROMP Macromonomers.....	52
2.6.	Conclusions.....	54

### **Chapter 3: Synthesis of Multifunctional Polyglycidol-Based**

<b>Macromonomers.....</b>	<b>56</b>	
3.1	State of the Art in the Preparation and Functionalization of Polyglycidol.....	57
3.2	Methods and Materials.....	63
3.2.1	Synthesis of $\alpha$ -Norbornenyl-Polyglycidol Macromonomers.....	63
3.2.1.1	Synthesis of Glycidol Acetal.....	63
3.2.1.2	Synthesis of $\alpha$ -Norbornenyl-Polyglycidol Macromonomers.....	63
3.2.1.2.1	Preparation of the Deprotonating Agent.....	63
3.2.1.2.2	Synthesis of $\alpha$ -Norbornenyl-Poly(glycidol acetal)	
Macromonomer.....	64	
3.2.1.3	Hydrolysis of $\alpha$ -Norbornenyl-Poly(glycidol acetal)	
Macromonomers.....	65	
3.2.2	Preparation of Biocide-Functionalized Macromonomers.....	65
3.2.2.1	Functionalization of the Polyglycidol Chains.....	65
3.2.2.2	Dodecylamine Functionalization of the Macromonomers.....	66
3.3	Results and Discussion.....	66
3.3.1	Synthesis of $\alpha$ -Norbornenyl-Polyglycidol Macromonomers.....	66
3.3.1.1	Synthesis of Glycidol Acetal.....	66
3.3.1.2	Synthesis of $\alpha$ -Norbornenyl-Poly(glycidol acetal)	
Macromonomers.....	67	
3.3.1.3	Hydrolysis of $\alpha$ -Norbornenyl-Poly(glycidol acetal)	
Macromonomers.....	71	
3.4	Preparation of Biocide-Functionalized Macromonomers.....	74
3.4.1	Functionalization of the Polyglycidol Chains.....	74
3.4.1.1	Optimization of Reaction for Macromonomer (3a, DP <sub>n</sub> = 25).....	77
3.5	Biocide Functionalization of the Macromonomers.....	79
3.5.1	Dodecylamine Functionalization of the Higher Molecular Weight Macromonomer (DP <sub>n</sub> = 103).....	79
3.5.2	Dodecylamine Functionalization of the Lower Molecular Weight Macromonomer (DP <sub>n</sub> = 25).....	83
3.6	Conclusions.....	88

### **Chapter 4: Preparation of Functionalized Polynorbornene-g-Polyglycidol-Based Particles by Dispersion ROMP..... 90**

4.1.	State of the Art in the Preparation of Polyglycidol-Based Particles.....	91
4.2.	Methods and Materials.....	96
4.2.1.	Preparation of Polynorbornene-g-Polyglycidol Particles by Dispersion ROMP.....	96
4.2.2.	Determination of the Conversion of Reactants.....	97
4.2.3.	Determination of Surface Functional Group Density.....	98

4.2.3.1. Determination of Hydroxyl Groups on the Non-Functionalized Particles.....	98
4.2.3.2. Determination of the Biocide Density in the Functionalized Particles.....	99
4.3. Results and Discussion.....	99
4.3.1. Preparation of Polynorbornene-g-Polyglycidol Particles by Dispersion ROMP.....	99
4.3.2. Preparation of Dodecylamine-Functionalized Polynorbornene-g-Polyglycidol Particles.....	104
4.3.3. Alternate Approaches for Increased Conversion of the Dodecylamine-Functionalized Macromonomer.....	108
4.4. Conclusions.....	109

**Chapter 5: Use of the Functionalized Macromonomer and Particles as Antifungal Agents Against *H. Resinae* ..... 111**

5.1 Identification of Fuel Contaminants and Treatment with Biocides.....	112
5.2 Materials and Methods.....	117
5.2.1 Materials.....	117
5.2.2 Methods.....	117
5.2.2.1 Evaluation of Biocide Release from the Macromonomer....	117
5.2.2.2 Preparation of Microbial Culture Stock.....	117
5.2.2.3 Preparation of Inoculum.....	118
5.2.2.4 Preparation of Culture Media.....	118
5.2.2.5 Evaluation of the Antifungal Properties of Macromonomer Solutions and Particle Dispersions.....	118
5.2.2.6 Evaluation of the Antifungal Properties of Particle Films...	119
5.3 Results and Discussion.....	120
5.3.1 Release Assessment of Dodecylamine.....	120
5.3.2 Agar Culture Medium for <i>H. Resinae</i> .....	122
5.3.3 Droplet Test with Macromonomer Solutions.....	123
5.3.4 Droplet Test on Particle Dispersions.....	126
5.3.4.1 Particle Conditioning.....	126
5.3.4.2 Droplet Test on Particle Dispersions.....	128
5.3.5 Tests with Particle-Based Films.....	130
5.3.5.1 Preparation and Characterization of the Films.....	131
5.3.5.2 Evaluation of the Antifungal Activity of the Particle Films	135
5.3.6 Incorporation of the Particles in a Model Coating.....	138
5.4 Conclusions.....	143

**Chapter 6: Concluding Remarks and Perspectives ..... 144**

6.1. Original Contributions to Knowledge.....	145
6.2. Suggestions for Future Work.....	147

**References ..... 150**

Chapter 1:.....	150
Chapter 2:.....	150
Chapter 3:.....	162

Chapter 4: .....	165
Chapter 5: .....	167
Chapter 6: .....	169

**Appendix A: Characterization Techniques..... 170**

A.1. Proton Nuclear Magnetic Resonance ( <sup>1</sup> H NMR) .....	171
A.2. Size Exclusion Chromatography (SEC) analysis .....	171
A.3. Matrix-Assisted Laser Desorption Ionization Time of Flight Mass Spectrometry (MALDI-ToF).....	171
A.4. Infrared Spectroscopy.....	171
A.5. Gas Chromatography.....	172
A.6. Dynamic Light Scattering (DLS) .....	172
A.7. Transmission Electron Microscopy (TEM).....	172
A.8. Atomic Force Microscopy (AFM) .....	172
A.9. Profilometry .....	173

**Appendix B: Supplementary Microbiology Methods..... 174**

B.1. Determination of Inoculum Concentration.....	175
---	-----

**Appendix C: Supplementary Characterizations..... 177**

## List of Figures

Figure 2.1.	Variations of the metathesis reaction.....	8
Figure 2.2.	Secondary ROMP mechanisms. ....	9
Figure 2.3.	Proposed ROMP mechanism for Ziegler-Natta catalysts. <sup>5</sup> .....	10
Figure 2.4.	Disproportionation reaction of propylene: First example of linear olefin metathesis. ....	10
Figure 2.5.	Early transition metal-based metathesis catalysts.....	11
Figure 2.6.	Well-defined ruthenium catalysts. ....	16
Figure 2.7.	Water-soluble ruthenium catalysts. ....	17
Figure 2.8.	Key components in the metal-free ROMP system: initiators 24-26; photoredox mediator 27; <i>endo</i> -cyclopentadiene monomer.....	19
Figure 2.9.	Synthesis of core-crosslinked cylindrical particles via tandem ROMP/NMP. <sup>57</sup> .....	22
Figure 2.10.	Synthesis of shell-crosslinked micelles with cobalt-functionalized core. <sup>62</sup> .....	23
Figure 2.11.	(A) Living ROMCopolymerization of dicarboximide norbornene with cyclooctatetraene; (B) Formation of caterpillar structures during the growth of the polycyclooctatetraene block. <sup>63</sup> .....	25
Figure 2.12.	Particles obtained by ROMP of a monomer containing a chelating group. (A) pH dependence of core-shell reversibility; (B) “Crosslinking” by complexation with Fe(II) or Cu(II) and metal ion exchange. <sup>67</sup> .....	25
Figure 2.13.	Representation of an emulsion polymerization system. ....	28
Figure 2.14.	Evolution of polymerization rate with conversion for a typical emulsion polymerization. ....	28
Figure 2.15.	Representation of miniemulsion polymerization.....	31
Figure 2.16.	Water-soluble miniemulsion ROMP initiator. <sup>76</sup> .....	32
Figure 2.17.	Latent ruthenium complex activated by protonation. ....	35
Figure 2.18.	Preparation of macroporous polymer beads by suspension ROMP. <sup>90</sup> .....	36
Figure 2.19.	Mechanism of particle formation in dispersion polymerization.....	38
Figure 2.20.	(A) Suspension ROMP of cyclooctadiene with $\alpha$ -norbornenyl-PS-PEO macromonomer; (B) Particles observed by optical microscopy. <sup>102</sup> .....	40
Figure 2.21.	Formation of polynorbornene (top) and polybutadiene (bottom) latexes by dispersion ROMP.....	42

Figure 2.22.	(A) Preparation of crosslinked polynorbornene particles by dispersion ROMP; (B) Observation of raspberry-shaped particles by TEM. <sup>106</sup>	43
Figure 2.23.	Mechanism for the formation of an acetal group assisted by an acid catalyst.	45
Figure 2.24.	Variation in the acetal hydrolysis rate with pH and the presence of substituents on PEG-based conjugates. <sup>110</sup>	45
Figure 2.25.	(A) Formation of polyplexes with acetalized polyethylenimine; (B) pH-dependence of the acetal bond hydrolysis. <sup>115</sup>	46
Figure 2.26.	Mechanism for the carbodiimide-mediated formation of an ester bond.	47
Figure 2.27.	(A) Formation of a hydrazone bond; (B) Typical release profiles for DOX as a function of pH. <sup>126</sup>	49
Figure 2.28.	Particle based on a dendritic core and poly(L-aspartate)- <i>b</i> -PEG for the acid-triggered release of DOX. <sup>145</sup>	49
Figure 2.29.	(A) Mechanism for the formation of an imine bond; (B) pH-dependent release profile of DOX from poly(alkyl methacrylate)-based copolymer micelles. <sup>147</sup>	50
Figure 2.30.	PEG-decorated Fe <sub>3</sub> O <sub>4</sub> particles functionalized with chromone.	51
Figure 2.31.	Preparation of pH-sensitive triazole-based prodrug and release under acidic pH. <sup>156</sup>	51
Figure 2.32.	Polynorbornene- <i>g</i> -PEO and polynorbornene- <i>g</i> -PCL particles prepared by dispersion ROMP for the pH-sensitive release of indomethacin, located at the periphery or within the core of the particles. <sup>158</sup>	53
Figure 2.33.	Biomaterials for the pH-sensitive delivery of antibiotic molecules. <sup>159, 160</sup>	54
Figure 3.1.	Initiating systems for the anionic ring-opening polymerization of glycidol: (A) Strong bases; (B) Deprotonating agents.	57
Figure 3.2.	Synthesis of "pom-pom like" structures by sequential generation copolymerization of glycidol acetal and ethylene oxide (Adapted from Dworak <i>et al.</i> ). <sup>12</sup>	60
Figure 3.3.	Examples of functional initiators for the anionic polymerization of glycidol.	61
Figure 3.4.	Strategies for the synthesis of polyglycidol-based macromonomers.	62
Figure 3.5.	<sup>1</sup> H NMR spectrum for glycidol acetal.	67
Figure 3.6.	<sup>1</sup> H NMR spectrum for $\alpha$ -norbornenyl-poly(glycidol acetal) macromonomer (1a) in CDCl <sub>3</sub> (DP <sub>n,Th</sub> = 25).	70
Figure 3.7.	SEC profiles for $\alpha$ -norbornenyl-poly(glycidol acetal) macromonomers (1a-c) in THF.	71
Figure 3.8.	MALDI-ToF of macromonomer (1a).	71
Figure 3.9.	<sup>1</sup> H NMR spectrum for $\alpha$ -norbornenyl-polyglycidol macromonomer (2a; DP <sub>n,NMR</sub> = 25) in D <sub>2</sub> O.	73

Figure 3.10.	SEC trace for the $\alpha$ -norbornenyl-polyglycidol macromonomer (2a) in DMF..	73
Figure 3.11.	$^1\text{H}$ NMR spectra in DMSO- $d_6$ for acetaldehyde diethyl acetal-functionalized $\alpha$ -norbornenyl-polyglycidol macromonomer (3c) versus amount of bromoacetal added.....	76
Figure 3.12.	SEC profile for (3a) with optimized yield. ....	78
Figure 3.13.	IR spectrum for macromonomer (4c). ....	82
Figure 3.14.	$^1\text{H}$ NMR spectrum for dodecylamine-functionalized macromonomer (4c). ....	83
Figure 3.15.	$^1\text{H}$ NMR spectrum for dodecylamine-functionalized $\alpha$ -norbornenyl-polyglycidol macromonomer (4a) (Solvent: $\text{CDCl}_3$ ; TEA: triethylamine).....	87
Figure 3.16.	SEC trace in THF for dodecylamine-functionalized $\alpha$ -norbornenyl-polyglycidol macromonomer (4a). ....	87
Figure 4.1.	Polyglycidol-based particles by crosslinking cinnamyl groups coupled with PEG- <i>b</i> -polyglycidol micelles. <sup>9</sup> .....	93
Figure 4.2.	Crosslinking reaction between the hydroxyl functions of polyglycidol and titanium tetraisopropoxide to form PS- <i>b</i> -polyglycidol particles. <sup>10</sup> .....	93
Figure 4.3.	Preparation of polyglycidol particles by ink jet deposition of allyl-functionalized polymer solution and crosslinking into spherical networks. <sup>14</sup> ..	95
Figure 4.4.	Polyglycidol-functionalized $\text{Fe}_3\text{O}_4$ particles for combined hyperthermia, drug-delivery and bioimaging applications. <sup>16</sup> .....	96
Figure 4.5.	$^1\text{H}$ NMR spectrum for polynorbornene- <i>g</i> -polyglycidol (5b) in $\text{CDCl}_3$ . ....	102
Figure 4.6.	Size distributions for polynorbornene- <i>g</i> -polyglycidol particles (5a-c) measured by DLS. (A): in ethanol/dichloromethane (65:35 v/v); (B) in water. ....	103
Figure 4.7.	Observation of polynorbornene- <i>g</i> -polyglycidol particles (5a) by TEM. ....	103
Figure 4.8.	IR spectrum for dodecylamine-functionalized polynorbornene- <i>g</i> -polyglycidol particles. ....	106
Figure 4.9.	(A) Size distribution for dodecylamine-functionalized particles measured by DLS in EtOH/ $\text{CH}_2\text{Cl}_2$ (65/35 v/v); (B) TEM imaging of the particles. ....	108
Figure 5.1.	Examples of synthesized biocides. (A) Benzalkonium derivatives, <sup>13</sup> (B) pyridylalkonium derivatives, <sup>14</sup> (C) glycosylamine derivatives. <sup>25</sup> .....	116
Figure 5.2.	$^1\text{H}$ NMR spectrum for free dodecylamine in ethanol- $d_6$ . ....	120
Figure 5.3.	Release of dodecylamine from the macromonomer by cleavage of the imine bond. (A) Observation by $^1\text{H}$ NMR spectroscopy, (B) release profile as a function of pH. ....	122
Figure 5.4.	<i>H. Resinae</i> growth on (a) PDA medium, (b) Czapek-Dox Agar medium after 7 days at 25°C. ....	123



Figure 5.5.	Droplet test against <i>H. resinae</i> on Czapek-Dox agar medium ( $10^6$ spores mL <sup>-1</sup> ): (a) Distribution of the droplet concentrations for plates (b-d); (b) Test with free dodecylamine; (c) Test with norbornenyl-polyglycidol macromonomer; (d) Test with dodecylamine-functionalized macromonomer; (e) Distribution of the droplet concentrations for plates (f-h); (f) Test with free dodecylamine; (g) Test with norbornenyl-polyglycidol macromonomer; (h) Test with dodecylamine-functionalized macromonomer. ....	124
Figure 5.6.	DLS observation of the particles (A-B) ultrafiltered in ethanol, and (C-D) transferred into DMSO by lyophilisation. (A and C) non-functionalized particles; (B and D) dodecylamine-functionalized particles. ....	127
Figure 5.7.	Droplet test with particle dispersions against <i>H. resinae</i> on PDA medium ( $10^5$ spores mL <sup>-1</sup> ): (a) Distribution of the droplet concentrations for plates (b-d); (b) Test with free dodecylamine; (c) Test with polynorbornene-g-polyglycidol particles; (d) Test with dodecylamine-functionalized particles. ....	128
Figure 5.8.	Droplet test against <i>H. resinae</i> on PDA medium ( $10^4$ spores mL <sup>-1</sup> ): (a) Distribution of the droplet concentrations for plates (b-d); (b) Test with free dodecylamine; (c) Test with polynorbornene-g-polyglycidol particles; (d) Test with dodecylamine-functionalized particles. ....	129
Figure 5.9.	Droplet test against <i>H. resinae</i> on Czapek-Dox agar medium ( $10^5$ spores mL <sup>-1</sup> ): (a) Distribution of the droplet concentrations for plates (b-d); (b) Test with free dodecylamine; (c) Test with polynorbornene-g-polyglycidol particles; (d) Test with dodecylamine-functionalized particles. ....	130
Figure 5.10.	Surface of glass plates after 10 depositions of 90 $\mu$ L by spin-coating: (A) Non-functionalized particles, (B) dodecylamine-functionalized particles. ....	132
Figure 5.11.	AFM imaging of the polynorbornene-g-polyglycidol particle films. Top: single-deposition films; bottom: multi-deposition films. Left: height imaging; center: phase imaging; right: 3D height imaging. ....	132
Figure 5.12.	AFM imaging of the dodecylamine-functionalized polynorbornene-g-polyglycidol particle films. Top: single-deposition films; bottom: multi-deposition films. Left: height imaging; center: phase imaging; right: 3D height imaging. ....	134
Figure 5.13.	Growth of <i>H. resinae</i> in inoculated agar media: (A) PDA medium with $10^4$ spores/Petri dish, (B) PDA medium with $10^3$ spores/Petri dish, (C) Czapek-Dox agar with $10^4$ spores/Petri dish, (D) Czapek-Dox agar with $10^5$ spores/Petri dish. ....	137
Figure 5.14.	Particle films tested against <i>H. resinae</i> in PDA medium containing a concentration of $10^3$ spores per Petri dish: (A) Dodecylamine-covered plate, (B) glass plate coated with non-functionalized particles, (C) glass plate coated with dodecylamine-functionalized particles. ....	138
Figure 5.15.	(A) Sanding technique utilized for the aluminum plates; (B) Aluminum plate coated with the VOC 2K K9550 formula. ....	139

Figure 5.16.	Aluminum plates coated with polyurethane resin and (A) non-functionalized particles; (B) dodecylamine-functionalized particles. ....	140
Figure 5.17.	Aluminum plates after neutral salt spray test. Column (1): after 7 days; column (2): after 14 days. Line (A): without particles; line (B): with non-functionalized particles; line(C): with dodecylamine-functionalized particles. ....	141
Figure 5.18.	Aluminum plates tested against <i>H. resinae</i> in PDA medium containing $10^3$ spores per Petri dish. Column (A) coated with resin alone; column (B) coated with resin and non-functionalized particles; column (C) coated with resin and dodecylamine-functionalized particles. Line (1) before neutral salt spray test; line (2) after salt spray test. ....	142
Figure B.1.	Hemocytometer grid (Cells are only counted in the green zones).....	175
Figure C.1.	$^1\text{H}$ NMR spectrum for $\alpha$ -norbornenyl-poly(glycidol acetal) macromonomer (1b) in $\text{CDCl}_3$ ( $\text{DP}_{n,\text{Th}} = 54$ ).....	178
Figure C.2.	$^1\text{H}$ NMR spectrum for $\alpha$ -norbornenyl-poly(glycidol acetal) macromonomer (1b) in $\text{CDCl}_3$ ( $\text{DP}_{n,\text{Th}} = 110$ ).....	178
Figure C.3.	MALDI-ToF spectrum for $\alpha$ -norbornenyl-poly(glycidol acetal) macromonomer (1b) ( $\text{DP}_n = 50$ ).....	179
Figure C.4.	MALDI-ToF spectrum for $\alpha$ -norbornenyl-poly(glycidol acetal) macromonomer (1c) ( $\text{DP}_n = 103$ ).....	179
Figure C.5.	MALDI-ToF mass spectrometry for acetaldehyde diethylacetal-functionalized macromonomer (3a).....	180
Figure C.6.	Profilometry measurements. Column (A): non-functionalized particle films; colomn (B): dodecylamine-functionalized particle films. Line (1): films by single deposition spin-coating; line (2): films by multi deposition spin-coating.....	181

## List of Tables

Table 2.1.	Functional group tolerance of early and late transition metal ROMP catalysts. ....	14
Table 3.1.	Characteristics of the $\alpha$ -norbornenyl-poly(glycidol acetal) macromonomers..	70
Table 3.2.	Characteristics of the $\alpha$ -norbornenyl-polyglycidol macromonomers. ....	72
Table 3.3.	Characteristics of the acetaldehyde diethyl acetal-functionalized $\alpha$ -norbornenyl-polyglycidol macromonomers. ....	77
Table 3.4.	Optimization of the conditions for the preparation of (3a).....	79
Table 3.5.	Characteristics of the macromonomers conjugated with dodecylamine. ....	81
Table 3.6.	Summary of the macromonomers synthesized and their composition. ....	88
Table 4.1.	Z-average diameter and conversion for particles synthesized via dispersion ROM-copolymerization of macromonomers (2a-c) with norbornene.....	104
Table 5.1.	Biocides against <i>H. resinae</i> suggested by Sheridan. <sup>10, 11</sup> .....	115
Table 5.2.	Evaluation of the release of dodecylamine from the functionalized macromonomer as a function of pH (percentage values determined by <sup>1</sup> H NMR). ....	122
Table 5.3.	Inhibition diameter measured for the antifungal properties of dodecylamine and dodecylamine-functionalized macromonomer. ....	125
Table 5.4.	Characteristics of the dodecylamine-functionalized polynorbornene-g-polyglycidol dispersions transferred in DMSO. ....	126
Table 5.5.	Average thickness of polynorbornene-g-polyglycidol particle films (standard deviation calculated from 4 repetitions). ....	135

## List of Schemes

Scheme 2.1.	Generalized ROMP mechanism. ....	11
Scheme 2.2.	Postulated mechanism for the photoredox ROMP of cyclic olefins.....	19
Scheme 3.1.	(A) Transfer reactions leading to the formation of branched species, (B) chain transfer to glycidol acetal. <sup>19</sup> .....	58
Scheme 3.2.	Hydrolysis of $\alpha$ -norbornenyl-poly(glycidol acetal) macromonomers.....	65
Scheme 3.3.	Synthesis of glycidol acetal. ....	67
Scheme 3.4.	Mechanism for the anionic ring-opening polymerization of glycidol acetal....	68
Scheme 3.5.	Functionalization of $\alpha$ -norbornenyl-polyglycidol macromonomers (2) with acetaldehyde diethyl acetal moieties. ....	74
Scheme 3.6.	Dodecylamine functionalization of macromonomer (3c).....	80
Scheme 3.7.	Intermolecular formation of hemiacetal groups under acidic conditions. ....	85
Scheme 3.8.	Synthesis of dodecylamine-functionalized $\alpha$ -norbornenyl-polyglycidol macromonomer (4a).....	85
Scheme 4.1.	Preparation of polynorbornene- <i>g</i> -polyglycidol particles by dispersion ROMP. ....	100
Scheme 4.2.	Preparation of dodecylamine-functionalized polynorbornene- <i>g</i> -polyglycidol particles by dispersion ROMP. ....	105
Scheme 4.3.	Dispersion ROMP of dodecylamine-functionalized macromonomer with the second generation Grubbs catalyst. ....	109

## List of Abbreviations

ADMET	Acyclic diene metathesis
AFM	Atomic force microscopy
AGE	Allyl glycidyl ether
ATRP	Atom transfer radical polymerization
Brij 700	Commercial macromolecular surfactant: C <sub>18</sub> H <sub>37</sub> -(CH <sub>2</sub> -CH <sub>2</sub> O) <sub>100</sub> -H
CM	Cross metathesis
CMC	Critical micelle concentration
DCM	Dichloromethane
DLS	Dynamic light scattering
DMF	N,N-Dimethylformamide
DMSO	Dimethylsulfoxide
DPMK	Dimethylphenyl potassium
DP <sub>n</sub>	Degree of polymerization
DTAB	Dodecyl trimethyl ammonium bromide
DOX	Doxorubicin
GC	Gas chromatography
<i>H. resiniae</i>	<i>Hormoconis resiniae</i>
HVLP	High volume low pressure
IR	Infrared
IUPAC	International Union of Pure and Applied Chemistry
MALDI-ToF	Matrix-assisted laser desorption/ionization time of flight mass spectroscopy
MMA	Methyl methacrylate
MSN	Mesoporous silica nanoparticles
MWCO	Molecular weight cut-off
NHC	N-Heterocyclic carbene
NMR	Nuclear magnetic resonance spectroscopy
PEO	Poly(ethylene oxide)
PEG	Poly(ethylene glycol)
PDSM	2-(2-Pyridyldisulfide)ethyl methacrylate
PMMA	Poly(methyl methacrylate)
PNb- <i>g</i> -PIP- <i>b</i> -PtBA	Polynorbornene- <i>g</i> -polyisoprene- <i>b</i> -poly( <i>tert</i> -butyl acrylate)

PS	Polystyrene
PS- <i>b</i> -PEO	Polystyrene- <i>b</i> -poly(ethylene oxide)
PTX	Paclitaxel
RAFT	Reversible addition-fragmentation chain transfer
RCM	Ring-closing metathesis
REACH	Registration, Evaluation and Authorisation of Chemicals
ROMP	Ring-opening metathesis polymerization
ROP	Ring-opening polymerization
scCO <sub>2</sub>	Supercritical carbon dioxide
SDBS	Sodium dodecylbenzenesulfonate
SDS	Sodium dodecyl sulphate
SEC	Size exclusion chromatography
Si-ATRP	Surface-initiated atom transfer radical polymerization
<i>t</i> -BA	<i>tert</i> -Butyl acrylate
<i>t</i> -BGE	<i>tert</i> -Butyl glycidyl ether
TEM	Transmission electron microscopy
THF	Tetrahydrofuran
UV	Ultraviolet
wt %	Percentage by weight

## List of Symbols

$a$	Number of sub-squares in a hemocytometer grid used for counting
$C_k^i$	Initial concentration of element k
$C_{sp}$	Spore concentration
$\mathfrak{D}$	Molecular weight dispersity
$F_d$	Dilution factor
$I_k$	Integration of element k by $^1\text{H}$ NMR
$M_k$	Molar mass of element k
$M_n$	Number-average molecular weight
$m_k^f$	Measured mass of element k
$m_k^i$	Initial mass of element k
$m_k^{th}$	Theoretical mass of element k
$N_k$	Number of units k
$n_k$	Molar amount of element k
$n_k^i$	Initial molar amount of element k
$n_{sp}$	Number of spores
$\pi_k$	Conversion of element k
$\rho_k$	Density of element k
$T_g$	Glass transition temperature
$v$	Volume of a sub-square
$V_k$	Volume of element k

# **Chapter 1: General Introduction**



## 1.1. Opening Remarks

Microbial contamination is a phenomenon that impacts many sectors of the industry. Various families of microorganisms, among which bacteria, fungi and moulds, represent a major issue in the food, pharmaceutical, or cosmetic and personal care sectors. Less known by the public is the contamination of aircraft fuel tanks by microorganisms. In this particular case, contamination is inevitable because of the simultaneous presence of fuel, whose hydrocarbon-based composition represents an adequate source of nutrients for the microorganisms, and water due to waterproofing defects in fuel storage tanks. Since the water ends up forming a layer at the bottom of the tank, microorganisms begin their development at the interface between the fuel and the water where they can meet all of their needs. The presence of microorganisms can have various severe consequences, as they are capable of degrading the fuel and alter its quality. After reaching a certain stage in their development, they can also affect various parts of the aircraft by travelling through the fuel. Their ability to form dense biofilm structures and to produce organic acids metabolically also causes considerable concern because these compounds can corrode the metallic walls of the fuel storage tanks. Treatment with biocide compounds is the common way of eliminating microorganisms and this represents a global market with an estimated worth of USD 6.4 billion in 2015, expecting to surpass USD 12 billion by 2022.<sup>1</sup> In the case of storage fuel tanks, biocides are dissolved in the fuel phase to prevent growth in the medium. This means that biocides must be added regularly in the tank to prevent microbial growth. Even in the presence of a biocide, water at the bottom of the tank should be drained daily to minimize the risks of contamination. Fuel tanks thus require continuous maintenance and permanent attention because regular sampling of the fuel should be made to check the presence of microorganisms. The interior of fuel tanks is also coated with chromium (VI) compounds, to provide additional biocidal properties to the walls and to inhibit chemical corrosion by the organic acids. Indeed, chromium is used for

passivation of the walls due to its reaction with oxygen and the creation of a protective layer. However, chromium was recently targeted by the European legislation REACh (Registration, Evaluation and Authorization of Chemicals) because of its carcinogenic effects and is planned to be forbidden from most of its current uses by the end of 2017. Efforts have thus focused on trying to find alternatives for chromium, with biocides having less toxicity towards humans to prevent microbial corrosion in fuel tanks. For this type of use, functionalized polymers can be a relevant choice as they offer the possibility to immobilize active molecules on their backbone. One can also take advantage of the production of organic acids to trigger a release of the biocide due to a decrease in pH. The combination of a polymer and a biocide through a pH-sensitive bond would enable the release of the active molecule into the fuel as a result of a remote trigger. This type of system would no longer need to be dissolved directly in the fuel and could thus be isolated on the tank walls without the need for regular additions.

## **1.2. Research Objectives and Thesis Outline**

The main objective of this Thesis work was to prepare a system of polymeric particles functionalized with a biocide, capable of delivering its active molecules when the medium becomes acidic. These particles could potentially be incorporated in a polymer-based coating and isolated on the walls of the tank for passive action against microbial-induced corrosion. The particles were synthesized by dispersion ring-opening metathesis polymerization (ROMP) of polyglycidol-based reactive surfactants, otherwise called macromonomers. A polyglycidol backbone was chosen because of its potential for multifunctionalization through the hydroxyl groups on each repeat unit. Dodecylamine, a chemical compound with proven antifungal properties and not targeted by the REACh legislation, was selected as biocide and conjugated to the macromonomer before its polymerization through its primary amine group to form a pH-sensitive imine bond. The synthesized particles were tested for their

microbiocidal activity against *Hormoconis resinae*, a fungus often encountered in fuel tanks that generates an acidic environment during its development.

This Thesis is divided into five Chapters. After this brief Foreword, the **second Chapter** consists in a literature review of the development of the ROMP reaction, and of the various techniques to prepare particles through ROMP in dispersed media or the self-assembly of copolymers synthesized by ROMP. In the case of dispersed media ROMP, the review clearly separates examples using non-reactive surfactants and reactive surfactants. In a second part, the review details various options for the synthesis of pH-sensitive bonds and their utilization for the conjugation between polymeric particles and active molecules in the prospect of achieving the pH-sensitive drug delivery of bioactive compounds.

The **third Chapter** of this Thesis reports the details on the synthesis and characterization of norbornene-functionalized linear polyglycidol macromonomers as multifunctional substrates for the immobilization of a biocide. Functionalization of the macromonomer and the formation of a pH-sensitive imine bond with dodecylamine are also discussed.

The **fourth Chapter** details the use of the macromonomers synthesized in the preparation of novel core-shell polynorbornene-g-polyglycidol particles by dispersion ROMP using metathesis of the active norbornene terminal groups. The versatility of this technique enabled the use of the biocide-multifunctionalized macromonomer without changes in the experimental method to give rise to highly functionalized biocide particles. Chemical and colloidal aspects of the latexes obtained are discussed.

In the **fifth Chapter**, testing of the biocide-functionalized macromonomer and particles for antifungal activity against the fuel fungus *Hormoconis resinae* is discussed. First, the release of dodecylamine by cleavage of the imine bond was confirmed by molecular analysis. Then, microbiology methods were implemented to demonstrate the bioactivity of the system. The

final goal of the project was to devise an antimicrobial coating for the aircraft industry. An attempt at incorporating the biocide-functionalized particles in a commercial coating under the guidance of members from the Bordeaux-based company Rescoll was performed.

The **final Chapter** of this Thesis summarizes the main conclusions drawn from the work presented in the previous Chapters, and discusses perspectives for future work on this topic.

**Chapter 2: Bibliography –  
Synthesis of Functional Particles  
by ROMP**

The ring-opening metathesis polymerization (ROMP) technique has emerged over the past decades as a powerful method for the creation of carbon-carbon double bonds. The reaction of a metal carbene initiator with a strained cyclic olefin leads to its polymerization through opening of the ring. Progress in understanding of the mechanism and the development of well-defined initiators allowed the preparation of materials with various functional groups. The field of particle synthesis by ROMP also emerged from this trend. Polymer particles can be obtained by the self-assembly of block copolymers synthesized by ROMP, or directly by ROMP in dispersed media. Stabilization of the particles can be achieved either with non-reactive or reactive surfactants. Reactive surfactants enable covalent anchoring of the stabilizer, thus preventing their desorption from the particles. By careful design, functionalization of the surfactant becomes possible, and with it the formation of functionalized particles. Among numerous possibilities for functionalization, the use of pH-sensitive bonds is an interesting option since pH variations are often encountered in the human body to signal a malfunction requiring treatment. Functionalization with adequate active molecules via pH-sensitive bonds is perfectly compatible with ROMP, to prepare polymer particles finding applications as systems for the delivery of drugs and other bioactive molecules.

## **2.1. General Concepts of Ring-Opening Metathesis Polymerization (ROMP)**

In chemistry, the term metathesis refers to the exchange of atoms between two molecules. In the specific case of olefins, it refers to a reaction which implies the exchange of unsaturated carbon atoms between two olefin reactants. This reaction includes several variations. Ring-Closing Metathesis (RCM), Ring-Opening Metathesis (ROM), and Cross Metathesis (CM) reactions all involve two molecules, while Ring-Opening Metathesis Polymerization (ROMP) and Acyclic Diene METathesis (ADMET) reactions lead to the formation of polymers (Figure

2.1). These reactions are catalyzed by organometallic compounds and are potentially reversible. The field of olefin metathesis is growing rapidly and has seen three researchers rewarded with the Nobel Prize in chemistry in 2005: Yves Chauvin from France for the understanding of the mechanism, and Robert H. Grubbs and Richard R. Schrock from the United States for their pivotal contributions in organometallic metathesis catalysts.

Among the different metathesis reactions, ROMP is the process that has attracted the most attention. This chain-growth polymerization process involves the reaction of cyclic olefins to form polyalkenamers. The reaction is driven by the release of ring strain, thus the more strained the cyclic olefins are, the more easily they can polymerize. For less strained monomers, the reaction can be reversible.<sup>1</sup> Some well-defined catalysts can promote controlled/living ROMP conditions and offer a wide range of opportunities in the field of macromolecular engineering, although the reaction of unsaturation sites in the polymer backbone can compete with cyclic olefin addition in the case of very active catalysts. These secondary reactions are referred to as backbiting and cross-metathesis for intrachain and interchain reactions, respectively, and are the main causes for loss of control in the ROMP process (Figure 2.2).

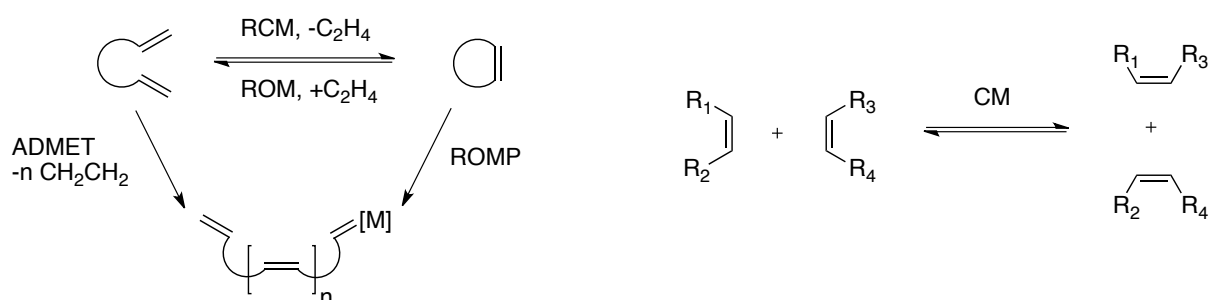


**Figure 2.1. Variations of the metathesis reaction.**

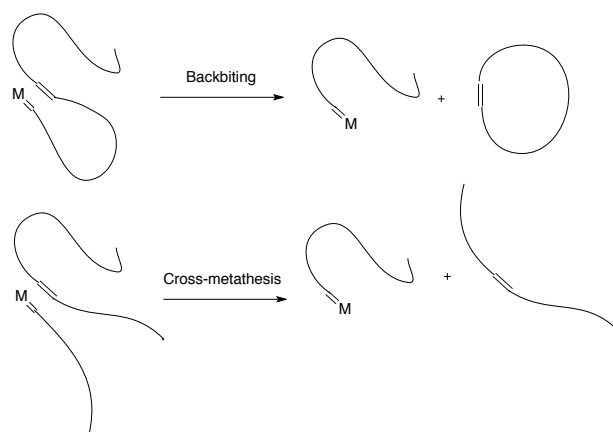


**Figure 2.2. Secondary ROMP mechanisms.**

### 2.1.1. Discovery of Olefin Metathesis Polymerization

The first ROMP reaction of norbornene and alkyl- or phenyl-substituted norbornenes was reported by researchers at DuPont in the mid-1950s.<sup>2,3</sup> The polymerization was catalyzed by the  $\text{TiCl}_4$  Ziegler-Natta catalyst with ethylmagnesium bromide as reducing agent. The reaction was first thought to take place as a regular Ziegler-Natta reaction, by complexation between the metal with a valence state of +2 and the unsaturated monomer.<sup>3</sup> No statement was made about opening of the norbornene ring, nor about the final structure of the polymer. Two years later, using a similar polymerization procedure with norbornene, Montague identified the formation of an unsaturated polymer chain consisting of cyclopentane rings.<sup>4</sup> The reaction was postulated to occur *via* coordination of the norbornene unsaturation with the metal center, and rearrangement to obtain an active site at the end of the propagating chain (Figure 2.3). Polynorbornene samples with different molecular weights were synthesized by varying the monomer to catalyst ratio. Eleuterio largely extended the scope of monomers utilized in a 1963 US patent, and various high molecular weight polyalkenamers were synthesized with catalysts derived from the group 6 metals.<sup>5</sup> A study by nuclear magnetic resonance spectroscopy (NMR) of the polymers confirmed the ring-opening hypothesis.<sup>6</sup> In



the meantime, teams at Standard Oil and Phillips Petroleum described the “disproportionation” of propylene into ethylene and *n*-butene isomers with molybdenum oxides supported on alumina, in what was the first example of linear olefin metathesis (Figure 2.4).<sup>7, 8</sup> *A priori* these reactions seemed unrelated, but in 1967 Calderon at Goodyear unified these two reactions, acknowledging the exchange of substituents in one unique process under the name *olefin metathesis*.<sup>9</sup> Using tungsten complexes, Chauvin<sup>9</sup> proposed a mechanism for the reaction that complied with the experimental observations.<sup>10</sup> The active centers for the polymerization were identified to be metal carbenes that could form a “metallacyclobutane” intermediate by coordination with a free olefin. Katz then managed to induce the polymerization of several cycloolefins with a single Fischer-type tungsten metal carbene compound (**1** in Figure 2.5).<sup>11-13</sup> In this way, the same metal carbene was shown to participate in both the initiation and the propagation steps of the polymerization process. The same complexes were used by Casey to help confirm the existence of a metallacyclobutane intermediate, and to gather insight on the selectivity of the reaction.<sup>14, 15</sup>

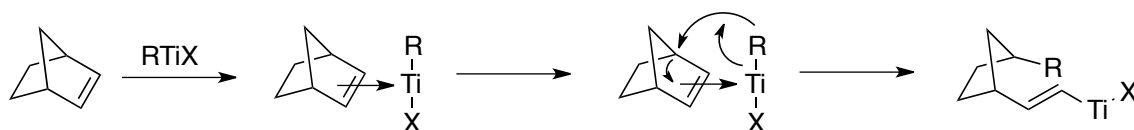


**Figure 2.3. Proposed ROMP mechanism for Ziegler-Natta catalysts.<sup>5</sup>**

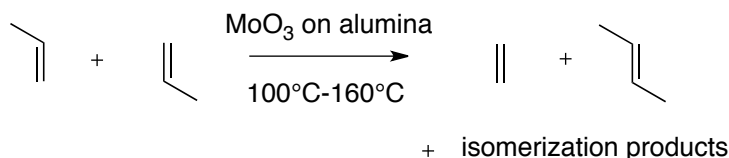
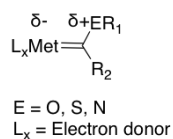
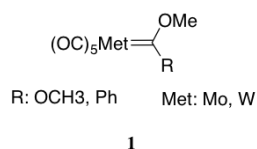


**Figure 2.4. Disproportionation reaction of propylene: First example of linear olefin metathesis.**

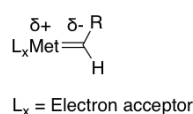
### Metal carbene complexes



### Examples



### Metal alkylidene complexes



### Examples

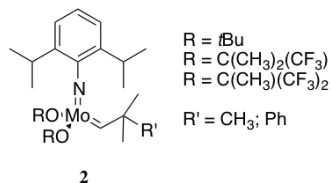
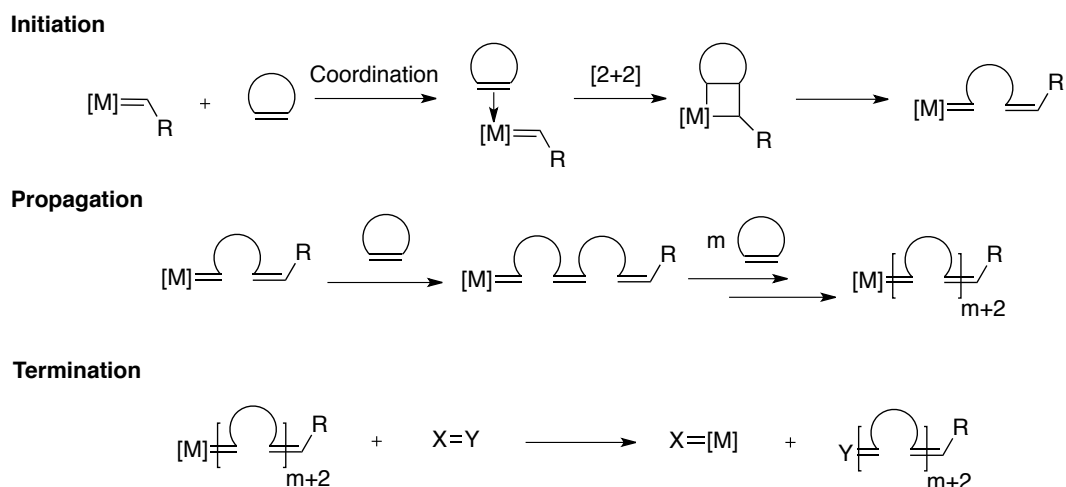


**Figure 2.5. Early transition metal-based metathesis catalysts.**

## 2.1.2. Mechanism

The mechanism of the ROMP reaction consists in a series of steps that apply to initiation as well as to propagation (Scheme 2.1). The first step is coordination of the free olefin with the unoccupied orbital of the metal center. Insertion of the olefin then leads to the formation of a metallacyclobutane intermediate. Subsequent cleavage of the bonds yields the metathesis products with recovery of the metal carbene bond as the active chain-end, and the last polymerized unit in the next position.



**Scheme 2.1. Generalized ROMP mechanism.**

### 2.1.3. Development of ROMP Catalysts

Promoting and controlling the metathesis reaction through catalyst design has been a challenge since the discovery of the ROMP process. Before recognition of the mechanism the mode of action of the catalyst and the importance of the metal carbene entity were not identified, thereby preventing major advances in key aspects of these compounds. It was nevertheless understood that the metathesis reaction involved a transition metal center. The goal of this review does not lie in the comprehensive coverage of all the metathesis catalyst systems developed over the past 65 years, but rather to focus on relevant examples of cycloolefin ROMP in organic and aqueous media. A distinction will be made between two families of catalysts however, namely ill-defined and well-defined catalysts.

#### 2.1.3.1. Ill-Defined Metathesis Catalysts

Various transition metals can be used for the ROMP of cycloolefins. Simple Ziegler-Natta catalysts of  $\text{TiCl}_4$  in combination with  $\text{Al}(\text{C}_2\text{H}_5)_3$  were found to open the cyclobutene ring and afford poly(1,4-butadiene) in high yield. Unfortunately, this catalyst also promoted a second addition mechanism leading to the formation of polycyclobutane along with poly(1,4-butadiene).<sup>16</sup> Other homogeneous catalysts such as  $\text{MoCl}_5$  or  $\text{WCl}_6$  only promoted the polymerization to pure polyalkenamers with modest conversions.<sup>17-19</sup> Other types of initiators based on  $\text{WCl}_6/\text{SnBu}_4$ ,  $\text{WOCl}_4/\text{EtAlCl}_2$ ,  $\text{MoO}_3/\text{SiO}_2$  or  $\text{Re}_2\text{O}_7$  were also found to promote the ROMP of cycloolefins. However the need for a strong Lewis acid to activate the catalyst led to limited tolerance towards functional groups and protic solvents. The lack of control over the activity and the number of active centers present in the reaction also limited their use.<sup>20, 21</sup> Water-soluble, ill-defined complexes were reported by Michelotti and Keaveney for the polymerization of norbornene.<sup>22</sup> The polymerization was conducted in anhydrous ethanol and in 95% ethanol using trichloride hydrates of ruthenium, osmium and iridium as catalysts, even at room temperature. However monomer conversion was incomplete, presumably because of

the heterogeneous reaction conditions used. It was only about 20 years later that the group of Grubbs reported the ROMP of ethoxy- and carboximide-functionalized 7-oxanorbornenes occurring in near quantitative yields in purely aqueous media. The  $\text{Ru}^{\text{II}}(\text{H}_2\text{O})_6(\text{tos})_2$  (tos = *p*-toluenesulfonate) ruthenium sulfonate salt still needed to be activated by heating, and the oxanorbornene derivatives polymerized to very high molecular weights, but with little control ( $\mathcal{D} > 1.7$ , where  $\mathcal{D}$  is the molar mass dispersity).<sup>23, 24</sup>

### 2.1.3.2. Well-Defined Catalysts

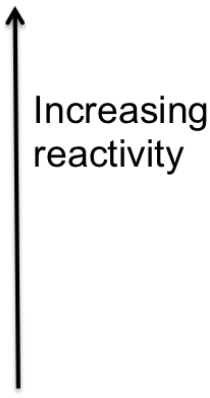
The metathesis mechanism could be further clarified through the use of well-defined catalysts, which enabled the characterization of the initiating and propagating species. The metal carbene moiety was thus identified as a key component in the reaction, and subsequent challenges consisted in preparing single component, active catalyst compounds. As mentioned previously, the first well-defined tungsten carbene complexes were synthesized by Fisher and Casey and later utilized for the ROMP of norbornene and other strained cycloolefins in the mid-1970s, yielding rather broad molecular weight distributions ( $\mathcal{D} > 1.85$ ; **1** in Figure 2.5).<sup>13-15</sup> Schrock used high oxidation state, early transition metal-based complexes to initiate metathesis reactions. The structure for such complexes typically consisted in a combination of two alkoxides and one imido ligand (**2** in Figure 2.5). The tolerance towards functional groups, oxygen or water, activity, selectivity towards free olefins, and livingness of the reaction could be tuned through variations in the metal (tungsten or molybdenum) and the ligands.<sup>25, 26</sup>

### 2.1.3.3. Ruthenium-Based Catalysts

Various transition metals have been tested for metathesis reactions. Early transition metal catalysts offer a very high activity, but at the expense of a lower tolerance to ambient conditions and functional groups. On the other side, late transition metals, and particularly

ruthenium, are much more tolerant towards functional groups, as shown in Table 2.1. Ruthenium-based catalysts thus favor the coordination to olefins rather than acids, alcohols or water, which makes these catalysts more user-friendly.

**Table 2.1. Functional group tolerance of early and late transition metal ROMP catalysts.**

<b>Titanium</b>	<b>Tungsten</b>	<b>Molybdenum</b>	<b>Ruthenium</b>	
Acids	Acids	Acids	<u>Olefins</u>	
Alcohols, Water	Alcohols, Water	Alcohols, Water	Acids	
Aldehydes	Aldehydes	Aldehydes	Alcohols, Water	
Ketones	Ketones	<u>Olefins</u>	Aldehydes	
Esters, Amides	<u>Olefins</u>	Ketones	Ketones	
<u>Olefins</u>	Esters, Amides	Esters, Amides	Esters, Amide	

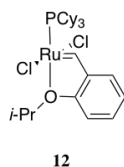
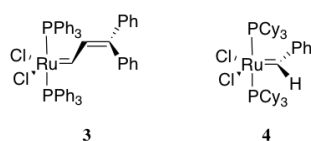
The “SonBinh catalyst” **3** (Figure 2.6) is the first well-defined ruthenium carbene complex, synthesized by the reaction of  $\text{RuCl}_2(\text{PPh}_3)_3$  and 3,3-diphenylcyclopropene. It polymerizes strained cycloolefins in organic solvents, but also in the presence of protic solvents, and has amazing tolerance to water and oxygen.<sup>27</sup> When the phosphine ligands are exchanged with more electron-donating tricyclohexylphosphine, the catalyst can even polymerize less strained olefins while keeping its high tolerance.<sup>28</sup> Unfortunately, this class of catalyst cannot be synthesized on a large scale. The reaction of diazoalkanes with  $\text{RuCl}_2(\text{PPh}_3)_3$  provided another series of well-defined catalysts that were more easily accessible. After phosphine ligand exchange, catalyst **4** displayed a high activity and polymerized hydrophobic norbornene and hydrophilic oxanorbornene derivatives in a living fashion, even in the presence of water, and yielded polycyclooctene or polycyclooctadiene with the lowest  $\bar{M}_n$

recorded thus far.<sup>29-31</sup> This family of complexes was the first generation of Grubbs metathesis catalysts.

The group of Herrmann started utilizing N-Heterocyclic carbenes (NHC) as ligands for ruthenium-based metathesis catalysts.<sup>32, 33</sup> Substitution of both or one of the phosphine ligands to obtain **5** and **6**, respectively, led to increased initiation rates and higher conversions in ROMP of the less strained cyclooctene. Grubbs exploited the lower dissociation energy of the phosphine ligands, in combination with the high activity offered by the NHC ligands, and synthesized complexes **7** and **8**.<sup>34, 35</sup> The latter is more active than **4** for the ROMP of a variety of strained, less strained and sterically hindered cycloolefins,<sup>36</sup> and is commonly known as the second-generation Grubbs metathesis catalyst. However the initiation rate of **8** is significantly lower than for its first-generation counterpart **4**.<sup>37</sup> The very fast-initiating catalysts **9** – **11** were synthesized by exchange of ligands between the second phosphine ligand and pyridine-based ligands.<sup>38</sup> Using catalyst **10** homopolymers, diblock and triblock copolymers were obtained with comparatively narrower molecular weight distributions than with catalyst **4**.<sup>39</sup> This catalyst also displayed remarkable activity for a wide range of monomers.

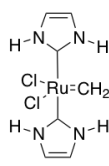
In parallel, the group of Hoveyda developed another popular generation of well-defined catalysts **12** and **13**, by replacing a tricyclohexylphosphine group of the Grubbs first- and second-generation catalysts with a chelating isopropoxyphenylmethylene ligand.<sup>40, 41</sup> Commonly referred to as Hoveyda-Grubbs first- and second-generation catalysts, these complexes display a high activity, recyclability, and unprecedented thermal stability.

## First-generation catalysts

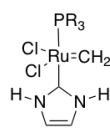


12

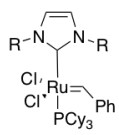
## Second-generation catalysts



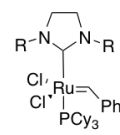
5



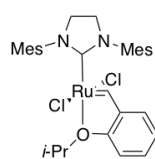
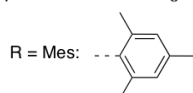
6



7

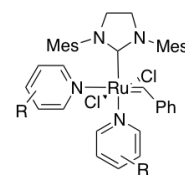


8



13

## Third-generation catalysts



9 (R = H)  
10 (R = 3-Br)  
11 (R = 4-Ph)

**Figure 2.6. Well-defined ruthenium catalysts.**

In view of promoting living polymerization in aqueous solutions, the catalyst system, even if well-defined, needs to be soluble in water/organic solvent mixtures or in water.<sup>31</sup> Indeed, low solubility leads to a low initiation efficiency because of the heterogeneity of the reaction, causing overall loss of control over the polymerization. A first approach to address this issue was to synthesize water-soluble catalysts with ionic ligands. Water-soluble complexes **14** – **19** were prepared by ligand exchange with either cationic<sup>42-44</sup> or anionic<sup>45, 46</sup> phosphines (Figure 2.7). Catalysts **14** and **15** promoted the first living ROMP of norbornene and 7-oxanorbornene derivatives in purely aqueous media, yielding homopolymers with dispersities lower than 1.24. Block copolymers could also be synthesized with complete conversion of the monomers.<sup>47</sup> These complexes are unfortunately prone to oxidative decomposition and must be handled in rigorously degassed solutions. Several other attempts were made to synthesize water-soluble ruthenium compounds by grafting poly(ethylene glycol) (PEG) chains on

commercial complexes. The chain can be either grafted on the NHC (**20** and **21**)<sup>48, 49</sup> or the pyridine ligands (**22** and **23**).<sup>45, 50</sup>

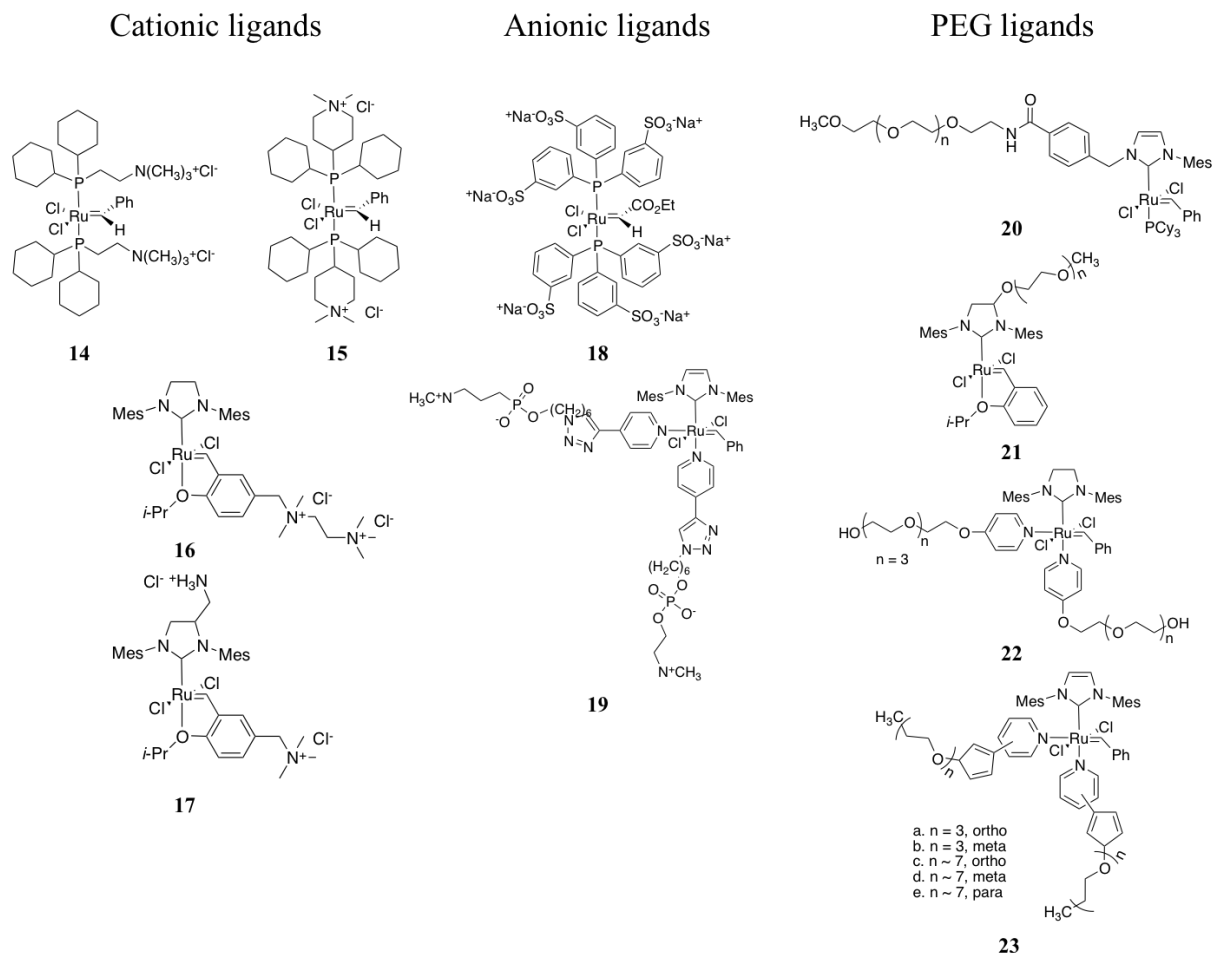


**Figure 2.7. Water-soluble ruthenium catalysts.**

Over a time span of 50 years and thanks to the work of many research teams over the world, ROMP has become a strong asset for the synthesis of polymers. Understanding the mechanism enabled the synthesis of a library of well-defined catalysts presenting advantages in terms of activity, control of the reaction, functional group tolerance or stability. In the application of ROMP to strained olefins, this provides a number of options for macromolecular engineering with the synthesis of star polymers, diblock or bottle-brush copolymers, or the synthesis of particles under different conditions.



#### 2.1.3.4. Metal-Free ROMP

While ruthenium catalysts are very efficient for the ROMP of strained and less strained cyclic olefins, traces of these compounds may contaminate the products. This can be problematic in the case of biomaterials synthesized by this technique. Very recently, efforts have been made into ways to recreate the ROMP mechanism without organometallic compounds. The team of Boydston thus developed a system composed of a vinyl ether initiator (**24** – **26**, Figure 2.8) and a photoredox mediator **27**. Because the active metal carbene center is absent in this technique, the mechanism differs from the classical ROMP reaction.<sup>51</sup> Initiation is performed by irradiation with blue LED light, which transfers an electron from the initiator to the mediator to form an activated radical cation (B, Scheme 2.2). The reaction of this compound with the cycloolefin yields a cyclobutane intermediate C. Because this reaction is also driven by the release of ring strain, compound D results from opening of the cycle. This propagation mechanism may continue until all the monomer is consumed. By this technique, norbornene was polymerized to over 50% conversion. The molecular weights obtained, in the range  $7\text{--}60\times 10^3\text{ g}\cdot\text{mol}^{-1}$ , were close to the expected values and could be controlled by varying the initiator to monomer ratio in the reaction. The redox state of the polymerization site was found to be reversible between an active and a dormant state, due to a dynamic equilibrium with the mediator. The authors also realized that the reaction could be terminated and reinitiated by switching the LED light source off and on. The reaction was extremely sensitive to water but resistant to oxygen. Functional monomers including silanes, chloro or alcohol functionalities, ether, ester or silyl ether protecting groups could be copolymerized with norbornene, but with varying success with respect to the target compositions.<sup>52</sup> The polymerization of *endo*-dicyclopentadiene (Figure 2.8) only proceeded with conversions below 20% and low molecular weight products, associated with intramolecular reactivity between both unsaturations of the monomer.<sup>53</sup> The results were improved by

copolymerization with a small amount of norbornene. The linear polymers could then be crosslinked through a thiol-ene click reaction between a dithiol and the cyclopentadiene moieties to form gels.

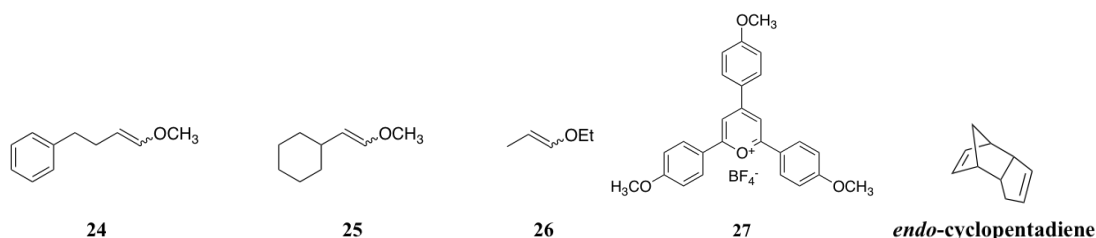
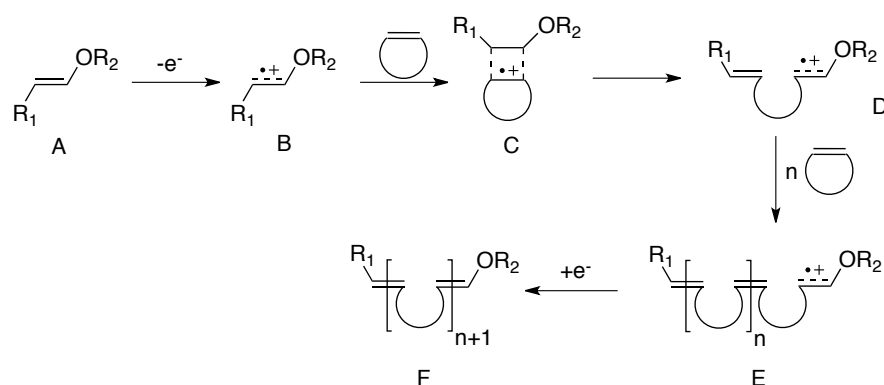


**Figure 2.8. Key components in the metal-free ROMP system: initiators 24-26; photoredox mediator 27; *endo*-cyclopentadiene monomer.**



**Scheme 2.2. Postulated mechanism for the photoredox ROMP of cyclic olefins.**

## 2.2. Particles by Self-Assembly of ROMP Copolymers

Self-assembly processes consist in the spontaneous organization of individual components in solution. The discovery of Grubbs-type ruthenium initiators, with fast initiation kinetics and enhanced functional group tolerance, enabled the synthesis of block copolymers with controlled compositions. The self-assembly of these copolymers into micelles soon became a logical choice for the synthesis of nanoparticles.

The terms “micelle” and “particle” are often utilized interchangeably to identify the same objects in the context of the self-assembly of block copolymers, but in this review we will distinguish between these two designations: A polymer micelle is strictly defined as the product of the self-assembly of amphiphilic block copolymer chains above their critical micelle concentration (CMC) in a poor or bad solvent for one of the blocks. The stability of these objects is mainly due to the presence of the selective solvent and the polymer concentration used. Polymer particles may be derived from micelles, but with further stabilization provided in the form of interchain interactions or covalent bonds. Changes in solvency conditions do not destabilize these particles. The focus of this section is on particles formed by the self-assembly of copolymers obtained by ROMP, and then further stabilized to hinder disassembly.

### **2.2.1. Core-Crosslinked Particles**

Monomers containing crosslinkable functions can be copolymerized as reactive blocks by ROMP. With careful choice of the solvent, these copolymers can self-assemble into micelles with the crosslinkable groups in the core. *Post*-assembly reaction of these groups enables crosslinking of the micelles into core-stabilized particles. Triblock copolymers were thus synthesized using hydrophilic oligoethylene glycol ester, more hydrophobic methyl ester and undecyl cinnamate derivatives of norbornenecarboxylic acid. The self-assembly and crosslinking were performed in methanol, a good solvent for the hydrophilic block. The use of a cinnamic acid-functionalized norbornene derivative enabled fast [2 + 2] cycloaddition by ultraviolet (UV) irradiation to induce crosslinking of the micelle cores.<sup>54</sup> The crosslinked particles thus remained stable in chloroform (CHCl<sub>3</sub>), a good solvent for both blocks, with diameters varying from 45 to 90 nm as the weight fraction of the hydrophobic block in the copolymers increased. The team of Xie performed a similar synthesis as a one-pot process in toluene by sequential addition of a bis-bromoisobutyl norbornene derivative and cinnamic

acid-functionalized oxanorbornene dicarboximide, with or without further addition of a bis-methyl ester oxanorbornene monomer.<sup>55</sup> The use of toluene as a selective solvent isolated the more hydrophilic oxanorbornene units in the core of the micelles, while the brominated units remained available on the surface for further functionalization. Crosslinking by UV irradiation was thus limited to the core and particles with diameters between 100-190 nm were obtained, and of larger diameters for shorter hydrophilic blocks. The team of Grubbs used a similar crosslinkable cinnamyl norbornene derivative along with a PEG-functionalized norbornene to form core-crosslinked particles in water, which were then functionalized with <sup>18</sup>F for application as imaging agent for cancerous tissues.<sup>56</sup> The diameters obtained varied from 47 to 142 nm as the molecular weight for the copolymers increased. The team of Wooley used brush polymers synthesized by ROMP of an alkoxyamine-functionalized norbornene monomer, followed by sequential nitroxide-mediated polymerization (NMP) of isoprene and *tert*-Butyl acrylate (t-BA, PNB-*g*-PIP-*b*-PtBA). The much higher degree of polymerization of the polynorbornene backbone as compared to the side chains led to cylindrical brush-like morphologies.<sup>57</sup> Crosslinking of the inner polyisoprene segments with sulphur chloride (S<sub>2</sub>Cl<sub>2</sub>) was then carried out to obtain 59 × 2.1 nm<sup>2</sup> soft-core hard-shell cylinders (Figure 2.9).

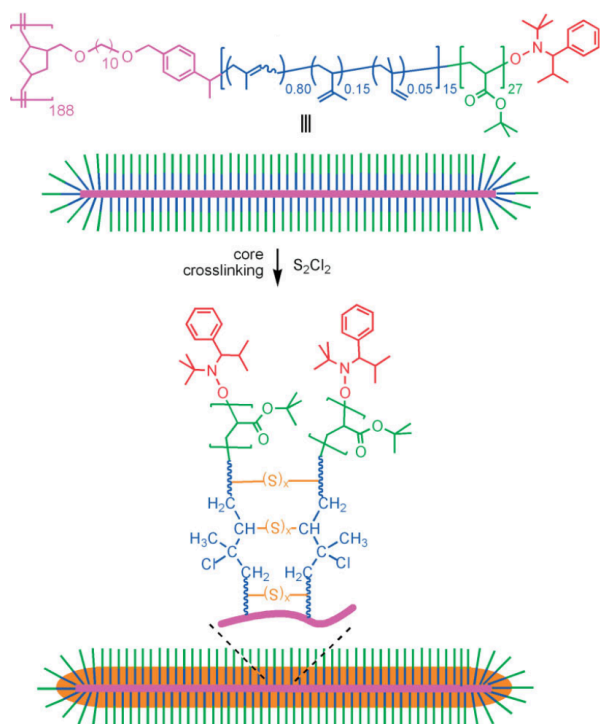


**Figure 2.9. Synthesis of core-crosslinked cylindrical particles via tandem ROMP/NMP.<sup>57</sup>**

### 2.2.2. Shell-Crosslinked Particles

In contrast to the preceding section, the crosslinkable groups of the block copolymers can be placed at the periphery of the micelles under appropriate solvency conditions. Triggering the crosslinking reaction after the formation of these micelles leads to shell-stabilized particles. PEG-grafted polyoctenamers were thus synthesized by ROM-copolymerization of cyclooctene with PEG-functionalized cyclooctene, and were allowed to self-assemble at the interface of toluene droplets in water. The addition of a PEG-grafted bis-cyclooctene monomer and reaction by ring-opening cross-metathesis with the intrachain unsaturation sites yielded 30  $\mu\text{m}$  crosslinked hollow microcapsules, useful for the encapsulation of hydrophobic drug molecules.<sup>58, 59</sup> Hollow capsules were also obtained by modifying the bromine-functionalized micelles synthesized by Xie<sup>55</sup> (described above) to polymerize 4-(3-butenyl)styrene by Atom Transfer Radical Polymerization (ATRP) on their surface. UV-

induced shell-crosslinking by Ring Closing Metathesis of the pendant olefin groups, and removal of the core by hydrolysis of the ester bonds from the hydrophilic monomer yielded 112 nm capsules in  $\text{CHCl}_3$ .<sup>60</sup> The t-BA units of the PNB-*g*-PIP-*b*-PtBA cylinders described previously were also hydrolyzed to allow shell-crosslinking with a diamino compound.<sup>61</sup> The crosslinking process induced a change to a globular morphology. The core of the particles was then removed by degrading the polyisoprene chains with ozone, to obtain hollow capsules with dimensions of 40 nm diameter  $\times$  2 nm thickness. The group of Weck prepared double-layer hollow shell particles from ROMP triblock copolymers containing hydrophilic PEG- and methyl ester- to hydrophobic octyl ester-functionalized norbornenes.<sup>62</sup> Norbornene monomers containing cinnamyl groups and salen ligands were also included in the hydrophobic core, to enable crosslinking by UV irradiation and the anchoring of cobalt salt particles, respectively. The final particles had diameters between 10-35 nm, depending on the copolymer composition. The activated Co(III)-salen complex embedded in the polymer shell was used as catalyst for the hydrolytic kinetic resolution of epichlorohydrin (Figure 2.10).

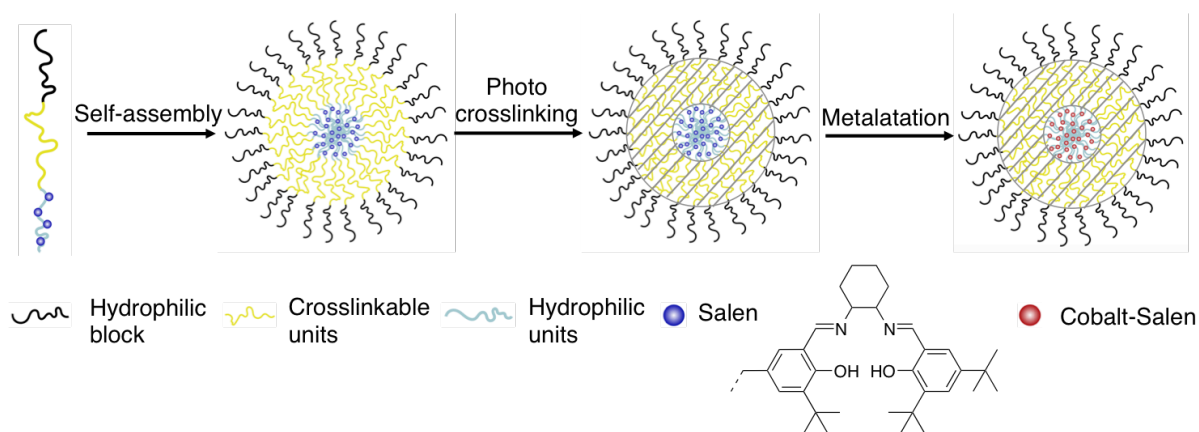


**Figure 2.10. Synthesis of shell-crosslinked micelles with cobalt-functionalized core.**<sup>62</sup>

### 2.2.3. Particles Stabilized by Interchain Interactions

By taking advantage of the antagonism between two blocks of a copolymer, same-block interactions can be favored under the right solvency conditions to create stable assemblies without resorting to crosslinking. In a series of papers, Choi thus described the preparation of caterpillar nanostructures through the copolymerization of dicarboximide norbornene with cyclooctatetraene using the third-generation Grubbs catalyst (Figure 2.11(A)).<sup>63</sup> After the synthesis of the polynorbornene block, the growth of a polyacetylene block induced the formation of polyacetylene/polynorbornene core-shell spheres during the synthesis in dichloromethane (Figure 2.11(B)). Further increase in the molecular weight of the polyacetylene block expanded the core to the point where the shell broke open. Alignment of the open spheres to shield the polyacetylene chains was then observed. Caterpillar structures with a length of 500 nm were ultimately formed, and were remarkably stable thanks to  $\pi$ - $\pi$  interactions between the polyacetylene chains. This process enabled the formation of air-stable semiconducting polyacetylene, potentially useful for applications in nanoelectronics. Optimization of the reaction conditions<sup>64</sup> and substitution of the norbornene derivative with a tricyclodiene strained olefin<sup>65</sup> enabled tuning of the size and assembly into higher order structures. The structures were still obtained by a one-pot polymerization technique, thanks to differences in reactivity between cyclooctatetraene and the strained olefin derivative.<sup>66</sup> Another example of heterogeneous particles was provided by Jäkle, with the copolymerization of a pyridylborate norbornene derivative with oxanorbornene diesters.<sup>67</sup> Hydrolysis of the ester groups in the shell promoted self-assembly in water, with pH-dependent reversibility of the core-shell structure (Figure 2.12(A)). The micelles were “crosslinked” by interchain complexation of Fe(II) or Cu(II) with the pyridylborate ligands to form an ionic network. The system displayed metal ion exchange ability and was proposed as a polymer-based cure for metal poisoning (Figure 2.12(B)).

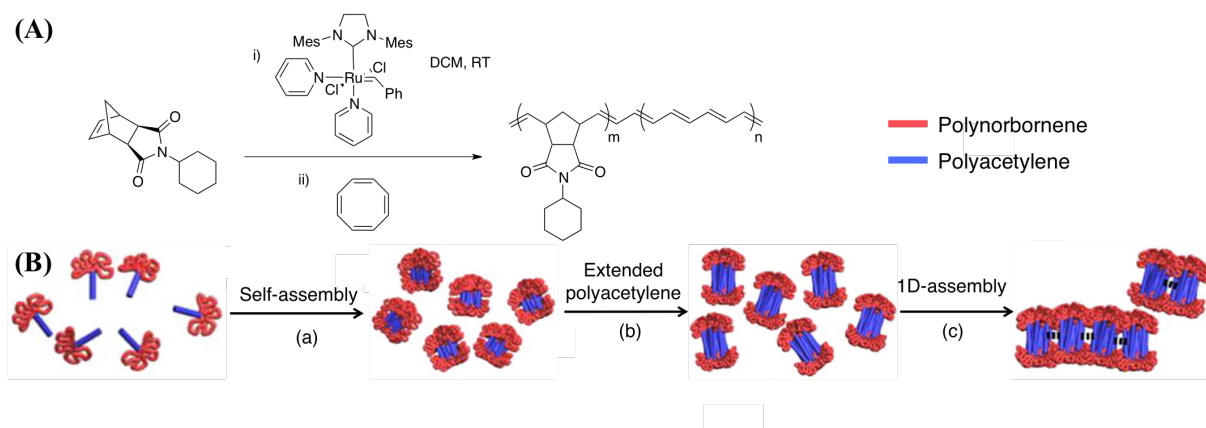


**Figure 2.11. (A) Living ROMCopolymerization of dicarboximide norbornene with cyclooctatetraene; (B) Formation of caterpillar structures during the growth of the polycyclooctatetraene block.<sup>63</sup>**

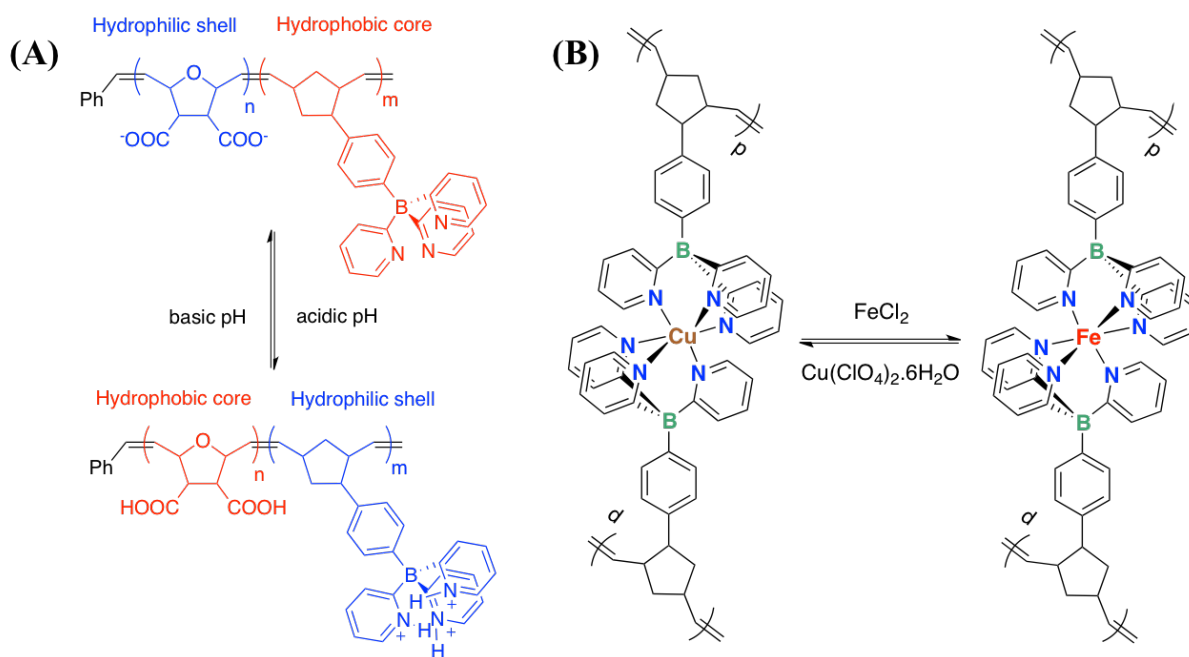


**Figure 2.12. Particles obtained by ROMP of a monomer containing a chelating group. (A) pH dependence of core-shell reversibility; (B) “Crosslinking” by complexation with Fe(II) or Cu(II) and metal ion exchange.<sup>67</sup>**



## **2.3. Particles by Dispersed Medium ROMP Using Non-Reactive Surfactants**

Polymer particles are commonly prepared via dispersed media polymerization. This alternative approach offers various strategies, depending on the type of particles needed. As later discussed, the polymerization mechanism involves either homogeneous or heterogeneous particle nucleation. Naturally, the ROMP process was adapted to these dispersed media conditions thanks to modifications in the catalysts and/or the surfactants to obtain dispersions of polymeric particles. In this section of the review, the particles were formed during the polymerization due to the specific reaction conditions used and are normally not crosslinked. They remain stable over a wide range of conditions however.

### **2.3.1. Emulsion ROMP**

In emulsion polymerization, a hydrophobic monomer is dispersed in water using a surfactant. Since the surfactant is employed at a concentration well above its CMC (typically 1-2%), a heterogeneous system with various components is obtained after stirring. Monomer droplets stabilized by the surfactant typically have a diameter of 1-10  $\mu\text{m}$ .<sup>68</sup> Micelles are also formed by the surfactant and are swollen by a small fraction of the monomer, to reach a diameter in the 5-80 nm range. Finally, depending on their solubility, a small fraction of monomer and free surfactant are solubilized in the continuous water phase (Figure 2.13). The polymerization is started by the addition of a water-soluble initiator, which typically begins the polymerization in the continuous medium after reaction with the solubilized monomer. Since the newly formed oligomeric species is insoluble in water, it may diffuse to a monomer-swollen micelle and propagate the polymerization inside of it. A polymer chain then starts growing and the micelle becomes a particle. During propagation, the newly formed particles grow by the addition of monomer from the aqueous phase, whose concentration is maintained at its solubility limit at all times by dissolution of the monomer from the droplets

acting as monomer reservoirs. This process, called *micellar nucleation*, is thought to be dominant under typical emulsion polymerization conditions, particularly for hydrophobic monomers. At the opposite end, particles can be formed by *homogeneous coagulative nucleation* when a significant fraction of the monomer can be solubilized in water, in which case the oligomeric species may collapse on themselves as oligomers when they reach a critical size. In that scenario, nucleation of the particles occurs through stabilization of the precipitated particles by surfactant adsorbed either from the micelles, the droplets or the surfactant solubilized in water. As before, particle growth then takes place by diffusion of the monomer from the water phase. Finally *droplet nucleation*, whereby an oligomeric radical enters a monomer droplet, is generally insignificant because the surface area of the micelles is far greater than that of the droplets, and thus the probability that these capture a radical is much higher.

In the kinetics of emulsion polymerization, three intervals can be distinguished (Figure 2.14). Nucleation of the particles occurs almost exclusively during interval I, where the rate of polymerization increases rapidly with the number of active particles. Interval II starts when all of the surfactant initially involved in micelle formation becomes employed to stabilize the particles formed. The number of particles in the system then stabilizes, and the polymerization rate remains constant thanks to diffusion of the monomer from the droplets, through the aqueous phase into the particles. The particles increase in size as the monomer droplets are gradually consumed. The end of interval II is marked by the disappearance of the monomer droplets. The monomer concentration in the particles then gradually decreases throughout interval III, which in turn also decreases the rate of polymerization. Emulsion polymerization is typically used to produce latexes with particle diameters of 0.1-1  $\mu\text{m}$ .

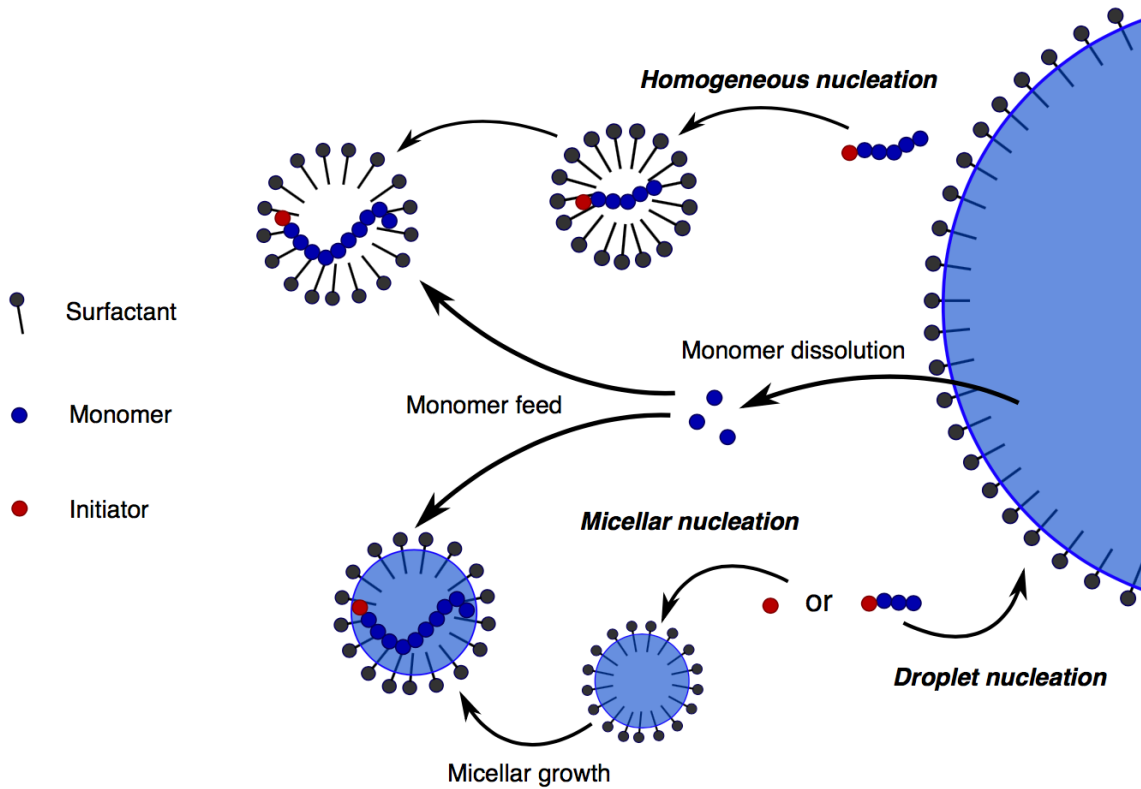


Figure 2.13. Representation of an emulsion polymerization system.

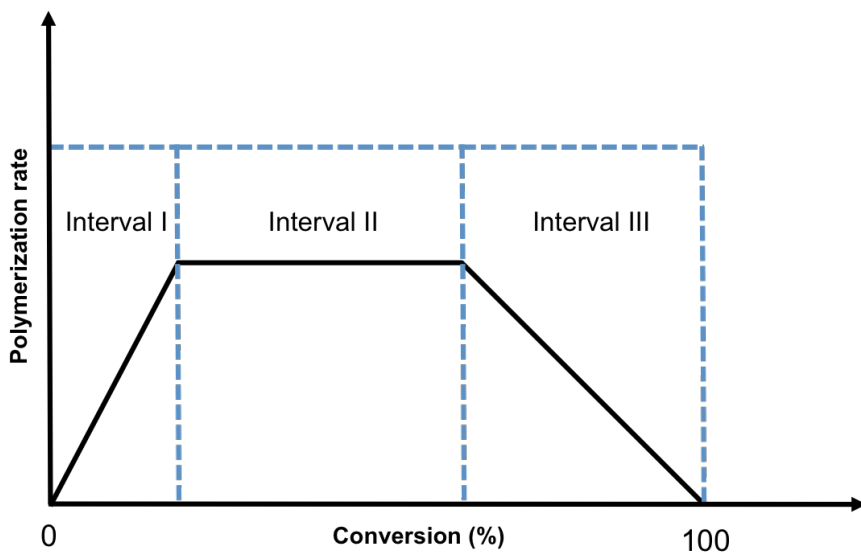


Figure 2.14. Evolution of polymerization rate with conversion for a typical emulsion polymerization.

### 2.3.1.1. ROMP in Aqueous Emulsions

The first emulsion ROMP reaction of norbornene and norbornene derivatives containing polar and halide groups, using water-soluble iridium, osmium and ruthenium salts as catalysts was reported by Rinehart and Smith.<sup>69, 70</sup> Non-ionic and anionic surfactants could be used, and the role of ethanol as reducing agent for the metallic catalysts was evidenced. However the monomer conversion only reached 10%, and no evidence for particle formation was provided. In 1995, Wache reported the emulsion polymerization of norbornene using new water-soluble ruthenium complexes as catalysts, and sodium dodecylbenzenesulfonate as surfactant.<sup>71</sup> No characterization results for the product were given either, but monomer conversions above 60% were attained in a matter of hours.

The first living emulsion ROMP reaction using well-defined ruthenium complexes (**3** and **4** in Figure 2.6) was achieved by the group of Grubbs in 1996.<sup>31</sup> Hydrophobic and hydrophilic norbornene and oxanorbornene monomers were emulsified with large quantities of dodecyl trimethyl ammonium bromide (DTAB). The water-insoluble catalysts needed to be dissolved in 5:1 water/organic solvent mixtures to reach the micelles. Homopolymers and diblock copolymers with  $\bar{M}_n$  lower than 1.35 were synthesized to demonstrate the living nature of the reaction. Water-insoluble sugar-functionalized norbornene derivatives were also polymerized to conversions higher than 70% by emulsion ROMP stabilized by DTAB, initiated with ruthenium carbene complexes **3**<sup>72</sup> and **4**.<sup>73</sup> However no details on the formation of a latex were disclosed. Characterization information on the particles was first provided in year 2000 by Claverie *et al.*<sup>46</sup> The emulsion ROMP of norbornene at 80°C initiated by water-soluble complexes **15** and **18** (Figure 2.7) was shown to form spherical particles with diameters between 50 and 150 nm depending on the monomer, catalyst and surfactant concentrations used. Interestingly, this system experienced predominantly homogeneous nucleation and a

constant increase in the number of particles throughout the reaction. However this system could not polymerize cyclooctene and cyclooctadiene in high yield.

### **2.3.1.2. ROMP in Non-Aqueous Emulsions**

As a variation of the emulsion polymerization technique, it is possible to use two immiscible organic solvents as the continuous and dispersed phases. The group of Müllen thus reported the preparation of particles by mixing *n*-hexane (as a continuous phase) with immiscible N,N-dimethylformamide (DMF, as a dispersed phase) to prepare non-aqueous emulsions stabilized by a polyisoprene-*b*-poly(methyl methacrylate) copolymer.<sup>74</sup> The ROMP of amide- and ester-functionalized norbornene derivatives inside the droplets led to the formation of 50-200 nm particles with Grubbs second-generation metathesis catalyst **8** (Figure 2.6). The spherical particles displayed excellent colloidal stability, with a size depending on both the *n*-hexane/DMF ratio and the stabilizer concentration. Core-shell particles were also obtained by sequential addition of the monomers, and opened the prospect of surface functionalization with clickable shell functionalities.

### **2.3.2. Miniemulsion ROMP**

The miniemulsion polymerization process consists of a monomer pre-emulsion obtained by sonication in the presence of a stabilizer to obtain 50-500 nm monomer droplets (Figure 2.15). A hydrophobic agent is also used to minimize the *Ostwald ripening* effect, due to diffusion of the monomer from the smaller droplets into the larger ones through the aqueous phase. The combined concentration of surfactant and hydrophobic agent is typically in the range of 1-3% by weight (wt %). A water-soluble initiator is introduced in the medium, and the reaction proceeds exclusively in the droplets to form particles with a final size similar to that of the droplets. The droplets can be considered as closed reactors, and the kinetics profile only consists in two intervals for miniemulsion polymerization. Interval I still corresponds to

nucleation, with a longer duration as compared to the emulsion process due to slow entry of the hydrophilic initiator into the droplets. There is no steady rate interval in the miniemulsion polymerization reaction, because monomer diffusion is not involved. Thus after nucleation, the rate of polymerization decreases as the monomer conversion increases. The closed reactor system does not require diffusion of the monomer for polymerization to proceed, which means that highly hydrophobic monomers can be polymerized by this technique. Hydrophobic drugs or other bioactive compounds can also be mixed with the monomer prior to sonication, to end up inside the droplets after droplet formation and thus be encapsulated once the particles have formed. Miniemulsion polymerization represents an economical way to obtain very stable particles with reasonable amounts of stabilizer, and to control the size by sonication.

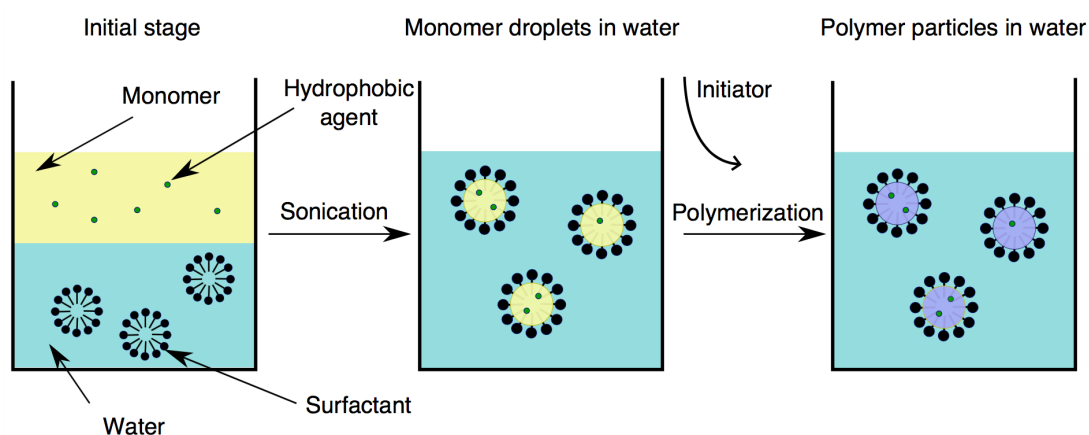


**Figure 2.15. Representation of miniemulsion polymerization.**

The synthesis of particles by ROMP in miniemulsions started with the work of Claverie *et al.* as an alternative to emulsion ROMP for norbornene, cyclooctene and cyclooctadiene.<sup>46</sup> While the polynorbornene latexes tended to flocculate, stable polybutadiene latexes with particle diameters between 200-600 nm were obtained. Rather than using the usual monomer miniemulsion polymerization protocol, a catalyst miniemulsion of hydrophobic initiator **4**

(Figure 2.6) was prepared and the monomer was directly transferred dropwise with a canula. The mini-reactor model was not followed in this case, because diffusion of the monomer to the catalyst droplets and redistribution of the miniemulsion were allowed. The group of Héroguez later achieved the miniemulsion ROMP of norbornene by addition of a water-soluble complex, either  $\text{RuCl}_3$  in alcoholic solution<sup>75</sup> or a well-defined macroinitiator **28** (Figure 2.16)<sup>76</sup> specially designed to prevent coagulation observed with the first-generation Grubbs catalyst **4** (Figure 2.6), and stable 200-500 nm particles were obtained with monomer conversions close to 100%. Hybrid particles were also prepared by tandem ROMP/ATRP in miniemulsion. Using **28** (Figure 2.16) as a water-soluble catalyst, homopolymer blends of polynorbornene and poly(methyl methacrylate) (PMMA), were obtained using ethyl 2-chloropropionate as ATRP initiator. Similarly, the use of a tandem ROMP-reactive, ATRP initiating norbornene molecule functionalized with ethyl 2-chloropropionate gave rise to graft and star-like copolymers.<sup>77</sup> A morphological study of the homopolymer blends revealed the formation of 200 nm Janus-type particles with segregation into two hemispheres.<sup>78</sup>

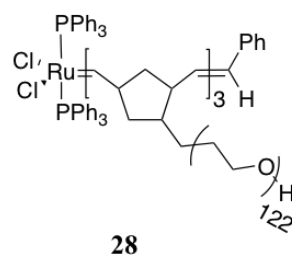


**Figure 2.16. Water-soluble miniemulsion ROMP initiator.**<sup>76</sup>

### 2.3.3. Microemulsion ROMP

Microemulsion polymerization bears similarities to emulsion and miniemulsion polymerization, but the monomer droplet size is in a range well below 100 nm. The final particles generally have a diameter around 5-50 nm.<sup>79</sup> In this case the droplets are stabilized

by a combination of surfactant (usually sodium dodecyl sulfate, SDS) at a concentration of 10-15 wt % and a co-surfactant, usually pentanol. Because of the high concentration of surfactant and the very small sizes involved, microemulsions are transparent or translucent and thermodynamically stable, in contrast to the emulsion and miniemulsion systems. The polymerization can be initiated with hydrophobic or hydrophilic initiators. Moreover, unlike emulsion polymerization, the nucleation process occurs continuously throughout polymerization. Microemulsion polymerization has attracted much interest because of the possibility of synthesizing very small particles and very high polymer molar masses. The transparency of the medium also represents an opportunity for photopolymerization processes.<sup>80-82</sup>

Grubbs described the first attempt at ROMP in microemulsions with a water-soluble catalyst **14** (Figure 2.7) and a 9-fold weight ratio of surfactant to norbornene.<sup>47</sup> Though quantitative monomer conversion was achieved, no characterization results were given for the latex. Mecking also reported the microemulsion ROMP of norbornene, as well as less strained cyclooctadiene and cyclooctene, initiated by the first-generation Grubbs metathesis catalyst **4** (Figure 2.6).<sup>83</sup> To retain stability of the droplets upon addition of the monomer, it was decided to use two separate microemulsions for the monomer and the catalyst, that were mixed to afford monomer and catalyst droplets. It seems that polymerization proceeded by diffusion of the monomer into the catalyst droplets. Particles with a diameter of 20-35 nm were obtained with respectable (55-100%) monomer conversion. The tandem ROMP/ATRP system in miniemulsion, described earlier (Section 2.3.2) for norbornene and methyl methacrylate, was also adapted for microemulsions.<sup>84, 85</sup> This method allowed the direct use of Grubbs first-generation metathesis catalyst **4** (Figure 2.6) by adding a microemulsion of both monomers to a catalyst microemulsion. Particles with diameters of 20-50 nm were thus obtained with various morphologies. Homopolymer blend particles with a core-shell morphology, having a



hard PMMA core and a soft polynorbornene shell, were obtained by adding ethyl 2-chloropropionate as ATRP initiator in the monomer droplets, while graft copolymer particles with an “acorn-like” shape were obtained using norbornene-functionalized ethyl 2-chloropropionate as a ROMP-reactive ATRP initiator. Substituting t-BA for MMA led to similar morphologies, but this time with polynorbornene at the core because of its faster polymerization rate.<sup>86</sup> The double microemulsion mixing ROMP technique was also implemented for the synthesis of fluorescently labeled anisotropic nanocrystals from trans-cyclooctene.<sup>87</sup> When a fluorescently labeled second-generation Hoveyda-Grubbs complex was used to introduce a single fluorescent molecule at the end of each chain, oblate-shaped polyethylene nanocrystals with dimensions of  $15 \times 45 \text{ nm}^2$  were obtained after hydrogenation. Another strategy used consisted in utilizing latent hydrophobic initiators, to prevent their reaction with the monomer during the emulsification process. Homogeneous mixing of the catalyst could thus be achieved before switching on the reaction. The group of Meier devised an imine imidazole ligand coordinated with the ruthenium center on the imine moiety (Figure 2.17) to that end.<sup>88</sup> Initiation was activated by the addition of HCl to protonate the imine and imidazole groups, to generate a vacant coordination site on the ruthenium center and promote the metathesis reaction. A stable microemulsion was prepared by that method, with 15 wt % of Tween 20 surfactant and droplets of initiator solution in 5-norbornene-2-yl acetate. The addition of HCl to the medium initiated the polymerization to yield particles with sizes between 10 and 21 nm in 2 hours. Variation of the HCl/Ru ratio provided control over the initiation rate.

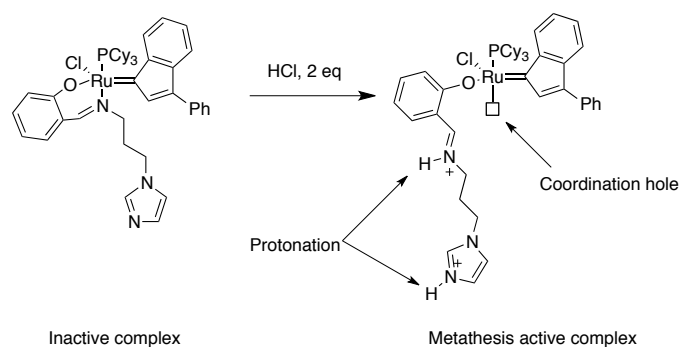


**Figure 2.17. Latent ruthenium complex activated by protonation.**

### 2.3.4. Suspension ROMP

Suspension polymerization consists in a hydrophobic monomer phase dispersed in a continuous water phase in the presence of a dispersing agent at low concentration. The hydrophobic nature of the initiator used implies that polymerization can only take place inside the monomer droplets. This technique leads to the formation of particles in a size range between 10  $\mu\text{m}$  and 5 mm. Because a low concentration of stabilizer is involved, the suspension is unstable by nature and can phase-separate upon interruption of stirring.

The first example of ROMP in suspension was reported by Grubbs in 1996, where norbornene and 7-oxanorbornene derivatives were polymerized in a living fashion using **4** (Figure 2.6), without characterization of the particles formed.<sup>31</sup> The group of Janda achieved the copolymerization of norbornene, 5-norbornene-2-methanol and norbornene-based crosslinkers by suspension ROMP with water-insoluble second-generation Grubbs catalyst **8** (Figure 2.6). After hydrogenation, this inexpensive procedure provided micrometric inert functional polymer beads that could serve as supports for the solid-state synthesis of various organic compounds.<sup>89</sup> Hilborn also performed the suspension ROMP of dicyclopentadiene in the presence of a porogen, poly(1,2-butylene glycol) monobutyl ether, in monomer droplets stabilized by hydroxypropyl cellulose.<sup>90</sup> The polymer phase-separated from the porogen as it

formed, and also crosslinked thanks to the difunctionality of the monomer (Figure 2.18). After washing off the surfactant and the porogen, 300-400  $\mu\text{m}$  porous beads were obtained.

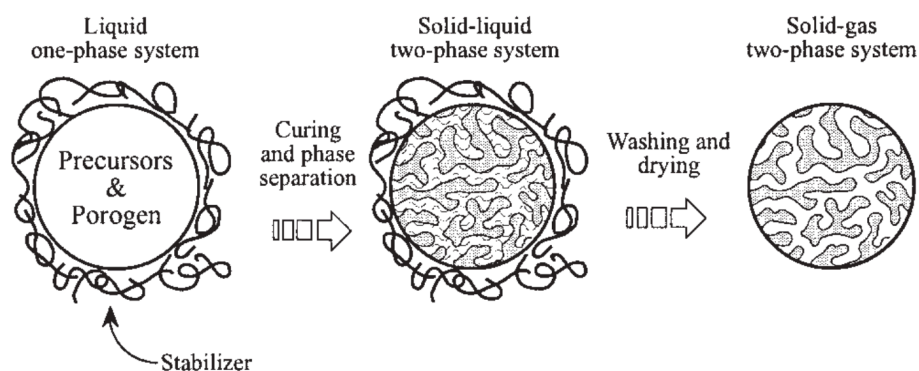


**Figure 2.18. Preparation of macroporous polymer beads by suspension ROMP.**<sup>90</sup>

### 2.3.5. Dispersion ROMP

The development of dispersion polymerization started in the 1950s, because of demand by the paints and coatings industry for high molecular weight polymers dispersed in organic solvents in replacement of solution or emulsion processes.<sup>91-93</sup>

The mechanism of dispersion polymerization consists in an initially homogeneous solution of monomer(s) and stabilizer in organic solvent(s). The stabilizer is a homopolymer or a block copolymer acting as steric stabilizer and can have a linear, branched or brush architecture. The addition of a soluble initiator to the medium starts the polymerization and particle nucleation by different mechanisms. The most frequent mechanism is thought to be *spontaneous nucleation*, whereby oligomeric active centers precipitate once they reach a certain critical chain length (Figure 2.19). The newly formed nuclei can be stabilized in the medium by the adsorption of stabilizer. *Aggregative nucleation* is a mechanism whereby polymer chains associate before reaching a critical chain length, forming non-soluble aggregates also stabilized by the adsorption of stabilizer. *Coagulative nucleation* involves

unstable nuclei associating with each other or with existing particles to form larger particles. Particle nucleation is a rather rapid process that is typically completed in a matter of minutes, so the number of particles in the system remains fairly constant after nucleation is completed. Further polymerization takes place in the form of particle growth, by adsorption or the precipitation of growing oligomers on the particles.

The kinetics of dispersion polymerization are complex because of the heterogeneity of the system. The reaction first takes place only in solution but after the appearance of particles, the reaction takes place both in solution (with the formation of oligomeric chains) and within the particles.

The size and size distribution of the particles are governed by several factors: the nature of the monomer influences the solubility of the oligomers, and thus the critical length at which nucleation begins. The monomer concentration also affects the polymerization kinetics. An increase in stabilizer concentration means that a larger area can be stabilized, so it leads to the formation of a larger number of smaller particles. Increasing the molecular weight of the steric stabilizer likewise promotes stabilization of the particles, which limits the coagulative nucleation process. Smaller nuclei are better stabilized, and the particle size thus decreases. Increasing the initiator concentration decreases the molecular weight of the polymer chains formed, but also increases the rate of aggregative and coagulative nucleation processes, causing an increase in particle size. An increase in temperature likewise increases the number of active sites, which increases the particle size.

The group of Booth polymerized water-soluble bis(methoxymethyl)-7-oxanorbornene using the  $\text{RuCl}_3 \cdot \text{H}_2\text{O}$  complex, and a non-ionic Pluronic® poly(ethylene oxide)-*b*-poly(propylene oxide)-*b*-poly(ethylene oxide) copolymer surfactant to stabilize the particles.<sup>94</sup> The surfactant concentrations used were between 9-27  $\text{g} \cdot \text{L}^{-1}$ , and the monomer concentration 18  $\text{g} \cdot \text{L}^{-1}$  to obtain stable particles. While the polymerization was conducted in water, the mechanism

described corresponded to a dispersion polymerization. The particles obtained had a diameter below 60 nm and were stable for over 5 months. Attempts at producing pure polynorbornene latexes were conducted in dichloromethane/ethanol mixtures using the first-generation Grubbs catalyst **4** (Figure 2.6). However neither PEO homopolymer, PS-*b*-PEO nor polynorbornene-*g*-PEO amphiphilic copolymers could stabilize the growing polynorbornene particles, which precipitated out.<sup>95</sup> The very fast kinetics of the reaction and incompatibility of the surfactant with the polymer formed prevented the efficient adsorption of the stabilizer during nucleation of the particles. Seeded dispersion ROMP with preformed polynorbornene latex was also attempted but only enabled more growth of the existing particles through capture of the new polynorbornene chains, and coalescence without promoting the nucleation of new particles.

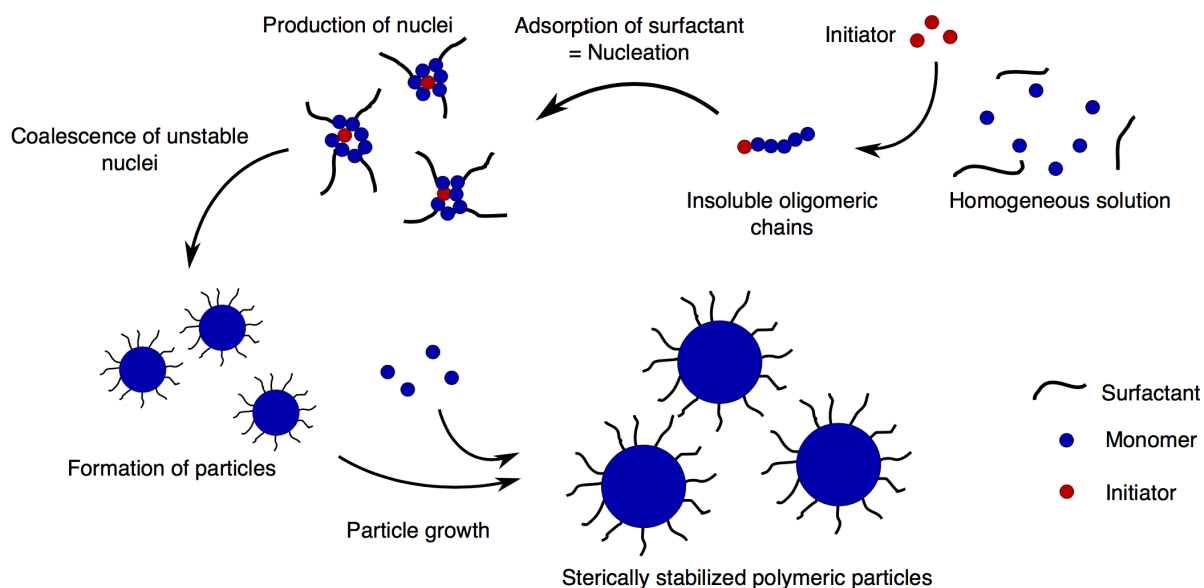


**Figure 2.19. Mechanism of particle formation in dispersion polymerization.**

## 2.4. Synthesis of Particles by ROMP Using Macromonomers

The IUPAC (International Union of Pure and Applied Chemistry) definition of a macromonomer is: “*A macromolecule that has one end-group which enables it to act as a monomer molecule, contributing only a single monomeric unit to a chain of the final macromolecule*”.<sup>96</sup> This definition highlights that a macromonomer is composed of two main elements, namely a monomeric end-group that can react in any of the conventional free radical or controlled polymerization techniques, and an attached chain that can be either an oligomeric or polymeric segment. Macromonomers find multiple uses as homopolymers and copolymers, in the synthesis of star and bottle-brush polymers, thanks to the *grafting through* technique.<sup>97-100</sup>

In the case of dispersed media polymerization, macromonomer chains can serve as stabilizer. The macromonomer is a reactive stabilizer, since it takes part in the polymerization but is also an integral part of the final particles. For ROMP in dispersed media, both the stabilizing chain and the polymerizable moiety can be selected depending on the intended application of the particles. The brief review of the synthesis of particles by ROMP using macromonomers provided in the following sections depicts recent advances for the various dispersed media techniques.

### 2.4.1. Miniemulsion ROMP

1,4-Polybutadiene-*g*-PEO copolymers were synthesized by miniemulsion ROMP,<sup>101</sup> using a cyclobutene-PEO macromonomer prepared by clicking an azide-functionalized PEO chain with an alkyne-functionalized cyclobutene. A mixture of macromonomer, hexadecane as hydrophobic agent, the third-generation Grubbs catalyst **10** (Figure 2.6) in dichloromethane, and an aqueous solution of Brij 700 (commercial macromolecular surfactant: C<sub>18</sub>H<sub>37</sub>-(CH<sub>2</sub>-CH<sub>2</sub>O)<sub>100</sub>-H) was sonicated to obtain a miniemulsion with limited (< 10%) polymerization of the macromonomer by the end of droplet formation, which marked the beginning of the

reaction. A polymacromonomer-based latex was obtained with a final maximum macromonomer conversion of 56% and the formation of 320 nm particles.

### 2.4.2. Suspension ROMP

Suspension ROMP of cyclooctadiene was first attempted using poly(diallylmethylammonium chloride) as a suspending agent, and the Grubbs first-generation complex **4** (Figure 2.6) as initiator. Polybutadiene beads were obtained, but insufficient stabilization combined with the low glass transition temperature of the polybutadiene product led to progressive aggregation. When an  $\alpha$ -norbornenyl-PEO macromonomer was added to the reaction in combination with the suspending agent, micrometer-sized particles were obtained, but the macromonomer conversion remained below 10% because of its high hydrophilicity. The stabilization level offered by this system was also insufficient to prevent coalescence of the particles. Amphiphilic character was introduced in the macromonomer by adding a PS block (Figure 2.20(A)). Conversion of the  $\alpha$ -norbornenyl-PS-PEO macromonomer was quantitative in that case, and stable 20  $\mu\text{m}$  beads were obtained by copolymerization with cyclooctadiene in a classical suspension technique (Figure 2.20(B)).<sup>102</sup>

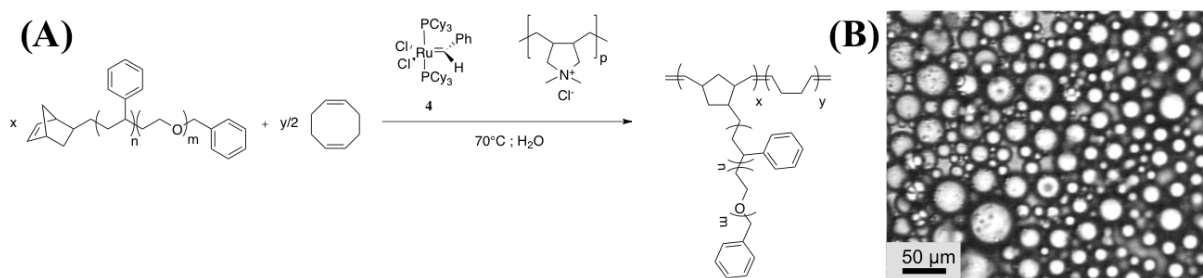


**Figure 2.20. (A) Suspension ROMP of cyclooctadiene with  $\alpha$ -norbornenyl-PS-PEO macromonomer; (B) Particles observed by optical microscopy.**<sup>102</sup>

### 2.4.3. Dispersion ROMP

The use of norbornene-functionalized macromonomers was studied in more details for the synthesis of particles by dispersion ROMP, in particular using norbornene as monomer and the first-generation Grubbs catalyst **4** (Figure 2.6). The growing chains quickly started precipitating in the dichloromethane/ethanol mixture, and stabilization of the nuclei was achieved by copolymerization with an  $\alpha$ -norbornenyl-PEO macromonomer. The particles continued to grow by reaction of the remaining norbornene and macromonomer to produce polynorbornene latexes (Figure 2.21, top).<sup>95, 103</sup> Measurement of the conversion rates for the monomer and the macromonomer implied the formation of a gradient copolymer, starting from a polynorbornene block. The final conversion was complete for norbornene, while 90% of the macromonomer was reacted. The particle diameter could be tuned in a range of 240-590 nm by varying the molecular weight and concentration of the macromonomer, and the concentrations of initiator and monomer. The introduction of a polystyrene (PS) block on the macromonomer chain, to obtain an  $\alpha$ -norbornenyl-PS-*b*-PEO stabilizer, did not prevent the formation of particles. The hydrophobic PS block rather provided better compatibility with polynorbornene, which increased the rate of macromonomer conversion as compared to its PEO counterpart. The consequences of this appeared to be a longer nucleation period and faster stabilization of the particles, which led to the formation of smaller particles with broader size distributions. When the copolymerization was conducted with cyclooctadiene, the lower ring strain as compared to norbornene enabled faster incorporation of the macromonomer and reversed gradient copolymer formation.<sup>104</sup> Redistribution reactions through back-biting or intermolecular cross-metathesis on the unsaturations of the polymer chains were also more favored, which resulted in delayed precipitation of the chains and the formation of a broad population of 2-15  $\mu\text{m}$  particles (Figure 2.21, bottom). The secondary reactions also generated soluble macromonomer-rich chains in the medium, that nucleated



later into a second smaller (200-500 nm) population, but also with a broad distribution. Nevertheless, the latex could be hydrogenated quantitatively to produce a polyethylene latex without changes in colloidal properties.<sup>105</sup> The only way found to produce a monomodal population, in this case, was to allow the macromonomer and cyclooctadiene to swell a preformed polynorbornene latex, and initiation for further growth of the existing particles.

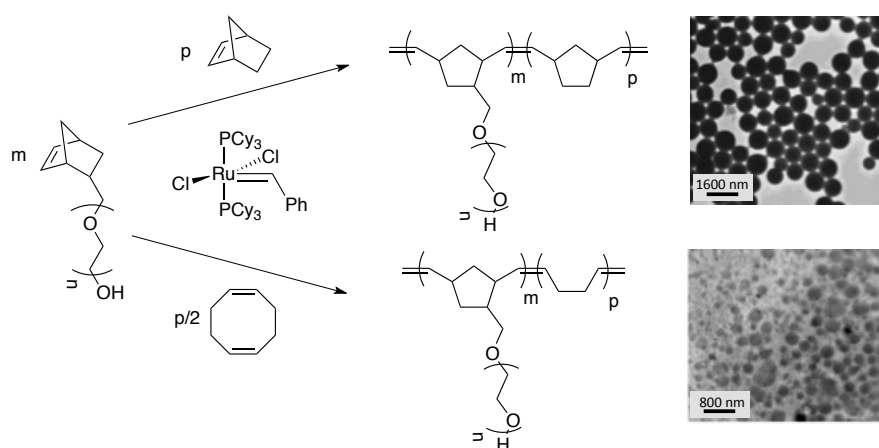


**Figure 2.21. Formation of polynorbornene (top) and polybutadiene (bottom) latexes by dispersion ROMP.**

The previously described system could also be crosslinked as the particles formed, by adding a di-norbornene crosslinker to the usual norbornene and  $\alpha$ -norbornenyl-PEO macromonomer composition (Figure 2.22(A)).<sup>106</sup> Raspberry-shaped particles around 400 nm in diameter were thus obtained (Figure 2.22(B)). The structure of the particles was explained by altered kinetics due to the presence of the crosslinker. Both norbornene and the crosslinker reacted quantitatively, while macromonomer conversion was slower in the presence of the crosslinker, with a lower final conversion (< 65%, versus 90% without crosslinker). It was determined that in the first stage of polymerization mainly norbornene and the crosslinker reacted, leading to poorly stabilized, highly crosslinked nuclei. The presence of the crosslinker and the stiff structure limited further incorporation of either component in this first

population. The next step of the polymerization consisted in the reaction of the remaining crosslinker with the macromonomer, which led to secondary nucleation. The newly formed particles then attached to the first population by reaction of the crosslinker.

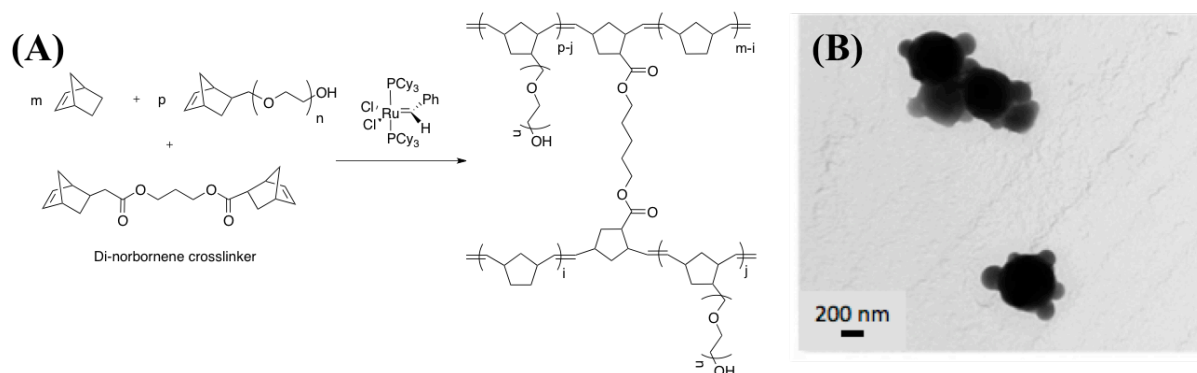


**Figure 2.22. (A) Preparation of crosslinked polynorbornene particles by dispersion ROMP; (B) Observation of raspberry-shaped particles by TEM.<sup>106</sup>**

## 2.5. pH-Sensitive Functionalized Polymeric Particles

The conjugation of active molecules with polymer particles is an efficient way for drug vectorization, or for the controlled delivery of bioactive compounds in general (such as the biocide of interest in this project). Polymer particles offer a high surface group density, which enables the synthesis of highly concentrated vectors. Conjugation can be achieved before the formation of the particles, to allow better control of the amount of conjugated molecules, but sometimes at the expense of incorporation in the final particles. Conjugation after the formation of the particles generally decreases the extent of control over the process, because of the heterogeneity of the reactions. The delivery of the active molecules can be triggered by variations in the redox, thermal, or pH characteristics of the environment. In the latter case, acidic conditions can be used to trigger the hydrolysis of a labile bond between the particle and the molecule. This concept is widely used in antibacterial, antifungal and anticancer drug

delivery systems, because a decrease in pH is typically caused by the singular metabolism of the targeted organisms.<sup>107-109</sup>

### **2.5.1. pH-Sensitive Bonds for the Formation of Drug-Polymer and Drug-Particle Conjugates**

The formation of pH-sensitive bonds is required in the context of releasing an active molecule upon acidification of the medium; thus acetal, ester, hydrazone and imine bonds are most commonly used for pH-sensitive conjugation to polymers. In each case, the nature of substituents surrounding the bond will influence the hydrolysis kinetics and the pH-sensitivity of the bond. The ease of synthesis and the compatibility of these bonds with a wide range of polymer substrates represent a good opportunity for the preparation of pH-sensitive polymer particles. Hereafter, the examples provided will illustrate the main families of polymers utilized with each bond type to prepare polymer-drug conjugates, since they relate to bioactive conjugates in general, as well as applications restricted to the use of polymer particles conjugated with active molecules through pH-sensitive bonds. For the sake of consistency with the earlier discussion, examples involving non-crosslinked polymeric micelles will not be included in this review.

#### **2.5.1.1. Conjugation with Acetal Bonds**

Acetal groups can be obtained by condensation of a carbonyl group with two alcohol moieties in the presence of either an acid or a base catalyst (Figure 2.23). In organic chemistry, this approach is usually utilized for the protection of hydroxyl functions. The acetal group is quite stable under neutral and alkaline conditions, but mildly acidic conditions (e.g. pH 5) can trigger the hydrolysis of the bond at rates varying from minutes to several hours, depending on the substituents present (Figure 2.24).<sup>110</sup> Acetal groups were thus utilized to attach

anticancer or chromophore molecules to PEG,<sup>110, 111</sup> poly(acrylic acid),<sup>112</sup> poly(methacrylate esters),<sup>113</sup> polylactide<sup>114</sup> and polyethylenimine<sup>115</sup> substrates.

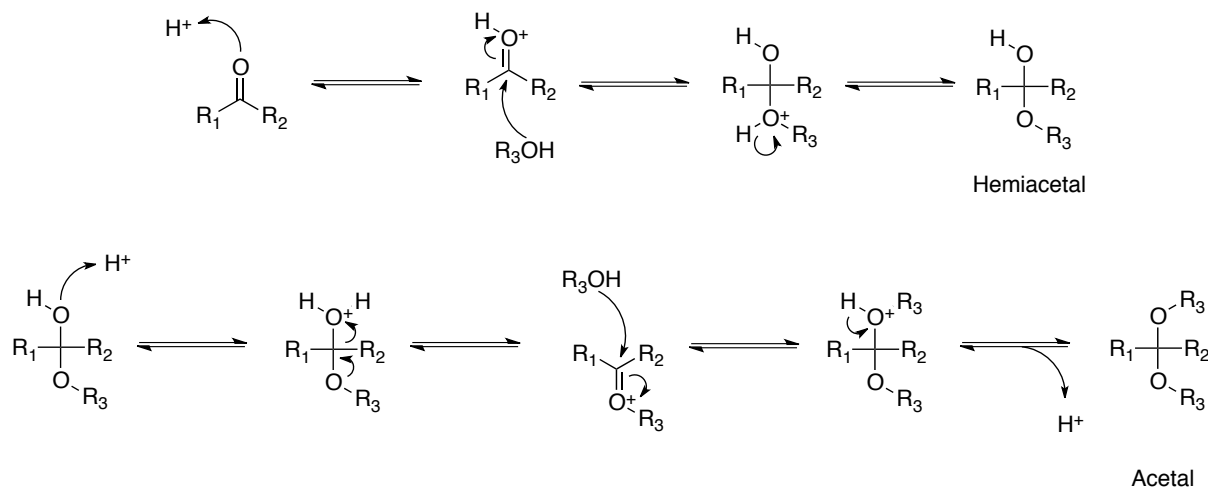


**Figure 2.23. Mechanism for the formation of an acetal group assisted by an acid catalyst.**

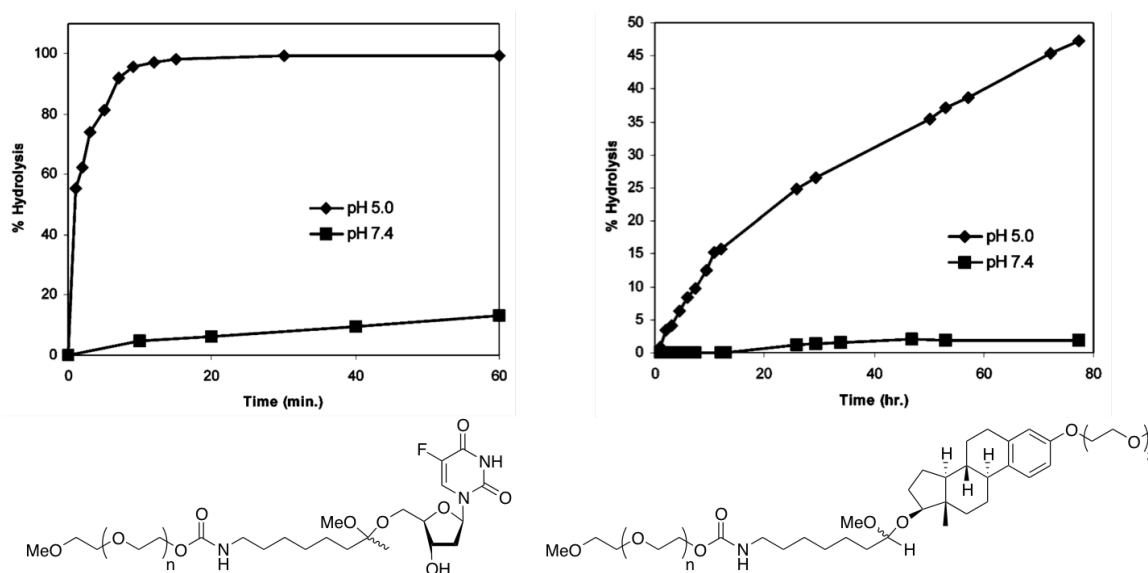


**Figure 2.24. Variation in the acetal hydrolysis rate with pH and the presence of substituents on PEG-based conjugates.<sup>110</sup>**

While acetal functionalities have been used as pH-sensitive components in the field of drug delivery,<sup>110</sup> literature on this topic is scarce when applied to polymer particles. For example, a

pH-sensitive acetal-based spacer was coupled with the amine groups of a polyethylenimine chain. This spacer also had terminal primary amine functions that served for the condensation of nucleic acids in various siRNA and DNA sequences, to form 80-200 nm polyplexes and achieve gene delivery to model cell lines (Figure 2.25(A)).<sup>115</sup> The hydrolysis kinetics of the acetal linkages were monitored *in vitro* by <sup>1</sup>H NMR spectroscopy and modeled with the Arrhenius equation. While the bonds still hydrolyzed at pH 7.4, three- and ten-fold increases in hydrolysis rate were observed at pH 6 and 5, respectively (Figure 2.25(B)).

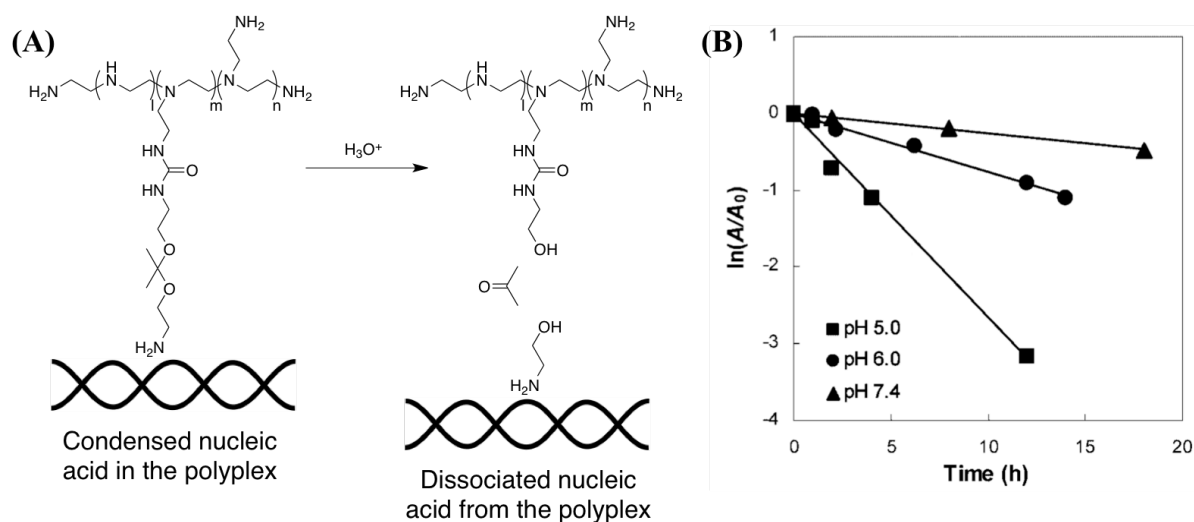


**Figure 2.25. (A) Formation of polyplexes with acetalized polyethylenimine; (B) pH-dependence of the acetal bond hydrolysis.**<sup>115</sup>

### 2.5.1.2. Conjugation with Ester Bonds

Ester bonds are formed by the reaction of an alcohol with a carboxylic acid (Figure 2.26). The formation of an ester using an acid catalyst is a slow process, which can be facilitated with the use of a carbodiimide to activate the acid. The peculiarity of ester bonds is that they can be cleaved at physiological pH (7.4), but also under acidic or basic conditions. In the specific case of polymers, the rate of hydrolysis depends more strongly on the hydrophilicity and the steric hindrance of the neighbouring groups than on the pH itself, higher rates being observed

for more hydrophilic, less hindered neighbouring groups.<sup>116, 117</sup> Esters have been employed as pH-sensitive linkers with PEG,<sup>118-120</sup> polypropylene,<sup>121</sup> poly(vinyl alcohol)<sup>122</sup> and polyacrylates<sup>117, 123-125</sup> for the conjugation of anti-inflammatory and anticancer drugs.

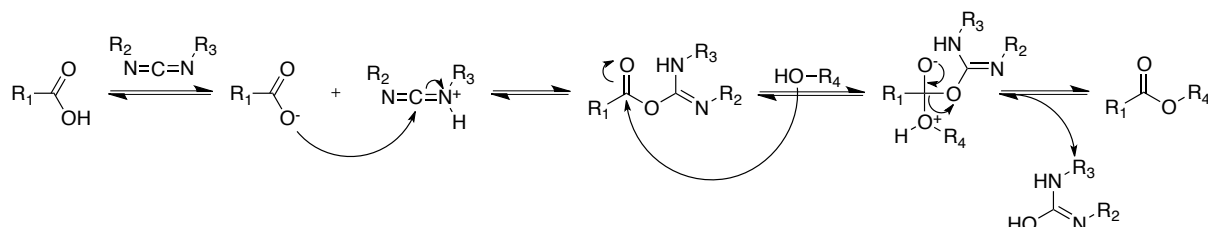


**Figure 2.26. Mechanism for the carbodiimide-mediated formation of an ester bond.**

### 2.5.1.3. Conjugation with Hydrazone Bonds

A third type of pH-sensitive linkage is the hydrazone bond, formed by the reaction of a hydrazine with a ketone (Figure 2.27(A)). This is a popular choice for the immobilization of doxorubicin (DOX) on polymer chains. This anticancer drug can be attached through its lone ketone group, to prevent the side effects of the free molecule. The hydrazone bond is rather stable under alkaline and neutral conditions, but hydrolysis takes place at or below pH 6, over several hours to several days, the process being accelerated under more acidic conditions. As shown in Figure 2.27(B), for a set duration, the release of DOX via hydrolysis of hydrazone bonds can increase from 0 to 100% as the pH is decreased from 7 to 3.<sup>126</sup> DOX and other anticancer agents were thus conjugated to various types of polymers, namely polyesters,<sup>127-131</sup> polyacrylates,<sup>132-138</sup> polyamides,<sup>126</sup> polysaccharides,<sup>139</sup> PEG,<sup>134</sup> and polyglycidol.<sup>140, 141</sup>

Several examples in the literature demonstrate the usefulness of the hydrazone bond to link active molecules to polymer particles. DOX was thus conjugated to a methacrylamide monomer through a hydrazone bond, to be placed in the core of polymer micelles composed of PEG-*b*-poly(N-(2-hydroxypropyl)methacrylamide lactate) copolymers, with functionalization with methacrylate groups at the end of the lactate chains. Crosslinking of the

micelles was achieved through free radical polymerization of the methacrylate groups in the core of the micelles, to simultaneously graft DOX covalently to the micelles.<sup>142</sup> The 80 nm particles thus obtained were able to release their entire drug load within 24 hours at pH 5, and displayed increased toxicity for cancer cells as compared to the free drug. In a different study, an amphiphilic block copolymer was synthesized by the reversible addition-fragmentation chain transfer (RAFT) copolymerization of 2-(2-pyridyldisulfide)ethyl methacrylate (PDSM) and N-(2-hydroxypropyl)methacrylamide. The pyridyldisulfide groups were then used to conjugate a maleimide-hydrazone derivative of DOX and to crosslink the core of the particles via disulfide bridges in a one-pot reaction.<sup>143</sup> Alternately, PEG was also grafted in the homopolymerization of the PDSM monomer by this method to form an amphiphilic copolymer.<sup>144</sup> The release of DOX was more rapid at pH 5 than at pH 7.4, and the system displayed enhanced cellular uptake and decreased cancer cell viability as compared to the free drug.<sup>144</sup> A dendritic core of Boltorn® H40 was also used to conjugate poly(L-aspartate)-*b*-PEG chains forming a shell (Figure 2.28). DOX was then conjugated via a hydrazone bond to the inner poly(L-aspartate) shell, while folic acid was conjugated to the PEG outer shell to enhance cellular uptake.<sup>145</sup> The particles obtained had a bimodal population, with sizes between 17-36 nm and 52-76 nm. DOX was released at acidic pH, with enhanced cell uptake and toxicity. Furthermore, the particles were degraded after two weeks at pH 5.3, which is useful for elimination of the carrier after use.

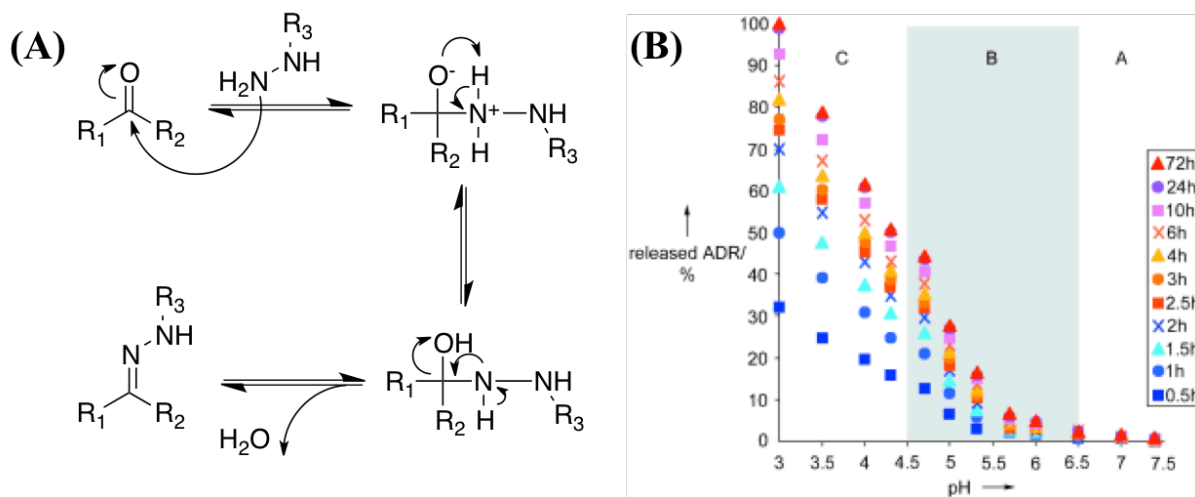


Figure 2.27. (A) Formation of a hydrazone bond; (B) Typical release profiles for DOX as a function of pH.<sup>126</sup>

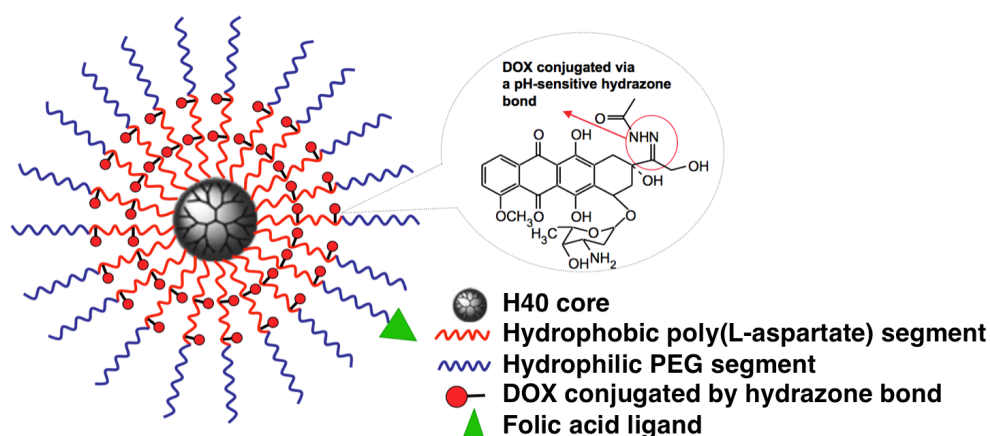


Figure 2.28. Particle based on a dendritic core and poly(L-aspartate)-*b*-PEG for the acid-triggered release of DOX.<sup>145</sup>

#### 2.5.1.4. Conjugation with Imine Bonds

The last important pH-labile linkage is the imine group, formed by the reaction of an aldehyde group and a non-protonated primary amine (Figure 2.29(A)). The bond is quite stable at neutral pH but cleaves under mildly acidic conditions ( $\text{pH} \leq 6$ ), with acceleration of the effect at lower pH (Figure 2.29(B)).<sup>146, 147</sup> Numerous examples of anticancer and antibiotic



drugs conjugated to polymers through an imine bond are reported in the literature, including polymers such as PEG,<sup>120, 146, 148-150</sup> polysaccharides,<sup>151-154</sup> polyacrylates,<sup>147, 155</sup> and polyamides.<sup>148</sup>

The imine bond was also utilized as a cleavable moiety for the delivery of molecules from polymeric particles. The group of Sun thus grafted PEG-NH<sub>2</sub> chains onto magnetic Fe<sub>3</sub>O<sub>4</sub> particles and conjugated the side chains to chromone, an anticancer agent, through its aldehyde group (Figure 2.30).<sup>149</sup> The final particle size was in a range of 60-110 nm and the conjugate was stable at pH 7.4. The release of chromone after 24 hours increased from 13 to 88% when the pH was decreased from 6 to 3. The imine bond also displayed increased tendency to hydrolyze when the temperature was raised from 25°C to 37°C. The system was tested as an anticancer agent with HeLa cancer cells, displaying a high uptake and toxicity due to the enhanced solubility of conjugated chromone.

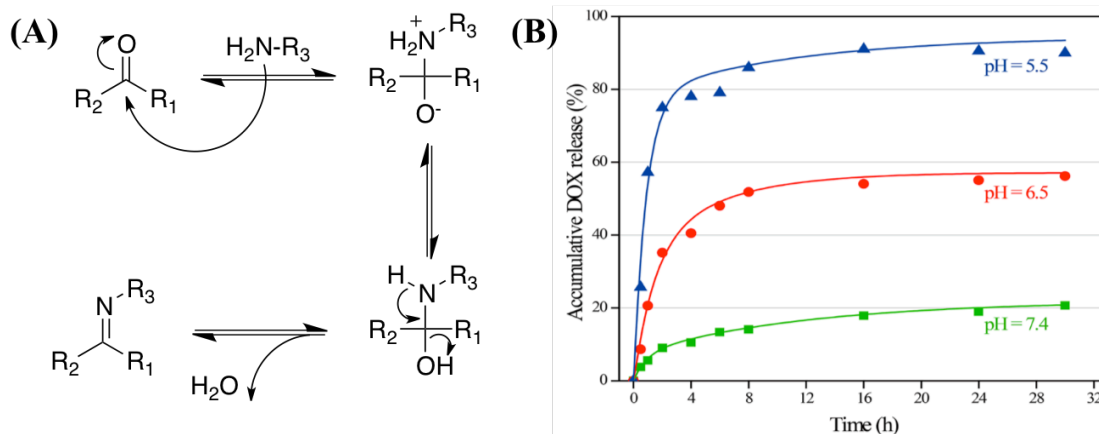


**Figure 2.29. (A) Mechanism for the formation of an imine bond; (B) pH-dependent release profile of DOX from poly(alkyl methacrylate)-based copolymer micelles.<sup>147</sup>**

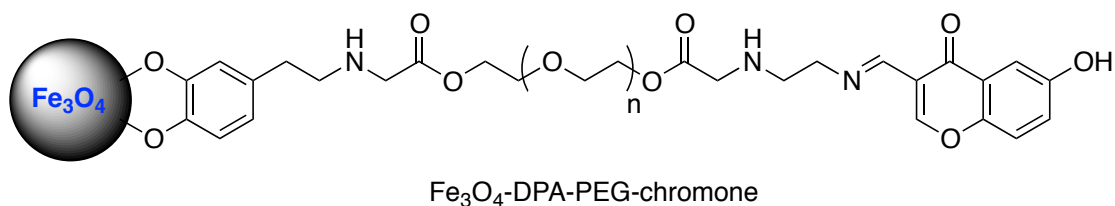


**Figure 2.30. PEG-decorated  $\text{Fe}_3\text{O}_4$  particles functionalized with chromone.**

### 2.5.1.5. Conjugation with pH-Sensitive Triazole Bonds

A single case involving a pH-sensitive derivative containing a trityl functionality was reported by Bertrand *et al.* The strategy consisted in replacing one of the phenyl groups in the trityl moiety with a triazole group obtained by a “click” reaction between a PEO-azide and a diarylpropargyl alcohol. Functionalization of the terminal hydroxyl groups with both an alkyne and an anticancer drug yielded a clickable, pH-sensitive prodrug (Figure 2.31). Through variations in the drug and the substituents on the phenyl groups, the hydrolysis half-life of the compounds could be tuned between 1 minute and 4 days.<sup>156</sup>

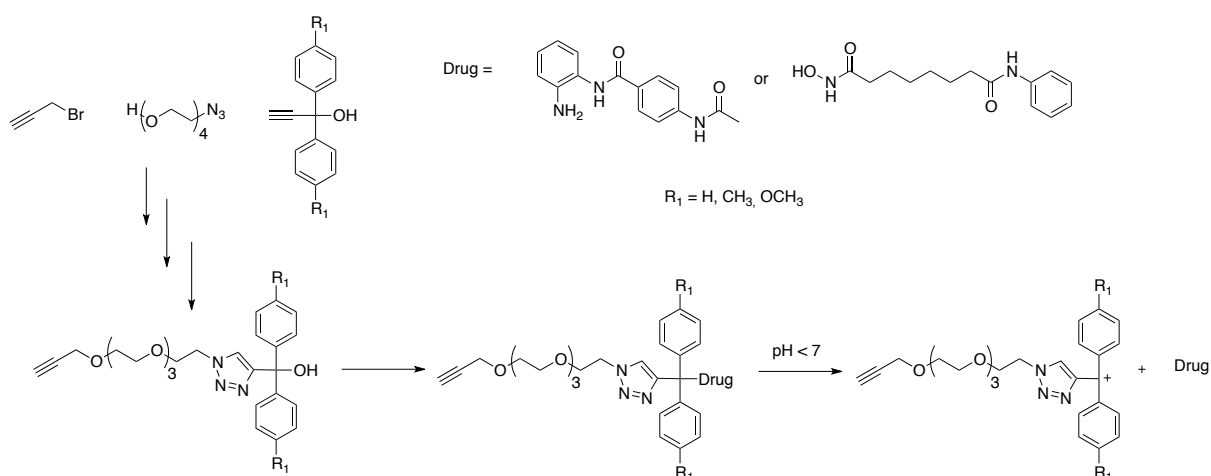


**Figure 2.31. Preparation of pH-sensitive triazole-based prodrug and release under acidic pH.**<sup>156</sup>

### 2.5.2. pH-Sensitive Particles Prepared with ROMP Macromonomers

The preparation of polynorbornene-PEO graft copolymers, by dispersion ROMP of norbornene with a macromonomer, enabled the formation of core-shell particles with a polynorbornene core, and PEO chains forming the shell and stabilizing the particles in the dispersion medium. The recognized biocompatibility of PEO, combined with the non-cytotoxicity of polynorbornene, naturally oriented the applications of these materials towards drug delivery. By terminating the anionic synthesis of the  $\alpha$ -norbornenyl-PEO macromonomer with acidified methanol, the PEO chains could be functionalized with a hydroxyl group.<sup>157, 158</sup> Functionalization of these hydroxyl groups with active molecules prior to the ROMP process made these active molecules available at the periphery of the core-shell particles obtained.

This methodology was first attempted with the anti-inflammatory drug indomethacin, conjugated via a pH-sensitive ester bond.<sup>158</sup> Dispersion ROMP yielded core-shell particles with diameters ranging from 300 to 600 nm. The incorporation of the active compound, and its release were confirmed by UV spectrophotometry to exceed 80% after 48 hours at pH 3 (Figure 2.32). Indomethacin was also introduced in the core of the particles, *via* conjugation with a norbornene monomer. A macromonomer including a hydrophobic and degradable polycaprolactone block was also used, and latex particles with a diameter of around 250 nm were obtained. Degradation of the polycaprolactone block under acidic conditions released the PEO chains, which destabilized the particles and exposed the conjugated indomethacin, thus triggering its release. The polynorbornene and PEO components could then be metabolically degraded. After 48 hours at pH 3, more than 85% release was observed, accompanied by degradation of the latex particles (Figure 2.32).

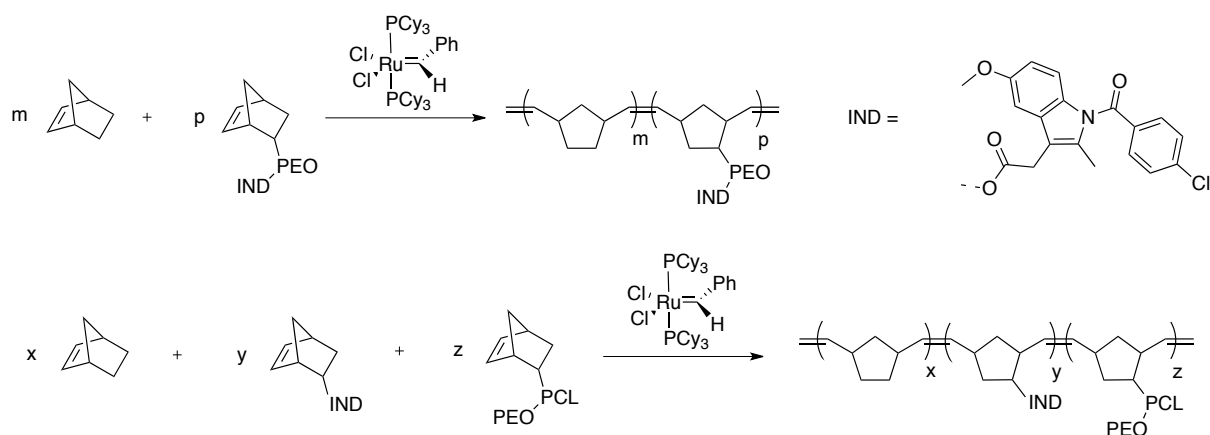


**Figure 2.32. Polynorbornene-*g*-PEO and polynorbornene-*g*-PCL particles prepared by dispersion ROMP for the pH-sensitive release of indomethacin, located at the periphery or within the core of the particles.<sup>158</sup>**

The use of pH-cleavable imine bonds to conjugate the  $\alpha$ -norbornenyl-PEO macromonomer with gentamicin sulphate, an antibiotic molecule, was also described.<sup>159, 160</sup> Particles were prepared by dispersion ROMP of norbornene along with a fraction of non-functionalized macromonomer. Core-shell particles with a diameter of 300 nm were obtained. Release of the drug and the inhibition of *Staphylococcus epidermidis* were studied at acidic pH (4-7), to mimic the acidic environment of infected tissues (Figure 2.33).<sup>159</sup> In a different investigation, the increasingly rapid release of gentamicin sulfate and the inhibition of *Staphylococcus aureus* were observed as the pH decreased below 6.<sup>160</sup> Copolymerization of the bactericide-functionalized macromonomer with a carboxylic acid-terminated macromonomer produced particles with diameters in the 200-350 nm range, which could be anchored onto titanium surfaces of bone implants via amide bonds, to serve in the localized treatment of post-surgery infections. After a 7-day exposure to buffer solutions at pH ranging from 7 to 4, the release of gentamicin from the grafted particles was observed from 0 up to 80% with decreasing pH.<sup>160</sup>

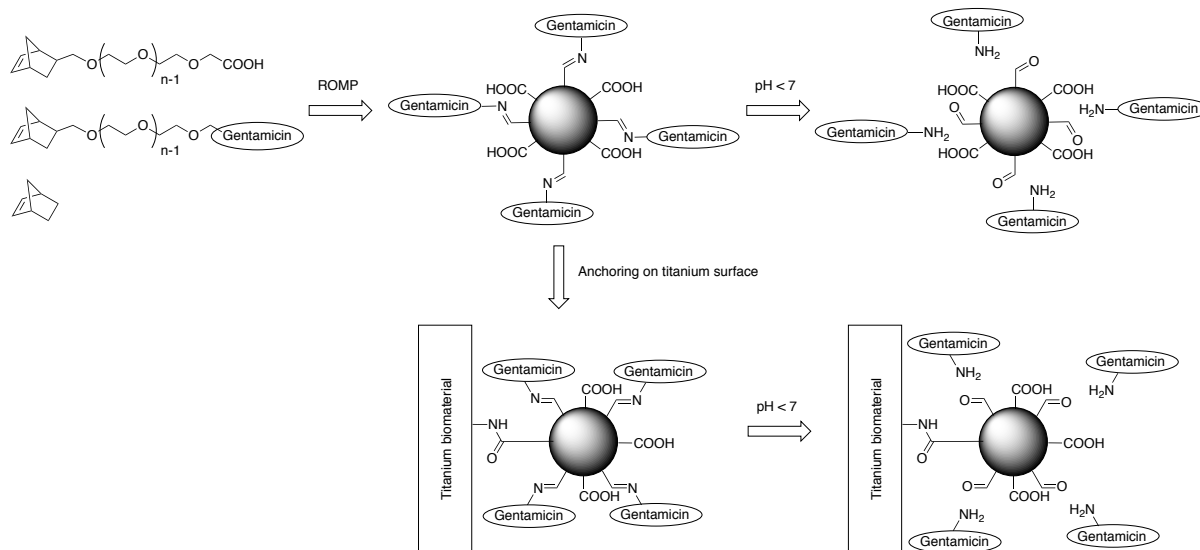


**Figure 2.33. Biomaterials for the pH-sensitive delivery of antibiotic molecules.**<sup>159, 160</sup>

Finally, the PEO-based macromonomers were functionalized with an azide terminal group to enable further conjugation by azide-alkyne click chemistry. Various clickable anticancer prodrugs containing the pH-sensitive triazole bond described previously were thus conjugated to obtain a library of functional macromonomers. Synthesis of the particles by dispersion ROMP led to the formation of 300-380 nm core-shell particles with the active molecules at their surface. Anti-tumor activity was assessed *in vitro*<sup>161</sup> and *in vivo*,<sup>162, 163</sup> with limited toxicity towards healthy organs as compared to the free drug.

## 2.6. Conclusions

The discovery of the ROMP reaction has enabled the preparation of unsaturated polymers starting from strained cyclic olefin monomers. The reaction soon became applicable to less strained cyclic olefins and more tolerant to functional monomers, air and water, thanks to significant advances in organometallic catalysis of the reaction. Various teams utilized this efficient reaction in dispersed media to prepare particles, first with surfactants and then with reactive macromonomers. The functionality of these macromonomers was exploited to conjugate active molecules and obtain surface-functionalized core-shell particles for

applications including anticancer agents and bactericides. The ROMP reaction tolerates well the incorporation of pH-sensitive bonds, which are popular for the design of smart release systems. Depending on the metabolism of the targeted species and the functionalities of the active molecules, various options can be envisioned to design suitable and efficient systems.

The development of fungal strains was inhibited with the use of amine-based biocide molecules. These species produce a decrease in the pH of their environment, even at low concentrations. The choice of pH-sensitive particles synthesized by ROMP is thus perfectly compatible with these applications. The use of macromonomers represents an opportunity for the immobilization of biocides using imine or other bonds, which is justified by the chemical nature of the biocide to conjugate and the range of required sensitivity. Dispersion polymerization permits the use of limited amounts of functional macromonomer to prepare highly surface-functionalized particles.

In the following Chapters, the preparation of multifunctional ROMP reactive macromonomers based upon polyglycidol will be discussed, with full characterization of the different components. The preparation of non-functionalized and biocide-functionalized particles by dispersion ROMP will then be discussed. Given the conjugation of the biocide to the macromonomer or the particles via a pH-sensitive imine bond, another section will report on the release of the biocide under acidic conditions, and on the antifungal properties of the system prepared.

**Chapter 3: Synthesis of  
Multifunctional Polyglycidol-Based  
Macromonomers**

### 3.1 State of the Art in the Preparation and Functionalization of Polyglycidol

Polyglycidol is a water-soluble polyether that attracts increasing interest in the biomedical field due to its biocompatibility<sup>1-3</sup> and high chemical functionality.<sup>4, 5</sup> Polyglycidol can be prepared by cationic ring-opening polymerization of glycidol initiated by Lewis or Brønsted acids,<sup>6-8</sup> but the most widely used method is anionic ring-opening polymerization (ROP). Anionic initiation can be performed with strong bases such as cesium hydroxide or potassium *tert*-butoxide (Figure 3.1(A) **1** and **2** respectively), or with initiators formed *in-situ* from a primary alcohol deprotonated by a strong base. Examples of deprotonating agents include potassium methoxide<sup>9</sup> and diphenylmethyl potassium<sup>10</sup> (DPMK; Figure 3.1(B) **3** and **4**, respectively). High molecular weight polyglycidol, with a molar mass reaching 800,000 g.mol<sup>-1</sup>, was also obtained using a coordinating ZnEt<sub>2</sub> catalyst. Control over the polymerization was reasonable with  $\bar{D} = 1.46$ , considering the high value of the molecular weight.<sup>11</sup>

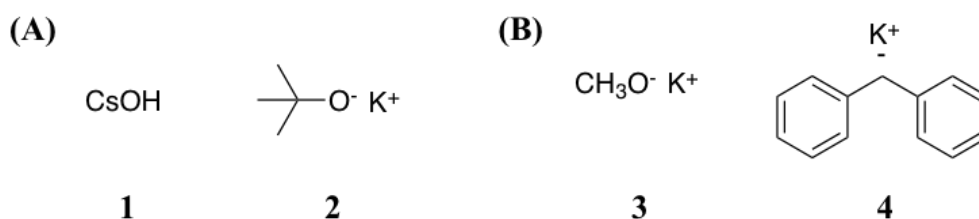
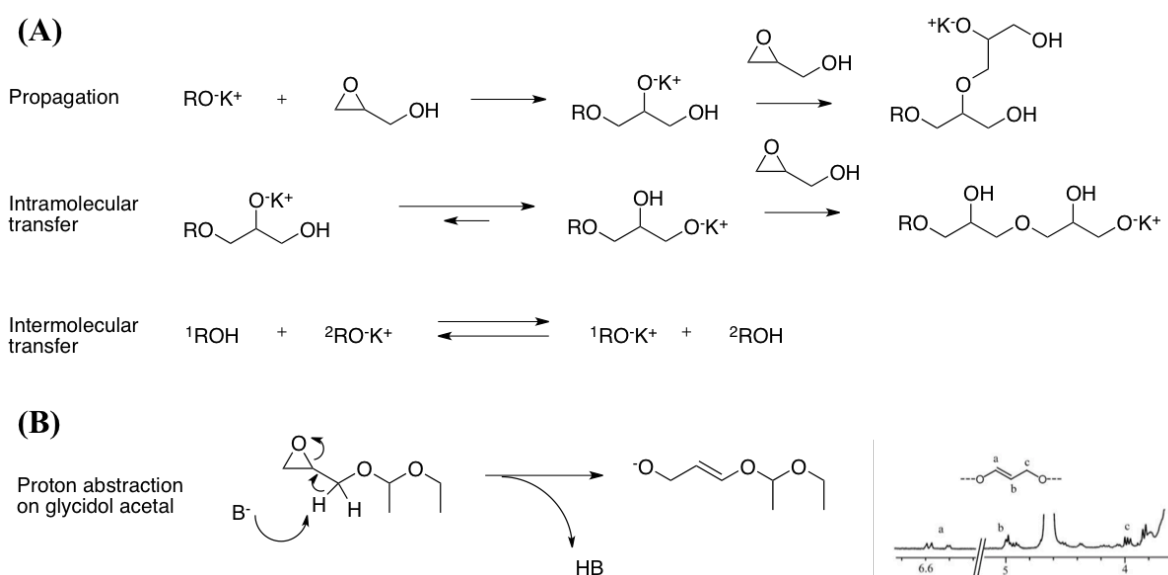


**Figure 3.1. Initiating systems for the anionic ring-opening polymerization of glycidol: (A) Strong bases; (B) Deprotonating agents.**

The polymerization of unprotected glycidol typically leads to the formation of hyperbranched macromolecules.<sup>9, 12-14</sup> This is because the free hydroxyl group in the molecule allows intra- or intermolecular transfer of the propagating center after the ring-opening step (Scheme 3.1(A)). The reaction may then take place on either or both hydroxyl groups to form branched



architectures. A linear polymer chain structure can only be achieved if this hydroxyl group is protected to prevent the chain transfer step. Several examples of protecting groups include ether derivatives,<sup>5, 15, 16</sup> but the most common method was developed by Spassky *et al.* and utilizes an acetal protecting group.<sup>17</sup> A post-polymerization hydrolysis step is therefore required to recover the original glycidol units.<sup>4, 17-20</sup> Control over the anionic ring-opening polymerization of glycidol acetal for alcoholate initiator systems with a potassium counterion was found to be optimal for molecular weights below 30,000 g·mol<sup>-1</sup>, because of a transfer reaction between the active center and the protected monomer. A strong base initiator can abstract a proton from the acetal moiety to form an allyl oxide, that can subsequently reinitiate the polymerization of glycidol acetal (Scheme 3.1(B)).<sup>19</sup> The consequences of this would be a decrease in the overall molecular weight and an increase in polydispersity index. The group of Harth also managed to polymerize unprotected glycidol in aqueous media. Under rather mild conditions (80°C and pH 6), polyglycidol with a low degree of branching, molecular weights around 1500 g·mol<sup>-1</sup> and polydispersity index values between 1.1 and 1.2 was obtained.<sup>21</sup>



**Scheme 3.1. (A) Transfer reactions leading to the formation of branched species, (B) chain transfer to glycidol acetal.<sup>19</sup>**

The combination of controlled polymerization with the protection of glycidol opens the way for controlling the architecture of polyglycidol. Triblock copolymers were thus synthesized by growing poly(glycidol acetal) chains from PEO, poly(propylene oxide) or PS difunctional blocks.<sup>18, 22, 23</sup> Star and dendritic block copolymers were obtained by sequential addition of glycidol derivatives or ethylene oxide to multifunctional alcohol initiators.<sup>24-26</sup> The protection of glycidol was also utilized as a means to control the branching density of copolymers: the group of Dworak synthesized arborescent polyglycidol by polymerization of glycidol acetal, complete deprotection and reinitiated polymerization of glycidol acetal on 10% of the existing hydroxyl groups. When the process was repeated 3 times, molecular weights of up to  $1.8 \times 10^6$   $\text{g} \cdot \text{mol}^{-1}$  were obtained.<sup>4</sup> The same group also obtained pom-pom-like structures by the growth of short poly(glycidol acetal) blocks from each end of a PEO midblock and subsequent hydrolysis of these protected blocks. PEO-*b*-poly(glycidol acetal) segments were then grafted from the hydroxyl functions for 2 additional generations (Figure 3.2). Dendritic polymers with molecular weights up to  $200,000$   $\text{g} \cdot \text{mol}^{-1}$  were obtained with  $\bar{D}$  close to unity by that approach.<sup>12</sup> Interestingly, the polymerization of glycidol from a PEO block was prone to chain transfer even with very slow addition of the monomer, which favored the formation of oligoglycidol and little amounts of grafted structures.

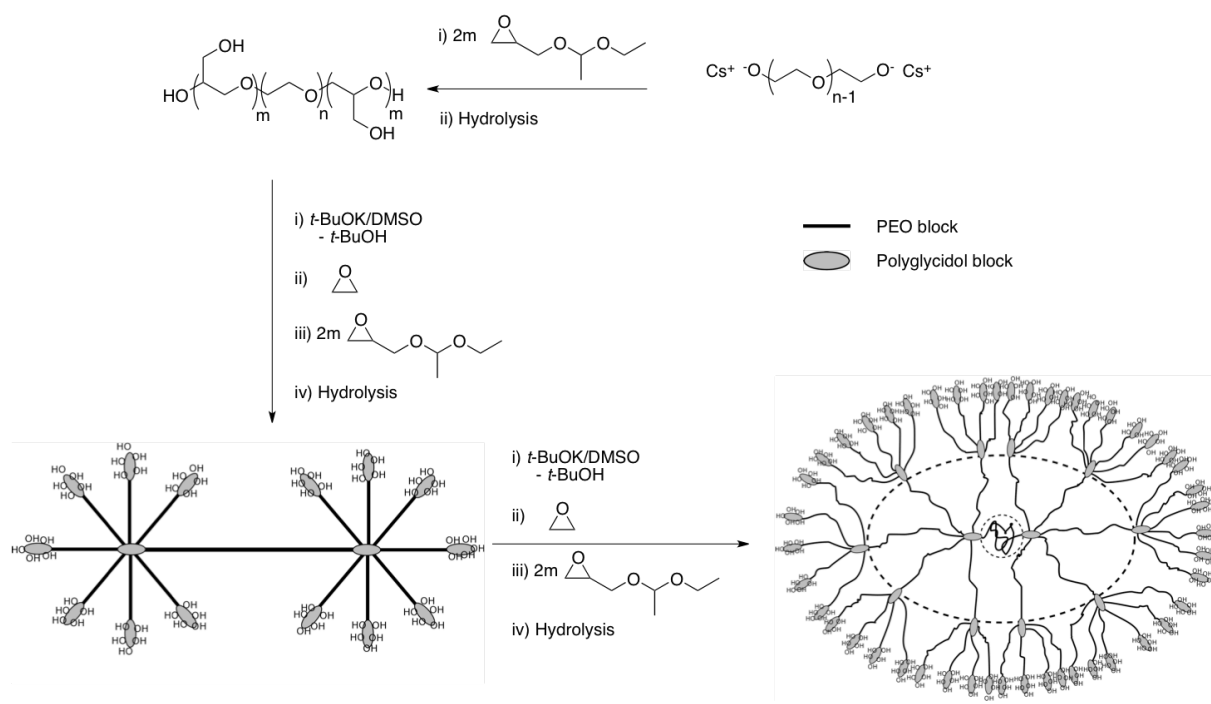


**Figure 3.2. Synthesis of "pom-pom like" structures by sequential generation copolymerization of glycidol acetal and ethylene oxide (Adapted from Dworak *et al.*).<sup>12</sup>**

The high chemical functionality of polyglycidol is an interesting asset because it provides opportunities for applications in a number of fields. Functionalization can be performed in several ways. One possibility consists in using a bifunctional initiator, bearing an additional functional group to yield an  $\alpha$ -functionalized polyglycidol. Amino-functionalized linear and hyperbranched polyglycidols were synthesized in this manner, by initiation with an N,N-dibenzylpropanol derivative and removal of the protecting groups by reduction to obtain a primary amine group (Figure 3.3(A)). These polymers were grafted on gold and glass surfaces to enhance their biocompatibility.<sup>27-29</sup> The group of Carlotti synthesized  $\alpha$ -azido and  $\alpha$ -bromo polyglycidol using a tetraalkylammonium azide initiator (Figure 3.3(B)), which presents opportunities to design architectures using "click-chemistry".<sup>30, 31</sup> Another strategy consists in preparing  $\omega$ -functionalized polyglycidol using a suitable terminating agent. For example, linear polyglycidol and poly(glyceryl glycerol) bearing a single clickable alkyne group were obtained by termination of the anionic ROP with propargyl bromide.<sup>32</sup>



hydroxymethacrylate by ATRP to give branched polymers.<sup>42</sup> Other methods involved additional steps after termination. Huck *et al.* thus reacted the terminal hydroxyl function with methacryloyl chloride (Figure 3.4(a)),<sup>43</sup> while Frey *et al.* terminated the reaction with propargyl bromide to introduce a terminal alkyne in the polymer, followed by reaction with an azide-functionalized methyl methacrylate derivative (Figure 3.4(d)).<sup>42</sup> It should be noted that, in spite of the wide range of polyglycidol-based macromonomers reported in the literature, no examples of ROMP-reactive macromonomers were found.

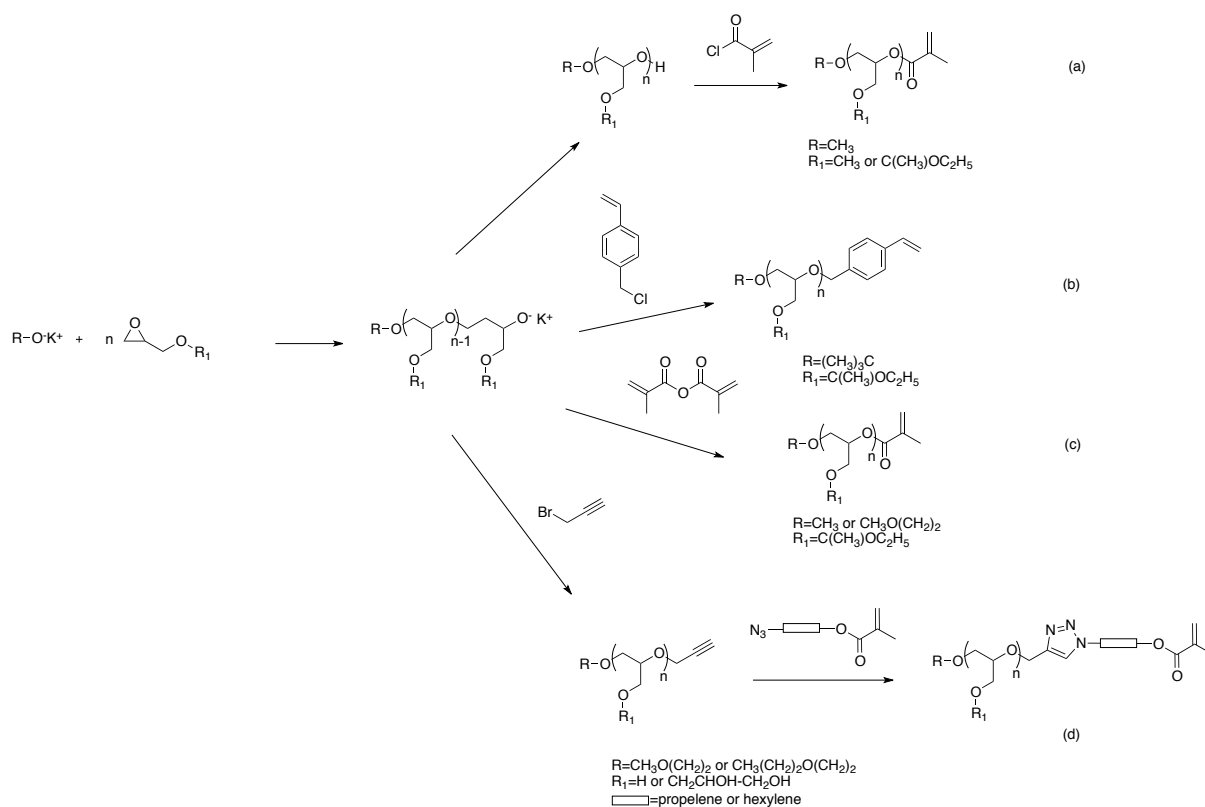


**Figure 3.4. Strategies for the synthesis of polyglycidol-based macromonomers.**

The main objectives of the research described in this Chapter were to investigate the  $\alpha$ -functionalization and post-polymerization functionalization reactions of polyglycidol to design ROMP-reactive macromonomers with immobilized biocide molecules, as building blocks for the design of pH-sensitive particles preventing the development of

microorganisms. A linear polyglycidol-based macromonomer provides multiple reactive sites on a single chain, such that the density of active molecules on the particles can be maximized. The synthesis of various  $\alpha$ -norbornenyl-polyglycidol macromonomers will first be described. Conjugation of the selected biocide with the macromonomer chain through a pH-sensitive imine bond will then be discussed.

## **3.2 Methods and Materials**

### **3.2.1 Synthesis of $\alpha$ -Norbornenyl-Polyglycidol Macromonomers**

The preparation of  $\alpha$ -norbornenyl-polyglycidol macromonomers consisted in three steps, namely the protection of glycidol with an acetal group, the synthesis of the linear macromonomer, and removal of the protecting groups in a final hydrolysis step.

#### **3.2.1.1 Synthesis of Glycidol Acetal**

The glycidol acetal monomer was synthesized by a well-established procedure.<sup>44</sup> *p*-Toluenesulfonic acid (TsOH, 1 g) was added portion-wise to a magnetically stirred solution of 40.0 g (0.54 mol) of 2,3-epoxypropanol (glycidol) in 200 mL (2.09 mol) of ethyl vinyl ether, so as to maintain the temperature below  $-15^{\circ}\text{C}$  while cooling in an ethanol-liquid nitrogen bath. The reaction mixture was stirred for 3 hours and then washed with 100 mL of saturated aqueous  $\text{NaHCO}_3$  solution. The organic phase was dried over  $\text{MgSO}_4$ , filtered, and excess ethyl vinyl ether was removed under reduced pressure. The product was purified by distillation and transferred to an ampoule under nitrogen.

#### **3.2.1.2 Synthesis of $\alpha$ -Norbornenyl-Polyglycidol Macromonomers**

##### **3.2.1.2.1 Preparation of the Deprotonating Agent**

The synthesis of diphenylmethyl potassium (DPMK) was performed as follows. In a flame-dried round-bottomed flask, pieces of potassium (4.95 g, 0.127 mol) were introduced under

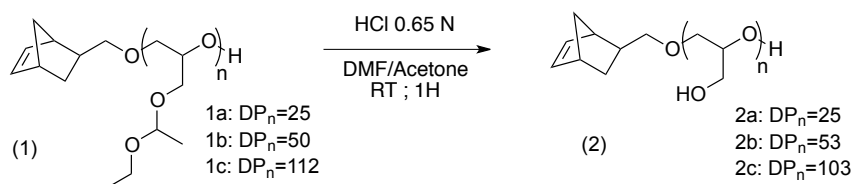
nitrogen flow followed by naphthalene (8.11 g,  $6.3 \times 10^{-2}$  mol, 0.5 equivalent/potassium). Dry tetrahydrofuran (THF, 160 mL) was then added, and the solution was left to stir for 5 hours before the addition of diphenylmethane (21.15 mL, 0.127 mol). The resulting solution was stirred for 2 days and used in the anionic ring-opening polymerization procedure. The DPMK solution needed to be titrated to determine the amount required in the reaction. A flame-dried round-bottomed flask was charged with dry dimethylsulfoxide (DMSO), followed by a few crystals of triphenylmethane, and more DPMK was added until the solution just turned red-orange. Acetanilide (0.200 g,  $1.48 \times 10^{-3}$  mol) was then added, instantly turning the solution to clear light yellow. The resulting solution was titrated with DPMK solution from a flame-dried burette under nitrogen until the orange coloration from the DPMK solution persisted in the titration mixture. Upon further addition of acetanilide, the titration was repeated. Each addition and titration was carried out under inert conditions. The average concentration of DPMK was determined to be  $0.64 \text{ mol} \cdot \text{L}^{-1}$ .

### **3.2.1.2.2 Synthesis of $\alpha$ -Norbornenyl-Poly(glycidol acetal) Macromonomer**

For a macromonomer with a number-average degree of polymerization ( $DP_n$ ) of 25, 1.60 mL ( $1.37 \times 10^{-2}$  mol) of 5-norbornene-2-methanol was added to 200 mL of freshly cryodistilled THF, followed by 17.1 mL of DPMK solution (0.8 equivalent, at  $0.64 \text{ mol} \cdot \text{L}^{-1}$  in THF). Then 50 g (0.342 mol) of glycidol acetal were added to the reaction medium. The reaction was left stirring for approximately 72 hours at  $65^\circ\text{C}$  to attain full monomer conversion. Degassed acidified methanol (5-7 drops of concentrated HCl in 5 mL) was then added drop-wise to stop the polymerization and the solvent was removed by rotary evaporation. The macromonomer was dialyzed for 2-3 days against ethanol in a regenerated cellulose membrane with a 1000 Da molecular weight cut-off (MWCO). The purified  $\alpha$ -norbornenyl-poly(glycidol acetal) macromonomer (**1a-c**) was dried under vacuum. Yield: 60%.

### 3.2.1.3 Hydrolysis of $\alpha$ -Norbornenyl-Poly(glycidol acetal) Macromonomers

The  $\alpha$ -norbornenyl-poly(glycidol acetal) macromonomers were hydrolyzed by the following method, adapted from Spassky (Scheme 3.2).<sup>17</sup> In a typical experiment, the macromonomer (**1a-c**; 1.65 g, 11.1 mmol acetal units) was dissolved in 75 mL of a mixture of N,N-dimethylformamide (DMF)/acetone (1:4 v/v), and 4.5 mL of concentrated hydrochloric acid solution (HCl; 11.7 mol.L<sup>-1</sup>) were added. The reaction was stirred for 1 hour, and enough saturated aqueous Na<sub>2</sub>CO<sub>3</sub> solution was added to reach pH 8 (monitored with pH paper). The solvent was removed under reduced pressure, the product was redissolved in 50 mL of ethanol, and the solution was filtered to remove residual salts. The ethanol was then evaporated and the macromonomer was redissolved in 50 mL of water. Further purification of the sample was carried out by ultrafiltration in water using a regenerated cellulose membrane with a MWCO of 1000 Da. The deprotected  $\alpha$ -norbornenyl-polyglycidol macromonomer (**2a-c**) was finally lyophilized in water. Yield: 65%.



**Scheme 3.2.** Hydrolysis of  $\alpha$ -norbornenyl-poly(glycidol acetal) macromonomers.

## 3.2.2 Preparation of Biocide-Functionalized Macromonomers

### 3.2.2.1 Functionalization of the Polyglycidol Chains

In a typical experiment, 1 g of macromonomer (**2c**; DP<sub>n</sub> = 103) was dissolved in 30 mL of dry DMF. Sodium hydride (NaH, dispersed in mineral oil 60% w/w; 3.24 g, 10 equivalents per hydroxyl units on the macromonomer), previously washed with heptane to remove the



mineral oil, was dispersed in 50 mL of dry DMF. The macromonomer solution was then added drop-wise with stirring under nitrogen. After 30 min, bromoacetaldehyde diethyl acetal (2, 3, 4 or 6 equivalents per hydroxyl unit) was added drop-wise and the reaction mixture was stirred for 12 hours at 60°C. Excess NaH was neutralized by drop-wise addition of concentrated HCl, the mixture was evaporated, the product was redissolved in dichloromethane (DCM), washed at least 5 times with 15 mL aliquots of water and brine, filtered and dialyzed against ethanol for 2 days. Finally, product (**3c**) was dried under vacuum. Yield: 40-60%.

### **3.2.2.2 Dodecylamine Functionalization of the Macromonomers**

The macromonomer (**3c**; 0.5 g;  $2.98 \times 10^{-5}$  mol;  $DP_n = 103$ ) was dissolved in 6 mL of 3 N HCl and stirred for 6 hours at room temperature. Triethylamine was added to the medium to neutralize the acid, and the pH was adjusted to 13 with 50 mL of alkaline solution (pH 13, composition: KCl 0.37%, NaOH 0.53%). Dodecylamine (0.345 g, 0.8 equivalent per acetaldehyde function on the macromonomer) was dissolved in 3 mL of absolute ethanol, and 40 mL of absolute ethanol were added to the reaction medium to reach a 60:40 ratio (H<sub>2</sub>O:EtOH v/v). The dodecylamine solution was then added dropwise and the reaction was left to stir overnight.

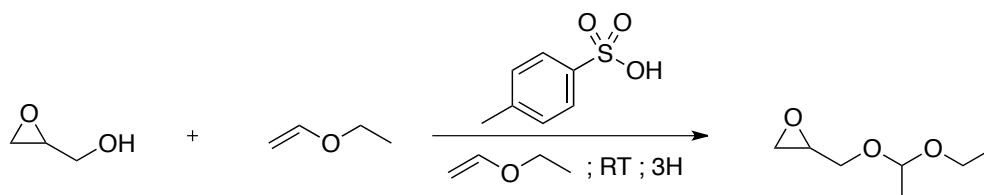
## **3.3 Results and Discussion**

### **3.3.1 Synthesis of $\alpha$ -Norbornenyl-Polyglycidol Macromonomers**

#### **3.3.1.1 Synthesis of Glycidol Acetal**

The first step in the  $\alpha$ -norbornenyl-polyglycidol macromonomer synthesis was the protection of the glycidol monomer (Scheme 3.3), to obtain a linear macromonomer devoid of branching. The structure of the protected monomer was confirmed by <sup>1</sup>H NMR analysis after

purification (Figure 3.5). Characteristic peaks corresponding to the acetal functionality were observed at  $\delta$  1-1.25 and 4.65 ppm. The good agreement of the peak integrals with the expected values also confirmed the purity of the compound.



**Scheme 3.3. Synthesis of glycidol acetal.**

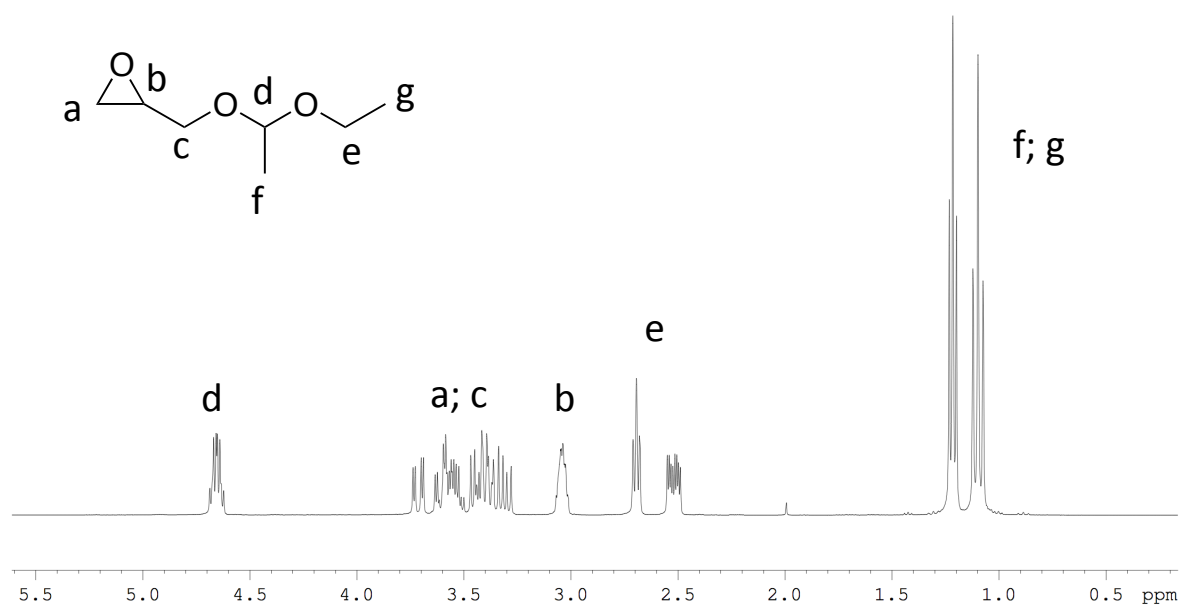
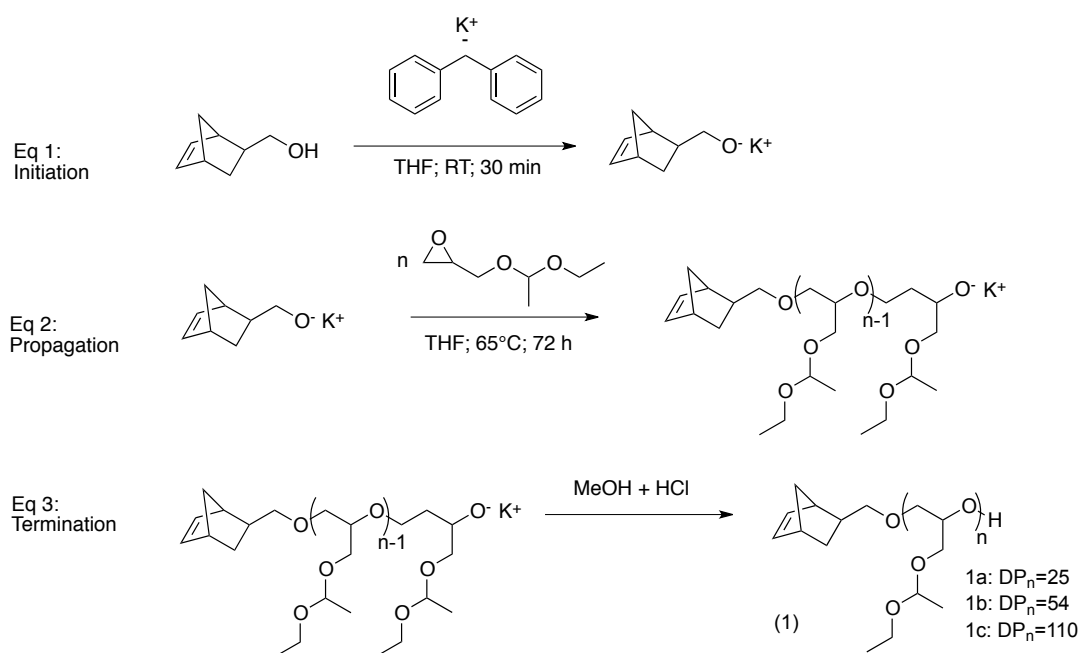


**Figure 3.5.  $^1\text{H}$  NMR spectrum for glycidol acetal.**

### 3.3.1.2 Synthesis of $\alpha$ -Norbornenyl-Poly(glycidol acetal) Macromonomers

In the second step, the glycidol acetal monomer was polymerized by anionic ring-opening polymerization initiated with 5-norbornene-2-methanol. DPMK was selected as a deprotonating agent to generate active alcoholate species. This approach provides a potassium

counterion for the controlled polymerization of glycidol acetal (Scheme 3.4, Eq. 1). The propagation step involves nucleophilic attack of the alcoholate active center on the glycidol acetal ring, which still leaves an alcoholate active chain-end (Scheme 3.4, Eq. 2). Termination was achieved with acidic methanol to re-protonate the alcoholate species (Scheme 3.4, Eq. 3).



**Scheme 3.4. Mechanism for the anionic ring-opening polymerization of glycidol acetal.**

Three poly(glycidol acetal) macromonomers (**1a-c**) were synthesized with different target degrees of polymerization ( $DP_{n,Th}$ ) depending on the relative amounts of monomer and initiator used. The macromonomers were characterized by  $^1H$  NMR spectroscopy to determine their structure (Figure 3.6; Figure C.3 and Figure C.4 in Appendix C.; Table 3.1). The expected peaks were observed in the  $^1H$  NMR spectra, as well as peaks at  $\delta$  5.9-6.15 ppm corresponding to the ethylenic protons of the norbornenyl moiety. By integration of these peaks and the peak corresponding to the CH protons of the glycidol acetal units ( $\delta$  4.71 ppm), the experimental  $DP_n$  ( $DP_{n,NMR}$ ) of the macromonomers was determined for comparison to the  $DP_{n,Th}$  calculated from the amounts of 5-norbornene-2-methanol and glycidol acetal monomer

used in the reactions. The good agreement between these two values confirmed that all the chains were functionalized with one norbornenyl moiety, without side reactions in the macromonomer synthesis. The  $DP_{n,NMR}$  values were also used to calculate the number-average molecular weight of the macromonomers ( $M_{n,NMR}$ ). Zooming in the area from 6.6 to 5 ppm in the  $^1H$  NMR spectrum showed little presence of allyl peaks (less than 2.5% versus the norbornene groups). Thus chain transfer to the monomer was very limited within the molecular weight range of interest.

Size exclusion chromatography (SEC) analysis of the polymers yielded monomodal distributions with narrow molecular weight distributions, which confirms good control over the anionic polymerization reaction for the conditions used (Figure 3.7). Indeed, the initiator was stirred for 30 minutes in the presence of DPMK to ensure complete deprotonation. Quick addition of the monomer and the thermodynamic equilibrium between the active  $R-O^-$  and inactive  $R-OH$  species enabled growth of all the chains at the same rate.

Analysis of sample (**1a**) by matrix-assisted laser desorption/ionization time of flight mass spectroscopy (MALDI-ToF) showed a dominant population that coincided with linear chains functionalized with norbornene with a peak-to-peak mass increment of  $146 \text{ g mol}^{-1}$ , corresponding to the molar mass of a glycidol acetal monomeric unit (Figure 3.8). A second population was observed with a much lower intensity. The assignment of the molar mass values corresponded to a partially hydrolyzed linear chain, which could be explained by hydrolysis of the sample inside the acidic analysis matrix. The number-average molecular weight obtained by this technique was also in good agreement with the  $^1H$  NMR results ( $M_{n,MALDI} = 3655 \text{ g mol}^{-1}$  vs  $M_{n,NMR} = 3780 \text{ g mol}^{-1}$ ). This method did not confirm nor infirm the importance of chain transfer to the monomer, as initiation by an allyl oxide moiety would yield a population with the exact same molecular weight as initiation with 5-norbornene-2-methanol. However, the very close agreement between the theoretical and experimental  $DP_n$

establishes that transfer to the monomer was insignificant. MALDI-ToF spectroscopies for compounds **(1a)** and **(1b)** are provided in Figure C.5 and Figure C.6 in Appendix C:

**Table 3.1. Characteristics of the  $\alpha$ -norbornenyl-poly(glycidol acetal) macromonomers.**

Macromonomer	$DP_{n;Th}$ <sup>1</sup>	$DP_{n;NMR}$ <sup>2</sup>	$M_{n;NMR}$ ( $g \cdot mol^{-1}$ ) <sup>3</sup>	$M_{n;SEC}$ ( $g \cdot mol^{-1}$ ) <sup>4</sup>	$\bar{D} (M_w/M_n)$ <sup>4</sup>
<b>(1a)</b>	25	23	3780	3710	1.06
<b>(1b)</b>	54	50	7420	7630	1.09
<b>(1c)</b>	110	103	15160	12080	1.14

<sup>1</sup> $DP_{n;Th} = n_{mono} / n_{NbOH}$ , where  $n_{mono}$  and  $n_{NbOH}$  are the initial amounts of monomer and 5-norbornene-2-methanol, respectively; <sup>2</sup> $DP_{n;NMR} = 2 I_{CH} / I_{Nb}$ , where  $I_{Nb}$ : integration of the ethylenic protons of norbornene,  $I_{CH}$ : integration of the CH proton of the acetal group; <sup>3</sup> $M_{n;NMR} = M_{Nb} + 146 DP_{n;NMR}$ ,  $M_{Nb} = 124 g mol^{-1}$  is the molecular weight of the norbornenyl moiety, 146 is the molecular weight of the glycidol acetal unit; <sup>4</sup> Determined by SEC analysis in THF.

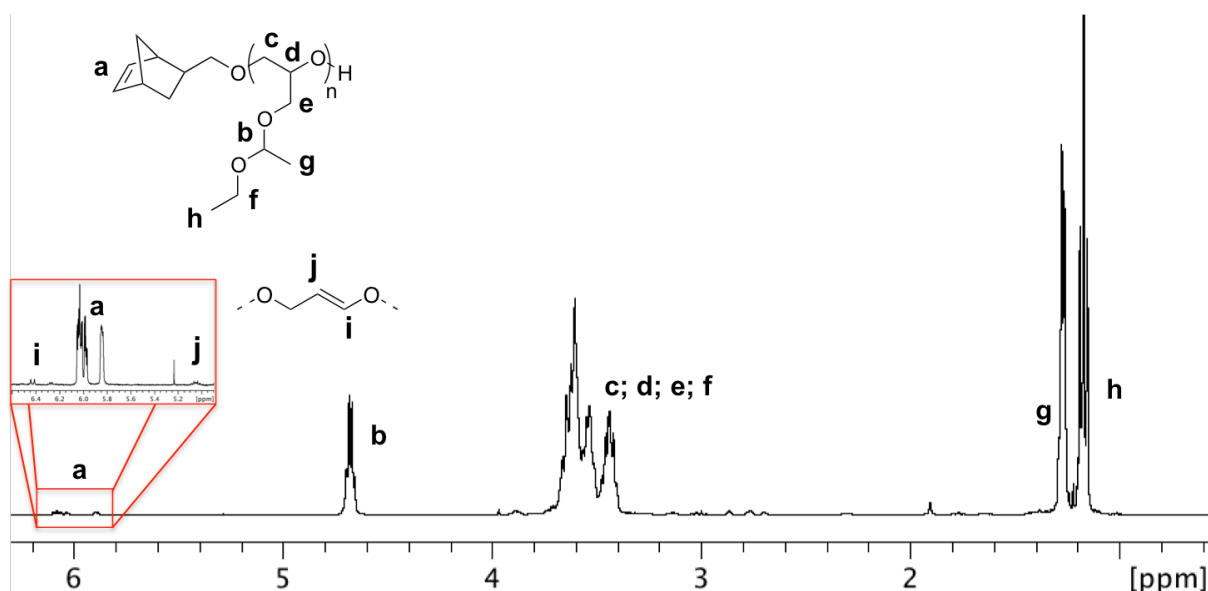


**Figure 3.6.** <sup>1</sup>H NMR spectrum for  $\alpha$ -norbornenyl-poly(glycidol acetal) macromonomer **(1a)** in  $CDCl_3$  ( $DP_{n;Th} = 25$ ).

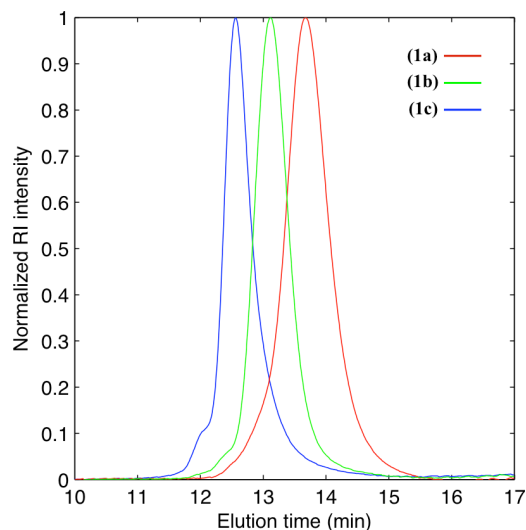


**Figure 3.7.** SEC profiles for  $\alpha$ -norbornenyl-poly(glycidol acetal) macromonomers (1a-c) in THF.

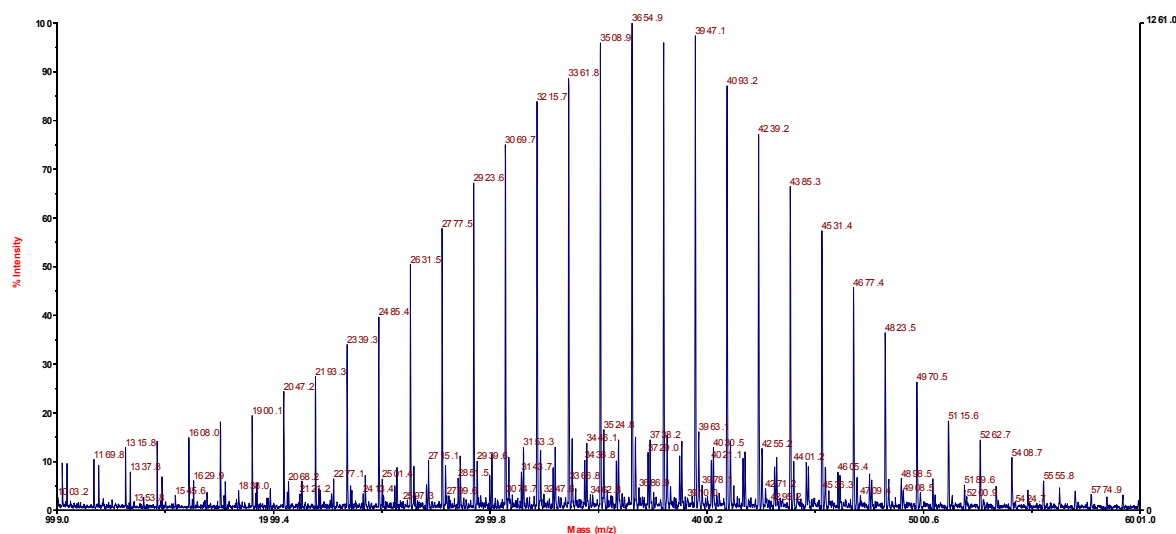


**Figure 3.8.** MALDI-ToF of macromonomer (1a).

### 3.3.1.3 Hydrolysis of $\alpha$ -Norbornenyl-Poly(glycidol acetal) Macromonomers

The hydroxyl functions of polyglycidol were recovered *via* hydrolysis of the acetal groups by a method adapted from Spassky (Scheme 3.2).<sup>17</sup> After one hour of reaction and purification by ultrafiltration, the products (**2a-c**) were characterized by <sup>1</sup>H NMR and SEC analysis. Total

disappearance of the peaks corresponding to the CH ( $\delta$  4.71 ppm) and the CH<sub>3</sub> ( $\delta$  1.12-1.48 ppm) units of the acetal groups was observed in the <sup>1</sup>H NMR spectrum, confirming total deprotection (Figure 3.9). By integration of the two protons for the norbornenyl moiety ( $I_{Nb}$ ) and the glycidol units (5 DP<sub>n</sub> protons), the number-average degree of polymerization of the deprotected macromonomer (DP<sub>n;NMR</sub>) could be calculated. This value was close to the DP<sub>n</sub> determined before deprotection, which confirms the preservation of the norbornenyl moiety and the absence of degradation of the polymer chains in the hydrolysis step. SEC analysis could not be performed in THF because the deprotected polyglycidol chains were insoluble in this solvent. Results obtained in DMF after deprotection still confirmed monomodal distributions with rather narrow distributions (Figure 3.10; Table 3.2).

The initiation of anionic ROP by a norbornene derivative, combined with the protection of glycidol, provided well-defined linear norbornene-functionalized polyglycidol macromonomers. The length of the polymer chains was controlled through variations in the monomer/initiator ratio. These polyhydroxylated macromonomers are foreseen as useful platforms for the conjugation of bioactive molecules.

**Table 3.2. Characteristics of the  $\alpha$ -norbornenyl-polyglycidol macromonomers.**

Macromonomer	DP <sub>n;Th</sub> <sup>1</sup>	DP <sub>n;NMR</sub> <sup>2</sup>	M <sub>n;NMR</sub> (g·mol <sup>-1</sup> ) <sup>3</sup>	M <sub>n;SEC</sub> (g·mol <sup>-1</sup> ) <sup>4</sup>	D (M <sub>w</sub> /M <sub>n</sub> ) <sup>4</sup>
<b>(2a)</b>	23	25	1975	2340	1.18
<b>(2b)</b>	50	53	4050	4000	1.15
<b>(2c)</b>	103	103	7750	n/a	n/a

<sup>1</sup>DP<sub>n;Th</sub> (2a-c) = DP<sub>n;NMR</sub> (1a-c), the hydrolysis reaction was assumed not to affect the DP<sub>n</sub>; <sup>2</sup>DP<sub>n;NMR</sub> = 2 I<sub>PGLD</sub> / 5 I<sub>Nb</sub>, where I<sub>PGLD</sub> is the integration of the polyglycidol protons, <sup>1</sup>H NMR spectra acquired in D<sub>2</sub>O; <sup>3</sup>M<sub>n;NMR</sub> = M<sub>Nb</sub> + 74 DP<sub>n;NMR</sub>, where M<sub>Nb</sub> = 124 g·mol<sup>-1</sup> is the molecular weight of the norbornenyl moiety, 74 is the molecular weight of the glycidol unit; <sup>4</sup>Determined by SEC analysis in DMF.

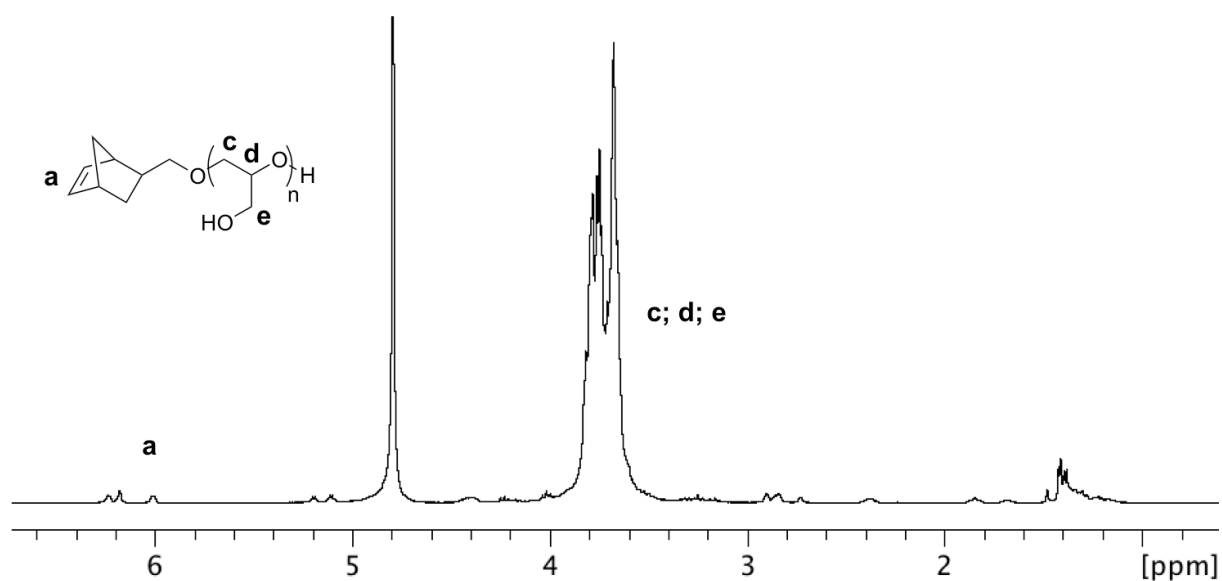


Figure 3.9.  $^1\text{H}$  NMR spectrum for  $\alpha$ -norbornenyl-polyglycidol macromonomer (2a;  $\text{DP}_{n;\text{NMR}} = 25$ ) in  $\text{D}_2\text{O}$ .

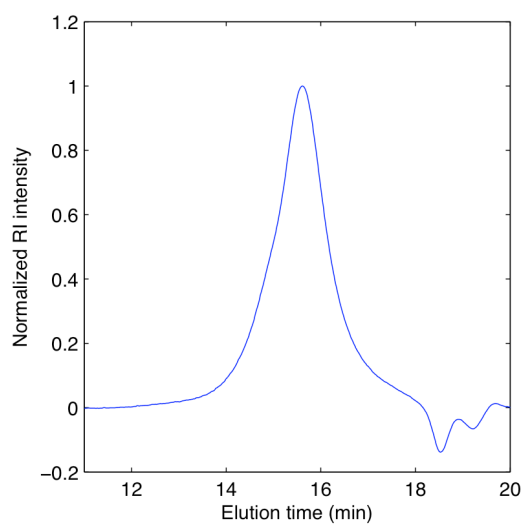


Figure 3.10. SEC trace for the  $\alpha$ -norbornenyl-polyglycidol macromonomer (2a) in DMF.

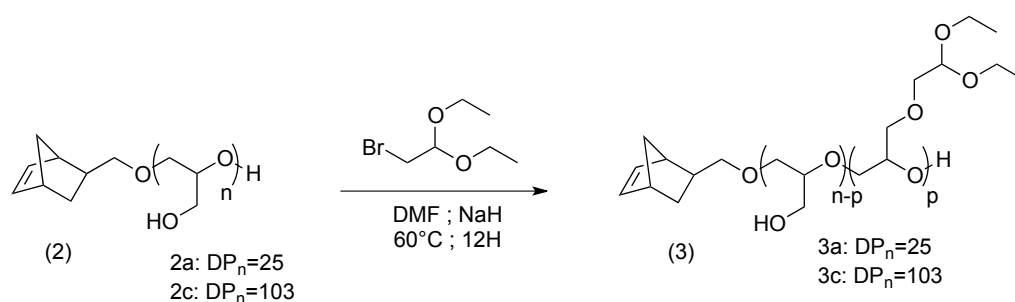


### 3.4 Preparation of Biocide-Functionalized Macromonomers

The well-defined linear polyglycidol macromonomers were utilized as multifunctional substrates, by making use of their hydroxyl groups to introduce a biocide through a pH-sensitive bond.

#### 3.4.1 Functionalization of the Polyglycidol Chains

As discussed in Chapter 2, the formation of an imine group requires the conjugation of a primary amine with an aldehyde moiety. To use the polyglycidol substrate as a host for active molecules, the hydroxyl functions of the repeating units needed to be derivatized to contain aldehyde groups. To avoid the degradation of these functional groups under the conditions used, a protected aldehyde derivative, namely an acetaldehyde diethyl acetal, was introduced on the backbone before further modification. The functionalization consisted in a Williamson nucleophilic substitution between the hydroxyl groups of the polyglycidol macromonomer and a bromine-functionalized acetaldehyde diethyl acetal (Scheme 3.5). Because the macromonomer with the highest  $DP_n$  had the largest number of hydroxyl groups available for conjugation, investigations were first undertaken with macromonomer (**2c**), having a  $DP_{n,NMR}$  of 103.



**Scheme 3.5. Functionalization of  $\alpha$ -norbornenyl-polyglycidol macromonomers (2) with acetaldehyde diethyl acetal moieties.**

For this study, different ratios of bromoacetal per hydroxyl group were tested to obtain a range of functionalized macromonomers (Table 3.3). These macromonomers were characterized by  $^1\text{H}$  NMR analysis (Figure 3.11), by confirming the appearance of a triplet for the  $-\text{CH}_3$  protons of the acetal moiety ( $I_{\text{CH}_3}$ ; 6H;  $\delta$  1.0-1.19 ppm). Assuming conservation of the  $\text{DP}_n$  of the macromonomer, the number of modified groups per chain was calculated using Equation (3.1):

$$N_{\text{Acetal}} = \frac{I_{\text{CH}_3}/6}{I_{\text{Nb}}/2} \quad (3.1)$$

As shown in Table 3.3, none of the attempts yielded quantitative functionalization of the hydroxyl functions, even for large excesses of brominated reagent. The acetaldehyde diethyl acetal group being quite bulky, it may hinder access to the remaining hydroxyl functions when it is coupled with the polyglycidol chain. As also shown in Table 3.3 and in Figure 3.11, when the number of hydroxyl groups per chain was constant, increasing the number of equivalents of bromoacetal resulted in an increase of the functionalization level. Hindrance may therefore be counterbalanced to some extent by higher reagent concentrations. With 6 equivalents of bromoacetal per hydroxyl group, a maximum of 78 units out of 103 were functionalized for **(3c)**. Consequently, these conditions were also used for the shorter macromonomer **(2a)** ( $\text{DP}_{n;\text{NMR}} = 25$ ) to obtain **(3a)**.

Comparatively to **(3c)**, the fraction of functionalized units for **(3a)** was not as high (Table 3.3), and more importantly, the reaction yield was below 20% as compared to 40-60% for **(3c)**. Indeed, the aqueous phase after the extraction step of the purification was ultrafiltered and analyzed by  $^1\text{H}$  NMR. The spectrum showed very low integrations for the  $-\text{CH}_3$  protons of the acetal group, suggesting very low functionalization yields (result not shown). It is postulated that NaH in DMF at  $60^\circ\text{C}$  was mainly involved in degradation of the solvent into

sodium formate and dimethylamine.<sup>45-47</sup> Its ability to deprotonate the hydroxyl functions of polyglycidol was limited, and the chains were thus poorly functionalized.

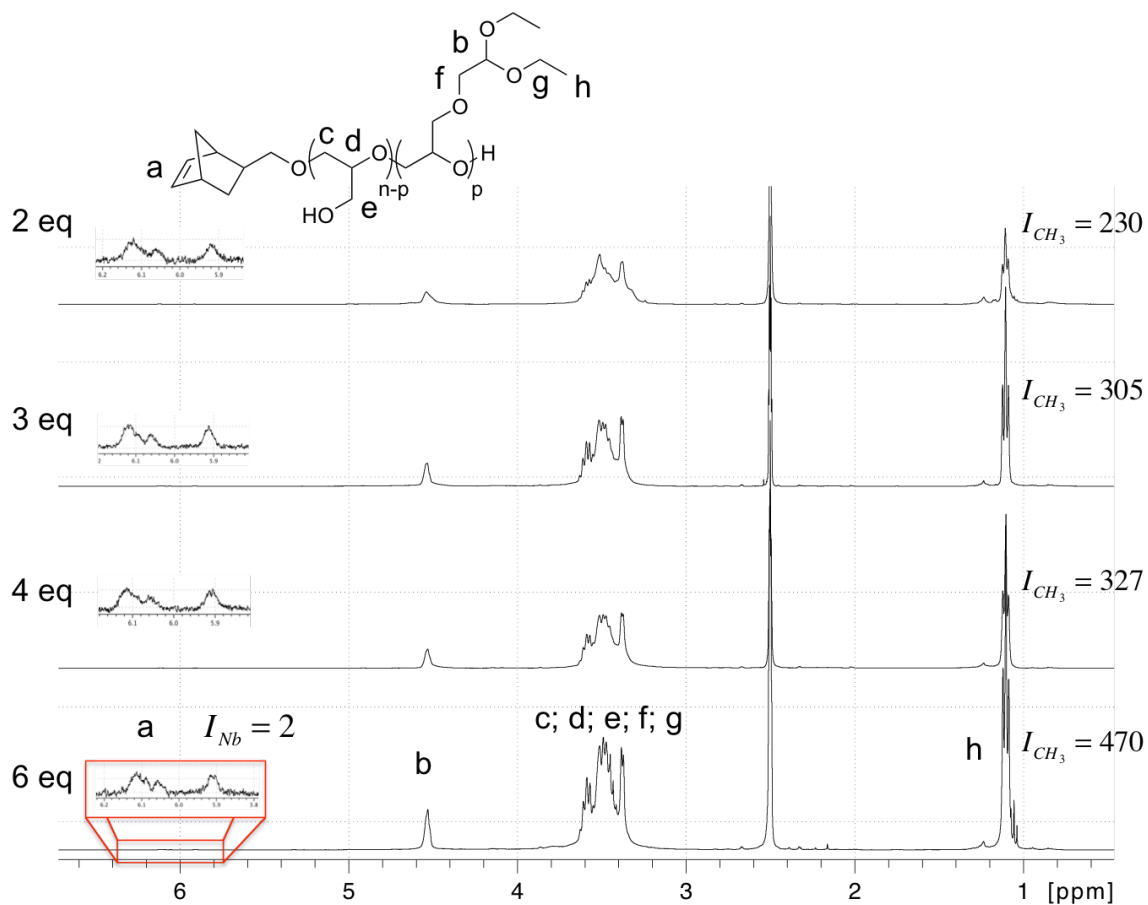


**Figure 3.11.**  $^1\text{H}$  NMR spectra in  $\text{DMSO-}d_6$  for acetaldehyde diethyl acetal-functionalized  $\alpha$ -norbornenyl-polyglycidol macromonomer (3c) versus amount of bromoacetal added.

**Table 3.3. Characteristics of the acetaldehyde diethyl acetal-functionalized  $\alpha$ -norbornenyl-polyglycidol macromonomers.**

Macromonomer	DP <sub>n,NMR</sub> (-OH groups/chain)	[Bromoacetal] /[-OH group]	Modified units/chain ( <sup>1</sup> H NMR)
<b>(3c)</b>	103	2	38
<b>(3c)</b>	103	3	51
<b>(3c)</b>	103	4	55
<b>(3c)</b>	103	6	78
<b>(3a)</b>	25	6	14

#### 3.4.1.1 Optimization of Reaction for Macromonomer (3a, DP<sub>n</sub> = 25)

Since the supposed preferential reaction of NaH with DMF may have been favored by the high temperature used (60°C), milder conditions were investigated in an attempt to reduce this secondary mechanism and favor the deprotonation of the hydroxyl functions. The reaction was thus attempted with **(3a)** at room temperature, with a maximum yield of 6% after 72 hours (Table 3.4). While these conditions prevented the degradation of DMF, the temperature may not have been elevated enough to promote subsequent substitution by the brominated compound. The reaction was thus left at room temperature for 4 hours after the reagents were added, to enable full deprotonation of the hydroxyl groups, and then heated to 60°C. Under these conditions the yield was increased to 65-90%, even when the amount of NaH was reduced to 5 equivalents per hydroxyl group (Table 3.4). <sup>1</sup>H NMR analysis of the resulting macromonomer showed that on average, 20 out of the 25 units were functionalized by this method. However the SEC traces showed a shoulder with a peak at a molecular weight doubled relatively to the main product (Figure 3.12). Analysis of the sample by MALDI-ToF

also showed several overlapping populations, assigned to linear chains containing varying numbers of glycidol and glycidol acetaldehyde diethyl acetal units and a single norbornenyl group (Figure C.7 in Appendix C:). No other population corresponding to degradation or coupling of the chains was observed, and functionalization with acetaldehyde diethyl acetal groups could thus be confirmed. The shoulder observed by SEC was therefore likely due to aggregation in the solvent. Moreover, the dominant peaks observed by MALDI corresponded to a  $DP_n$  of 29 with 15 functionalized units, which is in rather good agreement with the analysis by  $^1H$  NMR ( $DP_{n,NMR} = 25$ ).

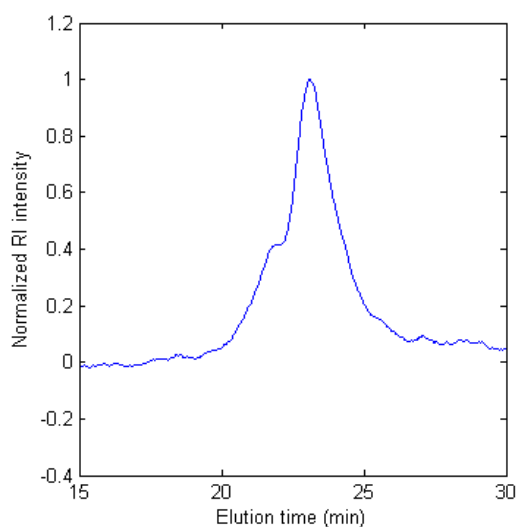


**Figure 3.12. SEC profile for (3a) with optimized yield.**

The method employing the Williamson reaction for the introduction of acetaldehyde diethyl acetal groups proved to be useful to obtain a range of activated  $\alpha$ -norbornenyl-polyglycidol macromonomers. For larger amounts of bromoacetal, very high functionalization levels could be reached to provide numerous sites per chain for further modification.

**Table 3.4. Optimization of the conditions for the preparation of (3a).**

Macromonomer	Temperature (°C)	Duration (h)	Yield (%)	Modified units/chain ( <sup>1</sup> H NMR)
(3c)	60	12	44	78
(3a) <sup>1</sup>	60	12	16	18
(3a) <sup>2</sup>	25	72	6	12
(3a) <sup>2</sup>	25/60	4 + 12	65	21
(3a) <sup>2</sup>	25/60	4 + 48	90	20

<sup>1</sup>  $\alpha$ -Norbornenyl-polyglycidol macromonomer with  $DP_{n,NMR}=23$ ; <sup>2</sup>  $\alpha$ -Norbornenyl-polyglycidol macromonomer with  $DP_{n,NMR}=25$ .

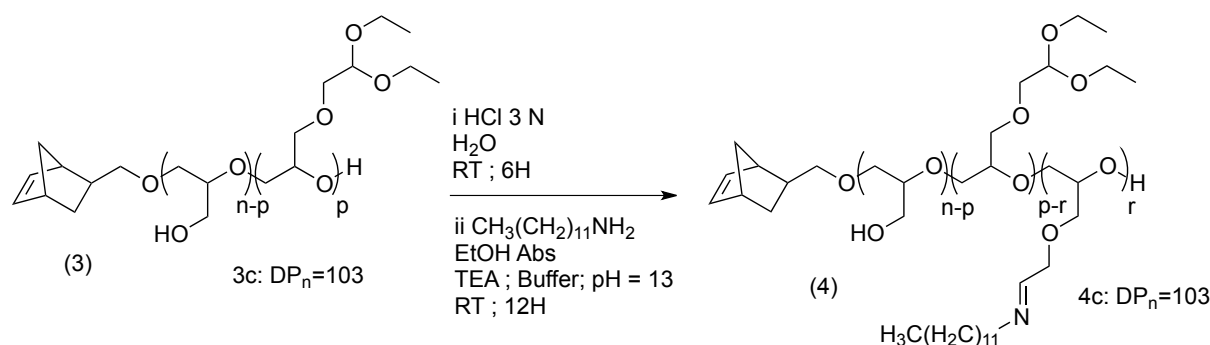
### 3.5 Biocide Functionalization of the Macromonomers

The method used for coupling dodecylamine was adapted from Héroguez *et al.*<sup>48, 49</sup> whereby the acetaldehyde diethyl acetal groups of the  $\alpha$ -norbornenyl-PEO macromonomer were deprotected to the aldehyde under acidic conditions, and then conjugated with a primary amine to form a pH-sensitive imine bond. These two reaction steps were carried out in one pot because of the instability of the aldehyde derivative. The reaction was first attempted with macromonomer (3c), having the most acetaldehyde diethyl acetal functions, to maximize the amount of coupled dodecylamine per chain.

#### 3.5.1 Dodecylamine Functionalization of the Higher Molecular Weight Macromonomer ( $DP_n = 103$ )

The introduction of pH-sensitive imine bonds was first attempted for macromonomer (3c), with a  $DP_n$  of 103 (Scheme 3.6). Taking advantage of the solubility of the macromonomer in water (Table 3.5), the hydrolysis step was performed in 3 N HCl. The pH of the solution was then brought to 13 for the second step of the synthesis. However, because dodecylamine was

not soluble in water, it was dissolved in absolute ethanol (0.8 equivalent per acetaldehyde functionality on macromonomer **(3c)**), and the reaction medium was diluted with absolute ethanol to reach a 60:40 ratio (H<sub>2</sub>O:EtOH v/v). The dodecylamine solution was added dropwise to the reaction medium which was left to stir overnight.



**Scheme 3.6. Dodecylamine functionalization of macromonomer (3c).**

When this method was implemented with macromonomer (3c), a precipitate started to form upon addition of the dodecylamine solution. After overnight stirring, massive precipitation had taken place. The compound was isolated by filtration, but attempts to solubilize it in common organic solvents were unfruitful. Neither <sup>1</sup>H NMR nor SEC studies could thus be conducted on this compound. Another reaction was attempted by replacing the buffer solution with triethylamine in absolute ethanol, to limit the amount of water present, but the same result was obtained. Analysis of the solid by infrared spectroscopy (IR) showed signals corresponding to the presence of imine groups at 1650-1850 cm<sup>-1</sup> (Figure 3.13), attesting that dodecylamine was conjugated to the macromonomer chains, and this was likely the reason for initial precipitation of the compound. Several explanations can be considered for the subsequent lack of solubility in common solvents. Precipitation of the compound would have brought the remaining aldehyde groups in close proximity. Under basic conditions, an aldol condensation reaction between these aldehyde functions would be favored to form an

insoluble network. The basic conditions could also have favored the interchain formation of acetal groups between the hydroxyl and aldehyde functions of the macromonomer, thus creating a crosslinked network. However, these side reactions were not observed previously in the conjugation of gentamicin on a polyglycidol macromonomer.<sup>50</sup> The formation of an insoluble product could also be related directly to the conjugation of dodecylamine with the polyglycidol chains, because the phenomenon appeared at the time of amine addition. The coupling of dodecylamine would lead to a high local density of alkyl segments along the polyglycidol chains, which may have crystallized upon conjugation to the macromonomer.

**Table 3.5. Characteristics of the macromonomers conjugated with dodecylamine.**

Macromonomer	DP <sub>n</sub> ; NMR	Solubility in ethanol, DCM and THF	Dodecylamine functions/chain
<b>(4c)<sup>1</sup></b>	103	No	n/a
<b>(4c)<sup>2</sup></b>	103	Yes	5
<b>(4a)<sup>3</sup></b>	25	No	n/a
<b>(4a)<sup>4</sup></b>	25	Yes	3

<sup>1</sup>Hydrolysis in 3N HCl (6 h), conjugation at pH 13 in absolute ethanol; <sup>2</sup>Hydrolysis in absolute ethanol with 3 N HCl (6 h), conjugation at pH 13 in absolute ethanol; <sup>3</sup>Hydrolysis in DMF/acetone (35/65, v/v) with 0.65 N HCl (6 h), conjugation at pH 7 in absolute ethanol; <sup>4</sup>Hydrolysis in DMF/acetone (35/65, v/v) with 0.65 N HCl (0.5 h), conjugation at pH 7 in absolute ethanol.



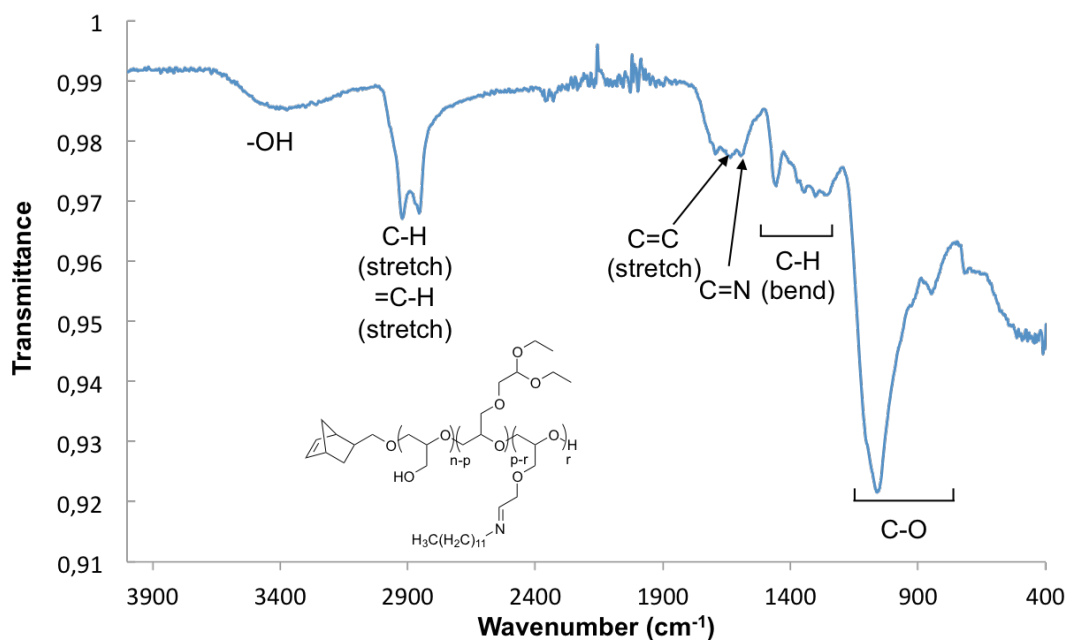


**Figure 3.13. IR spectrum for macromonomer (4c).**

The hydrolysis conditions were modified to decrease the density of coupling sites on the polyglycidol chains, so as not to affect their solubility significantly and/or to decrease their tendency to crystallize. The hydrolysis was thus performed in absolute ethanol with 3 N HCl for 6 hours, before dilution with ethanol and adjusting the pH above 7 with triethylamine. Dodecylamine in ethanol was then added drop-wise to the stirring solution. No precipitation was observed in this case, and the solution remained clear even after stirring overnight. The solution was concentrated on a rotary evaporator and ultrafiltered in ethanol using a polyethersulfone membrane with a MWCO of 5000 Da. The  $^1\text{H}$  NMR spectrum for the final product (**4c**) in Figure 3.14 displays peaks corresponding to both the polyglycidol chain and dodecylamine ( $\delta 0.8$  ppm for  $-\text{CH}_3$  and 1.2 ppm for the  $-\text{CH}_2-$  segments). The peak corresponding to the  $-\text{CH}_3$  protons of the acetaldehyde diethyl acetal groups was still present (30 out of the 78 units were hydrolyzed). Hydrolysis to the free aldehyde was thus effectively limited before the conjugation of dodecylamine with the macromonomer. The extent of

dodecylamine conjugation achieved in this way could be estimated by integration of the characteristic peak for dodecylamine at  $\delta 0.8$  ppm ( $I_{\text{DDA}}$ ; 3H) using Equation (3.2):

$$N_{\text{DDA}} = \frac{I_{\text{DDA}}/3}{I_{\text{Nb}}/2} \quad (3.2)$$

Approximately 9 molecules of dodecylamine were thus coupled per macromonomer chain with 103 repeating units (Table 3.5). This result is nevertheless significant, because the functionalization of a single macromonomer chain with multiple active species was achieved.

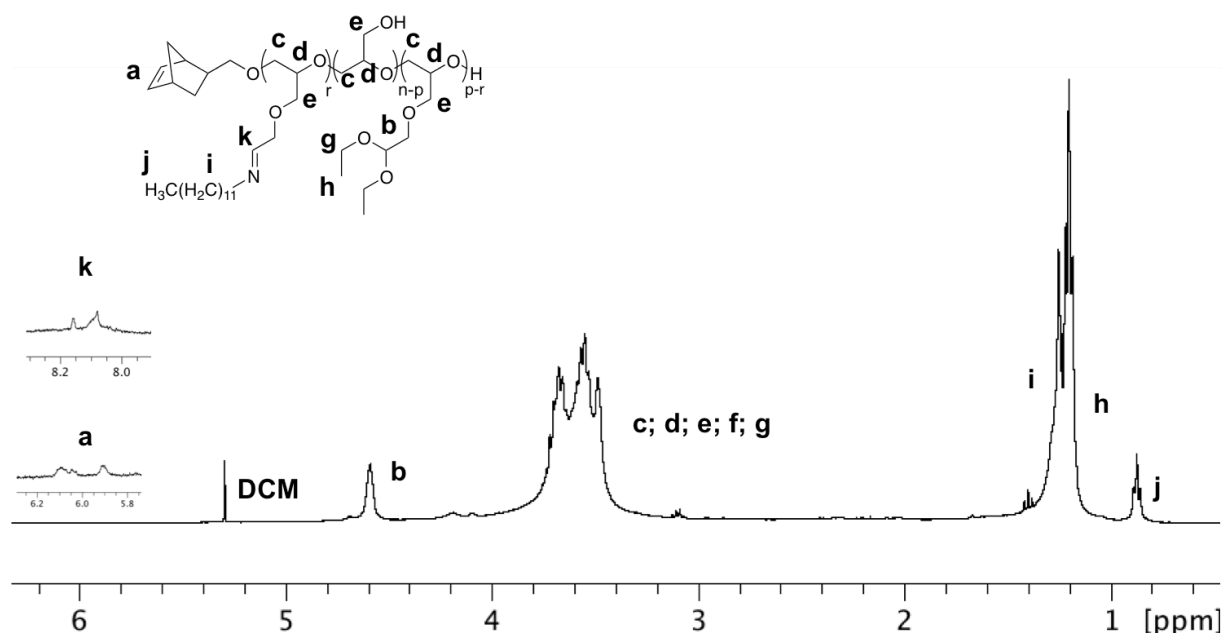


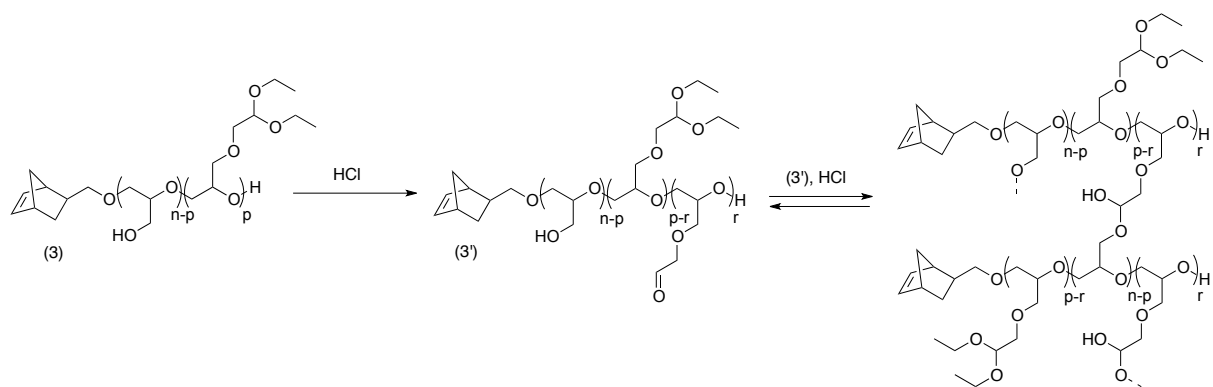
Figure 3.14.  $^1\text{H}$  NMR spectrum for dodecylamine-functionalized macromonomer (**4c**).

### 3.5.2 Dodecylamine Functionalization of the Lower Molecular Weight Macromonomer ( $\text{DP}_n = 25$ )

Considering the very low conjugation level obtained for macromonomer (**4c**) when the dodecylamine was added, the reaction was also attempted on the acetaldehyde diethyl acetal-functionalized macromonomer (**3a**), with a degree of polymerization 4 times lower. The

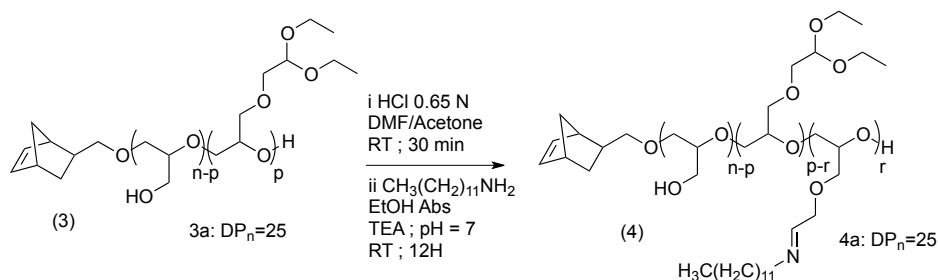
shorter chains should allow easier solubilization of the compound, decrease the crosslinking probability if side reactions of the aldehyde are involved, and would ensure a lower local concentration of dodecylamine, thus hindering crystallization. However the acetaldehyde diethyl acetal-functionalized macromonomer (**3a**) was insoluble in water. Because the hydrolysis of acetaldehyde diethyl acetal functionalities was very limited in absolute ethanol for (**3c**) even with 3 N HCl, a different method for the deprotection of the acetal functions on the poly(glycidol acetal) macromonomer was tested. Thus 0.25 g ( $6.6 \times 10^{-5}$  mol) of macromonomer (**3a**) was dissolved in 6 mL of DMF/acetone (1:4 v/v) and 360  $\mu\text{L}$  of concentrated HCl solution was added to reach a concentration of  $0.65 \text{ mol L}^{-1}$ . The reaction was left to stir for 6 hours.

With this procedure, a precipitate started to appear after about one hour. The solid compound was isolated by filtration. This compound was insoluble in common organic solvents and could not be characterized by  $^1\text{H}$  NMR or SEC analysis. Given the reaction conditions used, the insolubility was attributed to the reaction of the newly formed aldehyde groups on macromonomer (**3'**) under acidic conditions with free hydroxyl groups, to form hemiacetal groups (Scheme 3.7). Because of the multiple functional groups available on each macromonomer chain, intermolecular reactions would easily cause crosslinking of the material. When the reaction was performed in water with the higher molecular weight macromonomer, this crosslinking reaction was not observed. Hemiacetal formation is actually an equilibrium reaction driven by the elimination of water. In the latter case, using water as a solvent (in large excess) should drive the equilibrium towards the non-crosslinked compound (**3'**).



**Scheme 3.7. Intermolecular formation of hemiacetal groups under acidic conditions.**

The effects of this side reaction were thus minimized by decreasing the duration of the hydrolysis step to only 30 minutes (Scheme 3.8). No crosslinking was observed in this case. The reaction mixture was then diluted with absolute ethanol and the acid was neutralized by drop-wise addition of triethylamine. Upon addition of 0.8 equivalent of dodecylamine per acetaldehyde diethyl acetal group, no precipitation occurred even upon stirring overnight. Purification was performed by dialysis against ethanol.



**Scheme 3.8. Synthesis of dodecylamine-functionalized  $\alpha$ -norbornenyl-polyglycidol macromonomer (4a).**

Multiple new peaks were observed in the  $^1\text{H}$  NMR spectrum of product (4a) (Figure 3.15), for the protons of dodecylamine. Coupling was confirmed by the absence of the triplet at  $\delta$ 2.6 ppm, corresponding to the protons on the position alpha to the amino group in free dodecylamine.

Integration of the  $^1\text{H}$  NMR spectrum and Equation (3.2) yielded a conjugation level of 3.6 dodecylamine molecules per macromonomer chain. Integration of the signal for the acetaldehyde diethyl acetal functions corresponded to 5.5 hydrolyzed units when compared with **(3a)** (Table 3.5). The formation of imine linkages was thus quantitative in terms of the hydrolyzed units. A peak at  $\delta$  8.1 ppm, corresponding to the  $-\text{CH}=\text{N}-$  proton, also confirmed the formation of the imine bond but could not be utilized for quantification of the coupling yield because of its rapid exchange with the solvent.

In these reactions, complete preservation of the norbornene moieties and the polymer chains was postulated. It could indeed be confirmed that the acidic conditions used affected neither.

The molecular weight of **(4a)** was thus calculated using the equation

$$M_n = M_{\text{Nb}} + 17M_{\text{DIACTL}} + 3M_{\text{GLD;DDA}} + 5M_{\text{GLD}} = 4570 \text{ g}\cdot\text{mol}^{-1} \quad (3.3)$$

where  $M_{\text{Nb}}$  is the molecular weight of the 5-norbornene-2-methanol moiety ( $124 \text{ g}\cdot\text{mol}^{-1}$ );  $M_{\text{GLD}}$  is the molecular weight of a glycidol unit ( $74 \text{ g}\cdot\text{mol}^{-1}$ );  $M_{\text{DIACTL}}$  is the molecular weight of a glycidol unit functionalized with a diethylacetal group ( $190 \text{ g}\cdot\text{mol}^{-1}$ ); and  $M_{\text{GLD;DDA}}$  is the molecular weight of a glycidol unit functionalized with a dodecylamine molecule ( $283 \text{ g}\cdot\text{mol}^{-1}$ ).

Analysis by SEC in THF yielded a profile with the same shoulder observed for the macromonomer **(3a)**, again attributed to aggregation in the solvent. The molecular weight distribution remained rather narrow however ( $\text{Đ} = 1.25$ ), which also confirmed the absence of polymer degradation (Figure 3.16). Analysis by MALDI-ToF of macromonomer **(3a)** could not be performed, because no compatible matrix could be found yielding a useful signal.

A summary of the composition of all the macromonomers synthesized in this Chapter is provided in Table 3.6 for future reference in the following Chapters.

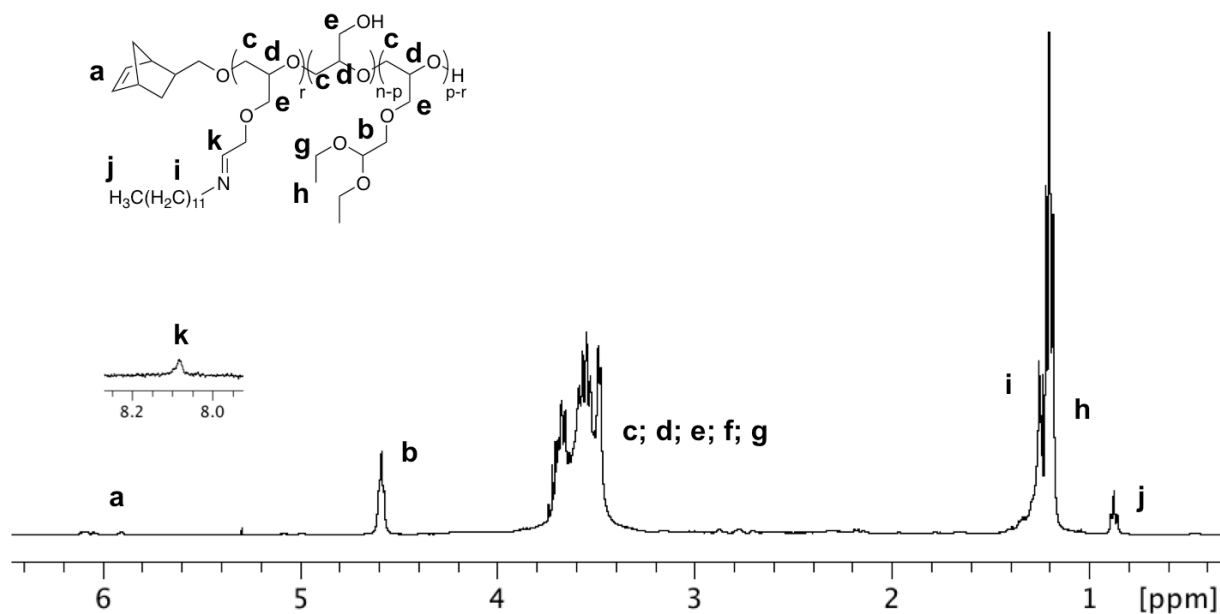


**Figure 3.15.**  $^1\text{H}$  NMR spectrum for dodecylamine-functionalized  $\alpha$ -norbornenyl-polyglycidol macromonomer (4a) (Solvent:  $\text{CDCl}_3$ ; TEA: triethylamine).

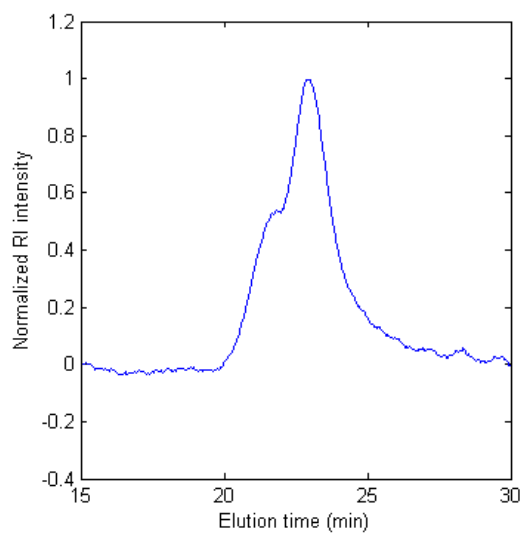


**Figure 3.16.** SEC trace in THF for dodecylamine-functionalized  $\alpha$ -norbornenyl-polyglycidol macromonomer (4a).

**Table 3.6. Summary of the macromonomers synthesized and their composition.**

Macromonomer	DP <sub>n, NMR</sub>	Glycidol acetal units	Glycidol units	Acetaldehyde units	Dodecylamine units
<b>(1a)</b>	23	23	/	/	/
<b>(1b)</b>	50	50	/	/	/
<b>(1c)</b>	103	103	/	/	/
<b>(2a)</b>	25	/	25	/	/
<b>(2b)</b>	53	/	53	/	/
<b>(2c)</b>	103	/	103	/	/
<b>(3a)</b>	25	/	11 – 4 <sup>1</sup>	14 – 21 <sup>1</sup>	/
<b>(3c)</b>	103	/	65 – 25 <sup>2</sup>	38 – 78 <sup>2</sup>	/
<b>(4a)</b>	25	/	5	17	3
<b>(4c)</b>	103 <sup>3</sup>	/	25	30	9

<sup>1</sup>Depending on the reaction conditions; <sup>2</sup>Depending on the [Bromoacetal]/[-OH] ratio; <sup>3</sup>Because of incomplete aldehyde-dodecylamine conjugation, the units do not add up to DP<sub>n, NMR</sub>.

### 3.6 Conclusions

An anionic ring-opening polymerization technique was implemented for the preparation of  $\alpha$ -norbornenyl-poly(glycidol acetal) macromonomers. The characterization results confirmed good control over the reaction, with degrees of polymerization close to the expected values and narrow molecular weight distributions. The macromonomers were linear due to the protection of glycidol with an acetal group. Hydrolysis of the macromonomers yielded polyglycidol macromonomers without notable change in DP<sub>n</sub>. The hydroxyl groups provided an opportunity for conjugation with dodecylamine through a pH-sensitive imine bond. Functionalization with protected aldehyde groups was first performed in high yield. Imine

bond formation was then investigated in a two-step one-pot procedure. Conjugation was achieved while keeping in mind potential crystallization of the dodecylamine side chains and crosslinking reactions. The lower molecular weight macromonomer provided comparatively higher conjugation yields than its higher molecular weight counterpart, and could serve as a building block in the preparation of bioactive particles.



**Chapter 4: Preparation of  
Functionalized Polynorbornene-g-  
Polyglycidol-Based Particles by  
Dispersion ROMP**

#### 4.1. State of the Art in the Preparation of Polyglycidol-Based Particles

The similarity in structure of polyglycidol and poly(ethylene oxide) (PEO) led different teams to consider the former as an alternative for the stabilization of particles. Depending on the polymerization conditions used, linear or branched polyglycidol may be obtained and both are useful for that application. In the literature, various strategies were described for the synthesis of polyglycidol-stabilized particles. Firstly, polyglycidol macromonomers were substituted for typical surfactants in dispersed medium polymerization. Particles can also be obtained by the self-assembly of block copolymers containing a polyglycidol block and functional groups for crosslinking. Droplets of polymer blends containing polyglycidol can be crosslinked into a network to form particles as well. Finally, polyglycidol can be grafted onto existing particles to provide additional functionality.

Linear styryl-polyglycidol macromonomers prepared by the termination of linear poly(glycidol acetal) with *p*-chloromethyl styrene were thus copolymerized with styrene in emulsion polymerization by the group of Dworak. The studies revealed the formation of spherical particles with diameters in a range of 200-900 nm, depending on the concentration and the molecular weight of the macromonomer, with a polyglycidol-rich surface layer.<sup>1</sup> This surfactant-free system found applications as photonic crystals<sup>2-4</sup> and in immunodiagnostics, whereby functionalization of the hydroxyl groups allowed the immobilization of antibodies.<sup>5-7</sup> Following a similar route, the group of Möller prepared particles using novel styryl-polyglycidol macromonomers obtained, in this case, by initiation with vinyl benzyl alcohol. This route allowed the formation of branched or linear structures with a single polymerizable group, and prevented the introduction of hydrophobic groups at both ends of a hydrophilic chain as in the case of Dworak. Depending on the concentration and the characteristics of the macromonomer, particles in a size range of 50-600 nm could be obtained.<sup>8</sup>

Various methodologies relied on the self-assembly into micelles of polyglycidol-containing block copolymers and their crosslinking, through suitable groups either introduced on the hydroxyl functionalities of polyglycidol or on the other block. Cinnamic acid was thus coupled with a polyglycidol block through its hydroxyl moiety, to provide hydrophobicity and reactivity to a PEG-*b*-polyglycidol double-hydrophilic block copolymer (Figure 4.1). After self-assembly into micelles in water, core crosslinking through the cinnamic acid groups was achieved by UV irradiation to form particles with diameters around 10 nm.<sup>9</sup> In another case, PS-*b*-polyglycidol copolymers with different sizes and block mass fractions were self-assembled in toluene. When the mass fraction of polyglycidol in the block copolymer was lower than 0.5, spherical core-shell micelles with a diameter between 12 and 23 nm were formed. The polyglycidol-rich core of the micelles was loaded with concentrated HCl, followed by titanium tetraisopropoxide. Crosslinking occurred by substitution of the hydroxyl groups catalyzed by HCl (Figure 4.2). In a good solvent for both polymer blocks, the particles were stable and reached a diameter of about 70 nm.<sup>10</sup> Novakov also copolymerized isoprene or butadiene with styrene to form the hydrophobic block of a poly(styrene-*co*-diene)-*b*-polyglycidol copolymer. Self-assembly into micelles was achieved in solvents selective for either block, locating polyglycidol in the core or at the periphery depending on the solvent used. Particles in the form of nano- and micro-sized micellar aggregates were obtained by performing core or shell crosslinking via UV radiation of the free unsaturation sites of the diene units in the hydrophobic block.<sup>11</sup>

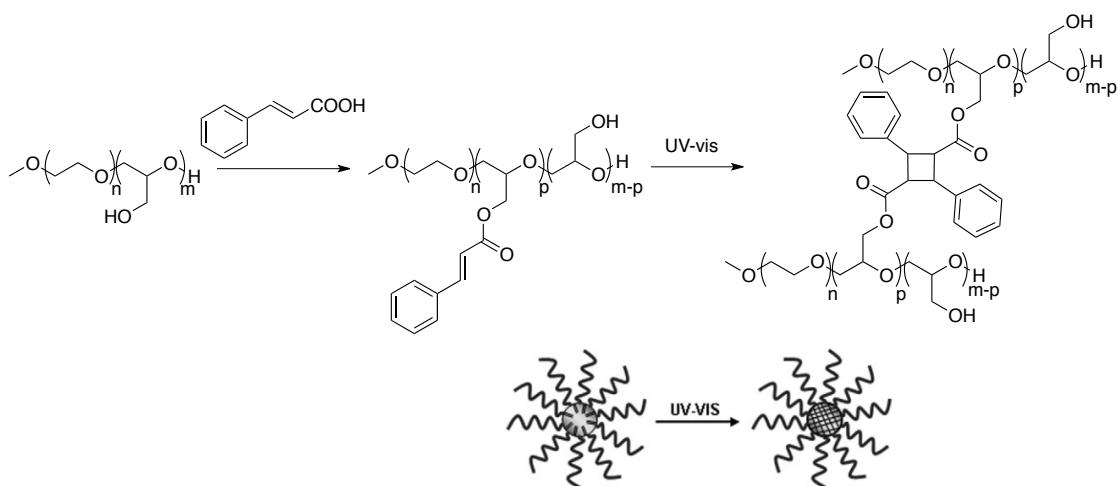


**Figure 4.1. Polyglycidol-based particles by crosslinking cinnamyl groups coupled with PEG-*b*-polyglycidol micelles.<sup>9</sup>**

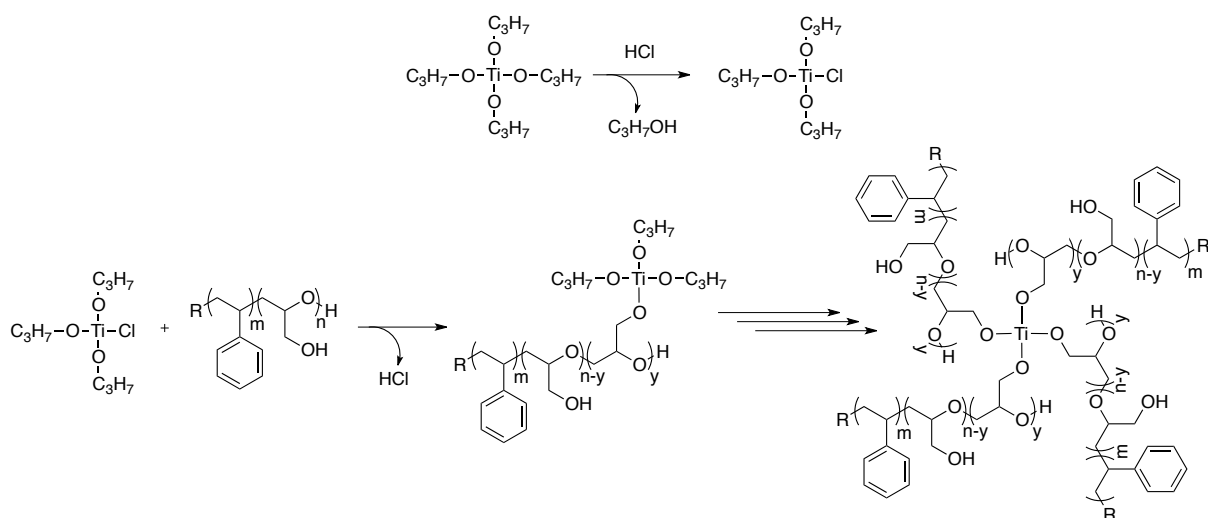


**Figure 4.2. Crosslinking reaction between the hydroxyl functions of polyglycidol and titanium tetraisopropoxide to form PS-*b*-polyglycidol particles.<sup>10</sup>**

Another way to prepare polyglycidol-stabilized particles is the compartmentalization of polymeric blends containing reactive polyglycidol, by crosslinking these compartments to form discrete networks. The group of Möller thus utilized hydrolyzable glycidol acetal, allyl glycidyl ether (AGE) and *tert*-butoxy glycidyl ether (t-BGE) units to prepare poly(glycidol acetal-*stat*-AGE), poly(glycidol acetal)-*b*-poly(AGE), poly(glycidol acetal-*stat*-t-BGE), and

poly(glycidol acetal)-*b*-poly(t-BGE). Compartmentalization was achieved by miniemulsification of the copolymers dissolved in toluene aided by SDS, and hexadecane as hydrophobic agent along with a dithiol crosslinker and a photoinitiator. The particles were crosslinked by UV irradiation, which induced thiol-ene “click” crosslinking and deprotection of the glycidol acetal units to form discrete microgels. The particles had diameters between 100-245 nm, with a size increasing for decreasing fractions of crosslinked AGE units. In the case of poly(glycidol acetal)-*stat*-AGE) and poly(glycidol acetal)-*b*-poly(AGE) the particles even displayed nanostructuring, with hydrophobic domains in the nanometer range.<sup>12</sup> The same miniemulsification process was utilized for blends of poly(glycidol acetal)-*b*-poly(AGE) and hydrophobic reactive poly(tetrahydrofuran-*stat*-allyloxy-3-ethyl-oxetane) or non-reactive PS in proportions of 10-50%. While the first blend series yielded diameters of 125-169 nm for particles with nanometric hydrophobic domains, non-reactive PS also phase-separated within the core of the particles due to its incompatibility with polyglycidol.<sup>13</sup> The group of Harth also prepared polyglycidol-stabilized particles by formulating homogeneous solutions of polymer with dithiol crosslinkers and radical initiators, loading them as an ink in a printer cartridge along with various dyes. Preparations containing branched allyl-functionalized polyglycidol, with or without allyl-functionalized polycarbonate, were also tested. Compartmentalization was observed when the preparations were printed as patterns of micrometric coloured dots onto glass surfaces and Teflon sheets. The substrates were then exposed to UV light to induce crosslinking of the droplets by a thiol-ene “click” reaction between the pendant allyl groups and a dithiol component. Confocal microscopy confirmed the presence of polycarbonate/polyglycidol and polyglycidol particles around 10  $\mu\text{m}$  and 2  $\mu\text{m}$ , respectively, with encapsulated dyes (Figure 4.3).<sup>14</sup> Alternatively, poly(glycidol)-*stat*-AGE) and PEG-dithiol gel precursors, and a radical initiator were encapsulated in large vesicles before exposure to UV light to induce crosslinking by a thiol-ene “click” reaction.

The process led to the formation of spherical gel particles between 132 and 148 nm, which could also encapsulate a model dye in the lipophilic film, and an antibacterial drug in the core of the vesicles, to promote their release by swelling of the network.<sup>15</sup>

Another recently reported approach involved grafting branched polyglycidol from silica-coated, amine-functionalized Fe<sub>3</sub>O<sub>4</sub> magnetic particles (Figure 4.4). The 100-120 nm diameter particles were then loaded with a fluorophore for bioimaging applications, and an anticancer drug to achieve cancer treatment through pH-sensitive drug-delivery, but could also be useful for cell hyperthermia because of their magnetic core.<sup>16</sup>

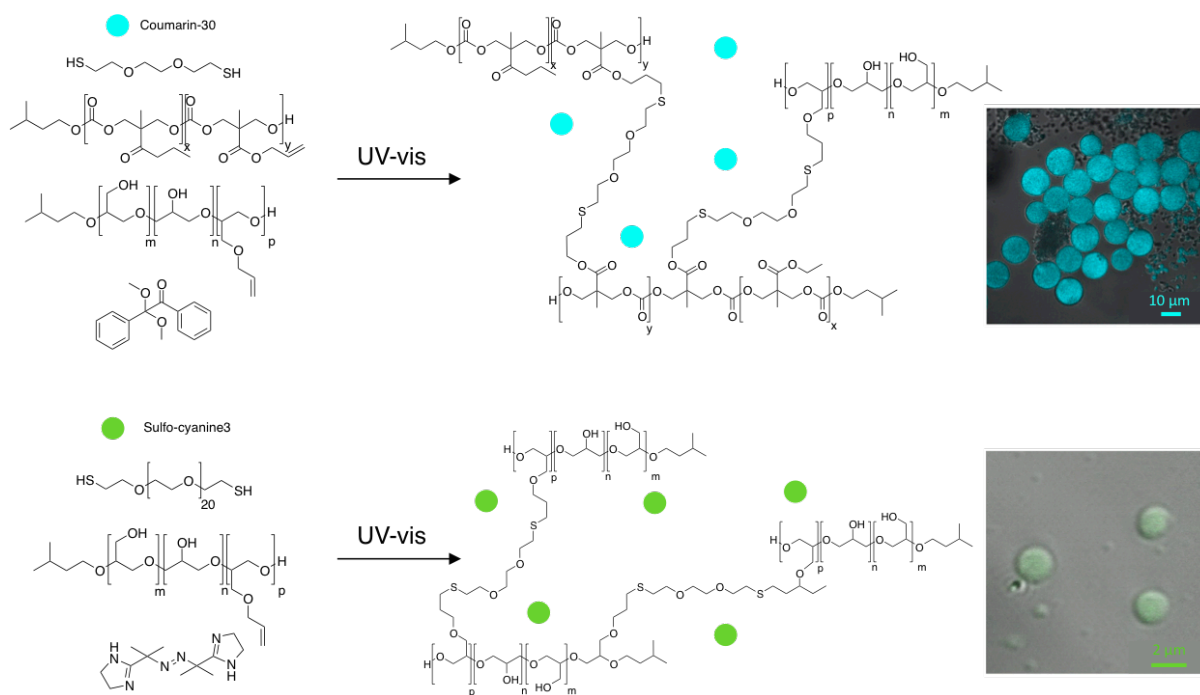


**Figure 4.3. Preparation of polyglycidol particles by ink jet deposition of allyl-functionalized polymer solution and crosslinking into spherical networks.<sup>14</sup>**

Among the different examples surveyed, none involved norbornenyl-polyglycidol macromonomers being used in dispersed medium polymerization, and even less so in combination with ROMP. The synthetic strategy selected for the current investigation enabled the functionalization of linear macromonomers with a single norbornene polymerizable

group. The synthesis of the bare macromonomer and the functionalized macromonomer prior to preparation of the particles provided good control over the macromonomer composition, and could potentially provide better control over the morphology of the particles.

Analysis results for non-functionalized polynorbornene-*g*-polyglycidol latexes prepared by the copolymerization of norbornene with  $\alpha$ -norbornenyl-polyglycidol macromonomers will first be provided. The synthesis of particles from multifunctional polyglycidol-based macromonomers will then be described.

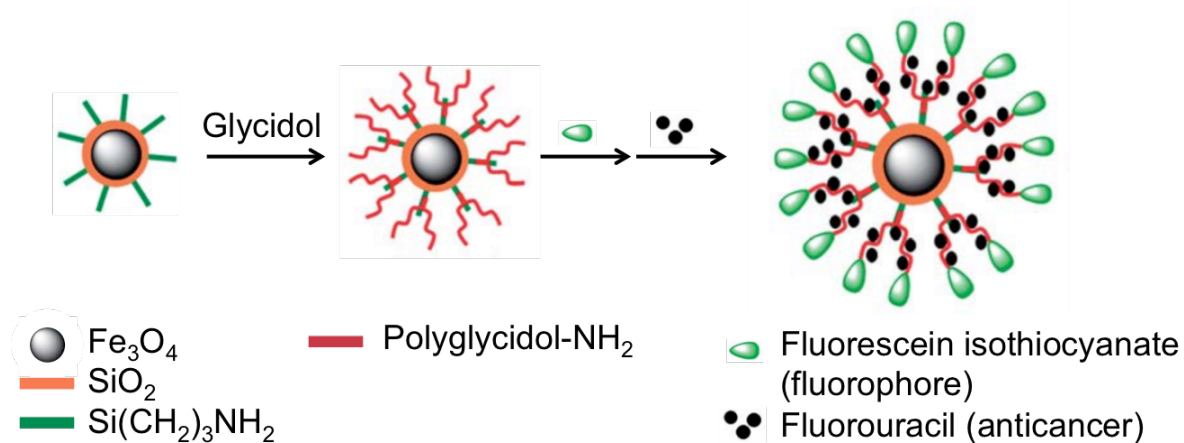


**Figure 4.4. Polyglycidol-functionalized  $\text{Fe}_3\text{O}_4$  particles for combined hyperthermia, drug-delivery and bioimaging applications.<sup>16</sup>**

## 4.2. Methods and Materials

### 4.2.1. Preparation of Polynorbornene-*g*-Polyglycidol Particles by Dispersion ROMP

Dispersion polymerization was carried out at room temperature with stirring, under inert atmosphere in a glove box. The solvents used were degassed by a freeze-pump-thaw process. In a typical experiment, 10 mg ( $1.2 \times 10^{-5}$  mol) of Grubbs first-generation complex was dissolved in 3.3 mL of dichloromethane/ethanol mixture (1:1 v/v). In these reactions, the

mass of norbornene and macromonomer was kept constant to maintain the same core-shell material ratio. Both norbornene (201 mg) and the macromonomer ( $\alpha$ -norbornenyl-polyglycidol macromonomer (**2a-c**), or the dodecylamine-functionalized macromonomer (**4a**), 241 mg) were dissolved in 6 mL of dichloromethane/ethanol solution (35:65 v/v) and were added to the catalyst solution, together with dodecane (206 mg) as an internal standard. The mixture was stirred for 24 hours and the reaction was terminated by addition of 0.3 mL ( $3.1 \times 10^{-3}$  mol) of ethyl vinyl ether. Determination of the size of the particles was achieved by dynamic light scattering (DLS) and transmission electron microscopy (TEM) analysis, after eliminating the unreacted macromonomer by centrifugation and decantation of the supernatant. The particles were then redispersed in a dichloromethane/ethanol mixture (35:65 v/v). For further characterization in an aqueous medium, the particles were transferred to an aqueous solution. With a 4-mL sample of the dispersion, dichloromethane was first carefully evaporated under reduced pressure, and then 4 mL of water were added drop-wise with stirring. The remaining ethanol was then evaporated under reduced pressure. The remaining unreacted macromonomer was eliminated by ultrafiltration of the sample in water (regenerated cellulose membrane with a MWCO of 10,000 Da)

#### 4.2.2. Determination of the Conversion of Reactants

The norbornene conversion was determined by gas chromatography using Equation (4.1),

$$\pi_{\text{Nb}} = 1 - \frac{I_{\text{Nb};t=24} / I_{\text{dod};t=24}}{I_{\text{Nb};t=0} / I_{\text{dod};t=0}} \quad (4.1)$$

where  $I_{i;t=24}$  is the integrated signal intensity for component  $i$  (with  $i=\text{Nb}$  for norbornene,  $\text{dod}$  for dodecane) at  $t=24$  hours, and  $I_{i;t=0}$  is the intensity of the signals at  $t=0$ .

The macromonomer conversion was determined by gravimetric analysis. Briefly, 4 mL of dispersion were centrifuged to isolate the solution from the particles. This process was repeated two more times with the supernatant, to isolate remaining suspended particles. The



particles were then dried under vacuum. The weight of the residue ( $m_{\text{polym}}^f$ : particles) was compared with the theoretical value to calculate the macromonomer conversion according to Equation (4.2):

$$\pi_{\text{macro}} = \frac{m_{\text{polym}}^f - \pi_{\text{Nb}} m_{\text{Nb}}^i}{m_{\text{macro}}^i} \quad (4.2)$$

where  $m_{\text{polym}}^{\text{th}}$  and  $m_{\text{polym}}^f$  are the theoretical and measured mass of polymer, respectively,  $m_{\text{Nb}}^i$  and  $m_{\text{macro}}^i$  are the initial mass of norbornene and macromonomer, respectively.

### 4.2.3. Determination of Surface Functional Group Density

#### 4.2.3.1. Determination of Hydroxyl Groups on the Non-Functionalized Particles

The number of moles of -OH groups per particle was estimated by first calculating the molar amount of -OH groups per gram of polymer according to Equation (4.3),

$$n_{\text{-OH/g}_{\text{polym}}} = \frac{DP_n n_{\text{macro}}^i \pi_{\text{macro}}}{\pi_{\text{macro}} m_{\text{macro}}^i + \pi_{\text{Nb}} m_{\text{Nb}}^i} \quad (4.3)$$

where  $DP_n$ ,  $n_{\text{macro}}^i$ ,  $\pi_{\text{macro}}$  and  $m_{\text{macro}}^i$  are the degree of polymerization, the initial amount (in moles), the conversion and the initial weight of macromonomer (4) used, respectively, and  $m_{\text{Nb}}^i$  and  $\pi_{\text{Nb}}$  are the initial weight and conversion of norbornene.

Using the information obtained by DLS analysis, the number of -OH groups per particle was calculated using Equation (4.4),

$$N_{\text{-OH/P}} = n_{\text{-OH/g}_{\text{polym}}} V_P \rho_P N_A \quad (4.4)$$

where  $V_P$  is the volume of a particle ( $V_P = \pi D_P^3/6$ ),  $\rho_P$  is the density of the particle approximated at  $1 \text{ g cm}^{-3}$ , and  $N_A$  is the Avogadro constant.

### 4.2.3.2. Determination of the Biocide Density in the Functionalized Particles

Similarly to the previous calculations, the molar amount of dodecylamine molecules per gram of polymer was calculated using Equation (4.5),

$$n_{DDA/g_{polym}} = \frac{N_{DDA} n_{macro}^i \pi_{macro}}{\pi_{macro} m_{macro}^i + \pi_{Nb} m_{Nb}^i} \quad (4.5)$$

where  $N_{DDA}$  is the number of units functionalized with dodecylamine on the macromonomer, and  $n_{macro}^i$ ,  $\pi_{macro}$  and  $m_{macro}^i$  are the initial amounts (in moles), the conversion and the initial weight of the macromonomer used, respectively.

The number of dodecylamine molecules per particle was then calculated using Equation (4.6),

$$N_{DDA/P} = n_{DDA/g_{polym}} V_P \rho_P N_A \quad (4.6)$$

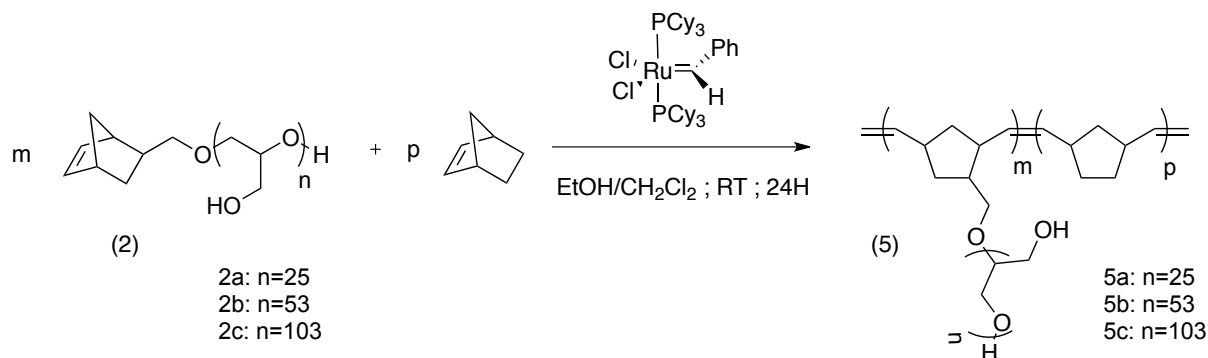
## 4.3. Results and Discussion

### 4.3.1. Preparation of Polynorbornene-g-Polyglycidol Particles by Dispersion ROMP

The particles were obtained by dispersion ROM copolymerization of norbornene with the  $\alpha$ -norbornenyl-polyglycidol macromonomer (**2a-c**) initiated by the Grubbs first-generation complex, in a mixture of ethanol/dichloromethane (65:35 v/v; Scheme 4.1). In this process, the norbornene and macromonomer are both soluble in the solvent mixture, while polynorbornene is insoluble. The particles remain dispersed since the polyglycidol chains stabilize the hydrophobic polynorbornene core, by forming a hydrophilic polyglycidol shell.

Three  $\alpha$ -norbornenyl-polyglycidol macromonomers were synthesized, as described in Chapter 3, by anionic ring-opening polymerization of glycidol acetal followed by hydrolysis of the acetal functions. Variation in the initiator/glycidol acetal ratio yielded macromonomers with

different molecular weights (**2a-c**). The influence of this parameter in the synthesis of the particles needed to be evaluated for this unprecedented dispersion ROMP process.



**Scheme 4.1. Preparation of polynorbornene-g-polyglycidol particles by dispersion ROMP.**

In all cases, after 24 hours of reaction, gas chromatography analysis of the final dispersion yielded no norbornene peak, in contrast to the initial measurement. The conversion of the monomer was thus complete. The macromonomer conversion determined by gravimetry was around 75%, regardless of the macromonomer molecular weight (Table 4.1). The conversion was incomplete in all cases, because even though the terminal norbornene group of the macromonomer was very reactive towards ROMP, the polyglycidol chain presumably shielded the norbornene group, making it less accessible. The polymerization kinetics of norbornene and the macromonomer could not be determined because of lack of solubility of the macromonomer and the graft copolymer in a common organic solvent. In analogy to dispersion ROMP with a norbornene-PEO macromonomer,<sup>17, 18</sup> it was nevertheless expected that most of the norbornene should react within the first minutes of the reaction, while only a small portion of the macromonomer could react. This means that the graft copolymer obtained is likely a gradient copolymer, with a norbornene-rich segment gradually turning into a macromonomer-rich segment on the outside of the particles. Thus, as the reaction

proceeds, the reactive sites should become embedded within a dense graft copolymer immobilized on the particles. Steric hindrance likely becomes so important under these conditions that it would eventually stop the reaction. An attempt at leaving the reaction running for 3 days did not improve the final macromonomer conversion. The macromonomer conversion may also be underestimated because in the gravimetric method used, since even after three centrifugation cycles some particles may have been left in the supernatant, which would reduce the final mass collected and thus decrease the calculated conversion.

$^1\text{H}$  NMR analysis was also carried out for the purified polynorbornene-*g*-polyglycidol particles. Signals confirming the incorporation of the macromonomer in the particles were observed (Figure 4.5), but the low solubility of polyglycidol in  $\text{CDCl}_3$  prevented quantitative analysis and the intensity of the characteristic peaks remained very low. The  $^1\text{H}$  NMR experiment was also carried out in  $\text{DMSO-}d_6$  to observe the polyglycidol chains, but in that case the characteristic peaks overlapped with the residual NMR solvent signal, again preventing quantitative analysis.

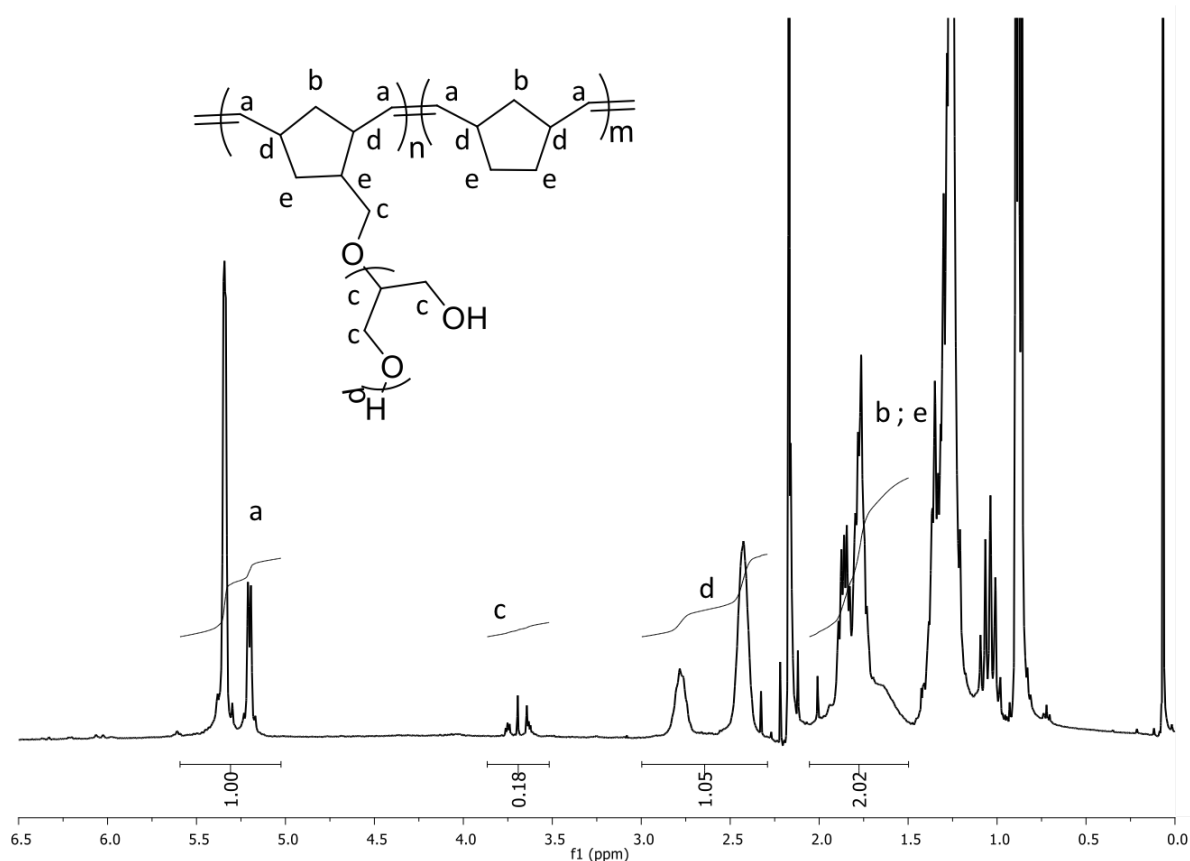


**Figure 4.5.**  $^1\text{H}$  NMR spectrum for polynorbornene-*g*-polyglycidol (**5b**) in  $\text{CDCl}_3$ .

The colloidal characterization of the particles was first approached by measuring the size of the particles by DLS in the reaction medium (ethanol/dichloromethane 65:35 v/v). Triplicate measurements on the samples yielded reproducible size distributions that were averaged. For each measurement, the size distributions in intensity, number and volume were identical. The Z-average diameter was thus chosen as the reference for the determination of particle sizes. The DLS diameter distribution plots for samples (**5a-c**) are provided in Figure 4.6. The Z-average diameter and the dispersity index obtained for each sample are also listed in Table 4.1. Diameters ranging from 280 to 420 nm were obtained for the particles, with diameters decreasing as the molecular weight of the macromonomer increased. This phenomenon can be explained by more effective stabilization of the precipitating polynorbornene for the higher molecular weight polyglycidol chains during dispersion ROMP. The particles can therefore

reach their equilibrium size more rapidly. A similar trend was observed for core-shell particles of polynorbornene-*g*-PEO in the same solvents.<sup>17</sup> Imaging of the particles (**5a**) by TEM yielded spherical objects (Figure 4.7).

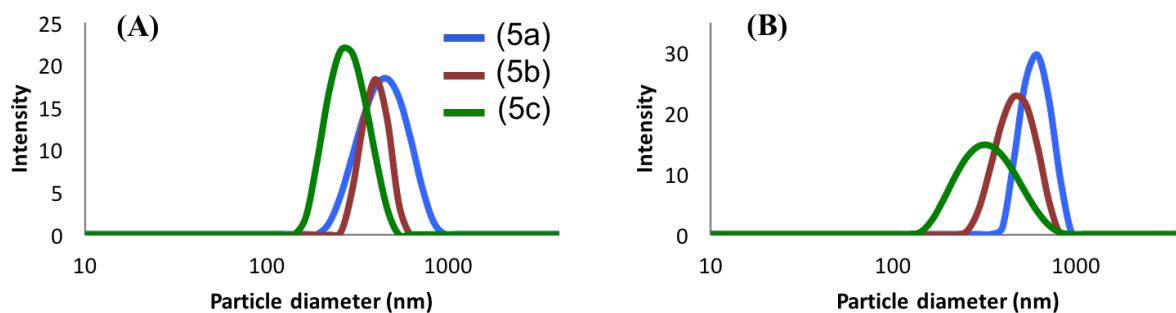


**Figure 4.6.** Size distributions for polynorbornene-*g*-polyglycidol particles (**5a-c**) measured by DLS. (A): in ethanol/dichloromethane (65:35 v/v); (B) in water.

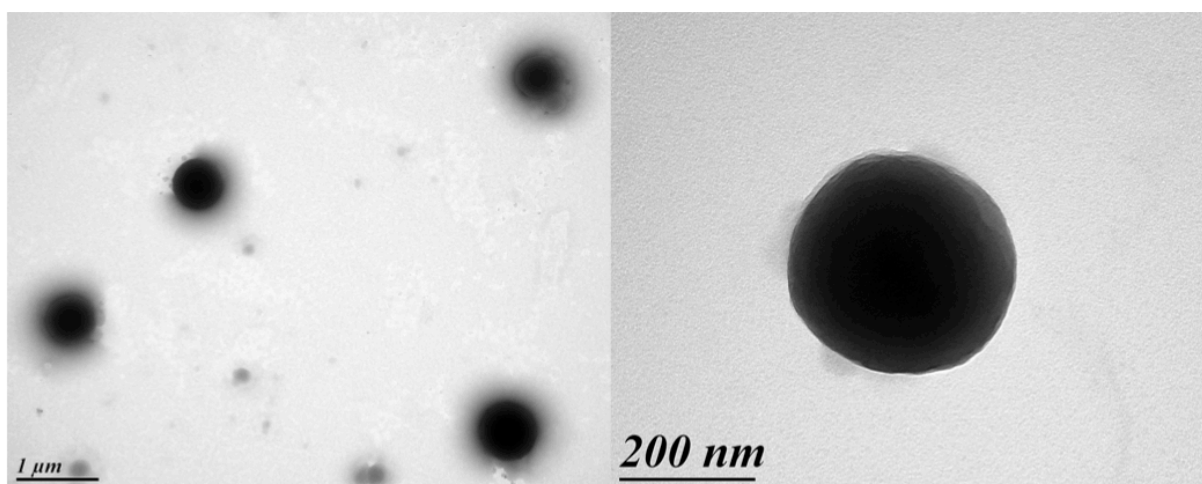


**Figure 4.7.** Observation of polynorbornene-*g*-polyglycidol particles (**5a**) by TEM.

The particles were also characterized by DLS after being transferred to water, and an increase in diameter was observed in all cases. This increase could be explained in part by contraction of the hydrophobic polynorbornene core, combined with swelling of the polyglycidol-rich shell of the particles in water, due to the presence of hydrophilic hydroxyl groups. This

nevertheless confirmed the formation of relatively stable polynorbornene particles with a corona of polyglycidol chains. Using Equations (4.3) and (4.4), the number of hydroxyl groups per particle was determined. As shown in Table 4.1, for comparable macromonomer conversions, the number of hydroxyl functions increased for decreasing  $DP_n$  of the macromonomer. This difference was most obvious upon transferring the particles in water, since **(5a)** showed a higher affinity than **(5c)** with more significant swelling in that solvent. The polyglycidol macromonomer provides a high density of hydroxyl functionalities, which can serve as anchoring sites for active molecules. For comparison, particles synthesized from macromonomer **(2a)** contained ca.  $1.4 \times 10^8$  hydroxyl groups per particle, vs.  $3 \times 10^6$  hydroxyl groups per particle for the analogous PEO-based particles having only one hydroxyl group at the end of each macromonomer chain.<sup>19</sup>

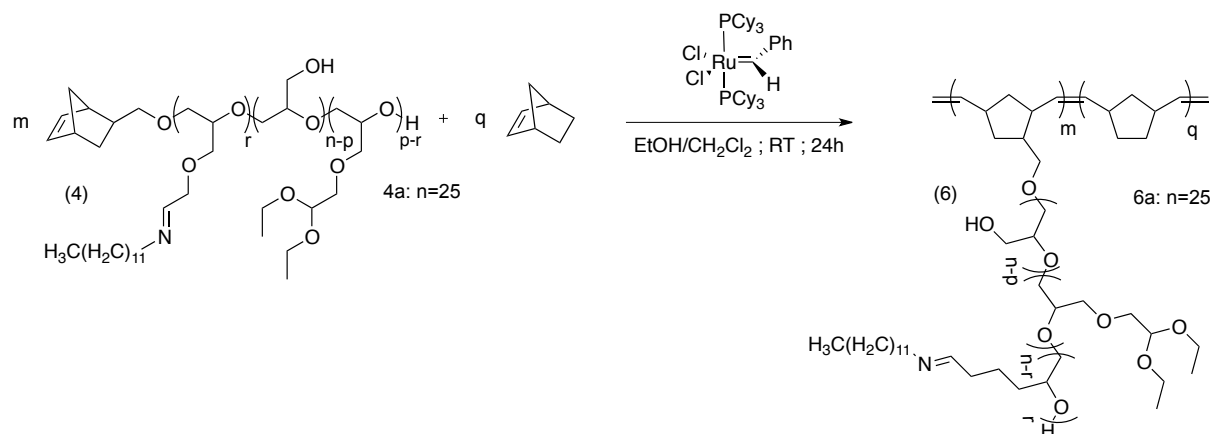
**Table 4.1. Z-average diameter and conversion for particles synthesized via dispersion ROM-copolymerization of macromonomers (2a-c) with norbornene.**

	Macromonomer $DP_n$	Macromonomer conversion (%)	Norbornene conversion (%)	Z-average diameter (nm) (DLS) and PD		-OH groups per NP/ $10^6$
				In EtOH/ CH <sub>2</sub> Cl <sub>2</sub>	In H <sub>2</sub> O	
<b>(5a)</b>	25	75	> 99%	420 (0.12)	610 (0.63)	140
<b>(5b)</b>	53	75	> 99%	390 (0.040)	540 (0.41)	110
<b>(5c)</b>	103	73	> 99%	280 (0.17)	340 (0.26)	43

### 4.3.2. Preparation of Dodecylamine-Functionalized Polynorbornene-g-Polyglycidol Particles

The next part of this investigation involved the copolymerization of norbornene with the dodecylamine-functionalized  $\alpha$ -norbornenyl-polyglycidol macromonomer **(4a)** in a dispersion

ROMP process, to prepare highly functionalized particles. The reaction was also initiated by the Grubbs first-generation complex (Scheme 4.2).



**Scheme 4.2. Preparation of dodecylamine-functionalized polynorbornene-g-polyglycidol particles by dispersion ROMP.**

The norbornene conversion, measured by gas chromatography, was determined to be complete. The macromonomer conversion, measured by gravimetric analysis and calculated according to Equation (4.2), was 25%. This conversion is 3 times lower than that obtained for non-functionalized  $\alpha$ -norbornenyl-polyglycidol macromonomers. Similarly to the non-functionalized macromonomers, as the ROMP reaction progressed, steric hindrance grew around the active centers until the reaction could no longer proceed. Since the dodecylamine-functionalized macromonomer is even bulkier with the alkyl chains coupled along its backbone, steric effects should be even more important. The terminal norbornene group should also be less accessible for incorporation in the graft copolymer. Furthermore, if the graft copolymer has a gradient composition with a macromonomer-rich final portion, successive reactions of the macromonomer units would become highly unfavorable. The activity of the reactive centers was verified by addition of a small portion of norbornene after the first 24 hours of reaction. Complete conversion of the monomer aliquot was confirmed by



gas chromatography. The limited conversion of the macromonomer thus cannot be attributed to deactivation of the metathesis-active centers. It is also postulated that dispersion ROMP generated low degree of polymerization, macromonomer-rich chain segments later in the reaction, after the very fast polymerization of norbornene. These chains would remain in solution because of their low polynorbornene content and could not be separated by centrifugation, thus decreasing the apparent macromonomer conversion.

Incorporation of the functionalized macromonomer in the particles was confirmed by IR analysis. Indeed, the spectrum displays characteristics of both the polynorbornene backbone, with peaks between 1250-1560  $\text{cm}^{-1}$  and 2780-3110  $\text{cm}^{-1}$ , and the functionalized polyglycidol chains, with peaks corresponding to ether, hydroxyl, carbonyl, and imine groups on the macromonomer (Figure 4.8).

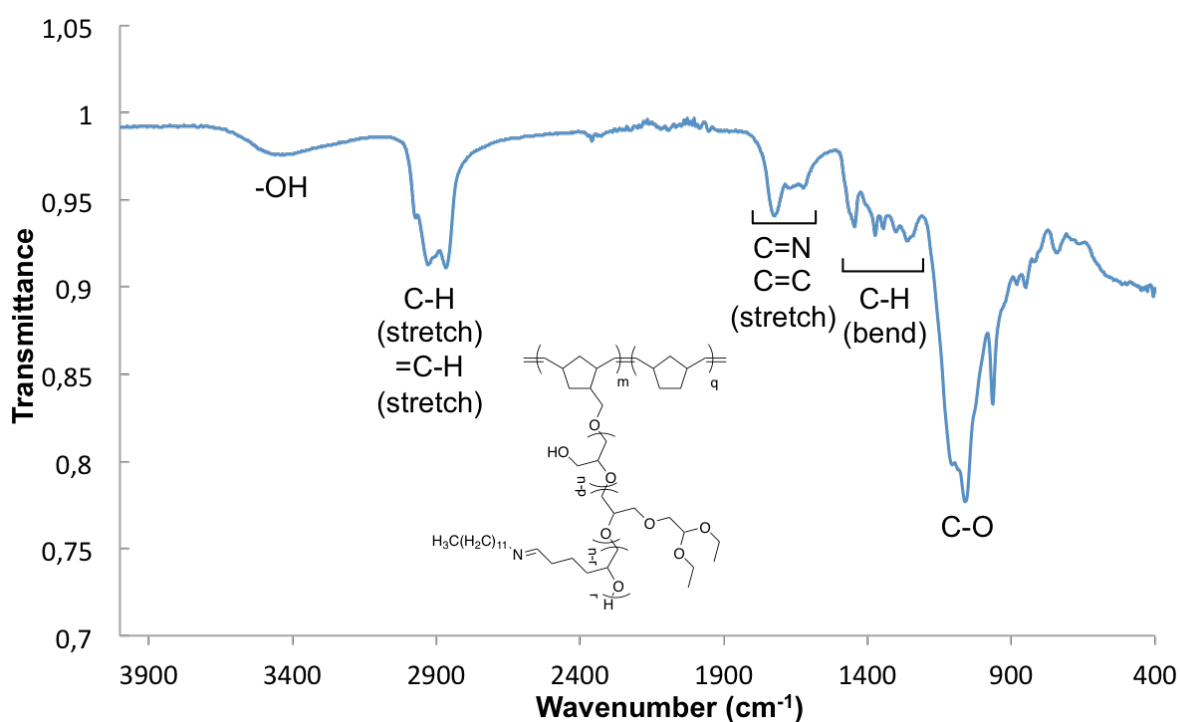


**Figure 4.8.** IR spectrum for dodecylamine-functionalized polynorbornene-g-polyglycidol particles.

DLS analysis of the dispersion confirmed the presence of particles with a Z-average diameter of 975 nm and a dispersity of 0.3 in the ethanol/dichloromethane solvent mixture (Figure 4.9(A)). Imaging of the particles by TEM (Figure 4.9(B)) yielded spherical objects with diameters around 600 nm. The difference in size with the DLS results can be explained by contraction of the dried particles for TEM as compared to their swollen state in the DLS measurements. In comparison to the polynorbornene-*g*-polyglycidol particles, the formation of larger objects can be explained by the higher solubility of the dodecylamine-functionalized macromonomer as compared to the non-functionalized macromonomer in the reaction medium, delaying the precipitation of the ROMP product. This higher solubility in the reaction medium may also have progressively decreased the tendency for the macromonomer to adsorb on the growing particles. The macromonomer would thus rather simply stay in solution in a favorable solvency environment rather than react with a heterogeneous system. The dodecylamine-functionalized particles could not be transferred to water, since massive aggregation was observed. The high intolerance of dodecylamine to water at the periphery of the particles should favor hydrophobic interactions between the particles. The amount of dodecylamine loaded, calculated according to Equations (5) and (6), was  $6.8 \times 10^7$  molecules per particle, corresponding to 4.3 wt %.

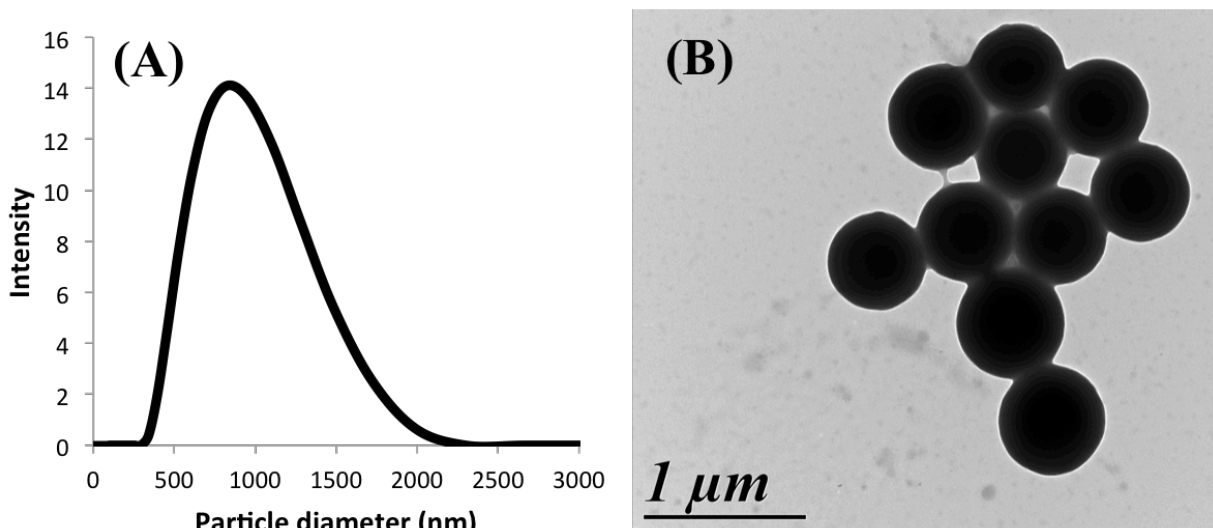


**Figure 4.9. (A) Size distribution for dodecylamine-functionalized particles measured by DLS in EtOH/CH<sub>2</sub>Cl<sub>2</sub> (65/35 v/v); (B) TEM imaging of the particles.**

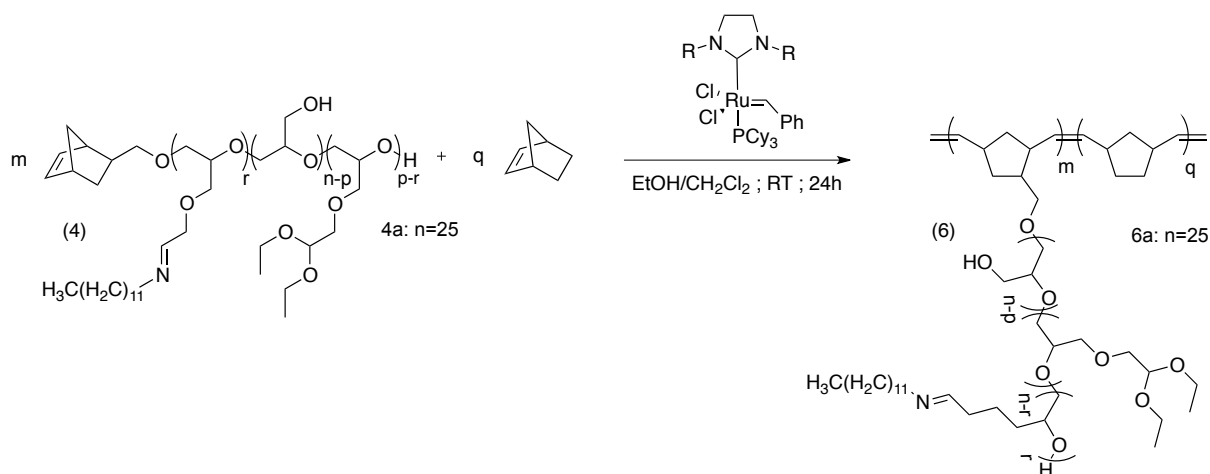
### **4.3.3. Alternate Approaches for Increased Conversion of the Dodecylamine-Functionalized Macromonomer**

The low conversion of dodecylamine-functionalized macromonomer achieved so far limited the density of dodecylamine moieties on the particles. To maximize the antifungal potential of the particles, attempts to enhance the macromonomer conversion were made.

Steric hindrance caused by the bulky dodecylamine-functionalized macromonomer chains around both the terminal norbornene unit of unreacted macromonomers and the active ROMP centers apparently brought the reaction to a stop. One way examined to circumvent this issue was to add more catalyst to the solution, to alleviate steric hindrance on each chain. The reaction was thus attempted with five times the usual concentration of Grubbs first-generation catalyst. The final macromonomer conversion was not increased in this way however.

It was already noted that the first-generation Grubbs complex has limited reactivity in the polymerization of sterically hindered macromonomers in solution.<sup>20, 21</sup> As an alternate approach, ROMP with the more reactive second-generation Grubbs catalyst proved to be

useful to obtain graft copolymers with very crowded brushes.<sup>22-24</sup> An attempt at dispersion ROMP with the dodecylamine-functionalized macromonomer was thus made with the second-generation Grubbs catalyst (Scheme 4.3). Even under these conditions, the macromonomer conversion was limited to 30%. The insignificant improvement in conversion was probably related to the anchorage of the active centers on the solid particle substrates, which dramatically limits their accessibility to free macromonomer, or to the good solubility of the macromonomer limiting its adsorption on the particles and favoring the formation of soluble oligomeric species.



**Scheme 4.3. Dispersion ROMP of dodecylamine-functionalized macromonomer with the second generation Grubbs catalyst.**

#### 4.4. Conclusions

Dispersion ROMP of norbornene with an  $\alpha$ -norbornenyl-polyglycidol macromonomer stabilizing agent was shown to be an efficient way to obtain core-shell particles of uniform size, with rather good conversion of the macromonomer. Variations in the molecular weight of the macromonomer enabled fine-tuning of the size of the particles. After functionalization of the macromonomer with dodecylamine as a biocide molecule, dispersion ROMP provided

larger particles. Incorporation of the macromonomer was also confirmed under these conditions, but the conversion suffered from high steric crowding around the norbornene chain end of the macromonomer and around the active centers. Modifications in the reaction conditions did not significantly improve the macromonomer conversion. Nonetheless, particles functionalized with a high content of biocide ( $6.8 \times 10^7$  molecules per particle, corresponding to 4.3 wt %) could be prepared by dispersion ROMP. The ability of this system to release the biocide molecule and to act as an antifungal agent will be discussed in the following Chapter.

**Chapter 5: Use of the  
Functionalized Macromonomer  
and Particles as Antifungal Agents  
Against *H. Resinae***

## 5.1 Identification of Fuel Contaminants and Treatment with Biocides

Microbial contamination in aircraft fuel tanks is an unavoidable phenomenon and represents a major industry concern, as it is a threat for the conformity and the durability of fuel distribution and tank parts, and thus for the safety of passengers.

Microorganisms can be found in fuel tanks because they find in these confined environments all the elements they need for their growth, namely glucose, water, phosphorous, sulphur, nitrogen, oxygen and various minerals. The microorganisms can proliferate by degrading some carbon sources to glucose, which then also induces the production of organic acids.

The major fraction of kerosene consists in a mixture of linear alkanes with chains between 10 and 16 carbons, which are particularly sensitive to enzymatic degradation for glucose production. Cyclic and aromatic alkanes are also found in the composition of kerosene but are more resistant to degradation. The additives contained in kerosene such as anti-oxidants or anti-icing agents provide phosphorous, sulphur and nitrogen sources to the microorganisms. Most importantly, kerosene is also able to solubilize 1 ppm of water per degree above 0°C. Knowing that microorganisms can proliferate at water levels as low as 10 ppm,<sup>1</sup> kerosene storage tanks at 25°C can be a favorable environment for the development of some microbial strains. Furthermore, the concentration of water can be increased by potential defects in the design of the tanks, or when the tank is linked to pipelines, which are also liable to leaks. The low temperatures experienced during the flights decrease the solubility of water in kerosene and favors the formation of a layer at the bottom of the tank. This phase separation is essential for the development of microorganisms.<sup>2</sup> Proliferation of the microorganisms will be favored first at the interface between kerosene and water, where the nutrients are readily available. Mandatory maintenance requirements include daily water drainage from the tanks, but this only reduces proliferation risks without eliminating them.

Numerous issues are associated with microbial growth. Degradation of the additives may result in significant loss of performance for the kerosene. Blockage of the valves, pipes or filters is observed because of the formation of large microbial colonies, as well as the formation of sludge due to the generation of biomass from the metabolism of the microorganisms.<sup>3</sup> The generation of organic acids mentioned before during the biodegradation process leads to a decreased pH in the aqueous phase, which is in direct contact with the metal walls of the tank. Long-term storage favors the development of large microbial populations, and implies higher damage levels to the metal pieces from chemical corrosion due to the acidic environment.

Several surveys were made to determine the different fuel contaminants, and numerous strains of bacteria, yeasts and filamentous fungi were identified.<sup>3-8</sup> The most commonly reported contaminant in kerosene is *Hormoconis resiniae* (*H. resiniae*), also known as *Cladosporium resiniae*, a filamentous fungus strain. This species is known for being notoriously resistant to extremely hostile conditions such as temperatures below 0°C, due to its ability to remain in a dormant state until the conditions are more adequate for its development. Indeed, a direct correlation between the growth of *H. resiniae* and corrosion was established in 1964 by Hendey by exposing aluminum foil pieces to the fungus, in solid or liquid media. After a 6-week incubation, all the samples were perforated with significant weight loss.<sup>9</sup>

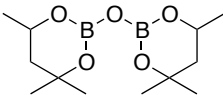
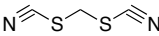
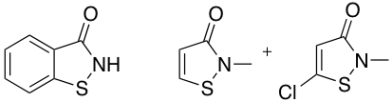
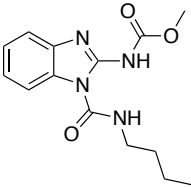
Fungal contamination is typically minimized with antifungal agents, among which chromium (VI) compounds are most commonly used for this type of environment, as coatings on the metallic walls in fuel tanks. It provides protection against electrochemical and microbial corrosion by passivation. However, due to its carcinogenic character, this compound is scheduled to be banned from the current markets starting in September 2017 by the European legislation REACh (Registration, Evaluation and Authorisation of Chemicals). New research is thus attempting to find alternate biocides less toxic to humans.



In the field of aeronautics, various organic biocides have been used against typical contaminants in fuel tanks. They are usually dissolved in the fuel phase. In the late 1980s, the groups of Neihof and Sheridan showed the efficacy of biocides with various chemical groups.<sup>10, 11</sup> The commercial izothiazolone compound Kathon (Table 5.1) induced a 10-fold decrease in biomass generated by several fungal contaminants in fuel at a concentration of only 10 ppm,<sup>5</sup> and was shown to reduce the concentration of *H. Resinae* in biofilms at concentrations above 50 ppm.<sup>12</sup>

Also among the most commonly used biocides, quaternary ammonium salts were found to exert bioactive effects due to their positive charge, that inhibits microorganisms by damaging their cell membrane. Commercial benzalkonium compounds and their more recent analogues with a pyridine ring displayed efficacy against a wide range of bacterial and fungal strains, including some contaminants potentially found in fuel tanks (Figure 5.1(A) and (B)).<sup>13, 14</sup> Molecular biocides based on quaternized aminoglucose were prepared by Coma *et al.* to induce partial inhibition of two wood fungi, with best results obtained for the longer alkyl substituents.<sup>15, 16</sup> Cationic polymers containing quaternary ammonium salts were prepared as a way to mimic antibacterial polypeptides. Kenawy *et al.* inhibited the growth of several bacterial and fungal stains with the use of poly(glycidyl methacrylate), which was chloroacetylated and quaternized with triethylamine.<sup>17</sup> The same process was utilized for copolymers of glycidyl methacrylate and hydroxyethyl methacrylate<sup>18</sup> and copolymers of chloro ethyl vinyl ether with either methyl methacrylate, hydroxyethyl methacrylate or vinylbenzyl chloride.<sup>19</sup> In this case, biocidal activity was only observed for the copolymer containing chloroethyl vinyl ether and vinylbenzyl chloride, with both monomers used to quaternize triethylamine through their halogen group. Polyquaternary ammonium compounds were also synthesized by atom transfer radical polymerization (ATRP)<sup>20, 21</sup> or ring-opening metathesis polymerization (ROMP)<sup>22, 23</sup> of quaternized ammonium monomers.

**Table 5.1. Biocides against *H. resinae* suggested by Sheridan.<sup>10, 11</sup>**

Chemical group	Example compound
Organoborate	Biobor <sup>®</sup> JF 
Thiocyanate	Methylene bis-thiocyanate 
Isothiazolone	Proxel (left), Kathon <sup>™</sup> 886 
Imidazole	Benomyl 

Non-quaternized amine-based compounds were also found to have antibacterial activity. N-Alkyl- $\beta$ -D-glycosylamine derivatives were thus synthesized by conjugation of glucose or galactose with primary or secondary amines (Figure 5.1(C)). Antifungal activity was demonstrated for these derivatives as well as for the non-conjugated free amines against *Coriolus versicolor*, *Poria placenta*<sup>24</sup> and *Aspergillus niger*.<sup>25</sup> The presence of a carbohydrate group facilitated the interaction between the active agent and the target microorganism, and thus enhanced its antifungal properties. It was also found that antifungal activity depended on the length of the conjugated amine, with maximum activity for free dodecylamine and the corresponding glycosylamine. Polymeric particles of dodecylglycosylamine were also obtained by emulsion polymerization of methacrylated sugars and derivatization with

dodecylamine. Moderate inhibition of fuel fungus *H. resinae* was observed by the liberation of glycosylamine through enzymatic hydrolysis of the methacrylate functions.<sup>26</sup>

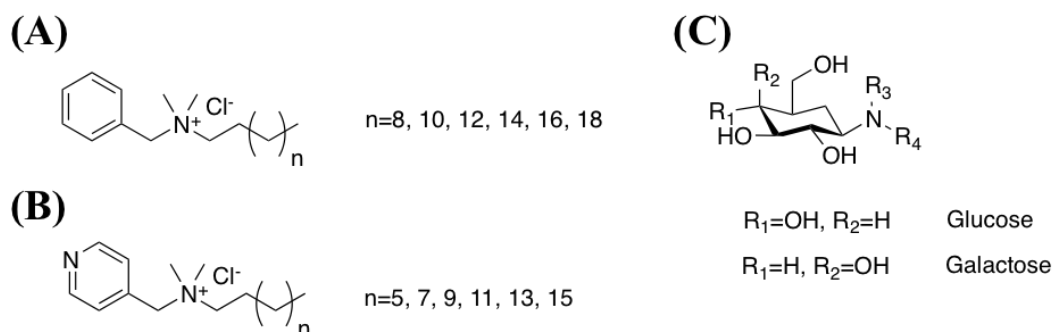


**Figure 5.1. Examples of synthesized biocides. (A) Benzalkonium derivatives,<sup>13</sup> (B) pyridylalkonium derivatives,<sup>14</sup> (C) glycosylamine derivatives.<sup>25</sup>**

In this Chapter, a system of polyglycidol-based particles obtained by ROMP was tested for its antifungal properties. Dodecylamine, a primary alkyl amine compound, was selected for its proven bioactive properties against several fungal strains as a free molecule, and its ability to be attached to the particles via a pH-sensitive imine bond. Effective release of the biocide from the system was monitored before testing the antifungal potential of both the dodecylamine-functionalized macromonomer and the functionalized particles. *H. resinae* was selected as a target strain, as it is representative of fuel tank contamination and could potentially trigger the release of the biocide through its own production of organic acids. Incorporation of the particles in a commercial model coating was also tested with verification that its original barrier properties were maintained.

## 5.2 Materials and Methods

### 5.2.1 Materials

Potato dextrose agar (PDA; Sigma Aldrich), Czapek-Dox agar (Sigma Aldrich) and malt broth (Difco) were used as received for preparation of the growth media. *H. resinae* (ATCC-20495) was purchased in a freeze-dried state and rehydrated according to the instructions provided. Sodium dodecyl sulphate (SDS; Sigma Aldrich), DMSO (Sigma Aldrich) and ethanol (VWR) were used without further purification.

### 5.2.2 Methods

#### 5.2.2.1 Evaluation of Biocide Release from the Macromonomer

A 50 mg sample of dodecylamine-functionalized macromonomer ((**4a**),  $M_n = 4460 \text{ g.mol}^{-1}$ ;  $N_{DiAc} = 16$ ,  $N_{DDA} = 3$ ) was dissolved in 375  $\mu\text{L}$  of ethanol- $d_6$  and the solution was transferred into an NMR tube. After measurement of the initial state ( $t_0$ ), 125  $\mu\text{L}$  of phosphate buffer (pH 5, 6, or 7;  $1 \text{ mol.L}^{-1}$ ) in  $\text{D}_2\text{O}$  was added to the tube. The extent of release was evaluated by comparing the integration of both peaks using Equation (5.1):

$$\%release = \frac{I_{t/m}}{I_{th}} \quad (5.1)$$

where  $I_{t/m}$  is the integration of either the triplet at  $\delta 2.9 \text{ ppm}$  or the multiplet at  $\delta 1.7 \text{ ppm}$ , and  $I_{th}$  is the theoretical integration for complete release ( $I_{th} = 2$  for the triplet and the multiplet when  $I_{\text{CH}_3, \text{dodecylamine}} = 3$ ).

#### 5.2.2.2 Preparation of Microbial Culture Stock

Approximately 10 mL of sterile PDA medium was poured into sterile screw-cap test tubes and aluminium caps were placed on the tubes. While the medium was still hot and liquid, the tubes were tilted onto a surface so that the medium in the tubes could gelify in a slanted

position. The tubes were held in this position until the medium was completely cooled. The slants were then inoculated with 100  $\mu$ L of a spore suspension described below.

### 5.2.2.3 Preparation of Inoculum

A sterile loop was used to scrape gently the surface of a stock culture and gather spores. The loop was then dipped into a tube filled with 3 mL of saline solution (0.9% NaCl). The tube was then vortexed and the spore concentration in the suspension was determined by microscopy (Figure B.2 in Appendix B:).

### 5.2.2.4 Preparation of Culture Media

PDA and Czapek-Dox agar media were prepared according to the guidelines provided by the manufacturer. The prepared medium (10-15 mL) was poured onto sterile Petri dishes (90 mm diameter) and allowed to gelify in a laminar flow fume hood.

### 5.2.2.5 Evaluation of the Antifungal Properties of Macromonomer Solutions and Particle Dispersions

After the synthesis, the particles were ultrafiltered in ethanol (regerenated cellulose membrane with a MWCO of 10,000 Da) to eliminate the unreacted macromonomer and deactivated initiator. The particles were then transferred in DMSO. The initial concentration of conjugated dodecylamine in the crude dispersion was calculated using Equation (5.2):

$$C_{DDA}^i = \frac{n_{macro}^i \pi_{macro} N_{DDA}}{V_d} \quad (5.2)$$

where  $n_{macro}^i$  and  $\pi_{macro}$  are the initial amount (in moles) and the conversion of macromonomer in the synthesis of the dispersion, respectively,  $N_{DDA}$  is the number of units on the macromonomer functionalized with dodecylamine, and  $V_d$  is the total volume of the dispersion. The concentration of dodecylamine in the dispersion was adjusted to the desired

values by adding dropwise a calculated volume of DMSO under stirring. Then the DCM/ethanol mixture was removed by lyophilization. The colloidal properties of the resulting dispersions were evaluated by DLS.

In a typical experiment, a PDA or Czapek-Dox agar Petri dish was inoculated with 100  $\mu\text{L}$  of spore suspension ( $C = 10^4$  or  $10^5$  spores per mL). Then 10  $\mu\text{L}$  of macromonomer solution in DMSO ((**4a**), with (**3a**) as negative control), or particle dispersion in DMSO ((**6a**) with (**5a**) as negative control) were pipeted directly onto the agar surface. In each test, 3 droplets corresponding to 3 dodecylamine concentrations (provided in the Discussion section) were tested on each dish. The Petri dishes were then incubated for 7 days at  $25^\circ\text{C}$ . The inhibition of *H. Resinae* was evaluated by measuring the diameter of the clear zone around each droplet.

#### **5.2.2.6 Evaluation of the Antifungal Properties of Particle Films**

For the preparation of particle films, dispersions of non-functionalized and dodecylamine-functionalized polynorbornene-g-polyglycidol particles ((**5a**) and (**6a**), respectively) were purified by ultrafiltration in ethanol with a  $5000 \text{ g}\cdot\text{mol}^{-1}$  molecular weight cut-off regenerated cellulose membrane. Successive 90  $\mu\text{L}$  samples of the dispersions were spin-coated 10 times on a  $15 \times 15 \text{ mm}^2$  glass cover slip substrate spinning at 2000 rotations per minute. The films were allowed to dry 30 seconds in-between each deposition of dispersion without interruption of the rotation. The films were then dried in a vacuum oven ( $T = 45^\circ\text{C}$ ) overnight before characterization.

For the bioactivity tests, a film-covered glass cover slip was put at the center of a Petri dish (52 mm diameter). Czapek-Dox agar medium was sterilized, inoculated with a spore suspension when the temperature was below  $40^\circ\text{C}$ , and mixed gently. A 4 mL aliquot of the inoculated agar medium was then deposited in the Petri dish containing the cover slip. After incubation for 7 days at  $25^\circ\text{C}$ , the inhibition of *H. Resinae* was evaluated by the presence or absence of a clear zone around the area of the cover slip.

## 5.3 Results and Discussion

### 5.3.1 Release Assessment of Dodecylamine

The release of dodecylamine from the macromonomer by cleavage of the imine bond in acidic medium is a critical step for this application, since it is necessary to induce a biocidal effect against fungal strains. As mentioned in Section 0 on the synthesis of the biocide-functionalized macromonomer, the successful conjugation of dodecylamine to the macromonomer could be confirmed by  $^1\text{H}$  NMR analysis through the absence of a triplet at  $\delta 2.6$  ppm and a multiplet at  $\delta 1.35$  ppm, corresponding to the protons in the positions alpha and beta to the amino group, respectively, of free dodecylamine. Cleavage of the imine bond on the macromonomer would release free dodecylamine, which could be quantified by the appearance of these characteristic peaks by  $^1\text{H}$  NMR.

Release studies were performed in ethanol- $d_6$  with the addition of phosphate buffer in  $\text{D}_2\text{O}$ . Analysis of the free biocide in ethanol- $d_6$  established that the triplet and multiplet were shifted at  $\delta 2.9$  ppm and  $\delta 1.7$  ppm respectively (Figure 5.2).

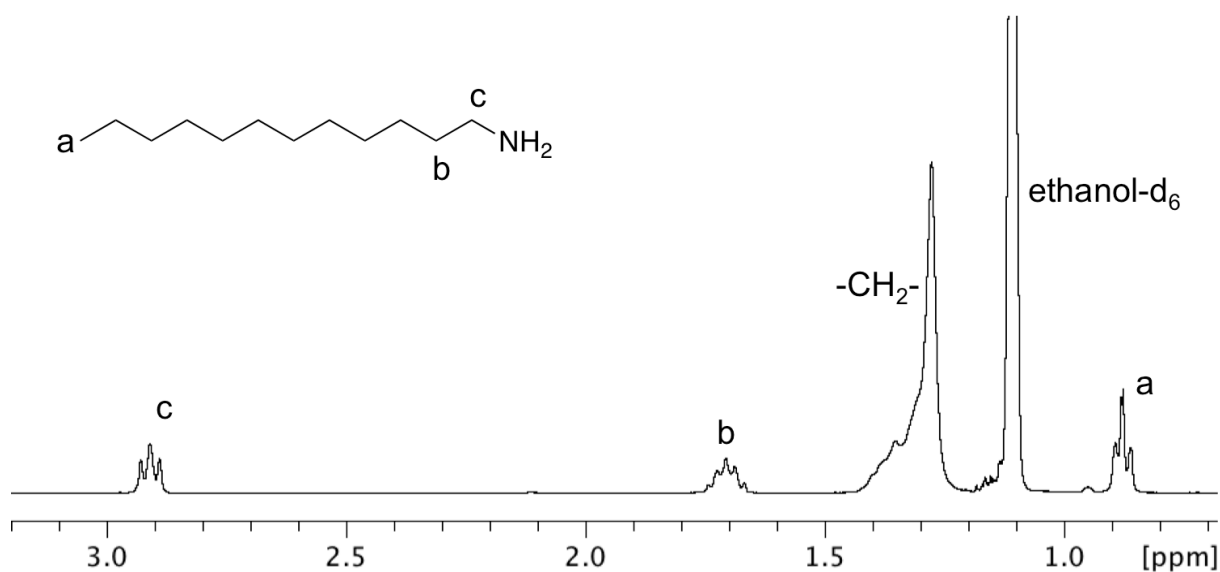
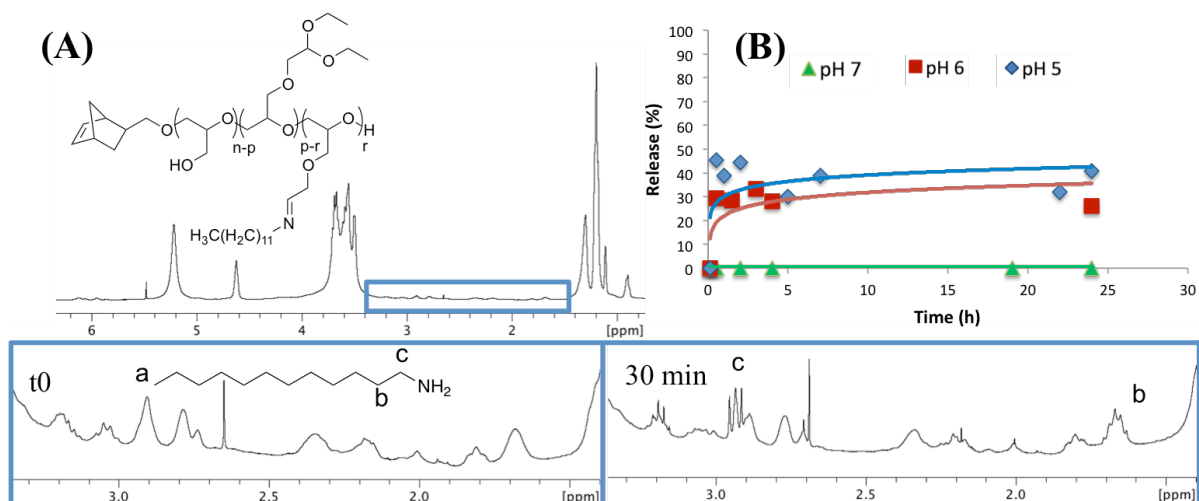


Figure 5.2.  $^1\text{H}$  NMR spectrum for free dodecylamine in ethanol- $d_6$ .

These signals were monitored in the  $^1\text{H}$  NMR spectrum of the macromonomer, before and after introduction of the buffer solution in the tube. At pH 5, as early as 30 minutes after the start of the experiment, the triplet and the multiplet could be observed, confirming the recovery of free dodecylamine (Figure 5.3). The extent of release, determined by integration of the peaks, was determined to be 45% (Table 5.2). Other measurements were performed for up to 7 days, but the release of the biocide leveled off around the initial value (41% after 24 h). The apparent decrease in release observed between 30 min and 24h is attributed to errors in the NMR peak integration and not to reformation of the imine bond. At pH 6, the same burst release was observed in the first 30 minutes of the experiment, with 30% of the biocide cleaved, but afterwards the release did not proceed further. When the experiment was performed at pH 7, however, no release of dodecylamine was observed. The release of free dodecylamine by cleavage of the imine bond thus depended on the acidity of the medium but was incomplete. This phenomenon could be explained by decreased solubility of the macromonomer in the medium, when the aqueous buffer was added to the solution to start the analysis. Phase separation was indeed observed upon addition of the buffer, which may have decreased the availability of the macromonomer to fully release the biocide.

When the experiment was attempted with the dodecylamine-functionalized particles, the intolerance of the system was even more pronounced upon addition of the aqueous buffer to the dispersion. The particles completely precipitated, thus preventing any measurement.





**Figure 5.3. Release of dodecylamine from the macromonomer by cleavage of the imine bond. (A) Observation by <sup>1</sup>H NMR spectroscopy, (B) release profile as a function of pH.**

**Table 5.2. Evaluation of the release of dodecylamine from the functionalized macromonomer as a function of pH (percentage values determined by <sup>1</sup>H NMR).**

Duration (h)	Release of dodecylamine (%)		
	0	0.5	24
pH = 7	0	0	0
pH = 6	0	30	26
pH = 5	0	45	41

### 5.3.2 Agar Culture Medium for *H. Resinae*

The growth of *H. resinae* on PDA and Czapek-Dox agar was tested to find two media with different responses: (1) a very favorable medium for optimal fungal growth, and (2) another medium that promoted decent but not ample growth of the fungus, so as to mimic a favorable but not optimal environment analogous to fuel tanks. On PDA medium, *H. resinae* grew as thick and grey-brownish colonies (Figure 5.4(a)). The aspect of the fungus was however very different on Czapek-Dox agar, where the colonies were rather thin and white (Figure 5.4(b)).

Therefore PDA was selected as the optimal growth medium, while Czapek-Dox agar was considered a less favorable medium for the development of *H. resinae*.

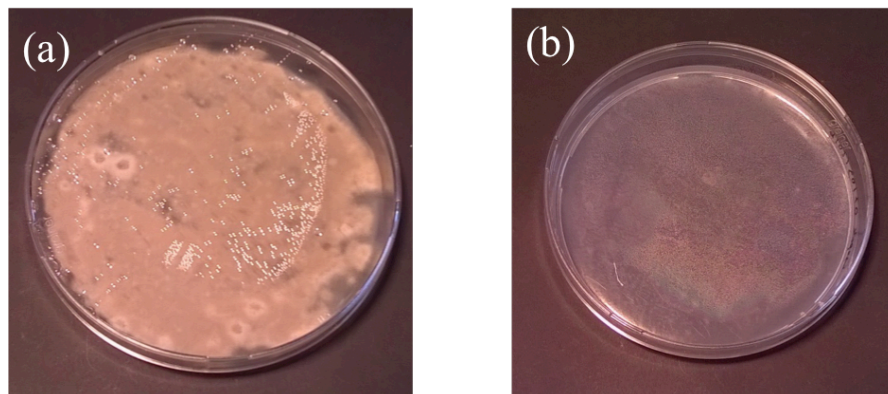


**Figure 5.4.** *H. Resinae* growth on (a) PDA medium, (b) Czapek-Dox Agar medium after 7 days at 25°C.

### 5.3.3 Droplet Test with Macromonomer Solutions

The dodecylamine-functionalized macromonomer was tested for its ability to inhibit the growth of *H. resinae*. A total of 6 macromonomer solutions in DMSO were prepared corresponding to 6 dodecylamine concentrations:  $1 \times 10^{-6}$ ,  $3 \times 10^{-6}$ ,  $5 \times 10^{-6}$ ,  $1 \times 10^{-5}$ ,  $3 \times 10^{-5}$  and  $5 \times 10^{-5} \text{ mol mL}^{-1}$ , and utilized in the droplet test on Czapek-Dox agar medium. As a positive control for the test, non-conjugated dodecylamine solutions in DMSO were prepared at the same concentrations as the macromonomer solutions. The negative control consisted in polyglycidol macromonomer solutions in DMSO. The macromonomer concentrations were calculated to be the same mass concentrations as the functionalized macromonomer solutions. For this test, a fungal suspension was prepared with a concentration of  $10^6 \text{ spores mL}^{-1}$ . The test was divided into 2 sets with dodecylamine concentrations ranging  $1-5 \times 10^{-6}$  and  $1-5 \times 10^{-5} \text{ mol mL}^{-1}$ . After deposition of the droplets, the Petri dishes were incubated for 7 days at 25°C. Results obtained are displayed in Figure 5.5, with photographs of the Petri dishes.

As expected for both sets of concentrations, the polyglycidol macromonomer did not inhibit the growth of *H. resinae* (Figure 5.5(c) and (g)). This test was useful to establish that the presence of DMSO did not interfere with the normal development of the fungus. The bioactivity of free dodecylamine was observed at all tested concentrations, with larger inhibition diameters for higher bioactive agent concentrations (Figure 5.5(b) and (f)). The dodecylamine-functionalized macromonomer did not inhibit the growth of *H. resinae* for concentrations  $1-5 \times 10^{-6} \text{ mol}\cdot\text{mL}^{-1}$  (Figure 5.5(d)), but inhibition zones were observed around the droplets for concentrations of  $1-5 \times 10^{-5} \text{ mol}\cdot\text{mL}^{-1}$  (Figure 5.5(h)). When conjugated to the macromonomer, the action of dodecylamine against *H. resinae* thus seemed reduced as expected due to delayed release of the amine.

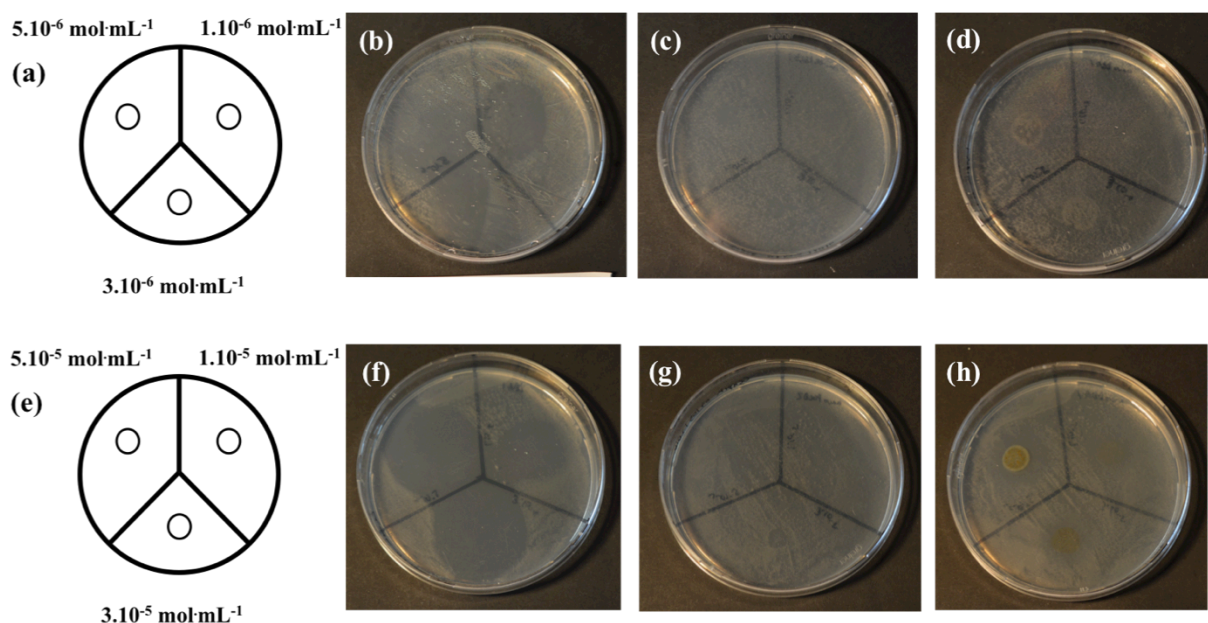


**Figure 5.5. Droplet test against *H. resinae* on Czapek-Dox agar medium ( $10^6$  spores $\cdot\text{mL}^{-1}$ ): (a) Distribution of the droplet concentrations for plates (b-d); (b) Test with free dodecylamine; (c) Test with norbornenyl-polyglycidol macromonomer; (d) Test with dodecylamine-functionalized macromonomer; (e) Distribution of the droplet concentrations for plates (f-h); (f) Test with free dodecylamine; (g) Test with norbornenyl-polyglycidol macromonomer; (h) Test with dodecylamine-functionalized macromonomer.**

The inhibition diameter of free dodecylamine and of the dodecylamine-functionalized macromonomer could be measured directly on the plates. The results displayed in Table 5.3 clearly show that for biocide concentrations increasing from  $1 \times 10^{-5}$  to  $5 \times 10^{-5}$  mol mL<sup>-1</sup>, the inhibition diameters increased, confirming higher antifungal activity against *H. resinae*. However, for equal overall biocide concentrations, the diameters were comparatively smaller for the dodecylamine-functionalized macromonomer than for free dodecylamine. This difference in efficacy is obviously due to the entire load of dodecylamine not being released from the macromonomer, but presumably also to the slower release due to gradual hydrolysis of the imine bonds. This result can be linked with the incomplete release of dodecylamine observed by <sup>1</sup>H NMR analysis, attributed to solubility issues in the medium (Section 5.3.1). The same phenomenon may have occurred in this case, since the aqueous agar medium may have caused collapse of the macromonomer chains, thus reducing their accessibility for the cleavage of the imine bond.

**Table 5.3. Inhibition diameter measured for the antifungal properties of dodecylamine and dodecylamine-functionalized macromonomer.**

<b>Biocide concentration (mol mL<sup>-1</sup>)</b>	<b>Inhibition diameter (mm)</b>	
	Dodecylamine	Dodecylamine- macromonomer
$1 \times 10^{-5}$	24	15
$3 \times 10^{-5}$	35	17
$5 \times 10^{-5}$	36	21

### 5.3.4 Droplet Test on Particle Dispersions

#### 5.3.4.1 Particle Conditioning

The multifunctional particles were tested for antifungal activity against *H. resinae*. The DCM/ethanol reaction mixture used for the synthesis of the particles was incompatible with fungal growth, however. Transfer of the particles in a suitable solvent was thus necessary before using the dispersions in the microbiological tests. DMSO was selected as a dispersant since it did not interfere with the normal development of the fungus. Samples for 3 dispersions were prepared corresponding to dodecylamine concentrations of  $1 \times 10^{-6}$ ,  $3 \times 10^{-6}$  and  $5 \times 10^{-6} \text{ mol mL}^{-1}$  after transfer in DMSO. In terms of polymer concentrations, this corresponded to values in the range of 14.6 - 73.2  $\text{mg mL}^{-1}$  (Table 5.4). Similarly to the tests with macromonomer solutions, dodecylamine solutions in DMSO were prepared at the same dodecylamine molar concentrations as positive controls. Polynorbornene-*g*-polyglycidol dispersions at the same polymer mass concentrations as the test dispersions (Table 5.4, bottom line) were used as negative controls. For consistency, these are also referred to as concentrations of  $1 \times 10^{-6}$ ,  $3 \times 10^{-6}$  and  $5 \times 10^{-6} \text{ mol mL}^{-1}$  for comparison with the other samples.

**Table 5.4. Characteristics of the dodecylamine-functionalized polynorbornene-*g*-polyglycidol dispersions transferred in DMSO.**

Dodecylamine concentration ( $\text{mol mL}^{-1}$ )	$1 \times 10^{-6}$	$3 \times 10^{-6}$	$5 \times 10^{-6}$
Polymer mass concentration ( $\text{mg mL}^{-1}$ )	15	44	73

The dispersions transferred into DMSO were characterized by DLS (Figure 5.6). The particle populations remained monomodal, apart from the dodecylamine-functionalized particles at a

concentration  $3 \times 10^{-6} \text{ mol}\cdot\text{mL}^{-1}$ , which showed a population around 100 nm. Considering that the dispersion was previously ultrafiltered without observing this population, there was no reason for free macromonomer to form this type of small objects in solution. This second population could be related to uncontrolled release of the conjugated dodecylamine during the lyophilization process. In DMSO, dodecylamine could have formed micelles giving rise to this population around 100 nm. Consequently, solvation of the particles would be altered, which would explain the increase in average diameter. The consequences of this phenomenon nevertheless remained limited, as no differences in biocidal properties were observed for this particular sample (Section 5.3.4.2). In other cases, transfer of the particles from ethanol to DMSO by lyophilization did not significantly affect their size, implying that the core-shell systems did not have a higher nor lower affinity with the new solvent. Attempts at preparing more concentrated dispersions in DMSO through lyophilization resulted in complete coagulation of the dispersions.

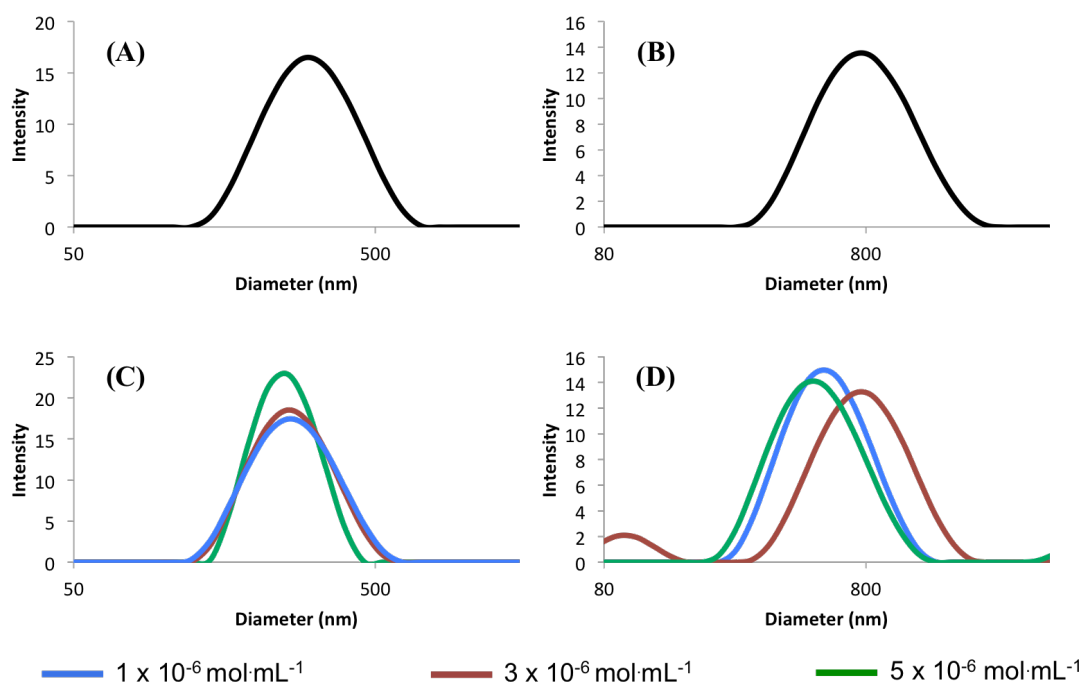


**Figure 5.6. DLS observation of the particles (A-B) ultrafiltered in ethanol, and (C-D) transferred into DMSO by lyophilisation. (A and C) non-functionalized particles; (B and D) dodecylamine-functionalized particles.**

### 5.3.4.2 Droplet Test on Particle Dispersions

The droplet test was first performed on PDA medium with Petri dishes inoculated with a spore suspension at  $10^5$  spores·mL<sup>-1</sup>. The results show that for concentrations  $1-5 \times 10^{-6}$  mol·mL<sup>-1</sup>, free dodecylamine led to small inhibition zones in the droplet deposition area (Figure 5.7(b)), while the non-functionalized particles expectedly did not inhibit the growth of *H. resinae* at all (Figure 5.7(c)). For the dodecylamine-functionalized particles, no clear zone could be observed at any of the concentrations tested. As explained in Section 5.3.3, the release mechanism of the biocide may be the reason for lower activity against *H. resinae*. In this particular case, the released dodecylamine may also remain entrapped in the solid layer created by the particles when the droplet was deposited, thus further reducing its action.

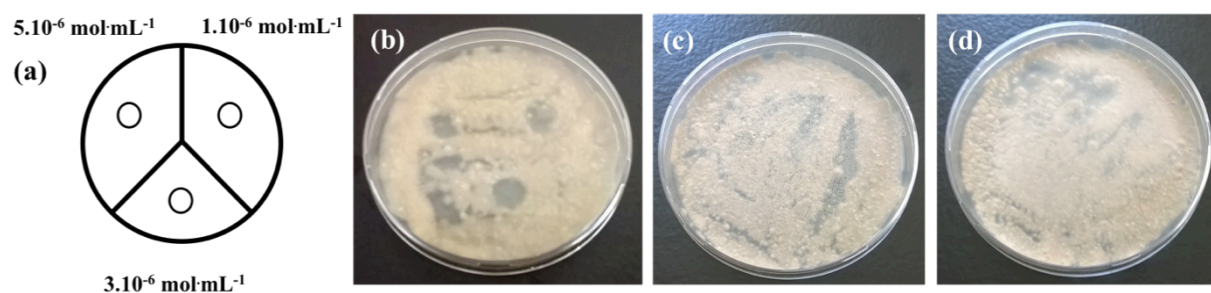


**Figure 5.7. Droplet test with particle dispersions against *H. resinae* on PDA medium ( $10^5$  spores·mL<sup>-1</sup>): (a) Distribution of the droplet concentrations for plates (b-d); (b) Test with free dodecylamine; (c) Test with polynorborene-*g*-polyglycidol particles; (d) Test with dodecylamine-functionalized particles.**

The use of a very favorable PDA medium, promoting fast growth of the fungus, combined with a low biocide/microbial load ratio, may overshadow the bioactive activity of the active compound. To enhance the response of the biocide against *H. resinae*, the spore concentration was reduced to  $10^4$  spores·mL<sup>-1</sup>. The fungus grew more sparsely under these conditions, as can be seen for the negative control with non-functionalized particles (Figure 5.8(c)). However, the lower spore concentration made the test rather inconclusive, as fewer colonies



spreaded homogeneously across the plates both for the positive control and the dodecylamine-functionalized particles (Figure 5.8(b) and (d) respectively). The spore concentration should thus be kept at a minimum of  $10^5$  spores·mL<sup>-1</sup> to maintain good legibility for the test.

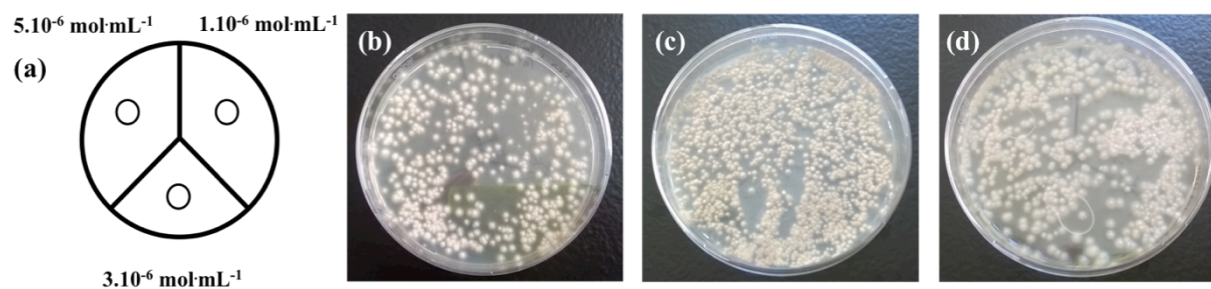


**Figure 5.8. Droplet test against *H. resinae* on PDA medium ( $10^4$  spores·mL<sup>-1</sup>): (a) Distribution of the droplet concentrations for plates (b-d); (b) Test with free dodecylamine; (c) Test with polynorbornene-*g*-polyglycidol particles; (d) Test with dodecylamine-functionalized particles.**

For the same biocide concentrations mentioned in the previous section ( $1-5 \times 10^{-6} \text{ mol} \cdot \text{mL}^{-1}$ ), particle dispersions in DMSO were tested against *H. resinae* on Czapek-Dox agar, a medium that is susceptible to show more biocide inhibition because it is less favorable to the development of the fungus and closer to growth conditions in fuel. As can be seen in Figure 5.9, the dodecylamine-functionalized particles did not inhibit the growth over the concentration range tested, since thin and white colonies were observed around the droplets as in the case of the negative control.



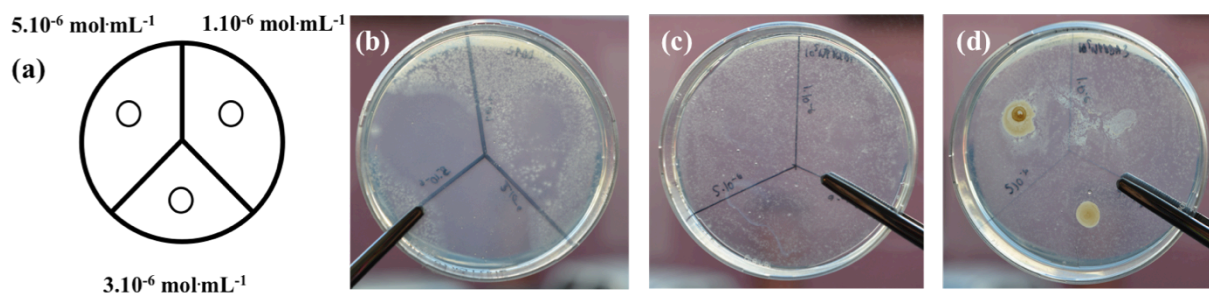


**Figure 5.9. Droplet test against *H. resinae* on Czapek-Dox agar medium ( $10^5$  spores·mL<sup>-1</sup>): (a) Distribution of the droplet concentrations for plates (b-d); (b) Test with free dodecylamine; (c) Test with polynorborene-*g*-polyglycidol particles; (d) Test with dodecylamine-functionalized particles.**

Dispersions of particles corresponding to biocide concentrations of  $1-5 \times 10^{-6}$  mol·mL<sup>-1</sup> were therefore unable to inhibit the growth of *H. resinae*, even in a less favorable environment for the fungus. The presumed limited release of the biocide, combined with its entrapment in the droplet, were provided as explanations for this observation. These effects may be counterbalanced to some extent by a higher biocide concentration achieved through a higher particle concentration. Transfer of the particles in DMSO by lyophilization was however limited to a maximum concentration of  $5 \times 10^{-6}$  mol·mL<sup>-1</sup>. Higher particle concentrations for microbiology tests may be achieved by preparing films from the dispersions.

### 5.3.5 Tests with Particle-Based Films

Negative results from dodecylamine-functionalized particle dispersions were previously obtained at amine equivalent concentrations of  $1-5 \times 10^{-6}$  mol·mL<sup>-1</sup>. Unfortunately, higher concentrations could not be achieved in the dispersions without coagulation. The preparation of particle films could be an alternative to using concentrated particle dispersions. The films could then be utilized in replacement of the droplets in microbiology tests.

### 5.3.5.1 Preparation and Characterization of the Films

The film preparation method described previously allowed the formation of homogeneous films with very little defects (Figure 5.10). Biocide-functionalized and non-functionalized particle films were observed by atomic force microscopy (AFM). Characterization was also performed on films obtained after a single 90- $\mu$ L deposition of the dispersion. In all cases, microscopy showed the presence of spherical particles. The single-deposition of non-functionalized particles yielded a film with a rather high density of particles (Figure 5.11), but AFM imaging in the phase mode to characterize the rigidity of the sample revealed soft particles that were not tightly packed, and apparently laying on a bed of undulated and equally soft matter. This tendency was enhanced on the multi-deposition films, which had a lower density of particles and a more uniform bed of soft material, as shown by three-dimensional imaging. This bed was most clearly observed with phase imaging at lower magnification, where the film seemed to embed most particles on the top but did not cover the whole sample, leaving open patches throughout the sample. The formation of this bed may be caused by deformation of the particles during the spin coating process.<sup>27</sup> Indeed, polyglycidol appeared to have moved away from the top of the particles to reveal the polynorbornene core in the AFM image. In the absence of solvent, favorable interactions between the particles, and particularly the polyglycidol shells, would cause their fusion to form a polymeric layer on the glass substrate. In the case of multi-deposition films, the bed would result from the fusion of several layers of particles to form a thicker and more homogeneous soft layer. Its capacity to embed particles would thus be increased, which would explain a seemingly lower concentration of particles in the film.

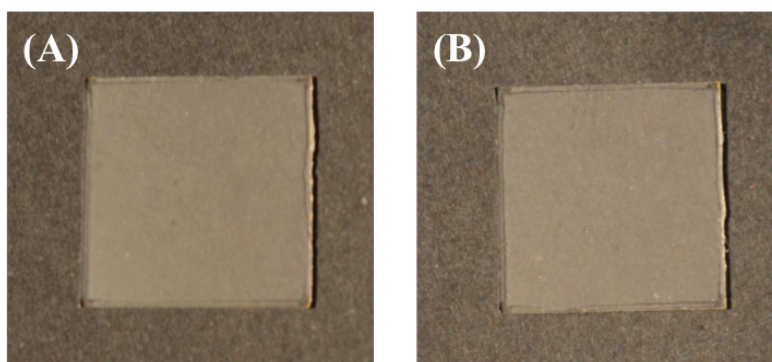


**Figure 5.10. Surface of glass plates after 10 depositions of 90  $\mu\text{L}$  by spin-coating: (A) Non-functionalized particles, (B) dodecylamine-functionalized particles.**

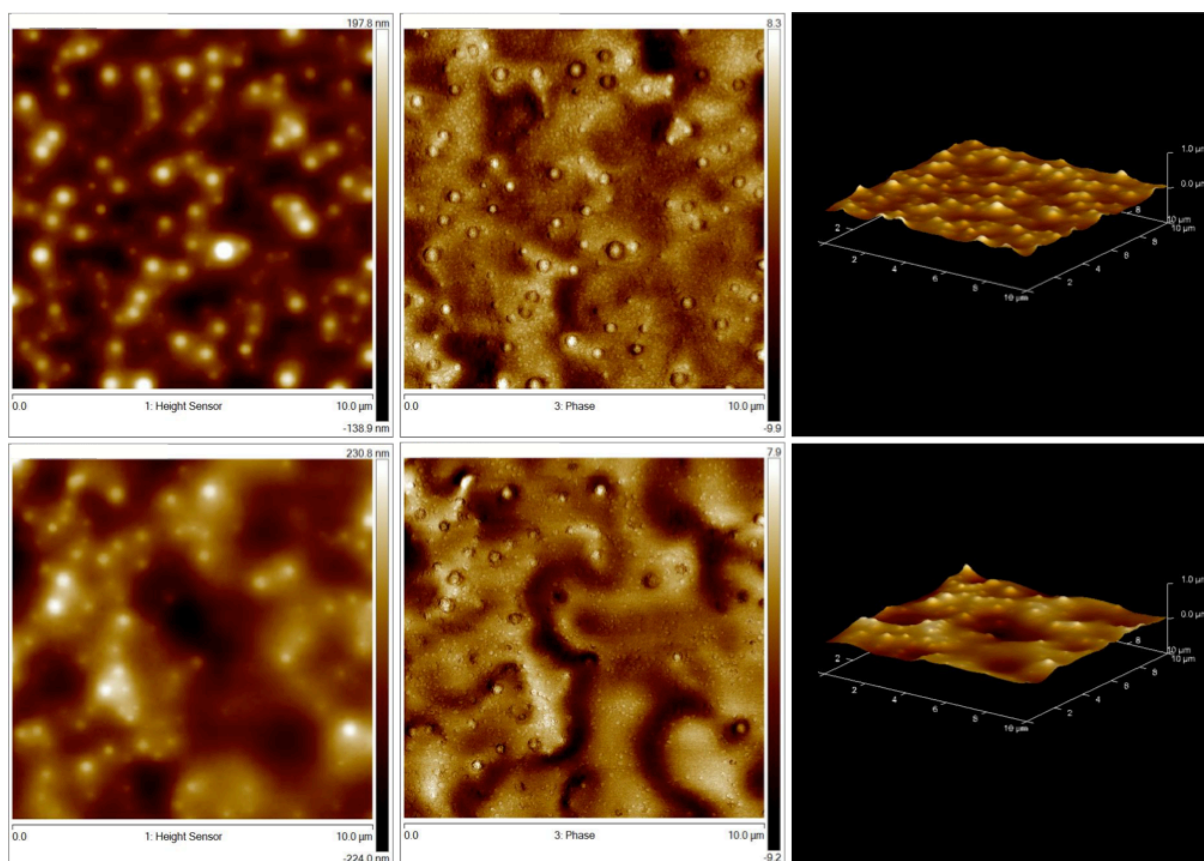


**Figure 5.11. AFM imaging of the polynorbornene-g-polyglycidol particle films. Top: single-deposition films; bottom: multi-deposition films. Left: height imaging; center: phase imaging; right: 3D height imaging.**

The same main features were observed for biocide-functionalized particle films (Figure 5.12). A soft matter bed was also formed and looked more homogeneous when multi-deposition was

achieved, as shown by three-dimensional imaging. Microscopy showed a denser population of particles with a tendency to form small clusters in this case. The biocide-functionalized particles thus appeared slightly less prone to deformation and fusion to form the bed of soft matter as compared to their non-functionalized counterpart. The polyglycidol-based chains should indeed be less inclined to flow, because of higher rigidity of the chains due to the presence of the acetaldehyde diethyl acetal and dodecylamine side groups. This propensity could be confirmed by phase imaging of the sample, which showed more rigid particles laying on top of a much softer surface. This lower tendency to deform could favor particle-particle interactions that would encourage their placement on top of each other when additional spin coating depositions are made. This difference in behavior between the non-functionalized particles and the biocide-functionalized particles is clearly illustrated with the profiles obtained by profilometry (Figure C.8 in Appendix C:). The non-functionalized particles, that easily deformed, tended to produce a more homogeneous surface with little roughness, and this tendency was maintained even after 10 spin-coating depositions. With a single deposition, the biocide-functionalized particles formed a quite homogeneous surface but as more depositions were made, particles depositing on top of each other created higher differentials in height and yielded a more heterogeneous surface.

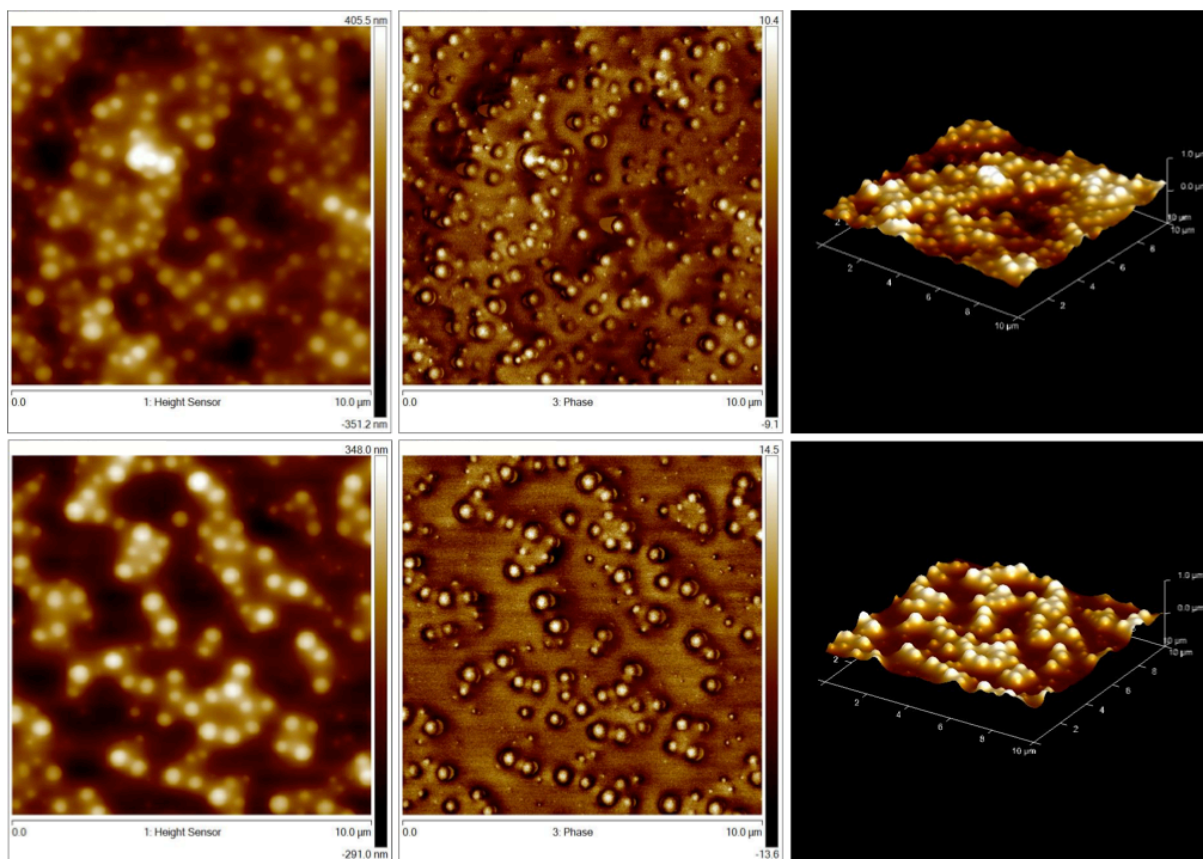


**Figure 5.12. AFM imaging of the dodecylamine-functionalized polynorbornene-g-polyglycidol particle films. Top: single-deposition films; bottom: multi-deposition films. Left: height imaging; center: phase imaging; right: 3D height imaging.**

Profilometry measurements were performed both on single and multi-deposition films of non-functionalized and biocide-functionalized particles to determine the thickness of the films. As summarized in Table 5.5, single-deposition particle films had thicknesses between 320 and 380 nm while multi-deposition films were between 1140 and 1250 nm. While an increase in thickness was observed when multi-deposition was used, the films obtained after 10 depositions obviously did not have thicknesses 10 times larger than the films obtained after a single deposition. This phenomenon could be explained by partial washing-off of the previously deposited particles by the solvent introduced in the next deposition step. This explanation appears highly probable, given the good affinity of the particles for the solvent. A second explanation may be the tendency to deform of the particles observed by AFM. The

deformation and fusion of the newly-deposited particles with the existing film would lead to a reduction in thickness of the film.

**Table 5.5. Average thickness of polynorbornene-g-polyglycidol particle films (standard deviation calculated from 4 repetitions).**

	Non-functionalized particle film		Biocide-functionalized particle film	
	Single-deposition	Multi-deposition	Single-deposition	Multi-deposition
Thickness (nm)	320±12	1140±39	380±4	1250±62

The amount of polymer deposited on the substrate was determined by gravimetry after drying the plates under vacuum. The molar amount of dodecylamine contained in the biocide-functionalized particle films was calculated to reach  $6 \times 10^{-9}$  mol. However, the molar amount of dodecylamine contained in a 10  $\mu$ L droplet for the most concentrated dispersion samples used in the droplet microbiology test ( $5 \times 10^{-6}$  mol mL<sup>-1</sup>) was  $5 \times 10^{-8}$  mol. While the spin-coating method was utilized in the hope of increasing the concentration of dodecylamine, this preparation method therefore did not yield more biocide-concentrated samples. The particle films were nevertheless tested for their antifungal properties in the following section, to observe any differences in behavior as compared with the particle dispersions.

### **5.3.5.2 Evaluation of the Antifungal Activity of the Particle Films**

The antifungal activity of the particles was verified again, this time using particles forming a homogeneous film on a glass plate. The films were not detached from the glass cover slips, so as to limit damage to the quite fragile material, and the antifungal activity of the materials was directly evaluated on the glass cover slips. The methodology thus required to be modified to maintain good contact between the fungus and the particles during the test. As described in

Section 5.2.2.6, the method consisted in putting the glass substrate at the bottom of a Petri dish, and to pour inoculated medium on top of the plate to cover the entire area of the Petri dish.

With this different methodology, the growth medium and the spore concentration needed to be optimized again. Test preparations were made by inoculating 100 mL of PDA and Czapek-Dox agar media with 2.5 mL of a  $10^5$  spores·mL<sup>-1</sup> suspension. By pipetting 4 mL of inoculated medium in each Petri dish containing a blank glass plate, their total charge would thus be  $10^4$  spores. Photos taken after a 7-day incubation time at 25°C revealed that *H. resinae* grew abundantly on PDA medium at this concentration while only little evidence of growth could be found on Czapek-Dox agar medium (Figure 5.13(A) and (C)). On PDA medium, the presence of the glass plate locally reduced the thickness of the medium and created a clearer zone of spores. An inhibiting response from the particle film could be observed more easily in this way.

With the objective of maximizing the potential inhibiting response, the inoculum concentration was reduced to  $10^4$  spores·mL<sup>-1</sup> for the more favorable PDA medium and increased to  $10^6$  spores·mL<sup>-1</sup> for the less favourable Czapek-Dox agar medium, to reach  $10^3$  and  $10^5$  spores per Petri dish, respectively. After 7 days of incubation, the PDA medium still displayed prominent growth of *H. resinae* with a clearer zone where the plate was inserted, while very thin and barely noticeable colonies were seen on Czapek-Dox agar (Figure 5.13(B) and (D)).



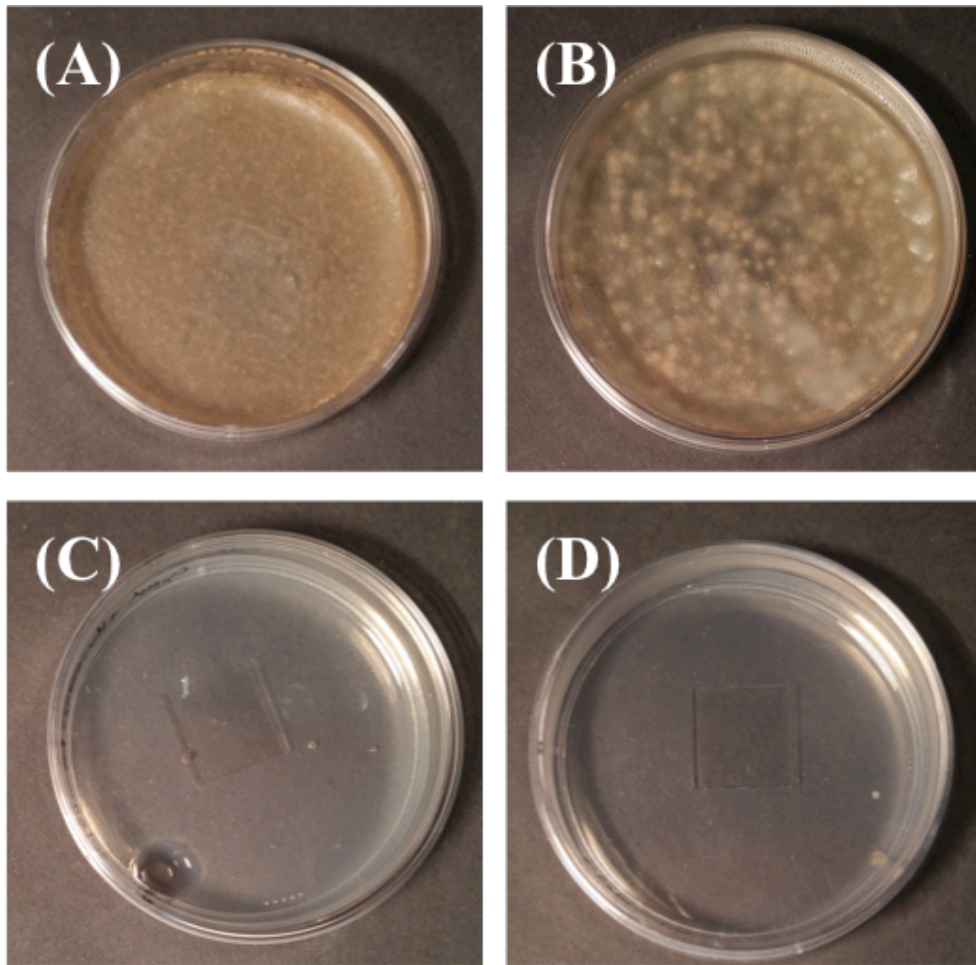


**Figure 5.13. Growth of *H. resinae* in inoculated agar media: (A) PDA medium with  $10^4$  spores/Petri dish, (B) PDA medium with  $10^3$  spores/Petri dish, (C) Czapek-Dox agar with  $10^4$  spores/Petri dish, (D) Czapek-Dox agar with  $10^5$  spores/Petri dish.**

For the following set of tests to evaluate the antifungal properties of particle films, a PDA medium with a concentration of  $10^3$  spores per Petri dish was thus selected, as it only allowed sufficient growth of the fungus. The response of the particle films may be enhanced in this way.

The dodecylamine-functionalized particle films, which were characterized in the previous Section (5.3.5.1), were tested for antifungal properties against *H. resinae* on PDA medium inoculated with a charge of  $10^3$  spores per Petri dish. Non-functionalized particle films were tested under the same conditions as negative control, while dodecylamine samples obtained after drying a solution of dodecylamine were used to ensure that dodecylamine on a glass



substrate could inhibit *H. resinae*. After 7 days of incubation, pictures were taken to account for inhibition of the fungus.

As can be seen in Figure 5.14, the dodecylamine-coated glass plate completely inhibited the growth of *H. resinae*, as no colonies could be observed after 7 days. The non-functionalized particle film enabled homogeneous growth of the fungus, with a lighter zone above the glass plate where the medium was thinner. The test with the dodecylamine-functionalized particle film presented the same aspect, meaning that *H. resinae* was not inhibited by the release of dodecylamine under these conditions. This result was not unexpected however, given the lower total molar amount of dodecylamine present on the glass substrate in comparison to a 10  $\mu$ L droplet used for the test with dispersions.

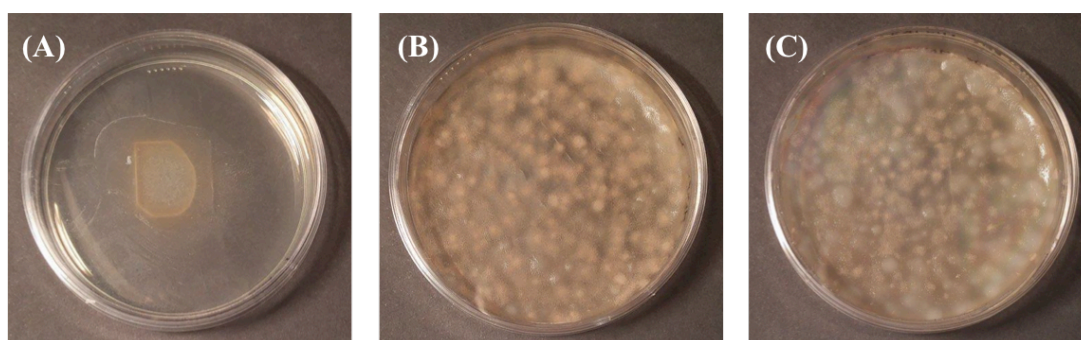


**Figure 5.14. Particle films tested against *H. resinae* in PDA medium containing a concentration of  $10^3$  spores per Petri dish: (A) Dodecylamine-covered plate, (B) glass plate coated with non-functionalized particles, (C) glass plate coated with dodecylamine-functionalized particles.**

### 5.3.6 Incorporation of the Particles in a Model Coating

Since one of the objectives of this work was to devise an anti-corrosion coating with biocidal properties, the particles were tested for incorporation in such a coating. This aspect needed to be verified regardless of the performance of the system because the particles should not disrupt the initial barrier properties if further work on their composition is to be undertaken.

Aluminum plates with dimensions of  $12.5 \times 8 \text{ cm}^2$  were utilized for spray coating. Preparation of the plates consisted in removing the adhesive protecting layer on the surface, and cleaning it with an acetone-soaked paper towel. The surface was then sanded with a 320-grade sandpaper according to the method illustrated in Figure 5.15(A). The coating formula selected was a commercial polyurethane resin from Standox (VOC 2K K9550), formulated by the addition of three components as described by the manufacturer. To 100 g of clear coat (K9550), 37 g of hardener (VOC 25-30) and 6 g of thinner (VOC 2K ADDITIVE) were added. The lifetime of this mixture was estimated to be between 1.25-1.5 h at  $20^\circ\text{C}$  by the manufacturer. The formulation was spray coated onto the aluminum plates with a High Volume Low Pressure (HVLP) spray gun equipped with a 1.4 mm spray nozzle and the spray pressure set at 0.7 bar. The plate was then left to dry for one week. This process led to the formation of a clear and glossy coating layer without defects (Figure 5.15(B)).

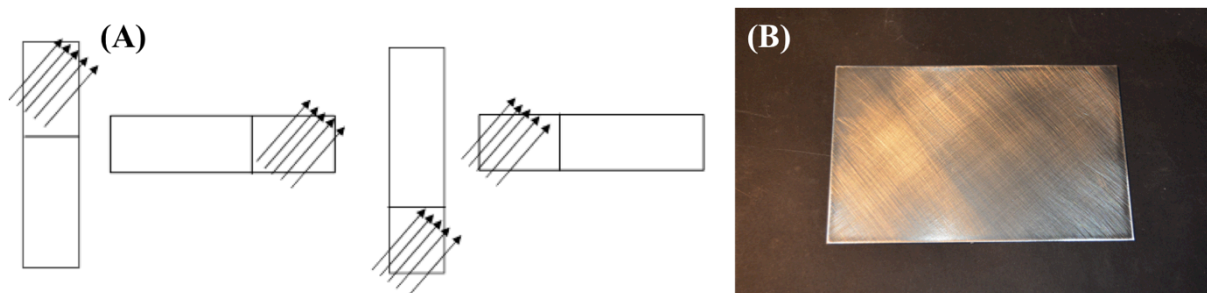


**Figure 5.15. (A) Sanding technique utilized for the aluminum plates; (B) Aluminum plate coated with the VOC 2K K9550 formula.**

Ultrafiltered non-functionalized and dodecylamine-functionalized particle dispersions in ethanol were then deposited on top of the dry coating by HVLP spray coating using a 0.8 mm spray nozzle and a spray pressure of 1 bar. The plates were then allowed to dry for 2 days. The pictures displayed in Figure 5.16 show that both particle types formed a homogeneous film.

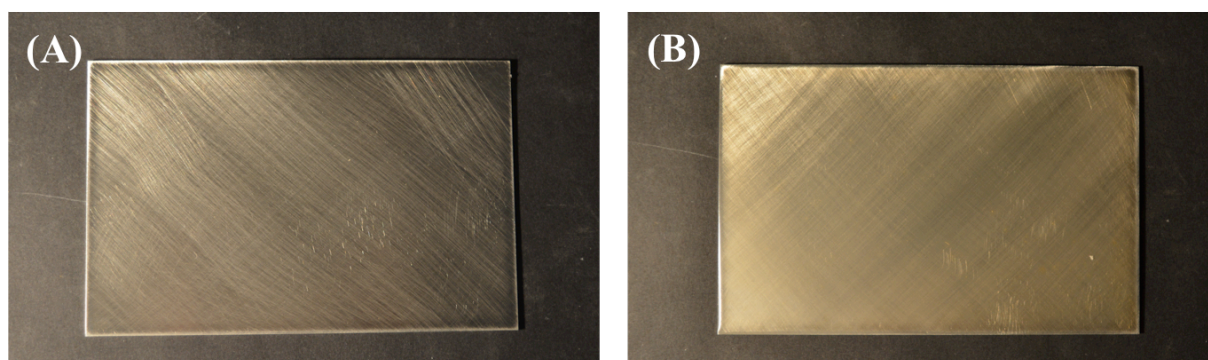


**Figure 5.16. Aluminum plates coated with polyurethane resin and (A) non-functionalized particles; (B) dodecylamine-functionalized particles.**

Resistance to chemical corrosion was tested for all the samples with a salt spray test under neutral conditions for a minimum duration of 14 days. The salt spray test consisted in placing the plates in a closed chamber where a salt water solution (5% NaCl) was constantly atomized through spray nozzles. This created an extremely corrosive environment for the plates in a 100% humidity atmosphere. The back of the plates was protected with a masking film, and the edges with insulating adhesive tape strips. Photos were taken after 7 and 14 days, to keep track of the appearance of corrosion pitting (Figure 5.17), which typically testifies that the coating no longer protects the aluminum plate.

After 7 and 14 days, the commercial resin did not show any sign of corrosion pitting, which was expected given its applications. When the resin was coated with non-functionalized and dodecylamine-functionalized particles this result remained unchanged, both after 7 and 14 days of exposure to the neutral salt spray. This means that the addition of particles by spraying on top of the resin did not create irregularities within the resin allowing the initiation of pitting. The particles may thus be added on top of the initial coating without affecting its properties. Furthermore, even after 14 days of constant exposure to the neutral salt spray and

a 100% humidity atmosphere, the particles did not seem to have been washed away from the plates, which indicates their good anchoring to the resin.

The bioactive properties of the plates were tested before and after exposure to neutral salt spray. The method applied was the same as for the particle films on glass substrates (methodology explained in Section 5.2.2.6). The PDA medium was also inoculated with a spore suspension at  $10^3$  spores  $\text{mL}^{-1}$  in this case.

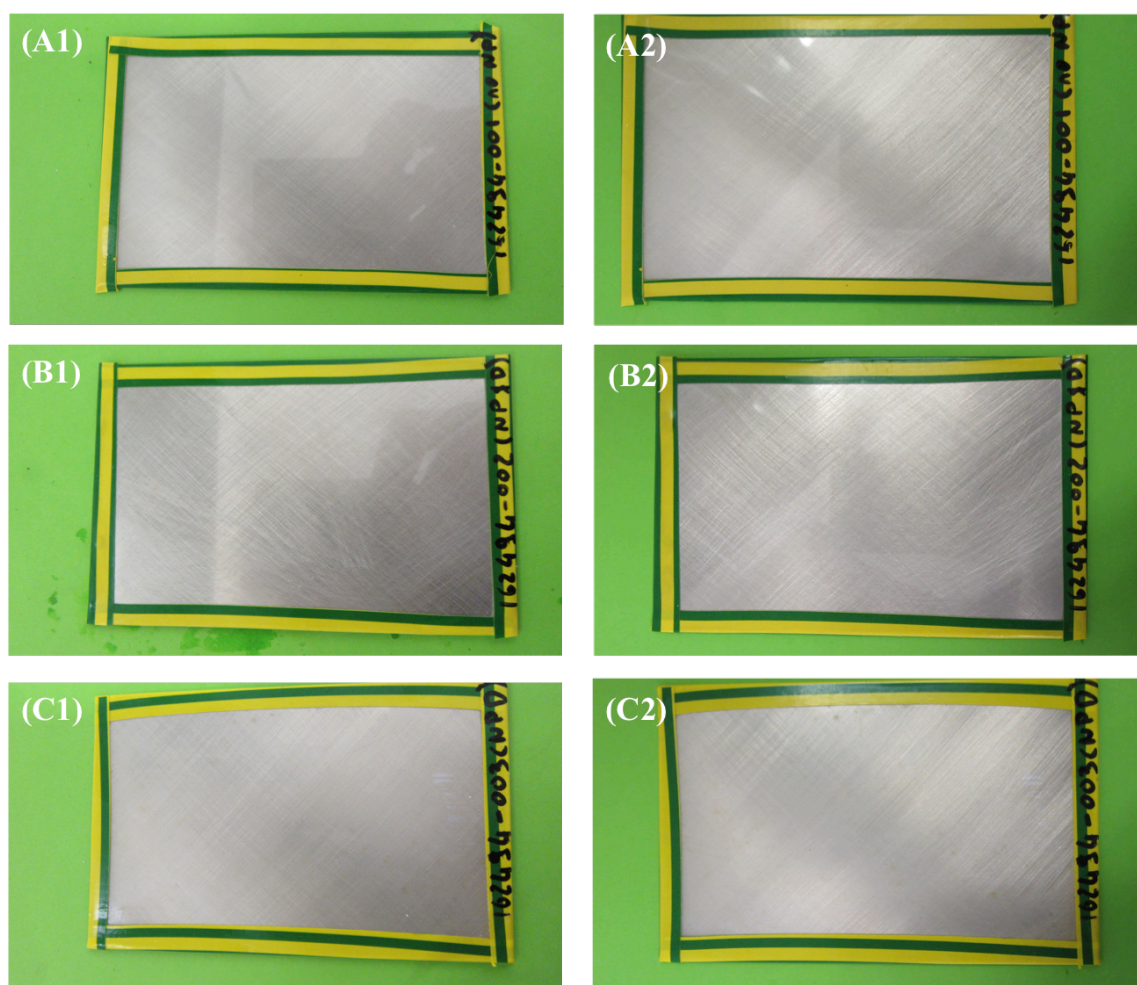


**Figure 5.17. Aluminum plates after neutral salt spray test. Column (1): after 7 days; column (2): after 14 days. Line (A): without particles; line (B): with non-functionalized particles; line(C): with dodecylamine-functionalized particles.**



The coated aluminum plates were therefore cut into  $1.5 \times 1.5 \text{ cm}^2$  squares and tested for their antifungal properties by the method described in Section 5.2.2.6, before and after the neutral salt spray test. Aluminum plates containing non-functionalized particles were used as negative control. As shown in the pictures of Figure 5.18, the plates containing the dodecylamine-functionalized particles did not inhibit the growth of *H. resinae*. The spraying method thus enabled the preparation of homogeneous films with no influence on the corrosion resistance for the commercial resin, but even in that case the concentration of dodecylamine in the particles was insufficient to promote antifungal activity.

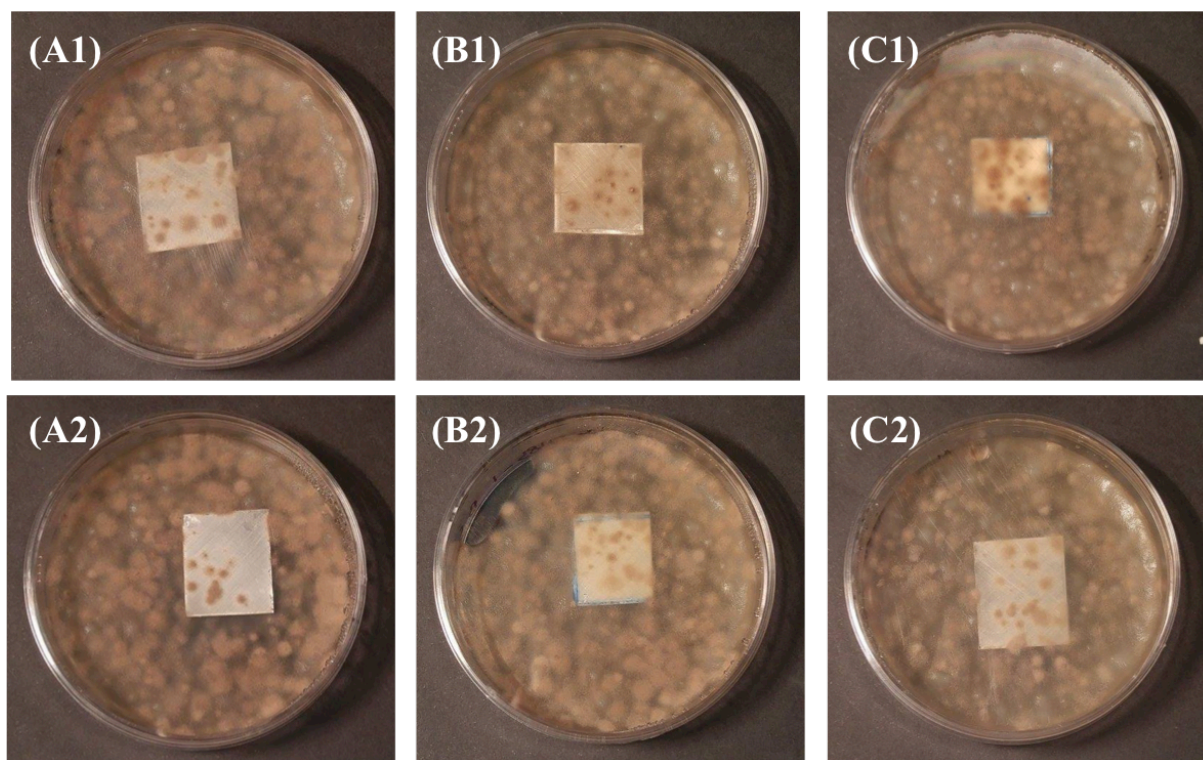


**Figure 5.18.** Aluminum plates tested against *H. resinae* in PDA medium containing  $10^3$  spores per Petri dish. Column (A) coated with resin alone; column (B) coated with resin and non-functionalized particles; column (C) coated with resin and dodecylamine-functionalized particles. Line (1) before neutral salt spray test; line (2) after salt spray test.

## 5.4 Conclusions

Dodecylamine-functionalized  $\alpha$ -norbornenyl-polyglycidol macromonomer and dodecylamine-functionalized polynorbornene-*g*-polyglycidol particles were tested for their antifungal properties. Cleavage of the imine bond to release free dodecylamine was observed by  $^1\text{H}$  NMR analysis for  $\text{pH} < 7$ , demonstrating the sensitivity of the macromonomer to a mildly acidic environment. Evaluation of the antifungal efficacy of both the functionalized macromonomer and the particle systems was performed against the fuel fungus *H. resinae*. While the macromonomer inhibited the fungus when using droplets of solution containing biocide concentrations ranging from  $1 \times 10^{-5}$  to  $5 \times 10^{-5} \text{ mol mL}^{-1}$  for both the macromonomer and free dodecylamine, these concentrations could not be attained for the particle dispersions, which understandably displayed no inhibition for these lower biocide concentrations. The antifungal properties of the particles were tested as films, either spin-coated on glass substrates or spray-coated on coated aluminum plates, but again the lower amounts of dodecylamine present on the substrates as compared to the droplets did not achieve fungal inhibition. The presence of the particles on the previously coated aluminum plates did not disturb the anti-corrosion properties of the resin, as the plates showed no sign of corrosion pitting even after 14 days of exposure to neutral salt spray. Better antifungal response may be achieved by enhancing the solubility of the macromonomer in water, which would induce better dispersibility of the particles in the medium to form the imine bond and make it more accessible for cleavage. Using the same family of biocides, it would be possible to test the conjugation of a shorter primary amine, for example hexylamine. Another way to proceed could be to find another primary amine biocide, with a higher water-solubility and a higher antifungal activity. The required concentration to observe a response against *H. resinae* may be decreased as compared to dodecylamine once they are conjugated on the particles, due to improved accessibility for cleavage and increased activity in the medium.

# **Chapter 6: Concluding Remarks and Perspectives**

## 6.1. Original Contributions to Knowledge

The main goals of this Ph.D. Thesis were to prepare a system of functional polymeric particles for application as antifungal agents to address the issue of microbial-induced corrosion of fuel tanks. The particles needed to be pH-sensitive for controlled delivery of a conjugated biocide molecule.

$\alpha$ -Norbornenyl-polyglycidol macromonomers with linear structures were synthesized by anionic ring-opening polymerization of protected glycidol, with initiation by norbornene-methanol. The polyglycidol backbone was then recovered by hydrolysis of the protected units. The polymerization reaction was well controlled with degrees of polymerization close to the expected values and low polydispersity indices. This procedure represents the first example of polyglycidol-based macromonomers functionalized with a ROMP-reactive norbornene moiety.

The available hydroxyl groups on each repeat unit of the macromonomer chain were utilized for functionalization with dodecylamine using an acid-sensitive bond. The process was performed in two steps, first with substitution of the hydroxyl groups with a bromoacetal compound to introduce protected aldehyde functions on the macromonomer. A one-pot two-step reaction then enabled the regeneration of the aldehyde functions and allowed the multifunctionalization of the macromonomer by the conjugation of dodecylamine through a pH-sensitive imine bond. Conjugation of the biocide to the macromonomer was preferred prior to its polymerization by ROMP as a reactive stabilizer, because this method allowed better control and characterization of the compound. The use of a polyglycidol backbone for the macromonomer instead of PEO used thus far enabled the preparation of multifunctionalized macromonomers bearing 3.6 dodecylamine molecules per chain. The former macromonomer could only be functionalized with a maximum of 1 active compound per chain using the lone terminal hydroxyl group of PEO.



Both the non-functionalized and the dodecylamine-functionalized macromonomers were utilized in a dispersion ROMP process to synthesize polynorbornene-*g*-polyglycidol particles. Spherical particles with diameters of 280-420 nm were obtained by copolymerization of norbornene with  $\alpha$ -norbornenyl-polyglycidol macromonomers with degrees of polymerization between 25 and 103. All the polymerizations yielded complete conversion of norbornene and a high conversion (about 75%) of the macromonomer. Core-shell conformation was confirmed by solvent transfer which caused selective swelling of the polyglycidol chains. The multifunctionality of the polyglycidol chains permitted to reach  $1.4 \times 10^8$  hydroxyl functions per particle available at their surface. This value represents a tremendous increase compared to an analogous polynorbornene-*g*-PEO latex which presented  $3 \times 10^6$  hydroxyl functions per particle.<sup>1</sup> Copolymerization with the dodecylamine-functionalized macromonomer also led to the formation of spherical particles whose diameter increased to 975 nm and the conversion of the macromonomer decreased to 25%. The substituted macromonomer chains were suspected to have decreased the accessibility of the terminal norbornene group and to have enhanced the solubility of the compound, thus decreasing its adsorption on the formed particles. This behavior contrasted with that of the functionalized  $\alpha$ -norbornenyl-PEO macromonomer. The reduced accessibility of the terminal norbornene group was not observed in this case because the lone active molecule was placed at the other end of the macromonomer chain. The ROMP reaction was not hindered and conversion of the functionalized macromonomer could be thus kept around the same values as the non-functionalized analogue.<sup>2,3</sup> The conversion of the  $\alpha$ -norbornenyl-polyglycidol macromonomer still enabled biocide functionalization to amount to  $6.8 \times 10^7$  molecules per particle, corresponding to 4.3 wt %.

Cleavage of the imine bond was observed by <sup>1</sup>H NMR analysis of the dodecylamine-functionalized macromonomer at pH 5-7. Incorporation of the particles in a commercial coating was achieved by spray coating on the surface to yield homogeneous surfaces. The

presence of the particles on the coating did not provoke premature pitting corrosion of the aluminum plates as compared to the control containing no particles. Both the functionalized macromonomer and the particles were tested for antifungal activity against *H. resinae*, a known fuel contaminant, with a droplet test on inoculated agar medium. A less favorable Czapek-Dox agar medium was necessary to observe inhibition of the fungus by a macromonomer solution at a biocide concentration of  $1-5 \times 10^{-5} \text{ mol mL}^{-1}$ . The particles were tested as spin-coated films on glass substrates and were tested against inoculated agar medium. In this method, the more favorable potato dextrose agar medium was necessary to observe growth of the fungus. The particle films did not show antifungal action against *H. resinae* however, presumably because the spin-coating technique did not allow for higher amounts of dodecylamine in the sample. When the aluminum plates coated with the particles were tested under the same conditions, no inhibition of the fungus was observed either.

## **6.2. Suggestions for Future Work**

The work presented in this Thesis confirmed that the polynorbornene-*g*-polyglycidol particle system synthesized by dispersion ROMP can be considered as a serious candidate for the preparation of functionalized particles. However, some aspects of this project could be studied in more depth.

Since one of the major issues with the preparation of the antifungal particles was low incorporation of the biocide-functionalized macromonomer, some elements of its structure could be modified to yield better results. One of the reasons hypothesized for this observation was reduced accessibility of the terminal norbornene group, due to the presence of bulky acetaldehyde diethylacetal and dodecylamine side groups. The functionalization steps could be modified to introduce the exact number of acetaldehyde diethylacetal group to be further conjugated with dodecylamine. In this way, the number of dodecylamine molecules introduced might be improved and no other side groups would be present on the

macromonomer. This study would still require preventing potential crystallization of the chains associated with dodecylamine. Another reason for low incorporation of the macromonomer could be its increased solubility in the dispersing medium due to its substituents. In this case, the introduction of a hydrophobic block between the norbornene group and the polyglycidol chain would favor the adsorption of the macromonomer onto the nucleated particles by decreasing the affinity of the macromonomer with the solvent mixture. The preparation methodology could also be reversed, by first synthesizing non-functionalized polynorbornene-*g*-polyglycidol particles by the usual dispersion ROMP reaction, and then functionalization of the hydroxyl groups in the shell. The tremendous increase in hydroxyl functionality of the particles compared to their polynorbornene-*g*-PEO counterparts would potentially offer more numerous sites of conjugation with the biocide. While macromonomer conversion could be enhanced by that approach, this would likely be achieved at the expense of decreased control over the functionalization process, and would lead to difficulties in the characterization of the system. Close attention should also be paid in this case to the long term stability of the particles.

The versatility of the ROMP reaction could potentially allow the polymerization of macromonomers substituted with different biocides. The investigation of antifungal molecules with higher solubility in water may be preferable to maintain good dispersibility of the particles in water. In this way, the antifungal properties of the system could be more thoroughly studied using tests in liquid media containing both the particles and a suspension of spores, to enhance contact between them and possibly observe a better response. By selecting a biocide with UV-absorbing properties, it would also be possible to monitor precisely the rate of release of that compound from the particles by cleavage of the imine bond under various conditions, and thus to predict its potential efficacy against *H. resinae*.

By conjugation of other types of active molecules, this system may find applications in different fields such as antibiotics or anticancer agents, where the targeted pH-sensitive release of drugs is often desired.

## References

### Chapter 1:

1. Report by Global Market Insights, Inc, February 2017.

### Chapter 2:

1. N. Calderon, E. A. Ofstead, J. P. Ward, W. A. Judy and K. W. Scott, *Journal of the American Chemical Society*, 1968, **90**, 4133-4140.
2. A. W. Anderson and N. G. Merckling, *US2721189*, 1955.
3. A. W. Anderson, N. G. Merckling and P. H. Settlage, *US2799668*, 1957.
4. W. L. Truett, D. R. Johnson, I. M. Robinson and B. A. Montague, *Journal of the American Chemical Society*, 1960, **82**, 2337-2340.
5. H. S. Eleuterio, *US3074918*, 1963.
6. N. Calderon, E. A. Ofstead and W. A. Judy, *Journal of Polymer Science Part A-1: Polymer Chemistry*, 1967, **5**, 2209-2217.
7. B. L. Evering and E. F. Peters, *US2963447*, 1960.
8. R. L. Banks and G. C. Bailey, *I&EC Product Research and Development*, 1964, **3**, 170-173.
9. N. Calderon, H. Y. Chen and K. W. Scott, *Tetrahedron Letters*, 1967, **8**, 3327-3329.
10. P. Jean-Louis Hérisson and Y. Chauvin, *Die Makromolekulare Chemie*, 1971, **141**, 161-176.
11. T. J. Katz, S. J. Lee and N. Acton, *Tetrahedron Letters*, 1976, **17**, 4247-4250.
12. T. J. Katz and N. Acton, *Tetrahedron Letters*, 1976, **17**, 4251-4254.

13. E. O. Fischer and A. Maasböl, *Angewandte Chemie International Edition in English*, 1964, **3**, 580-581.
14. C. P. Casey and T. J. Burkhardt, *Journal of the American Chemical Society*, 1974, **96**, 7808-7809.
15. C. P. Casey, H. E. Tuinstra and M. C. Saeman, *Journal of the American Chemical Society*, 1976, **98**, 608-609.
16. G. Dall'Asta, G. Mazzanti, G. Natta and L. Porri, *Die Makromolekulare Chemie*, 1962, **56**, 224-227.
17. G. Natta, G. Dall'Asta and G. Mazzanti, *Angewandte Chemie International Edition in English*, 1964, **3**, 723-729.
18. G. Natta, G. Dall'Asta, G. Mazzanti and G. Motroni, *Die Makromolekulare Chemie*, 1963, **69**, 163-179.
19. G. Natta, G. Dall'Asta, I. W. Bassi and G. Carella, *Die Makromolekulare Chemie*, 1966, **91**, 87-106.
20. K. J. Ivin and J. C. Mol, *Olefin Metathesis and Metathesis Polymerization*, 1997.
21. T. M. Trnka and R. H. Grubbs, *Accounts of Chemical Research*, 2001, **34**, 18-29.
22. F. W. Michelotti and W. P. Keaveney, *Journal of Polymer Science Part A: General Papers*, 1965, **3**, 895-905.
23. B. M. Novak and R. H. Grubbs, *Journal of the American Chemical Society*, 1988, **110**, 7542-7543.
24. M. A. Hillmyer, C. Lepetit, D. V. McGrath, B. M. Novak and R. H. Grubbs, *Macromolecules*, 1992, **25**, 3345-3350.
25. R. R. Schrock, *Accounts of Chemical Research*, 1990, **23**, 158-165.
26. R. R. Schrock, *Angewandte Chemie International Edition*, 2006, **45**, 3748-3759.

27. S. T. Nguyen, L. K. Johnson, R. H. Grubbs and J. W. Ziller, *Journal of the American Chemical Society*, 1992, **114**, 3974-3975.
28. S. T. Nguyen, R. H. Grubbs and J. W. Ziller, *Journal of the American Chemical Society*, 1993, **115**, 9858-9859.
29. P. Schwab, M. B. France, J. W. Ziller and R. H. Grubbs, *Angewandte Chemie International Edition in English*, 1995, **34**, 2039-2041.
30. P. Schwab, R. H. Grubbs and J. W. Ziller, *Journal of the American Chemical Society*, 1996, **118**, 100-110.
31. D. M. Lynn, S. Kanaoka and R. H. Grubbs, *Journal of the American Chemical Society*, 1996, **118**, 784-790.
32. T. Weskamp, W. C. Schattenmann, M. Spiegler and W. A. Herrmann, *Angewandte Chemie International Edition*, 1998, **37**, 2490-2493.
33. T. Weskamp, F. J. Kohl, W. Hieringer, D. Gleich and W. A. Herrmann, *Angewandte Chemie International Edition*, 1999, **38**, 2416-2419.
34. M. Scholl, T. M. Trnka, J. P. Morgan and R. H. Grubbs, *Tetrahedron Letters*, 1999, **40**, 2247-2250.
35. M. Scholl, S. Ding, C. W. Lee and R. H. Grubbs, *Organic Letters*, 1999, **1**, 953-956.
36. C. W. Bielawski and R. H. Grubbs, *Angewandte Chemie International Edition*, 2000, **39**, 2903-2906.
37. M. S. Sanford, J. A. Love and R. H. Grubbs, *Journal of the American Chemical Society*, 2001, **123**, 6543-6554.
38. J. A. Love, J. P. Morgan, T. M. Trnka and R. H. Grubbs, *Angewandte Chemie International Edition*, 2002, **41**, 4035-4037.
39. T.-L. Choi and R. H. Grubbs, *Angewandte Chemie International Edition*, 2003, **42**, 1743-1746.

40. J. S. Kingsbury, J. P. A. Harrity, P. J. Bonitatebus and A. H. Hoveyda, *Journal of the American Chemical Society*, 1999, **121**, 791-799.
41. S. B. Garber, J. S. Kingsbury, B. L. Gray and A. H. Hoveyda, *Journal of the American Chemical Society*, 2000, **122**, 8168-8179.
42. J. P. Jordan and R. H. Grubbs, *Angewandte Chemie International Edition*, 2007, **46**, 5152-5155.
43. B. Mohr, D. M. Lynn and R. H. Grubbs, *Organometallics*, 1996, **15**, 4317-4325.
44. D. M. Lynn, B. Mohr and R. H. Grubbs, *Journal of the American Chemical Society*, 1998, **120**, 1627-1628.
45. D. Samanta, K. Kratz, X. Zhang and T. Emrick, *Macromolecules*, 2008, **41**, 530-532.
46. J. P. Claverie, S. Viala, V. Maurel and C. Novat, *Macromolecules*, 2001, **34**, 382-388.
47. D. M. Lynn, B. Mohr, R. H. Grubbs, L. M. Henling and M. W. Day, *Journal of the American Chemical Society*, 2000, **122**, 6601-6609.
48. J. P. Gallivan, J. P. Jordan and R. H. Grubbs, *Tetrahedron Letters*, 2005, **46**, 2577-2580.
49. S. H. Hong and R. H. Grubbs, *Journal of the American Chemical Society*, 2006, **128**, 3508-3509.
50. K. Breitenkamp and T. Emrick, *Journal of Polymer Science Part A: Polymer Chemistry*, 2005, **43**, 5715-5721.
51. K. A. Ogawa, A. E. Goetz and A. J. Boydston, *J Am Chem Soc*, 2015, **137**, 1400-1403.
52. A. E. Goetz, L. M. M. Pascual, D. G. Dunford, K. A. Ogawa, D. B. Knorr and A. J. Boydston, *ACS Macro Letters*, 2016, **5**, 579-582.
53. A. E. Goetz and A. J. Boydston, *Journal of the American Chemical Society*, 2015, **137**, 7572-7575.



54. M. Sandholzer, S. Bichler, F. Stelzer and C. Slugovc, *Journal of Polymer Science Part A: Polymer Chemistry*, 2008, **46**, 2402-2413.
55. J. Liu, Y. Liao, X. He, J. Yu, L. Ding and M. Xie, *Macromolecular Chemistry and Physics*, 2011, **212**, 55-63.
56. J. B. Matson and R. H. Grubbs, *Journal of the American Chemical Society*, 2008, **130**, 6731-6733.
57. C. Cheng, K. Qi, D. S. Germack, E. Khoshdel and K. L. Wooley, *Advanced Materials*, 2007, **19**, 2830-2835.
58. K. Breitenkamp and T. Emrick, *Journal of the American Chemical Society*, 2003, **125**, 12070-12071.
59. K. Breitenkamp, D. Junge and T. Emrick, in *Polymeric Drug Delivery I*, American Chemical Society, 2006, vol. 923, ch. 18, pp. 253-267.
60. M. Xie, L. Zhang, Y. Liao, L. Ding, C. Zeng and Z. You, *Journal of Polymer Science Part A: Polymer Chemistry*, 2011, **49**, 4955-4963.
61. C. Cheng, K. Qi, E. Khoshdel and K. L. Wooley, *Journal of the American Chemical Society*, 2006, **128**, 6808-6809.
62. Y. Liu, V. Pinon and M. Weck, *Polymer Chemistry*, 2011, **2**, 1964-1975.
63. K.-Y. Yoon, I.-H. Lee, K. O. Kim, J. Jang, E. Lee and T.-L. Choi, *Journal of the American Chemical Society*, 2012, **134**, 14291-14294.
64. K.-Y. Yoon, I.-H. Lee and T.-L. Choi, *RSC Advances*, 2014, **4**, 49180-49185.
65. K.-Y. Yoon, S. Shin, Y.-J. Kim, I. Kim, E. Lee and T.-L. Choi, *Macromolecular Rapid Communications*, 2015, **36**, 1069-1074.
66. S. Shin, K.-Y. Yoon and T.-L. Choi, *Macromolecules*, 2015, **48**, 1390-1397.
67. G. M. Pawar, R. A. Lalancette, E. M. Bonder, J. B. Sheridan and F. Jäkle, *Macromolecules*, 2015, **48**, 6508-6515.

68. G. Odian, *Principles of Polymerization*, 2004.
69. R. E. Rinehart and H. P. Smith, *Journal of Polymer Science Part B: Polymer Letters*, 1965, **3**, 1049-1052.
70. R. E. Rinehart, 1968, **US3367924**.
71. S. Wache, *Journal of Organometallic Chemistry*, 1995, **494**, 235-240.
72. C. Fraser and R. H. Grubbs, *Macromolecules*, 1995, **28**, 7248-7255.
73. D. D. Manning, X. Hu, P. Beck and L. L. Kiessling, *Journal of the American Chemical Society*, 1997, **119**, 3161-3162.
74. R. Haschick, M. Klapper, K. B. Wagener and K. Müllen, *Macromolecular Chemistry and Physics*, 2010, **211**, 2547-2554.
75. D. Quémener, V. Héroguez and Y. Gnanou, *Macromolecules*, 2005, **38**, 7977-7982.
76. D. Quémener, V. Héroguez and Y. Gnanou, *Journal of Polymer Science Part A: Polymer Chemistry*, 2006, **44**, 2784-2793.
77. D. Quémener, A. Bousquet, V. Héroguez and Y. Gnanou, *Macromolecules*, 2006, **39**, 5589-5591.
78. C. Airaud, V. Héroguez and Y. Gnanou, *Macromolecules*, 2008, **41**, 3015-3022.
79. C.-S. Chern, in *Principles and Applications of Emulsion Polymerization*, John Wiley & Sons, Inc., 2008, DOI: 10.1002/9780470377949.ch6, pp. 154-174.
80. A. S. De Buruaga, I. Capek, J. C. De La Cal and J. M. Asua, *Journal of Polymer Science Part A: Polymer Chemistry*, 1998, **36**, 737-748.
81. G. David, F. Özer, B. C. Simionescu, H. Zareie and E. Pişkin, *European Polymer Journal*, 2002, **38**, 73-78.
82. K. Jain, J. Klier and A. B. Scranton, *Polymer*, 2005, **46**, 11273-11278.
83. V. Monteil, P. Wehrmann and S. Mecking, *Journal of the American Chemical Society*, 2005, **127**, 14568-14569.

84. C. Airaud, E. Ibarboure, C. Gaillard and V. Héroguez, *Macromolecular Symposia*, 2009, **281**, 31-38.
85. C. Airaud, E. Ibarboure, C. Gaillard and V. Héroguez, *Journal of Polymer Science Part A: Polymer Chemistry*, 2009, **47**, 4014-4027.
86. M. N. Nguyen, S.-J. Mougner, E. Ibarboure and V. Héroguez, *Journal of Polymer Science Part A: Polymer Chemistry*, 2011, **49**, 1471-1482.
87. B. Scheinhardt, J. Trzaskowski, M. C. Baier, B. Stempfle, A. Oppermann, D. Wöll and S. Mecking, *Macromolecules*, 2013, **46**, 7902-7910.
88. B. Ö. Öztürk, S. Karabulut Şehitoğlu and M. A. R. Meier, *European Polymer Journal*, 2015, **62**, 116-123.
89. B. S. Lee, S. Mahajan, B. Clapham and K. D. Janda, *The Journal of Organic Chemistry*, 2004, **69**, 3319-3329.
90. A. Della Martina, R. Graf and J. G. Hilborn, *Journal of Applied Polymer Science*, 2005, **96**, 407-415.
91. E. D. Sudol, in *Polymeric Dispersions: Principles and Applications*, ed. J. M. Asua, Springer Netherlands, Dordrecht, 1997, DOI: 10.1007/978-94-011-5512-0\_10, pp. 141-153.
92. S. Kawaguchi and K. Ito, in *Polymer Particles*, ed. M. Okubo, Springer Berlin Heidelberg, Berlin, Heidelberg, 2005, DOI: 10.1007/b100118, pp. 299-328.
93. K. E. J. Barrett, *British Polymer Journal*, 1973, **5**, 259-271.
94. S. Y. Lu, P. Quayle, C. Booth, S. G. Yeates and J. C. Padget, *Polymer International*, 1993, **32**, 1-4.
95. A. Chemtob, V. Héroguez and Y. Gnanou, *Macromolecules*, 2002, **35**, 9262-9269.
96. A. D. Jenkins, P. Kratochvíl, R. F. T. Stepto and U. W. Suter, *Journal*, 1996, **68**, 2287.

97. V. Héroguez, Y. Gnanou and M. Fontanille, *Macromolecular Rapid Communications*, 1996, **17**, 137-142.
98. N. Hadjichristidis, M. Pitsikalis, H. Iatrou and S. Pispas, *Macromolecular Rapid Communications*, 2003, **24**, 979-1013.
99. G. Morandi, S. Piogé, S. Pascual, V. Montembault, S. Legoupy and L. Fontaine, *Materials Science and Engineering: C*, 2009, **29**, 367-371.
100. J. Liu, A. O. Burts, Y. Li, A. V. Zhukhovitskiy, M. F. Ottaviani, N. J. Turro and J. A. Johnson, *Journal of the American Chemical Society*, 2012, **134**, 16337-16344.
101. D. Le, V. Montembault, S. Pascual, F. Collette, V. Héroguez and L. Fontaine, *Polymer Chemistry*, 2013, **4**, 2168-2173.
102. A. Chemtob, V. Héroguez and Y. Gnanou, *Macromolecules*, 2004, **37**, 7619-7627.
103. V. Héroguez, M. Fontanille and Y. Gnanou, *Macromolecular Symposia*, 2000, **150**, 269-274.
104. A. Chemtob, V. Héroguez and Y. Gnanou, *Journal of Polymer Science Part A: Polymer Chemistry*, 2004, **42**, 1154-1163.
105. A. Chemtob, V. Héroguez and Y. Gnanou, *Macromolecular Rapid Communications*, 2005, **26**, 1711-1715.
106. A.-C. Le Meur, C. Aymonier and V. Héroguez, *Journal of Polymer Science Part A: Polymer Chemistry*, 2012, **50**, 1746-1754.
107. G. Helmlinger, A. Sckell, M. Dellian, N. S. Forbes and R. K. Jain, *Clinical Cancer Research*, 2002, **8**, 1284.
108. A. C. Issekutz and S. Bhimji, *Infection and Immunity*, 1982, **36**, 558-566.
109. H.-P. Simmen and J. Blaser, *The American Journal of Surgery*, 1993, **166**, 24-27.
110. E. R. Gillies, A. P. Goodwin and J. M. J. Fréchet, *Bioconjugate Chemistry*, 2004, **15**, 1254-1263.

111. J. Zou, G. Jafr, E. Themistou, Y. Yap, Z. A. P. Wintrob, P. Alexandridis, A. C. Ceacareanu and C. Cheng, *Chemical Communications*, 2011, **47**, 4493-4495.
112. Y. Gu, Y. Zhong, F. Meng, R. Cheng, C. Deng and Z. Zhong, *Biomacromolecules*, 2013, **14**, 2772-2780.
113. Y. Li, Y. Tang, K. Yang, X. Chen, L. Lu and Y. Cai, *Macromolecules*, 2008, **41**, 4597-4606.
114. M. Li, M. Gao, Y. Fu, C. Chen, X. Meng, A. Fan, D. Kong, Z. Wang and Y. Zhao, *Colloids and Surfaces B: Biointerfaces*, 2016, **140**, 11-18.
115. M. S. Shim and Y. J. Kwon, *Biomacromolecules*, 2008, **9**, 444-455.
116. S.-i. Kondo, Y. Sasai, M. Kuzuya and S. Furukawa, *Chemical and Pharmaceutical Bulletin*, 2002, **50**, 1434-1438.
117. S.-i. Kondo, K. Murase and M. Kuzuya, *Chemical & Pharmaceutical Bulletin*, 1994, **42**, 2412-2417.
118. T. Ouchi, H. Kuroda and Y. Ohya, in *Poly(ethylene glycol)*, American Chemical Society, 1997, vol. 680, ch. 19, pp. 284-296.
119. Y. Ohya, H. Kuroda, K. Hirai and T. Ouchi, *Journal of Bioactive and Compatible Polymers*, 1995, **10**, 51-66.
120. M. Sedlák, M. Pravda, F. Staud, L. Kubicová, K. Týčová and K. Ventura, *Bioorganic & Medicinal Chemistry*, 2007, **15**, 4069-4076.
121. H. Magaña, K. Palomino, J. M. Cornejo-Bravo, L. Díaz-Gómez, A. Concheiro, E. Zavala-Lagunes, C. Alvarez-Lorenzo and E. Bucio, *International Journal of Pharmaceutics*, 2016, **511**, 579-585.
122. R. Jantas, Z. Draczyński, L. Herczyńska and D. Stawski, *American Journal of Polymer Science*, 2012, **2**, 79-84.
123. M. Babazadeh, *International Journal of Pharmaceutics*, 2006, **316**, 68-73.

124. M. Babazadeh, *Journal of Applied Polymer Science*, 2007, **104**, 2403-2409.
125. R. Jantas and L. Herczyńska, *Polymer Bulletin*, 2010, **64**, 459-469.
126. Y. Bae, S. Fukushima, A. Harada and K. Kataoka, *Angewandte Chemie International Edition*, 2003, **42**, 4640-4643.
127. H. R. Ihre, O. L. Padilla De Jesús, F. C. Szoka and J. M. J. Fréchet, *Bioconjugate Chemistry*, 2002, **13**, 443-452.
128. S. Aryal, C.-M. J. Hu and L. Zhang, *ACS Nano*, 2010, **4**, 251-258.
129. X.-B. Xiong and A. Lavasanifar, *ACS Nano*, 2011, **5**, 5202-5213.
130. G. Min, C. Chao, F. Aiping, Z. Ju, K. Deling, W. Zheng and Z. Yanjun, *Nanotechnology*, 2015, **26**, 275101.
131. H. Li, M. Li, C. Chen, A. Fan, D. Kong, Z. Wang and Y. Zhao, *International Journal of Pharmaceutics*, 2015, **495**, 572-578.
132. T. Etrych, M. Jelínková, B. Říhová and K. Ulbrich, *Journal of Controlled Release*, 2001, **73**, 89-102.
133. K. Ulbrich, T. Etrych, P. Chytil, M. Jelínková and B. Říhová, *Journal of Controlled Release*, 2003, **87**, 33-47.
134. K. Ulbrich, T. Etrych, P. Chytil, M. Pechar, M. Jelinkova and B. Rihova, *International Journal of Pharmaceutics*, 2004, **277**, 63-72.
135. O. Sedláček, M. Hrubý, M. Studenovský, D. Větvička, J. Svoboda, D. Kaňková, J. Kovář and K. Ulbrich, *Bioorganic & Medicinal Chemistry*, 2012, **20**, 4056-4063.
136. L. Sivak, V. Subr, J. Tomala, B. Rihova, J. Strohalm, T. Etrych and M. Kovar, *Biomaterials*, 2017, **115**, 65-80.
137. A. Braunová, L. Kostka, L. Sivák, L. Cuchalová, Z. Hvězdová, R. Laga, S. Filippov, P. Černoch, M. Pechar, O. Janoušková, M. Šírová and T. Etrych, *Journal of Controlled Release*, 2017, **245**, 41-51.

138. J. Cui, Y. Yan, Y. Wang and F. Caruso, *Advanced Functional Materials*, 2012, **22**, 4718-4723.
139. S. B. Shashwat and C. Dong-Hwang, *Nanotechnology*, 2008, **19**, 505104.
140. M. Hrubý, Č. Koňák and K. Ulbrich, *Journal of Controlled Release*, 2005, **103**, 137-148.
141. L. Zhou, R. Cheng, H. Tao, S. Ma, W. Guo, F. Meng, H. Liu, Z. Liu and Z. Zhong, *Biomacromolecules*, 2011, **12**, 1460-1467.
142. M. Talelli, M. Iman, A. K. Varkouhi, C. J. F. Rijcken, R. M. Schiffelers, T. Etrych, K. Ulbrich, C. F. van Nostrum, T. Lammers, G. Storm and W. E. Hennink, *Biomaterials*, 2010, **31**, 7797-7804.
143. Z. Jia, L. Wong, T. P. Davis and V. Bulmus, *Biomacromolecules*, 2008, **9**, 3106-3113.
144. L. Wong, M. Kavallaris and V. Bulmus, *Polymer Chemistry*, 2011, **2**, 385-393.
145. M. Prabakaran, J. J. Grailer, S. Pilla, D. A. Steeber and S. Gong, *Biomaterials*, 2009, **30**, 5757-5766.
146. H. Saito, A. S. Hoffman and H. I. Ogawa, *Journal of Bioactive and Compatible Polymers*, 2007, **22**, 589-601.
147. J. Mao, Y. Li, T. Wu, C. Yuan, B. Zeng, Y. Xu and L. Dai, *ACS Applied Materials & Interfaces*, 2016, **8**, 17109-17117.
148. M. Sedlák, M. Pravda, L. Kubicová, P. Mikulčíková and K. Ventura, *Bioorganic & Medicinal Chemistry Letters*, 2007, **17**, 2554-2557.
149. B. Wang, C. Xu, J. Xie, Z. Yang and S. Sun, *Journal of the American Chemical Society*, 2008, **130**, 14436-14437.
150. L. Zhu, L. Zhao, X. Qu and Z. Yang, *Langmuir*, 2012, **28**, 11988-11996.
151. N. Xiao, H. Liang and J. Lu, *Soft Matter*, 2011, **7**, 10834-10840.

152. D. Hua, J. Jiang, L. Kuang, J. Jiang, W. Zheng and H. Liang, *Macromolecules*, 2011, **44**, 1298-1302.
153. W. Huang, Y. Wang, S. Zhang, L. Huang, D. Hua and X. Zhu, *Macromolecules*, 2013, **46**, 814-818.
154. J. Shi, W. Guobao, H. Chen, W. Zhong, X. Qiu and M. M. Q. Xing, *Polymer Chemistry*, 2014, **5**, 6180-6189.
155. E.-R. Kenawy, F. Imam Abdel-Hay, A. Abou El-Magd and Y. Mahmoud, *Journal of Applied Polymer Science*, 2006, **99**, 2428-2437.
156. R. Delatouche, I. Denis, M. Grinda, F. E. Bahhaj, E. Baucher, F. Collette, V. Héroguez, M. Grégoire, C. Blanquart and P. Bertrand, *European Journal of Pharmaceutics and Biopharmaceutics*, 2013, **85**, 862-872.
157. V. Héroguez, S. Breunig, Y. Gnanou and M. Fontanille, *Macromolecules*, 1996, **29**, 4459-4464.
158. D. Quémener, V. Héroguez and Y. Gnanou, *Journal of Polymer Science Part A: Polymer Chemistry*, 2005, **43**, 217-229.
159. L. Pichavant, C. Bourget, M.-C. Durrieu and V. Héroguez, *Macromolecules*, 2011, **44**, 7879-7887.
160. L. Pichavant, G. Amador, C. Jacqueline, B. Brouillaud, V. Héroguez and M.-C. Durrieu, *Journal of Controlled Release*, 2012, **162**, 373-381.
161. I. Denis, F. el Bahhaj, F. Collette, R. Delatouche, F. Gueugnon, D. Pouliquen, L. Pichavant, V. Héroguez, M. Grégoire, P. Bertrand and C. Blanquart, *European Journal of Medicinal Chemistry*, 2015, **95**, 369-376.
162. I. Denis, F. el Bahhaj, F. Collette, R. Delatouche, F. Gueugnon, D. Pouliquen, L. Pichavant, V. Héroguez, M. Grégoire, P. Bertrand and C. Blanquart, *Biomacromolecules*, 2014, **15**, 4534-4543.



163. F. el Bahhaj, I. Denis, L. Pichavant, R. Delatouche, F. Collette, C. Linot, D. Pouliquen, M. Grégoire, V. Héroguez, C. Blanquart and P. Bertrand, *Theranostics*, 2016, **6**, 795-807.

### Chapter 3:

1. R. K. Kainthan, J. Janzen, E. Levin, D. V. Devine and D. E. Brooks, *Biomacromolecules*, 2006, **7**, 703-709.
2. R. K. Kainthan, S. R. Hester, E. Levin, D. V. Devine and D. E. Brooks, *Biomaterials*, 2007, **28**, 4581-4590.
3. R. K. Kainthan and D. E. Brooks, *Biomaterials*, 2007, **28**, 4779-4787.
4. W. Walach, A. Kowalczyk, B. Trzebicka and A. Dworak, *Macromolecular Rapid Communications*, 2001, **22**, 1272-1277.
5. M. Gervais, A.-L. Brocas, G. Cendejas, A. Deffieux and S. Carlotti, *Macromolecules*, 2010, **43**, 1778-1784.
6. E. J. Goethals, R. R. De Clercq, H. C. De Clercq and P. J. Hartmann, *Makromolekulare Chemie. Macromolecular Symposia*, 1991, **47**, 151-162.
7. R. Tokar, P. Kubisa, S. Penczek and A. Dworak, *Macromolecules*, 1994, **27**, 320-322.
8. A. Dworak, W. Walach and B. Trzebicka, *Macromolecular Chemistry and Physics*, 1995, **196**, 1963-1970.
9. A. Sunder, R. Hanselmann, H. Frey and R. Mülhaupt, *Macromolecules*, 1999, **32**, 4240-4246.
10. R. Francis, D. Taton, J. L. Logan, P. Masse, Y. Gnanou and R. S. Duran, *Macromolecules*, 2003, **36**, 8253-8259.
11. M. Jamróz-Piegza, A. Utrata-Wesołek, B. Trzebicka and A. Dworak, *European Polymer Journal*, 2006, **42**, 2497-2506.

12. W. Walach, B. Trzebicka, J. Justynska and A. Dworak, *Polymer*, 2004, **45**, 1755-1762.
13. F. Wurm, J. Nieberle and H. Frey, *Macromolecules*, 2008, **41**, 1184-1188.
14. S.-E. Stiriba, H. Kautz and H. Frey, *Journal of the American Chemical Society*, 2002, **124**, 9698-9699.
15. M. Yamane, Y. Hirose and K. Adachi, *Macromolecules*, 2005, **38**, 10686-10693.
16. M. Erberich, H. Keul and M. Möller, *Macromolecules*, 2007, **40**, 3070-3079.
17. D. Taton, A. Le Borgne, M. Sepulchre and N. Spassky, *Macromolecular Chemistry and Physics*, 1994, **195**, 139-148.
18. A. Dworak, I. Panchev, B. Trzebicka and W. Walach, *Macromolecular Symposia*, 2000, **153**, 233-242.
19. M. Hans, H. Keul and M. Moeller, *Polymer*, 2009, **50**, 1103-1108.
20. H. Keul and M. Möller, *Journal of Polymer Science Part A: Polymer Chemistry*, 2009, **47**, 3209-3231.
21. B. R. Spears, M. A. Marin, J. R. Montenegro-Burke, B. C. Evans, J. McLean and E. Harth, *Macromolecules*, 2016, DOI: 10.1021/acs.macromol.6b00305.
22. A. Dworak, G. Baran, B. Trzebicka and W. Wałach, *Reactive and Functional Polymers*, 1999, **42**, 31-36.
23. S. Halacheva, S. Rangelov and C. Tsvetanov, *Macromolecules*, 2006, **39**, 6845-6852.
24. A. Dworak and W. Wałach, *Polymer*, 2009, **50**, 3440-3447.
25. M. Libera, B. Trzebicka, A. Kowalczyk, W. Wałach and A. Dworak, *Polymer*, 2011, **52**, 250-257.
26. M. Libera, W. Wałach, B. Trzebicka, S. Rangelov and A. Dworak, *Polymer*, 2011, **52**, 3526-3536.
27. M. Wyszogrodzka and R. Haag, *Langmuir*, 2009, **25**, 5703-5712.

28. M. Weinhart, I. Grunwald, M. Wyszogrodzka, L. Gaetjen, A. Hartwig and R. Haag, *Chemistry – An Asian Journal*, 2010, **5**, 1992-2000.
29. M. Weinhart, T. Becherer, N. Schnurbusch, K. Schwibbert, H.-J. Kunte and R. Haag, *Advanced Engineering Materials*, 2011, **13**, B501-B510.
30. M. Gervais, A. Labbé, S. Carlotti and A. Deffieux, *Macromolecules*, 2009, **42**, 2395-2400.
31. M. Gervais, A.-L. Brocas, G. Cendejas, A. Deffieux and S. Carlotti, *Macromolecular Symposia*, 2011, **308**, 101-111.
32. A. Thomas, K. Niederer, F. Wurm and H. Frey, *Polymer Chemistry*, 2014, **5**, 899-909.
33. A. M. Hofmann, R. Wipf, B. Stühn and H. Frey, *Macromolecules*, 2011, **44**, 6767-6775.
34. A. Dworak, B. Trzebicka, A. Utrata and W. Walach, *Polymer Bulletin*, 2003, **50**, 47-54.
35. P. Dimitrov, E. Hasan, S. Rangelov, B. Trzebicka, A. Dworak and C. B. Tsvetanov, *Polymer*, 2002, **43**, 7171-7178.
36. P. Dimitrov, M. Jamróz-Piegza, B. Trzebicka and A. Dworak, *Polymer*, 2007, **48**, 1866-1874.
37. M. Backes, L. Messenger, A. Mourran, H. Keul and M. Moeller, *Macromolecules*, 2010, **43**, 3238-3248.
38. S. Lee, K. Saito, H.-R. Lee, M. J. Lee, Y. Shibasaki, Y. Oishi and B.-S. Kim, *Biomacromolecules*, 2012, **13**, 1190-1196.
39. A. Mendrek, S. Mendrek, B. Trzebicka, D. Kuckling, W. Walach, H.-J. Adler and A. Dworak, *Macromolecular Chemistry and Physics*, 2005, **206**, 2018-2026.
40. A. Dworak, I. Panchev, B. Trzebicka and W. Walach, *Polymer Bulletin*, 1998, **40**, 461-468.

41. M. Gosecka, J. Pietrasik, P. Decorse, B. Glebocki, M. M. Chehimi, S. Slomkowski and T. Basinska, *Langmuir*, 2015, **31**, 4853-4861.
42. A. Thomas, F. K. Wolf and H. Frey, *Macromolecular Rapid Communications*, 2011, **32**, 1910-1915.
43. G. Gunkel, M. Weinhart, T. Becherer, R. Haag and W. T. S. Huck, *Biomacromolecules*, 2011, **12**, 4169-4172.
44. A. O. Fitton, J. Hill, D. E. Jane and R. Millar, *Synthesis*, 1987, **12**, 1140-1142.
45. *Chemical & Engineering News Archive*, 1982, **60(28)**, 4-5.
46. *Chemical & Engineering News Archive*, 1982, **60(37)**, 4-5.
47. D. Heseck, M. Lee, B. C. Noll, J. F. Fisher and S. Mobashery, *The Journal of Organic Chemistry*, 2009, **74**, 2567-2570.
48. L. Pichavant, G. Amador, C. Jacqueline, B. Brouillaud, V. Héroguez and M.-C. Durrieu, *Journal of Controlled Release*, 2012, **162**, 373-381.
49. L. Pichavant, C. Bourget, M.-C. Durrieu and V. Héroguez, *Macromolecules*, 2011, **44**, 7879-7887.
50. L. Pichavant, H. Carrie, M. C. Durrieu and V. Heroguez, *Polymer Chemistry*, 2016, **7**, 7019-7028.

## Chapter 4:

1. T. Basinska, S. Slomkowski, A. Dworak, I. Panchev and M. M. Chehimi, *Colloid Polym Sci*, 2001, **279**, 916-924.
2. T. Basinska, L. Kergoat, C. Mangeney, M. M. Chehimi and S. Slomkowski, *e-Polymers*, 2007, **7**, 1008-1017.
3. N. Griffete, M. Dybkowska, B. Glebocki, T. Basinska, C. Connan, A. Maître, M. M. Chehimi, S. Slomkowski and C. Mangeney, *Langmuir*, 2010, **26**, 11550-11557.

4. M. Gosecka, N. Griffete, C. Mangeney, M. M. Chehimi, S. Slomkowski and T. Basinska, *Colloid Polym Sci*, 2011, **289**, 1511-1518.
5. I. Radomska-Galant and T. Basinska, *Biomacromolecules*, 2003, **4**, 1848-1855.
6. T. Basinska, M. Wisniewska and M. Chmiela, *Macromolecular Bioscience*, 2005, **5**, 70-77.
7. T. Basinska, S. Krolik and S. Slomkowski, *Macromolecular Symposia*, 2009, **281**, 96-105.
8. S. Pargen, C. Willems, H. Keul, A. Pich and M. Möller, *Macromolecules*, 2012, **45**, 1230-1240.
9. M. Jamróz-Piegza, W. Wałach, A. Dworak and B. Trzebicka, *Journal of Colloid and Interface Science*, 2008, **325**, 141-148.
10. M. Siebert, A. Henke, T. Eckert, W. Richtering, H. Keul and M. Möller, *Langmuir*, 2010, **26**, 16791-16800.
11. E. Haladjova, N. Dishovsky, W. Meier, C. B. Tsvetanov and C. P. Novakov, *Soft Matter*, 2011, **7**, 9459-9467.
12. B. Schulte, A. Walther, H. Keul and M. Möller, *Macromolecules*, 2014, **47**, 1633-1645.
13. B. Schulte, K. Rahimi, H. Keul, D. E. Demco, A. Walther and M. Moller, *Soft Matter*, 2015, **11**, 943-953.
14. B. R. Spears, M. A. Marin, A. N. Chaker, M. W. Lampley and E. Harth, *ACS Biomaterials Science & Engineering*, 2016, **2**, 1265-1272.
15. J. N. Lockhart, D. B. Beezer, D. M. Stevens, B. R. Spears and E. Harth, *Journal of Controlled Release*, 2016, **244**, Part B, 366-374.
16. M. S. Moorthy, Y. Oh, S. Bharathiraja, P. Manivasagan, T. Rajarathinam, B. Jang, T. T. Vy Phan, H. Jang and J. Oh, *RSC Advances*, 2016, **6**, 110444-110453.

17. A. Chemtob, V. Héroguez and Y. Gnanou, *Macromolecules*, 2002, **35**, 9262-9269.
18. A. Chemtob, V. Héroguez and Y. Gnanou, *Journal of Polymer Science Part A: Polymer Chemistry*, 2004, **42**, 2705-2716.
19. L. Pichavant, C. Bourget, M.-C. Durrieu and V. Héroguez, *Macromolecules*, 2011, **44**, 7879-7887.
20. S. Jha, S. Dutta and N. B. Bowden, *Macromolecules*, 2004, **37**, 4365-4374.
21. G. Morandi, V. Montembault, S. Pascual, S. Legoupy and L. Fontaine, *Macromolecules*, 2006, **39**, 2732-2735.
22. G. Morandi, G. Mantovani, V. Montembault, D. M. Haddleton and L. Fontaine, *New Journal of Chemistry*, 2007, **31**, 1826-1829.
23. F. Leroux, V. Montembault, S. Pascual, W. Guerin, S. M. Guillaume and L. Fontaine, *Polymer Chemistry*, 2014, **5**, 3476-3486.
24. D. A. N'Guyen, F. Leroux, V. Montembault, S. Pascual and L. Fontaine, *Polymer Chemistry*, 2016, **7**, 1730-1738.

## Chapter 5:

1. D. Allsopp, K. J. Seal and C. C. Gaylarde, *Introduction to Biodeterioration*, Cambridge University Press, Cambridge, 2 edn., 2004.
2. B. M. Rosales and M. Iannuzzi, *Materials Science and Engineering: A*, 2008, **472**, 15-25.
3. C. C. Gaylarde, F. M. Bento and J. Kelley, *Revista de Microbiologia*, 1999, **30**, 01-10.
4. E. Odier, *Annales de microbiologie*, 1976, **127b**, 213-225.
5. F. M. Bento and C. C. Gaylarde, *International Biodeterioration & Biodegradation*, 2001, **47**, 107-112.
6. K. Watanabe, Y. Kodama and N. Kaku, *BMC Microbiology*, 2002, **2**, 23-23.

7. M. E. Rauch, H. W. Graef, S. M. Rozenzhak, S. E. Jones, C. A. Bleckmann, R. L. Kruger, R. R. Naik and M. O. Stone, *Journal of Industrial Microbiology and Biotechnology*, 2006, **33**, 29-36.
8. V. Raikos, S. S. Vamvakas, J. Kaposos, A. Koliadima and G. Karaiskakis, *Fuel*, 2011, **90**, 695-700.
9. N. I. Hendey, *Transactions of the British Mycological Society*, 1964, **47**, 467-IN461.
10. G. Andrykovitch and R. A. Neihof, *Journal of Industrial Microbiology*, 1987, **2**, 35-40.
11. G. E. G. Hettige and J. E. Sheridan, *International Biodeterioration*, 1989, **25**, 175-189.
12. P. S. Guiamet and C. C. Gaylarde, *World Journal of Microbiology & Biotechnology*, 1996, **12**, 395-397.
13. S. El Hage, B. Lajoie, J.-L. Stigliani, A. Furiga-Chusseau, C. Roques and G. Baziard, *Journal of Applied Biomedicine*, 2014, **12**, 245-253.
14. B. Brycki, I. Małecka, A. Koziróg and A. Otlewska, *Molecules*, 2017, **22**.
15. T. Muhizi, S. Grelier and V. Coma, *Journal of Agricultural and Food Chemistry*, 2009, **57**, 8770-8775.
16. T. Muhizi, V. Coma and S. Grelier, *Pest Management Science*, 2011, **67**, 287-293.
17. E.-R. Kenawy, F. I. Abdel-Hay, A. E.-R. R. El-Shanshoury and M. H. El-Newehy, *Journal of Controlled Release*, 1998, **50**, 145-152.
18. E.-R. Kenawy, F. I. Abdel-Hay, A. E.-R. R. El-Shanshoury and M. H. El-Newehy, *Journal of Polymer Science Part A: Polymer Chemistry*, 2002, **40**, 2384-2393.
19. E.-R. Kenawy and Y. A. G. Mahmoud, *Macromolecular Bioscience*, 2003, **3**, 107-116.
20. T. Ravikumar, H. Murata, R. R. Koepsel and A. J. Russell, *Biomacromolecules*, 2006, **7**, 2762-2769.

21. H. Murata, R. R. Koepsel, K. Matyjaszewski and A. J. Russell, *Biomaterials*, 2007, **28**, 4870-4879.
22. M. F. Ilker, K. Nüsslein, G. N. Tew and E. B. Coughlin, *Journal of the American Chemical Society*, 2004, **126**, 15870-15875.
23. K. Lienkamp, A. E. Madkour, A. Musante, C. F. Nelson, K. Nüsslein and G. N. Tew, *Journal of the American Chemical Society*, 2008, **130**, 9836-9843.
24. T. Muhizi, V. Coma and S. Grelier, *Carbohydrate Research*, 2008, **343**, 2369-2375.
25. V. Neto, A. Voisin, V. Héroguez, S. Grelier and V. Coma, *Journal of Agricultural and Food Chemistry*, 2012, **60**, 10516-10522.
26. A. Voisin, PhD thesis, Université Bordeaux I, 2012.
27. M. F. Winnik, in *Emulsion Polymerization and Emulsion Polymers*, eds. P. A. Lovell and M. S. El-Aasser, John Wiley & Sons, Ltd, 1997, ch. 14, pp. 467-518.

## Chapter 6:

1. L. Pichavant, C. Bourget, M.-C. Durrieu and V. Héroguez, *Macromolecules*, 2011, **44**, 7879-7887.
2. L. Pichavant, G. Amador, C. Jacqueline, B. Brouillaud, V. Héroguez and M.-C. Durrieu, *Journal of Controlled Release*, 2012, **162**, 373-381.
3. L. Pichavant, H. Carrie, M. N. Nguyen, L. Plawinski, M. C. Durrieu and V. Héroguez, *Biomacromolecules*, 2016, **17**, 1339-1346.



# **Appendix A: Characterization Techniques**

### **A.1. Proton Nuclear Magnetic Resonance ( $^1\text{H}$ NMR)**

$^1\text{H}$  NMR spectra were obtained on a Bruker 400 MHz spectrometer in deuterated chloroform ( $\text{CDCl}_3$ ), DMSO ( $\text{DMSO-}d_6$ ), ethanol (ethanol- $d_6$ ) or water ( $\text{D}_2\text{O}$ ). A sample of 5-10 mg was dissolved in 500  $\mu\text{L}$  of the deuterated solvent, and the analysis was performed with 32 scans and a relaxation time of 2 seconds.

### **A.2. Size Exclusion Chromatography (SEC) analysis**

SEC analysis was carried out on a Varian apparatus equipped with TosoHaas TSK gel columns and a differential refractometer detector. THF or DMF served as eluents at a flow rate of 1  $\text{mL}\cdot\text{min}^{-1}$ , and calibration was achieved with low polydispersity PS standards.

### **A.3. Matrix-Assisted Laser Desorption Ionization Time of Flight Mass Spectrometry (MALDI-ToF)**

MALDI-ToF was performed at the CESAMO (Bordeaux, France) using a Voyager ABSciex mass spectrometer. Spectra were recorded in the positive-ion mode using the reflectron and an accelerating voltage of 20 kV. A trans-3-indoleacrylic acid matrix was used for all the measurements.

### **A.4. Infrared Spectroscopy**

Infrared spectra were obtained on a Vertex 70 Bruker Fourier transform-Infrared spectrometer. For each sample, the diamond crystal of an attenuated total reflectance accessory was brought into contact with the area to be analyzed. All the spectra were recorded between 4000 and 400  $\text{cm}^{-1}$  at a resolution of 4  $\text{cm}^{-1}$  with 16 scans per sample.

## **A.5. Gas Chromatography**

Gas chromatography analysis was performed using a Varian GC3900 instrument equipped with a Varian FactorFour™ polydimethylsiloxane capillary column (VF-1ms, 15m × 0.25 mm, ID DF = 0.25). The injected volume for the sample was 1 μL.

## **A.6. Dynamic Light Scattering (DLS)**

DLS measurements were performed on a Malvern Zetasizer Nano ZS90 instrument (scattering angle 90°) equipped with a He-Ne laser (4 mW; 633 nm). Before the measurements, the latex samples were diluted about 800-fold to minimize multiple scattering caused by high concentrations. The samples were transferred into a capped glass cuvette, and analysis was performed in triplicate with 3 runs of 60 seconds to ensure reproducibility.

## **A.7. Transmission Electron Microscopy (TEM)**

TEM measurements were performed at the Bordeaux Imaging Center (France) with a Hitachi H7650 microscope operating at an accelerating voltage of 80 kV. Pictures were recorded with the Digital Micrograph (Gatan) software. For the size, distribution and morphology observation, the latex samples were diluted about 400-fold and 4 μL were deposited on a 200-mesh carbon film-coated copper grid and allowed to dry for 3 minutes.

## **A.8. Atomic Force Microscopy (AFM)**

AFM was performed on a Dimension Icon (Veeco) apparatus in the tapping mode. Height, phase and three-dimensional images were generated using the Nanoscope analysis software (Bruker).

## **A.9. Profilometry**

Profilometry measurements were performed with a Bruker DektakXT-A mechanical profilometer. The particle films were directly analyzed on their glass substrate. A scratch was made with pliers before analysis of the sample.

# **Appendix B: Supplementary**

## **Microbiology Methods**

## B.1. Determination of Inoculum Concentration

The spore concentration in the inoculum suspension was determined by microscopy. The suspension (10  $\mu\text{L}$ ) was pipetted onto a hemocytometer grid that was then observed on a microscope with a magnification of typically 100. The spores were counted on each sub-squares of the hemocytometer grid highlighted in green (Figure B.2). The spores touching the bottom and bottom-right lines of each square were not counted to avoid redundancy. The spore concentration was determined using equation (B.1):

$$C_{sp} = \frac{n_{sp}}{av} F_d \quad (\text{B.1})$$

where  $n_{sp}$  is the number of spores,  $a$  is the number of sub-squares used in the counting,  $v$  is the volume of a sub-square and  $F_d$  is the dilution factor.

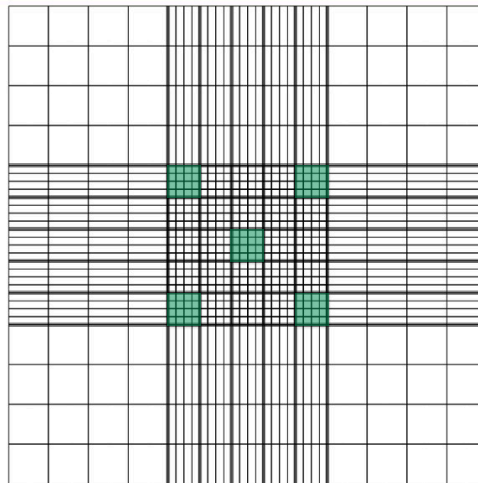


**Figure B.2. Hemocytometer grid (only cells in the green zones are counted).**

Once the initial concentration was determined, it could be adjusted as required by successive dilutions. Briefly, for a dilution factor of 100, two sterile tubes are filled with 9 mL of physiological water. Then a 1-mL sample was pipetted from the initial suspension and

deposited into a tube. After homogenization, 1 mL of the new suspension was pipeted and put into a second tube.

# **Appendix C: Supplementary Characterizations**



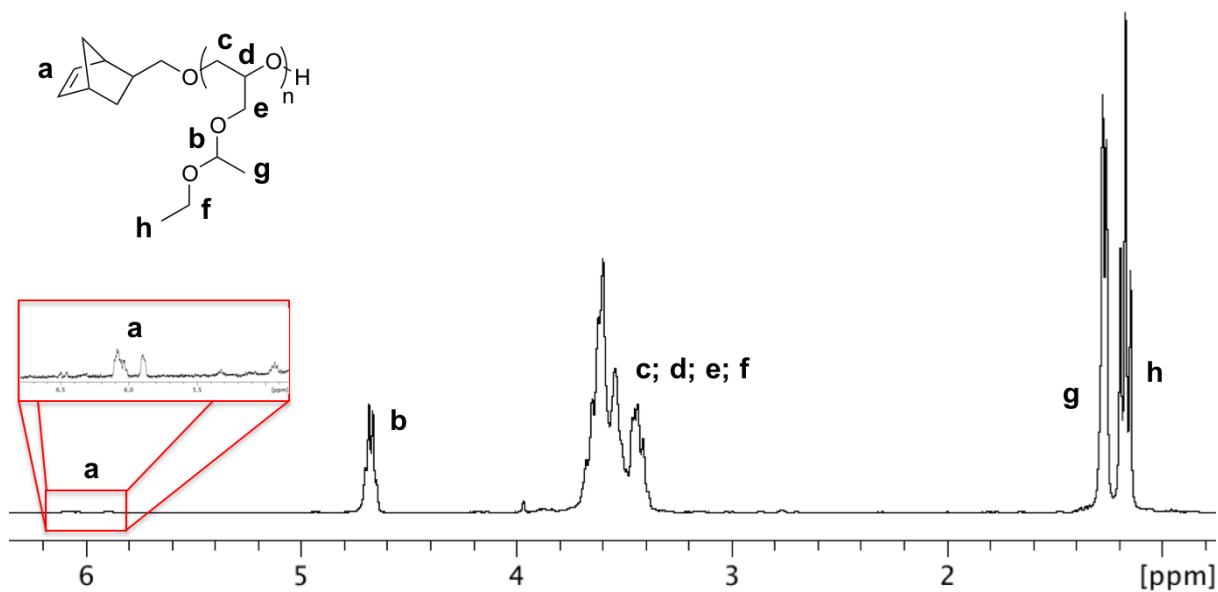


Figure C.3.  $^1\text{H}$  NMR spectrum for  $\alpha$ -norbornenyl-poly(glycidol acetal) macromonomer (1b) in  $\text{CDCl}_3$  (DP<sub>n</sub>:Th = 54).

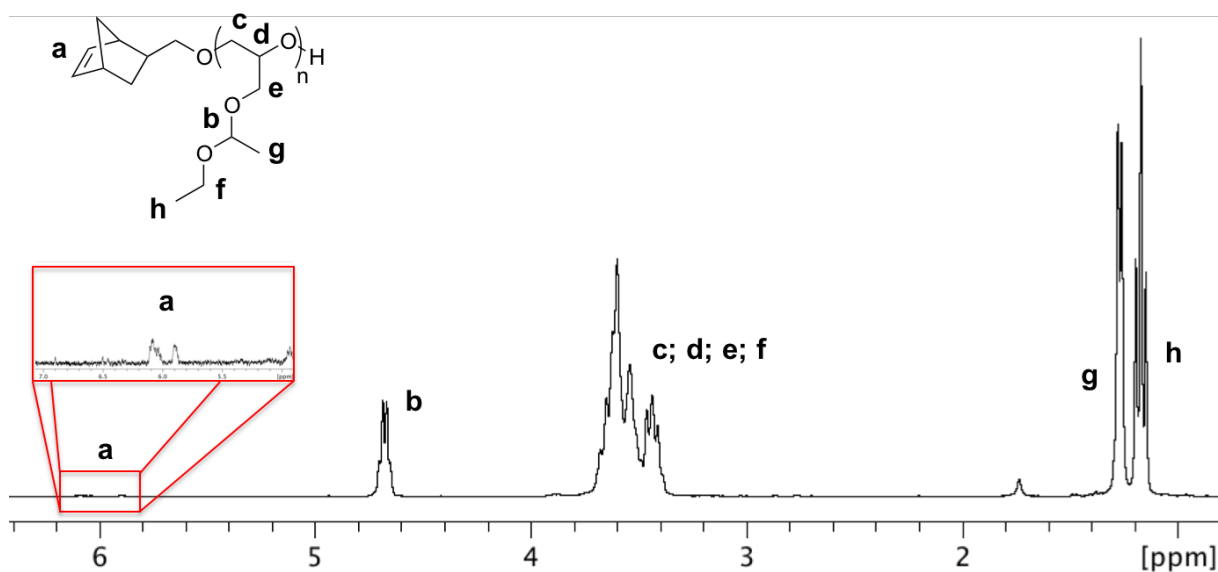
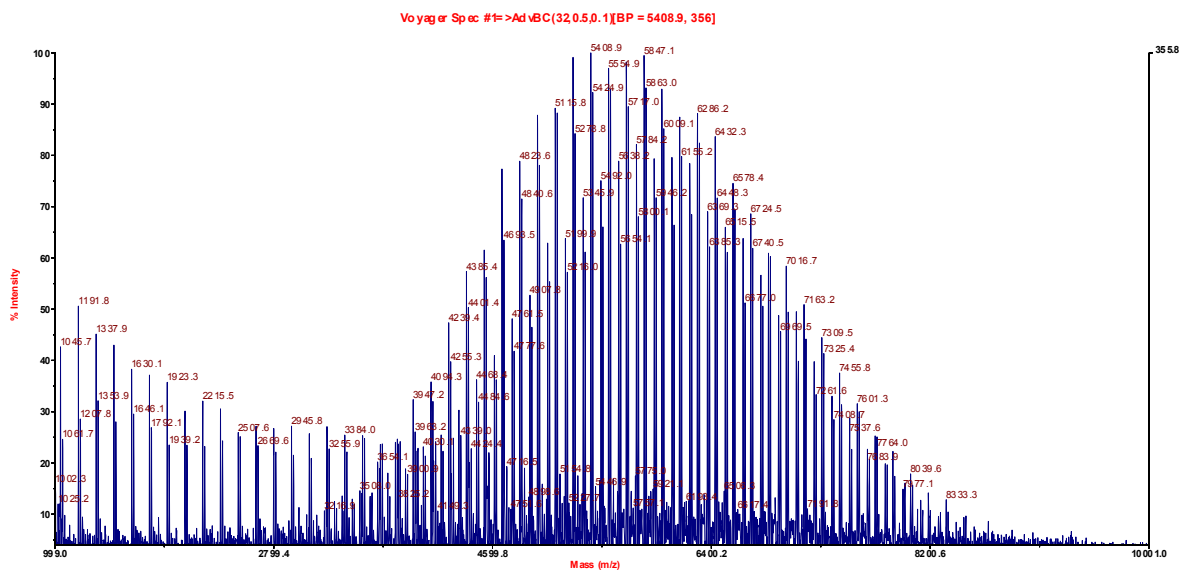
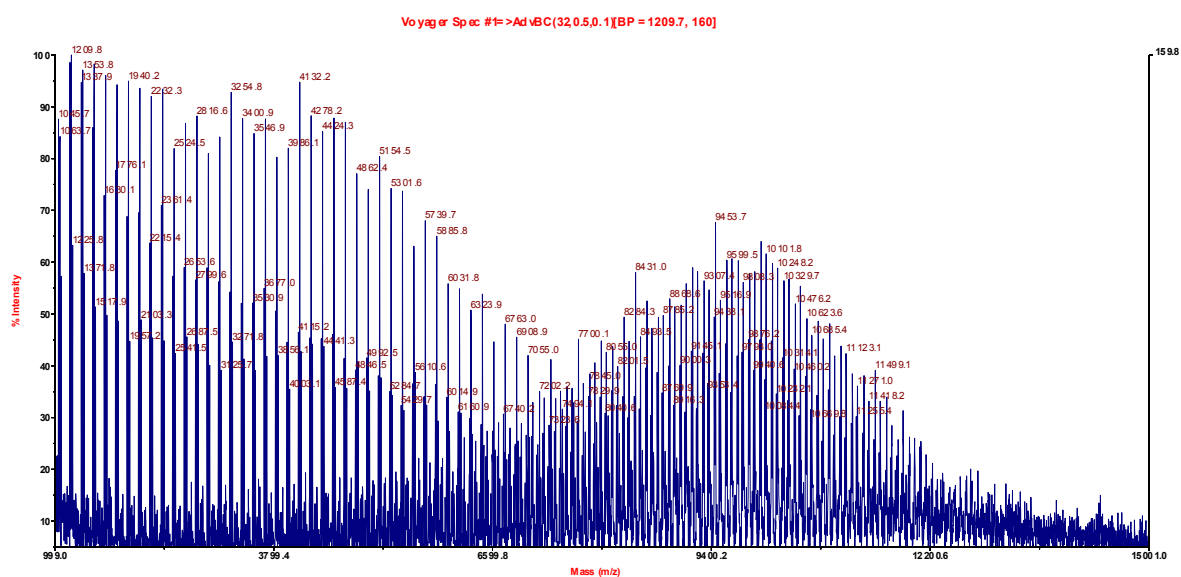


Figure C.4.  $^1\text{H}$  NMR spectrum for  $\alpha$ -norbornenyl-poly(glycidol acetal) macromonomer (1b) in  $\text{CDCl}_3$  (DP<sub>n</sub>:Th = 110).



**Figure C.5. MALDI-ToF spectrum for  $\alpha$ -norbornenyl-poly(glycidol acetal) macromonomer (1b) ( $DP_n = 50$ ).**



**Figure C.6. MALDI-ToF spectrum for  $\alpha$ -norbornenyl-poly(glycidol acetal) macromonomer (1c) ( $DP_n = 103$ ).**

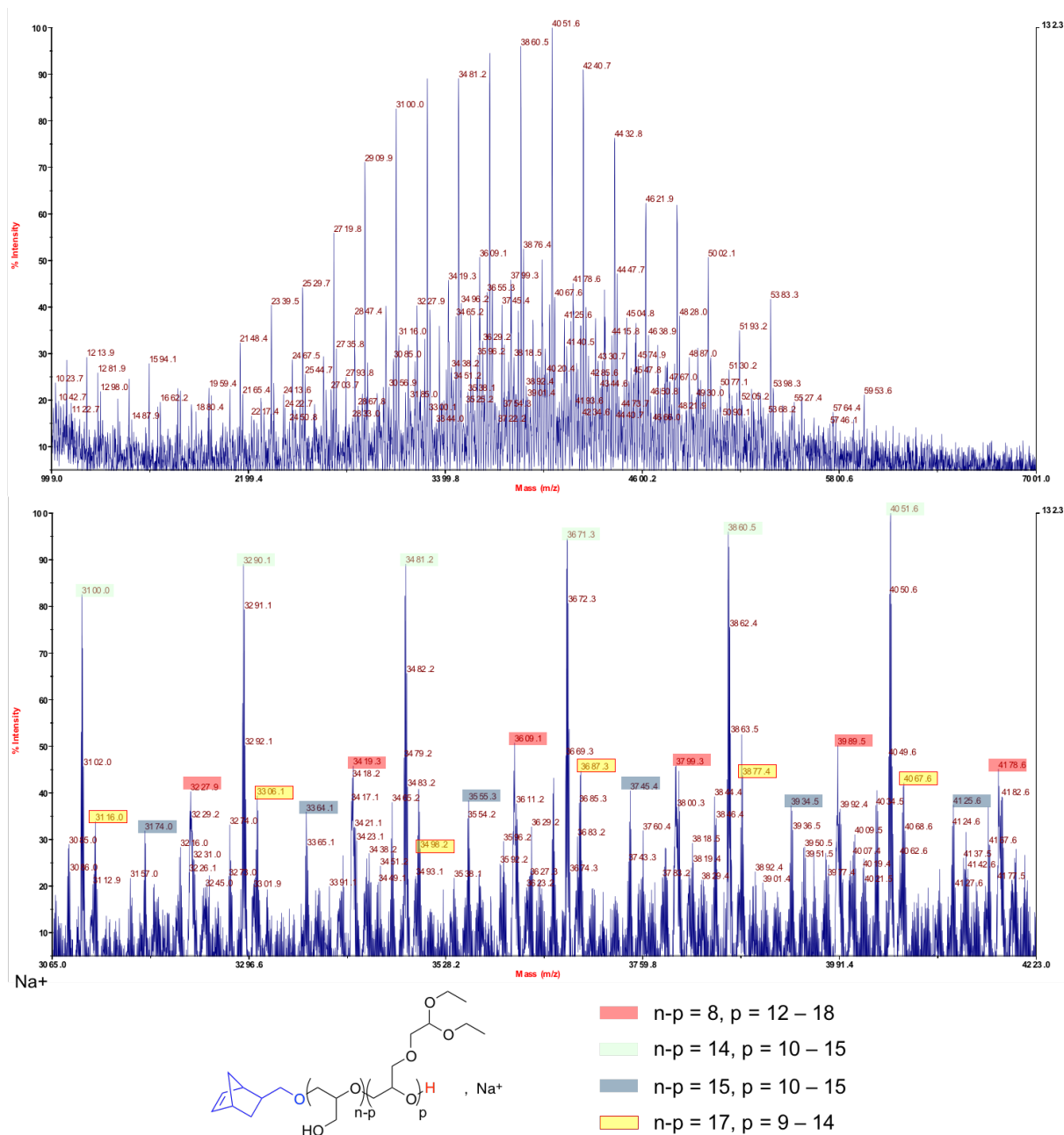


**Figure C.7. MALDI-ToF mass spectrometry for acetaldehyde diethylacetal-functionalized macromonomer (3a).**

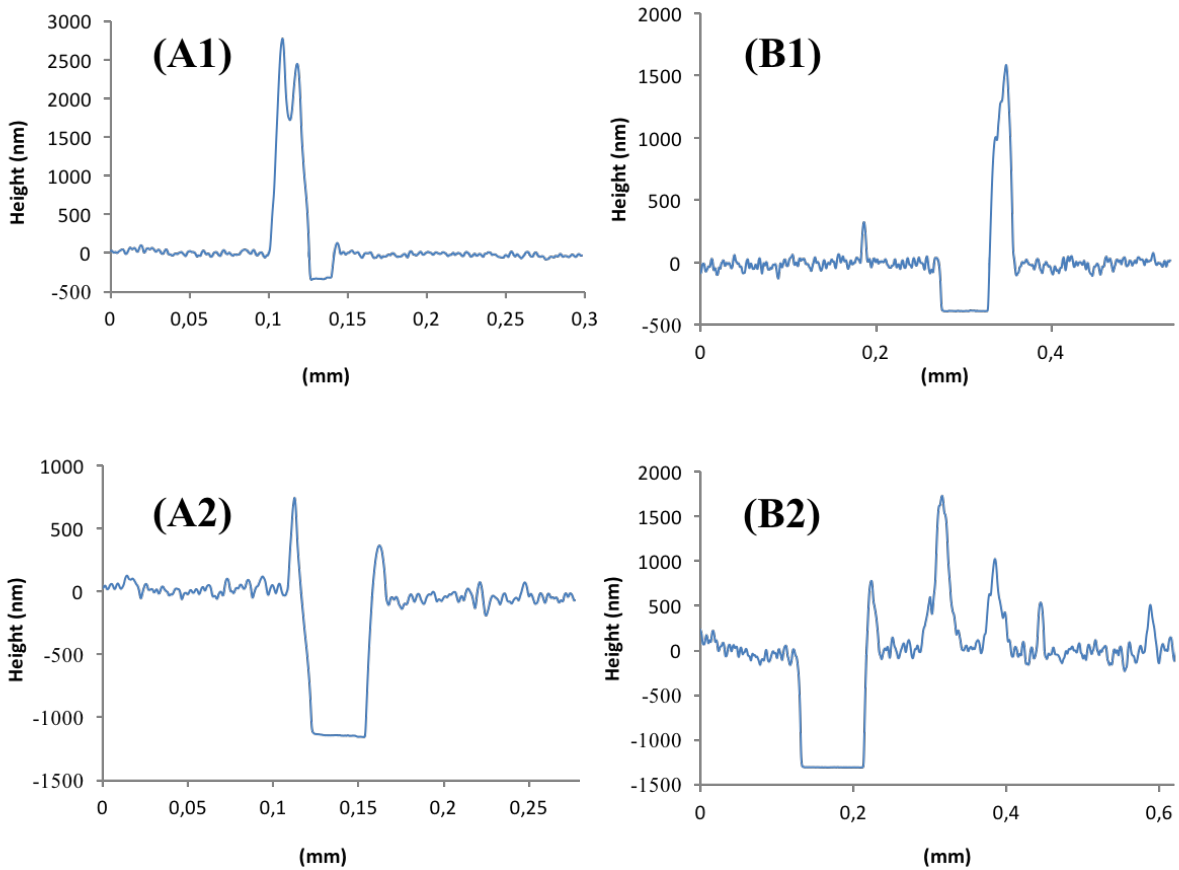


**Figure C.8. Profilometry measurements. Column (A): non-functionalized particle films; colomn (B): dodecylamine-functionalized particle films. Line (1): films by single deposition spin-coating; line (2): films by multi deposition spin-coating.**